

Carbene-Catalyzed Enantioselective Sulfenylation of Enone Aryl Aldehydes: A New Mode of Breslow Intermediate Oxidation

Rui Deng,^{a§} Shuquan Wu,^{a§} Chengli Mou,^{b§} Jianjian Liu,^a Pengcheng Zheng,^{a*} Xinglong Zhang^{d*} and Yonggui Robin Chi^{ac*}.

^aState Key Laboratory Breeding Base of Green Pesticide and Agricultural Bioengineering, Key Laboratory of Green Pesticide and Agricultural Bioengineering, Ministry of Education, Guizhou University, Huaxi District, Guiyang 550025, China.

^bSchool of Pharmacy, Guizhou University of Traditional Chinese Medicine, Huaxi District, Guiyang 550025, China.

^cDivision of Chemistry & Biological Chemistry, School of Physical & Mathematical Sciences, Nanyang Technological University, Singapore 637371, Singapore.

^dInstitute of High-Performance Computing, A*STAR (Agency for Science, Technology and Research), Singapore 138632, Singapore.

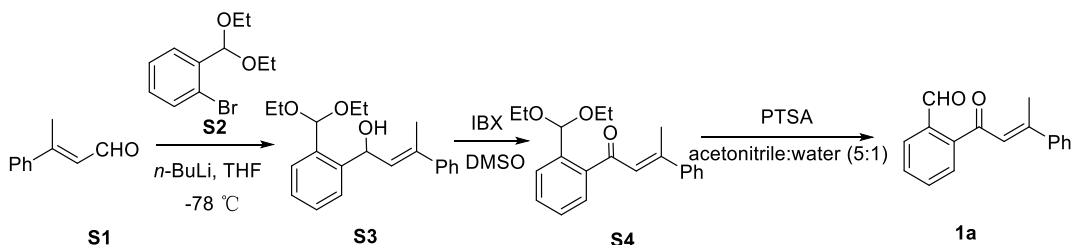
Content

I. General information	2
II. Preparation of substrates	3
III. Experimental section: condition optimization for the synthesis of 3a	4
IV. General procedure for the catalytic reactions.....	6
V. Mechanistic Studies.....	8
VI. LC-HRMS semi-quantitative analysis and ¹ H NMR of adduct 8	9
VII. The effect of added pTsOH instead of water	14
VIII. HRMS analysis of intermediates	15
IX. The rate of the NHC-catalyzed TsCl hydrolysis by LC-MS	16
X. Computational Methods	18
XI. Stereochemistry determination <i>via</i> X-ray crystallographic analysis	41
XII. References.....	42
XIII. Characterization of substrates and products	45
XIV. ¹ H NMR, ¹³ C NMR, ¹⁹ F NMR and HPLC spectra	69

I. General information

Commercially available materials purchased from Energy Chemical or Aladdin were used as received. Toluene was distilled. Unless otherwise specified, all reactions were prepared using 4 mL vial under N₂ atmosphere in glove-box from M Braun (UNILAB SP). Proton nuclear magnetic resonance (¹H NMR) spectra were recorded on a Bruker (AVANCE III HD 400 MHz) spectrometer. Chemical shifts were recorded in parts per million (ppm, δ) relative to tetramethylsilane (δ 0.00) or chloroform (δ = 7.26, singlet). ¹H NMR splitting patterns are designated as singlet (s), doublet (d), triplet (t), quartet (q), dd (doublet of doublets); m (multiplets), and etc. All first-order splitting patterns were assigned on the basis of the appearance of the multiplet. Splitting patterns that could not be easily interpreted are designated as multiplet (m) or broad (br). Carbon nuclear magnetic resonance (¹³C NMR) spectra were recorded on a Bruker (AVANCE III HD 101 MHz) spectrometer. Fluorine (¹⁹F) nuclear magnetic resonance (¹⁹F NMR) spectra were recorded on a Bruker (AVANCE III HD 376 MHz) spectrometer. The melting points (m.p.) of the title compounds were determined when left untouched on an XT-4-MP apparatus from Beijing Tech. Instrument Co. (Beijing, China). High resolution mass spectrometer analysis (HRMS) was performed on Waters Xevo G2-S QToF. Infrared spectra (IR) were obtained on a Thermo Fisher FT/IR-Nicolet iS50 spectrometer, and the absorptions have been reported in wavenumbers (cm⁻¹). Absolute configuration of the products was determined by X-ray crystallography (Bruker d8 quest). HPLC analyses were measured on Waters systems with Empower3 system controller, Alliance 2695, and 2998 Diode Array Waters 2489 UV/Vis detector. Chiralcel brand chiral columns from Daicel Chemical Industries were used with models IA, IB, IE or OD-H in 4.6 x 250 mm size. The racemic products used to determine the ee values were synthesized using racemic catalyst. Optical rotations were measured on an Insmark IP-digi Polarimeter in a 1 dm cuvette at 25 °C. The concentration (c) is given in g/100 mL. Analytical thin-layer chromatography (TLC) was carried out pre-coated silica gel plate (0.2 mm thickness). Visualization was performed using a UV lamp.

II. Preparation of substrates



Substrates **S1**, **S2** and **1a** were synthesized according to the reported method.¹⁻⁶

A 250 mL Schlenk flask was charged with **S2** (4.25 g, 16.4 mmol) 30 mL dry THF and placed at -78 °C. *n*-BuLi (2.5 M in hexane, 7.7 mL, 19.1 mmol) was added drop wise at same temperature and stirred for 30 min. **S1** (2g, 1 mmol) dissolved in 2 mL of dry THF, was added dropwise over 2 min and stirred for additional 30 min. The mixture was warmed to room temperature over 30 min. The reaction mixture was quenched with saturated aqueous ammonium chloride solution and extracted using ethyl acetate. The organic extracts were combined dried over anhydrous sodium sulphate and concentrated, the residual viscous crude **S3** was given.

The crude product **S3** was dissolved in DMSO (40 mL), and IBX (1.5 mmol) was added at room temperature for 30 min. After completion of the reaction, monitored by TLC, the mixture was quenched with water and filtered through Buchner funnel. The filter cake was washed with 3×5 mL of ethyl acetate. Organic extracts were combined and worked up using saturated sodium bicarbonate solution to remove excess iodobenzoic acid. The extract was dried over anhydrous sodium sulphate and concentrated under vacuum to give compound **S4**.

Compound **S4** was dissolved in acetonitrile/water (30 mL, 5:1) mixture in an oven dried round bottom flask and PTSA (0.1 eq) was added and stirred at rt until the reactant **S4** disappeared as monitored by TLC. The reaction mixture was quenched with saturated aqueous sodium bicarbonate solution and extracted with ethyl acetate. The organic extracts were combined, dried over anhydrous sodium sulphate and concentrated. The crude product was purified by silica gel column chromatography using petroleum ether/ethyl acetate (20:1) as eluent to afford compound **1a**.

III. Experimental section: condition optimization for the synthesis of 3a

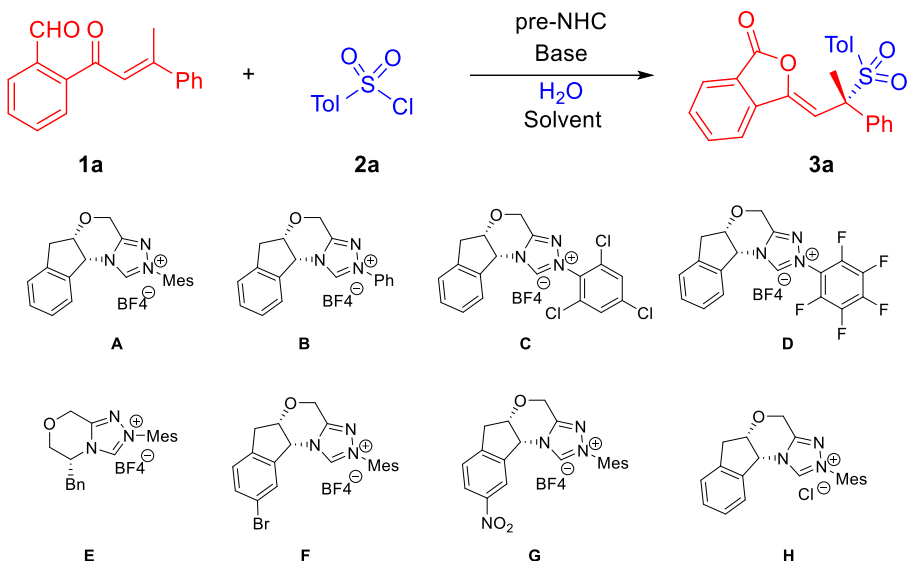


Table S-1. The effects of catalysts, bases^a

Entry	Pre-NHC	Base	Solvent	Additive	Time(h)	Yield(%) ^b	ee(%) ^c
1	A	K ₂ CO ₃	EA	-	12	13	96
2	A	K ₂ CO ₃	EA	4 Å	12	< 5%	96
3	A	K ₂ CO ₃	EA	H ₂ O	12	44	94
4	B	K ₂ CO ₃	EA	H ₂ O	12	29	77
5	C	K ₂ CO ₃	EA	H ₂ O	12	nr	nr
6	D	K ₂ CO ₃	EA	H ₂ O	12	nr	nr
7	E	K ₂ CO ₃	EA	H ₂ O	12	50	98
8	F	K ₂ CO ₃	EA	H ₂ O	12	33	98
9	G	K ₂ CO ₃	EA	H ₂ O	12	33	98
10	H	K ₂ CO ₃	EA	H ₂ O	12	36	94
11	E	DBU	EA	H ₂ O	12	nr	nr
12	E	Et ₃ N	EA	H ₂ O	12	nr	nr
13	E	DIPEA	EA	H ₂ O	12	nr	nr
14	E	DABCO	EA	H ₂ O	12	nr	nr
15	E	Cs ₂ CO ₃	EA	H ₂ O	12	52	97
16	E	Na ₂ CO ₃	EA	H ₂ O	12	31	95
18	E	K ₃ PO ₄	EA	H ₂ O	12	33	95
20	E	K ₂ HPO ₄	EA	H ₂ O	12	45	96
21	E	KOAc	EA	H ₂ O	12	53	93

^aUnless otherwise specified, the reactions were carried using **1a** (0.1 mmol), **2a** (0.12 mmol), pre-NHC (0.02 mmol), base (0.12 mmol), solvent (2.0 mL) and H₂O (0.05 mmol) at 45 °C for 12 h. ^bIsolated yield of **3a**. ^cThe ee values were determined via HPLC on chiral stationary phase. EA = Ethyl acetate. DBU = 1,8-Dizabicyclo[5.4.0]undec-7-ene. Et₃N = Triethylamine. DIPEA = Diisopropylethy. DABCO = 1,4-Diazabicyclo[2.2.2]octane;triethylenediamine. KOAc = Potassium Acetate. nr = no reaction.

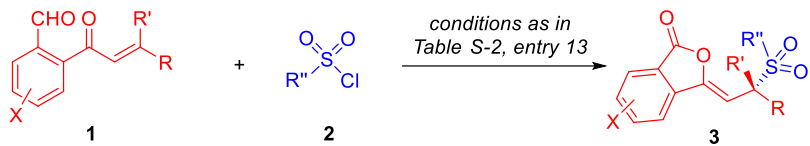
Table S-2. The effects of solvents and temperatures^a

Entry	Pre-NHC	Base	Solvent	Additive	Time(h)	Yield(%) ^b	ee(%) ^c
1	E	Cs ₂ CO ₃	THF	H ₂ O	12	64	97
2	E	Cs ₂ CO ₃	2-MeTHF	H ₂ O	12	71	95
3	E	Cs ₂ CO ₃	1,4-dioxane	H ₂ O	12	74	90
4	E	Cs ₂ CO ₃	Toluene	H ₂ O	12	75	98
5	E	Cs ₂ CO ₃	Et ₂ O	H ₂ O	12	41	92
6	E	Cs ₂ CO ₃	DME	H ₂ O	12	nr	nr
7	E	Cs ₂ CO ₃	DCM	H ₂ O	12	nr	nr
8	E	Cs ₂ CO ₃	PhCF ₃	H ₂ O	12	45	96
9 ^d	E	Cs ₂ CO ₃	Toluene	H ₂ O	12	69	95
10 ^e	E	Cs ₂ CO ₃	Toluene	H ₂ O	12	90	98
11 ^e	E	Cs ₂ CO ₃	Toluene	H ₂ O	1	50	93
12 ^e	E	Cs ₂ CO ₃	Toluene	H ₂ O	2	63	95
13 ^e	E	Cs ₂ CO ₃	Toluene	H ₂ O	4	90	98
14 ^e	E	Cs ₂ CO ₃	Toluene	H ₂ O	6	90	98
15 ^{e,f}	E	Cs ₂ CO ₃	Toluene	H ₂ O	4	29	99
16 ^{e,g}	E	Cs ₂ CO ₃	Toluene	H ₂ O	4	51	98
17 ^{e,h}	E	Cs ₂ CO ₃	Toluene	H ₂ O	4	90	98

^aUnless otherwise specified, the reactions were carried using **1a** (0.1 mmol), **2a** (0.12 mmol), pre-NHC (0.02 mmol), base (0.12 mmol), solvent (2.0 mL) and H₂O (0.05 mmol) at 45 °C for 12 h. ^b Isolated yield of **3a**. ^cThe ee values were determined via HPLC on chiral stationary phase. ^d0.1 mmol **2a** was used. ^e0.15 mmol **2a** was used. ^f0.01 mmol H₂O was used. ^g0.02 mmol H₂O was used. ^h0.1 mmol H₂O was used. THF = Tetrahydrofuran. 2-MeTHF = 2-Methyltetrahydrofuran. Et₂O = Diethyl ether. DME = 1,2-Dimethoxyethane. DCM = Dichloromethane. PhCF₃ = Benzotrifluoride.

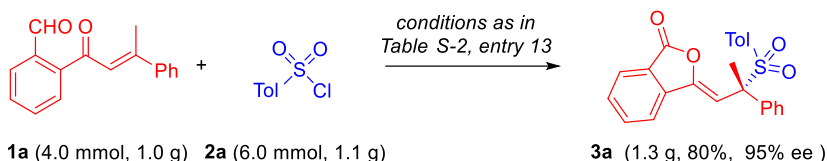
IV. General procedure for the catalytic reactions

General procedure for the catalytic reactions of **1** and **2** to synthesize product **3**



To a dry Schlenk tube equipped with a magnetic stir bar, was added **1** (0.1 mmol), **2** (0.15 mmol), triazolium salt NHC-E (0.02 mmol) and Cs_2CO_3 (0.12 mmol). The vial was then sealed, purged and backfilled with N_2 three times in glovebox before adding Toluene (2.0 mL) and H_2O (0.05 mmol), and the reaction mixture was stirred in oil bath at 45 °C for 4 h. The mixture was concentrated under reduced pressure. The resulting crude residue was purified *via* column chromatography on silica gel by using petroleum ether/ethyl acetate (5:1) to afford the desired product **3**.

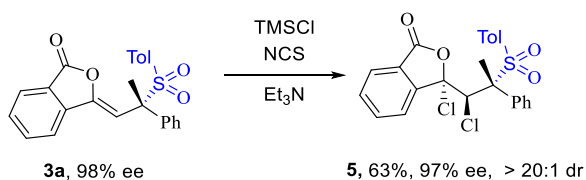
Scale-Up Synthesis of **3a**



To a dry Schlenk tube equipped with a magnetic stir bar, was added **1a** (4 mmol), **2a** (6 mmol), triazolium salt NHC-E (0.8 mmol) and Cs_2CO_3 (4.8 mmol). The vial was then sealed, purged and backfilled with N_2 three times in glovebox before adding Toluene (80 mL) and H_2O (2 mmol), and the reaction mixture was stirred in oil bath at 45 °C for 4 h. The mixture was concentrated under reduced pressure. The resulting crude residue was purified *via* column chromatography on silica gel by using petroleum ether/ethyl acetate (5:1) to afford the desired product **3a**.

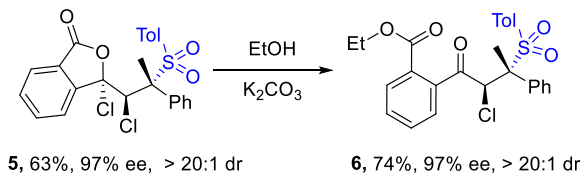
Synthetic transformations of chiral products **3a**

Preparation of **5** from product **3a**



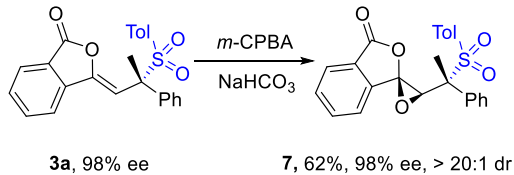
To a 25 mL flask, **3a** (0.40 mmol, 98% ee), TMSCl (0.80 mmol), NEt_3 (0.80 mmol) dissolved in anhydrous DCM (2.0 mL) at 0 °C and then warmed up to room temperature. After this mixture was stirred for 1 h, NCS (4.0 mmol) was added, and then, this was stirred at 60 °C for 5 h. The mixture was concentrated under reduced pressure. The resulting crude residue was purified *via* column chromatography on silica gel by using petroleum ether/ethyl acetate (5:1) to afford the desired product **5**.

Preparation of **6** from product **5**



To a 25 mL flask, product **5** (0.1 mmol, 97% ee) and K_2CO_3 (0.12 mmol) were added in EtOH (2.0 mL) and the mixture was stirred at 35 °C for 12 h. The reaction mixture was poured into a mixture of saturated aqueous ammonium chloride solution (10 mL). The aqueous phase was extracted with CH_2Cl_2 (10 mL × 2). The combined organic layer was washed with brine (30 mL) and dried over anhydrous sodium sulphate. The solvent was removed in vacuo and the residue was purified by flash column chromatography on silica gel by using petroleum ether/ethyl acetate (5:1) to afford the product **6** in 74% yield.

Preparation of **7** from product **3a**

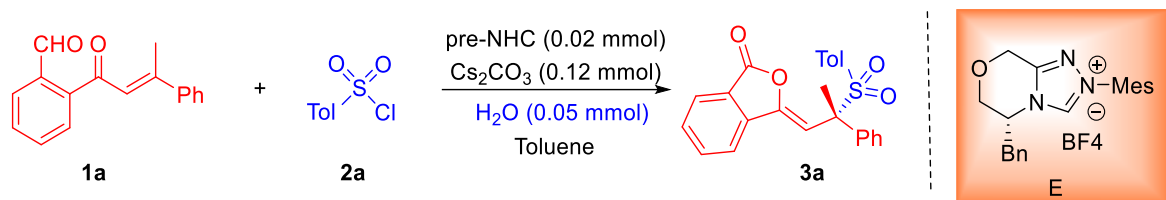


To a solution of **3a** (0.1 mmol, 98% ee) in CH_2Cl_2 (2.0 mL) was added *m*-CPBA (1 mmol) and saturated aqueous solution of NaHCO_3 (1 mL). The reaction mixture was stirred at room temperature for 12 h. The solvent was removed in vacuo and the residue was purified by flash column chromatography on silica gel by using petroleum ether/ethyl acetate (5:1) to afford the product **7** in 62% yield.

V. Mechanistic Studies

Linear effect studies

To elucidate the mode of stereochemical induction from the chiral NHC pre-catalyst to the sulfonated product, the linear effect study was conducted by building a relationship between the ee values of pre-NHC and that of the product. The specified ee values of pre-NHC was made by mixing certain amounts of optically pure *R*-NHC with optically pure *S*-NHC. Six reactions containing pre-NHC of racemic, 20%, 40%, 60%, 80% and 100% optical purity were run in parallel. The ee values of the products and the ee values of the catalysts exhibited a strongly linear positive correlation ($R^2=0.9981$) (Figure S-1). This linearity suggests that the stereochemical information on the chiral NHC pre-catalyst directly influences the stereochemical outcome of the product formation, as evidenced by the productive NCIs of the major enantioselective transition state (*Re*-TS5) (Figure S-13).



Entry	ee of pre-NHC (%)	ee of product (%)
1	0	0
2	20	19.5
3	40	40
4	60	55.2
5	80	73.5
6	100	95.3

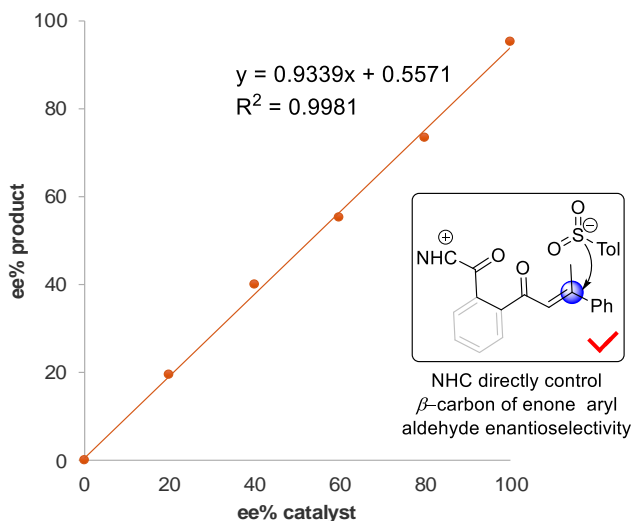


Figure S-1. Linear effect studies

VI. LC-HRMS semi-quantitative analysis and ^1H NMR of adduct 8

LC-HRMS semi-quantitative analysis of adduct 8

To a dry Schlenk tube equipped with a magnetic stir bar, was added **1a** (0.1 mmol), **2a** (0.15 mmol), triazolium salt NHC-E (0.02 mmol) and Cs_2CO_3 (0.12 mmol). The vial was then sealed, purged and backfilled with N_2 three times in glovebox before adding Toluene (2.0 mL) and H_2O (0.05 mmol), and the reaction mixture was stirred in oil bath at 45 °C for 4 h (Entry A). Based on the optimal reaction condition (Entry A), using 50 mg 4Å MS as additive and anhydrous toluene as solvent (Entry B). It was found that NHC directly reacted with toluenesulfonyl chloride **2a** to form by-product **8**, which was determined by liquid chromatography-high resolution mass spectrum (LC-HRMS). These numbers are semi-quantitative, and can provide certain insights on the reaction mechanism.

The intensity of by-product **8** was detected by the Waters BEH-C18 column of length 50 mm, 2.1 mm internal diameter and 1.7 μm particle thickness. 100% acetonitrile as mobile phase and the flow rate of the mobile phase was 300 $\mu\text{L}/\text{min}$ throughout the gradient. Column temperatures were tested at 40°C. The samples were taken 1 μl from the reaction solution with a micro syringe and diluted to 1 ml with pure acetonitrile and analyzed in full scan mode in the mass range of 50 to 1500 m/z. We repeated each experiment three times under the same conditions. Our current attempts in detecting the exact intensity of adduct **8** in the reaction mixture were not successful because this adduct was short-lived and highly reactive. A semi-quantitative analysis was performed, and the intensity of adduct **8** in the absence of water was found to be 30-130 times higher than that in the presence of water. These observations suggest water plays an important role in releasing the NHC catalyst from adduct **8**, thus recovering the deactivated NHC-Ts complex to regenerate the NHC for a productive catalytic cycle.

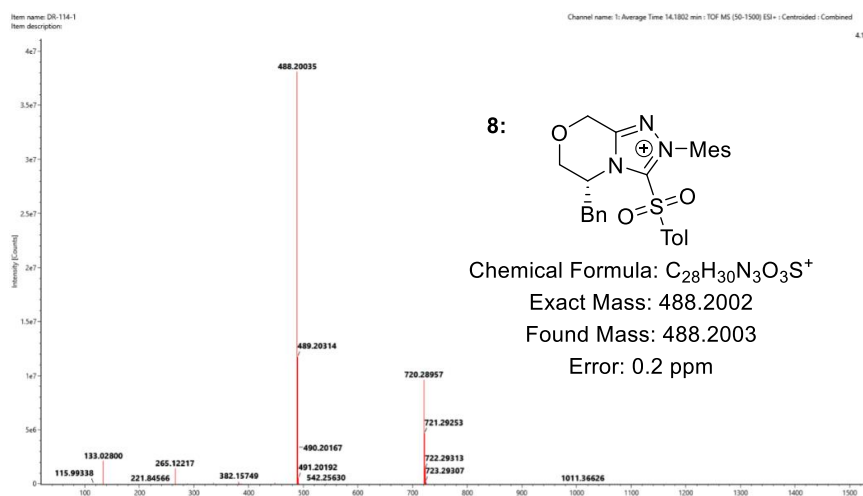
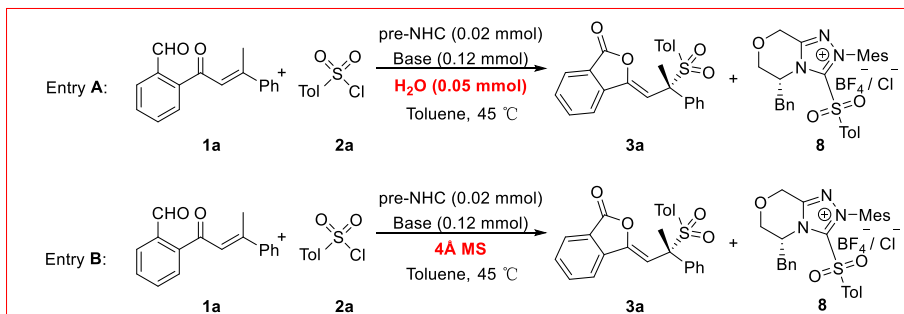


Figure S-2. HRMS spectra of by-product 8

LC-HRMS analysis of entry A

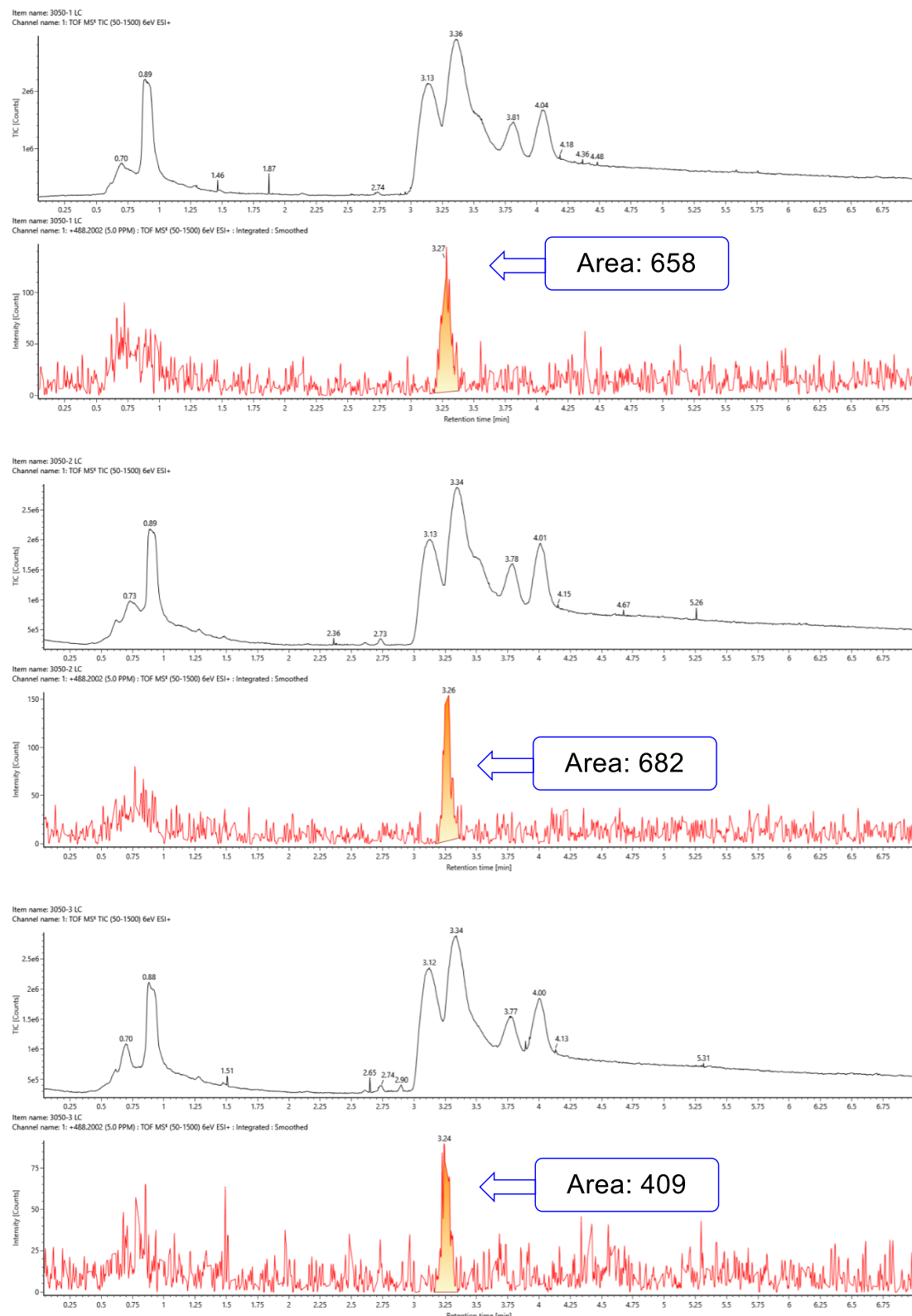


Figure S-3. LC-HRMS analysis of entry A

LC-HRMS analysis of entry B

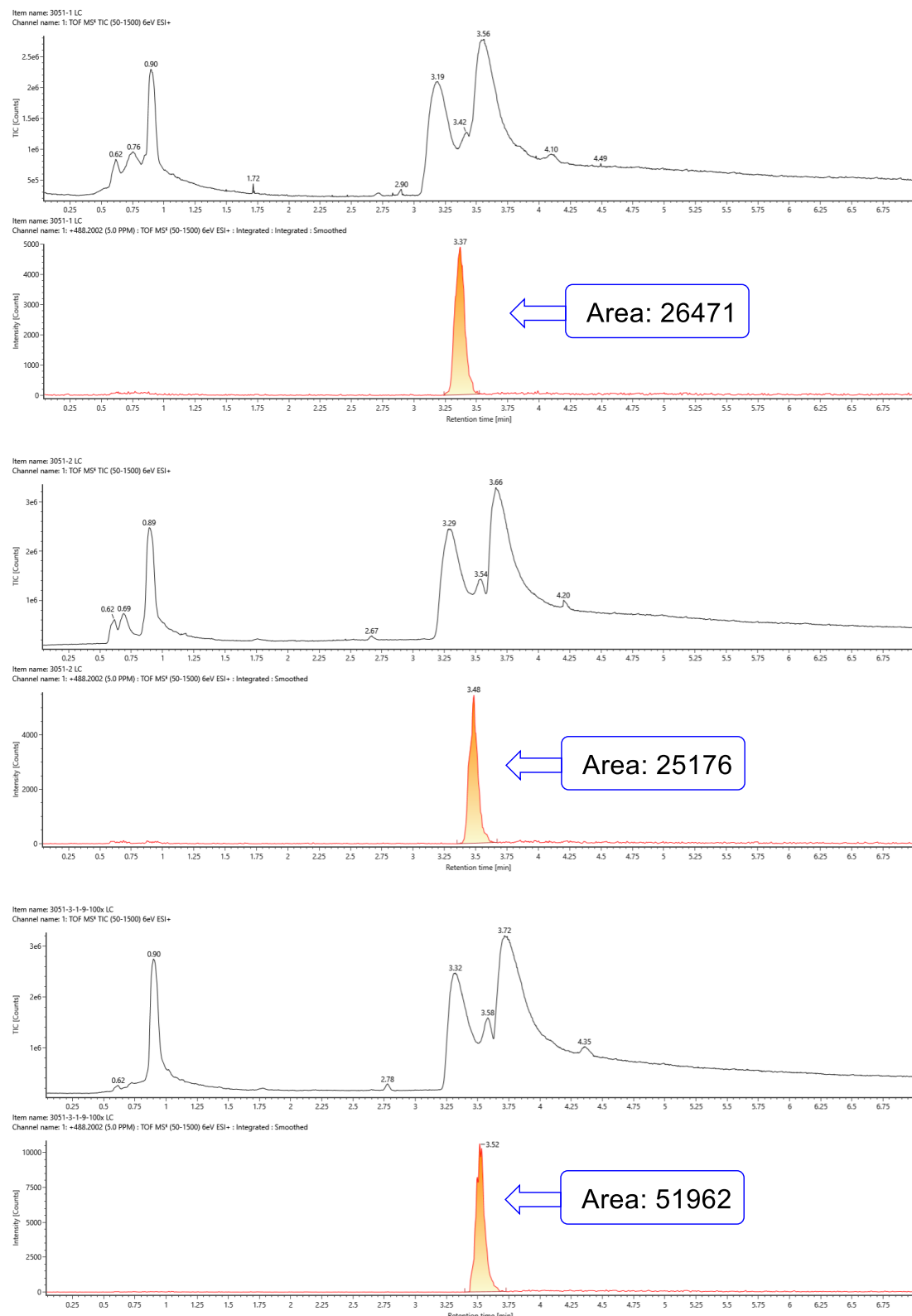
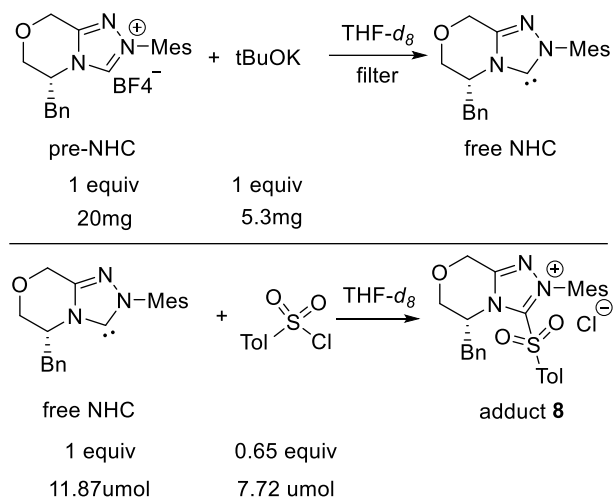


Figure S-4. LC-HRMS analysis of entry B

¹H NMR of adduct 8

The adduct **8** was determined by HRMS. Our efforts at that time to isolate this adduct were unsuccessful.

During this revision, we examined multiple methods to pre-prepare adduct **8**. The most successful results are illustrated in the following Figures. The adduct **8** was not stable for purifications (such as *via* silica gel column purification or crystallization). We managed to use ¹H NMR to study the formation of this adduct *in situ* (detailed result provided below). The hydrolysis of this adduct was also studied. Since adduct **8** can easily undergo hydrolysis (when solvent is not anhydrous and sufficient water is present), it can be used as an NHC pre-catalyst (in the presence of water).



Experimental details:

To an anhydrous THF-*d*₈ solvent (1 mL) in a 4 mL vial in a glove box, was added NHC pre-catalyst (20 mg) and tBuOK (5.3 mg). The mixture was stirred for 10 minutes at room temperature. The reaction was filtered and the solution containing free NHC (47.48 μmol/mL) was collected in an NMR tube (all the operations were performed in the glove box) and analyzed *via* ¹H NMR (Figure S-5).

In a separate set of experiments, free NHC was prepared as above in a THF-*d*₈ solution. To an NMR tube was added TsCl (1.5 mg, 7.72 μmol) and anhydrous THF-*d*₈ (0.3 mL). The 0.25 mL (47.48 μmol/mL) free NHC solution (11.87 μmol) and TsCl solution (both in THF-*d*₈) were mixed (right in the NMR equipment room) and immediately analyzed *via* ¹H NMR. This analysis indicates the formation of adduct **8** (Figure S-6).

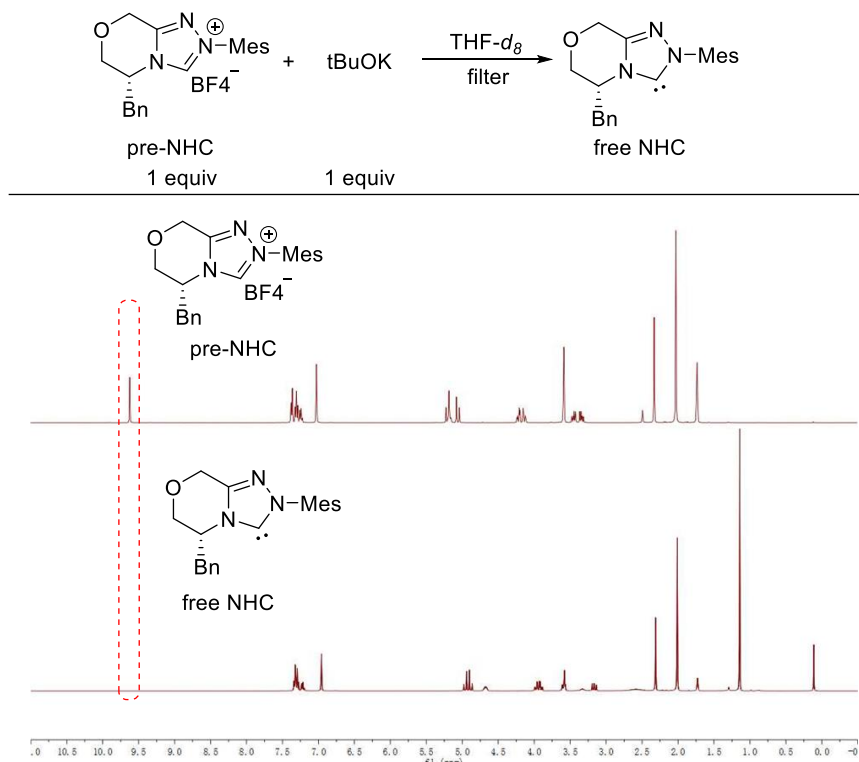


Figure S-5. ^1H NMR of pre-NHC and free NHC

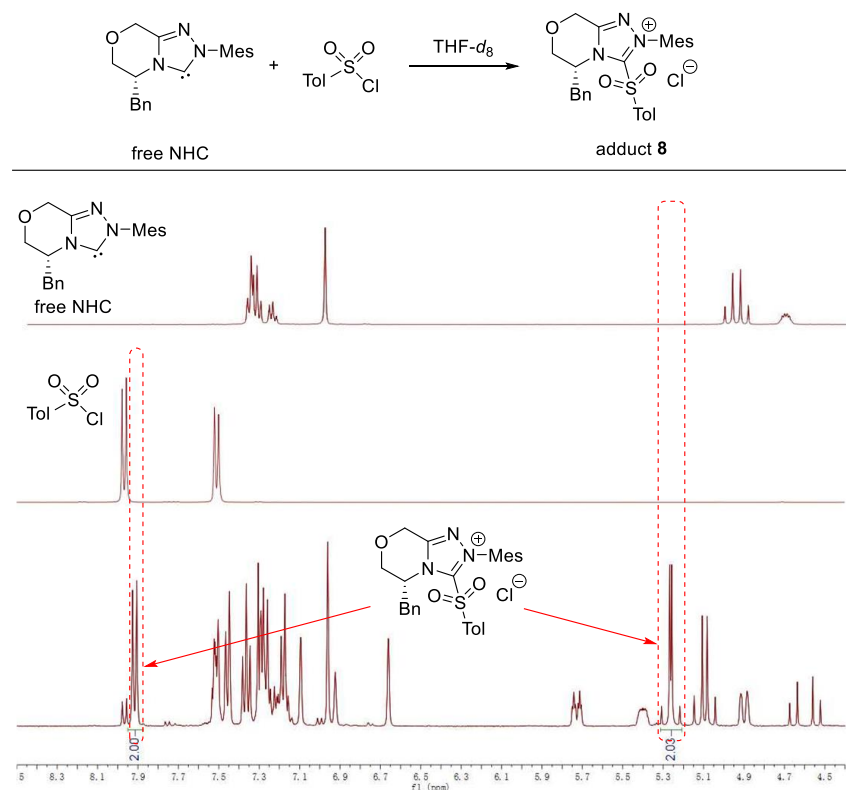
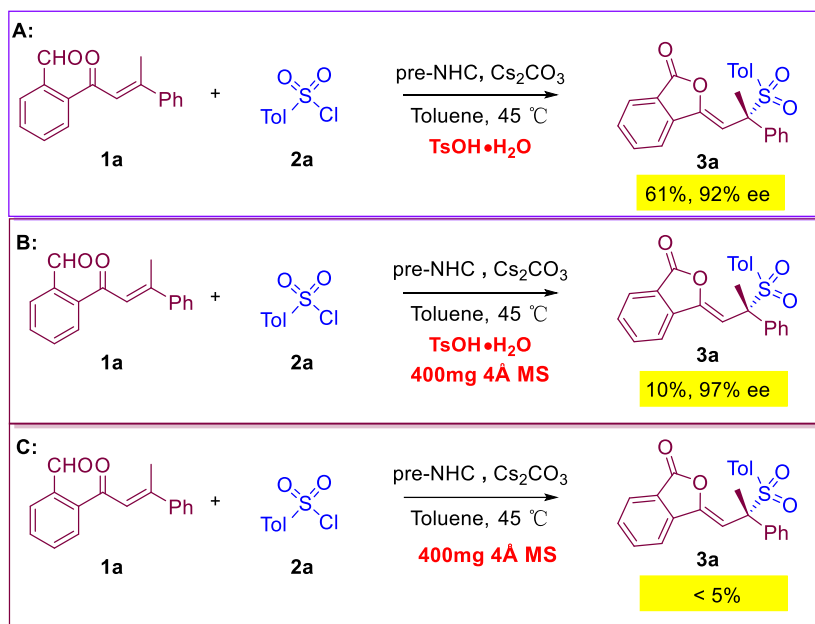


Figure S-6. The in situ ^1H NMR analysis of the formation of adduct 8

VII. The effect of added pTsOH instead of water

To investigate the effect of added pTsOH instead of water. Commercially available pTsOH·H₂O (CAS: 6192-52-5) is a monohydrate, to remove the effect of water, three control experiments were carried out.

To a dry Schlenk tube equipped with a magnetic stir bar, was added **1a** (0.1 mmol), **2a** (0.15 mmol), triazolium salt pre-NHC (0.02 mmol) and Cs₂CO₃ (0.12 mmol). The vial was then sealed, purged and backfilled with N₂ three times in glove box before adding Toluene (2.0 mL). In control experiment **A**, pTsOH·H₂O (0.05 mmol) was added, and the reaction mixture was stirred in oil bath at 45 °C for 4 h. The mixture was concentrated under reduced pressure. The resulting crude residue was purified to afford product **3a** in 61% yield and 92% ee. In control experiment **B**, 400mg 4Å molecular sieves and pTsOH·H₂O were added in the reaction, product **3a** was obtained in 10% yield and 97% ee. In control experiment **C**, 400mg 4Å molecular sieves was added (without pTsOH·H₂O and water), **3a** was obtained less than 5% yield. These observations suggested that water cannot be replaced by pTsOH.



VIII. HRMS analysis of intermediates

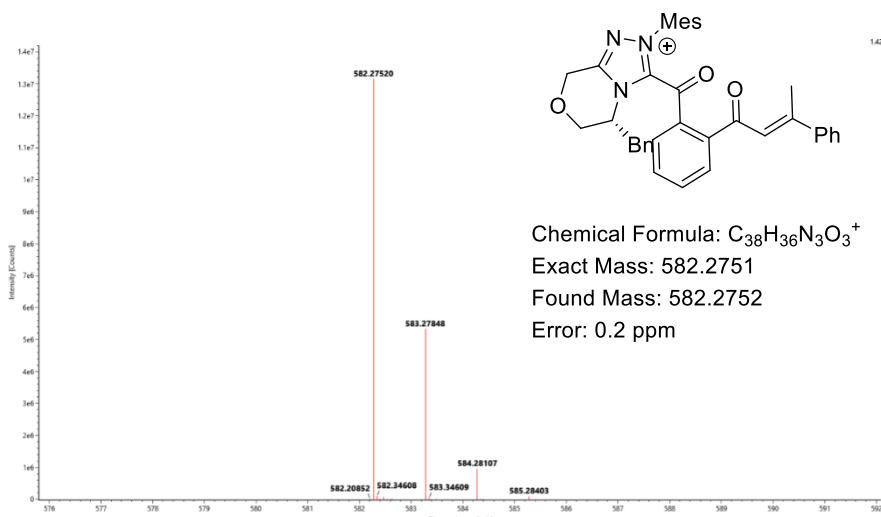


Figure S-7. HRMS(ESI⁺) spectra of acyl azonium intermediate

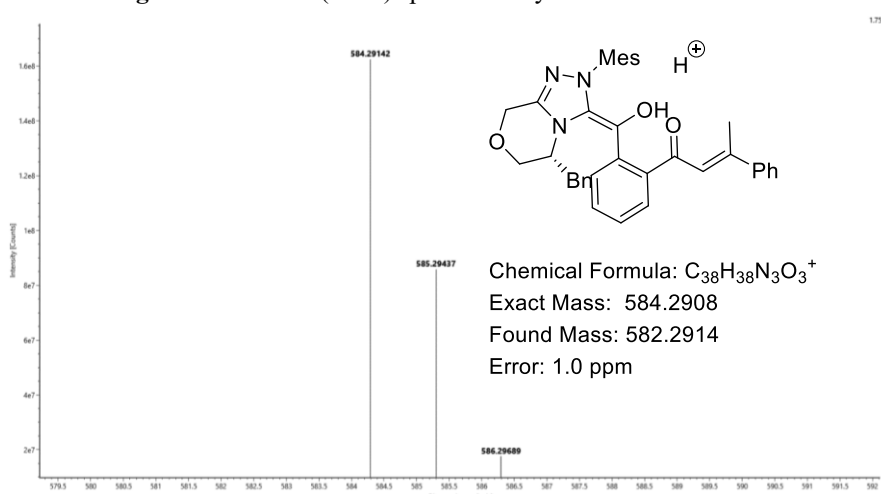


Figure S-8. HRMS(ESI⁺) spectra of Breslow intermediate

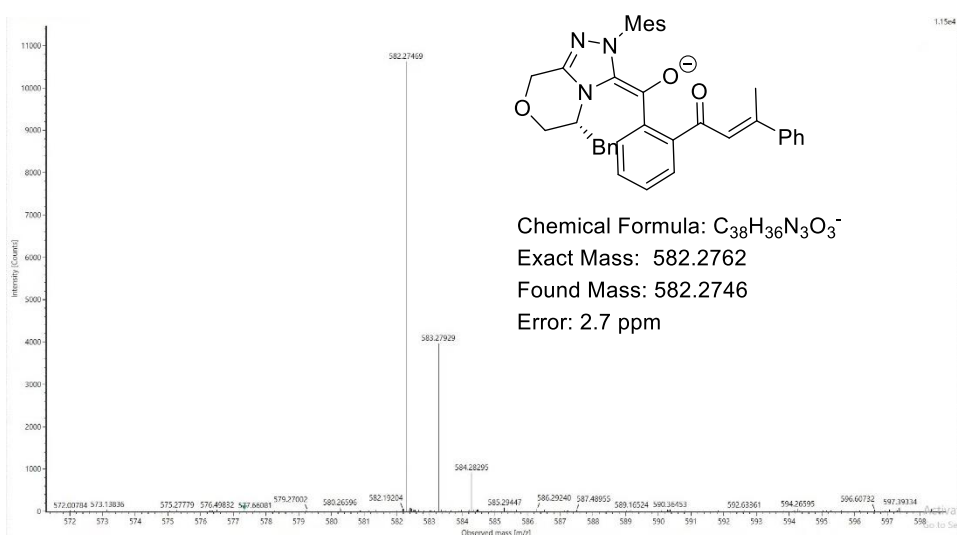
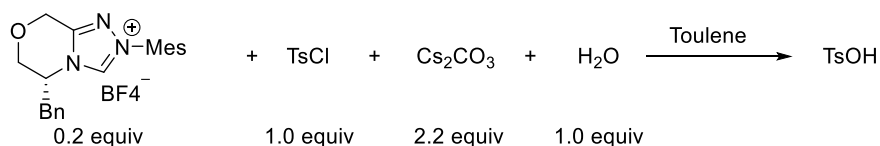


Figure S-9. HRMS(ESI⁻) spectra of intermediate I-a

IX. The rate of the NHC-catalyzed TsCl hydrolysis by LC-MS

To understand the rate of the NHC-catalyzed TsCl hydrolysis, we detected the TsOH concentration as a function of time by LC-MS/MS. Chromatographic separation of TsOH was performed on a SCIEX ExionLC AD system (Foster City, CA, USA). The column was an Agilent Eclipse XDB-C₁₈ column (4.6 mm × 150 mm, 5 μm particle size; Santa Clara, CA, USA) maintained at 40 °C. The injection amount was 2 μL. The mobile phase was composed of 30% solvent A (1% formic acid water) and 70% solvent B (acetonitrile) at a flow rate of 0.8 mL/min. The retention time of TsOH was approximately 2.7 min. Detection was performed on a SCIEX triplequad 4500 mass spectrometer (Foster City, CA, USA) fitted with electrospray ionization probe operated in the negative mode. The following optimal parameters were used: curtain gas pressure, 20 psi; ion source gas (GS1) pressure, 50 psi; ion source gas (GS2) pressure, 50 psi; ion source temperature, 500 °C; and ion spray voltage, -4500 V. Nitrogen (99.99%) was employed as the curtain, nebulizer and collision gases. Detection was carried out in multiple reactions monitoring mode. The mass parameters for TsOH were as follows: mass-to-charge ratio, 170.9 m/z; qualitative ion, 107.0 m/z (-25.28 eV, collision energy); quantitative ion, 79.9 m/z (-39.89 eV, collision energy); declustering potential, -67.8 V; entrance potential, -10 V; collision cell exit potential, -11 V.



We have detected the peak area of TsOH (concentrations range from 0.005 to 5 ug/mL), and the working curve equation is:

$$\text{Area} = 2.247 \times 10^6 \times [\text{TsOH}] + 4.493 \times 10^5 \quad (\text{R}^2 = 0.9998) \quad (\text{eq 1})$$

Table S-3. The peak area of TsOH

[TsOH] (μg/mL)	Area
0.005	5.49E+05
0.250	9.27E+05
0.500	1.64E+06
2.500	6.13E+06
5.000	1.17E+07

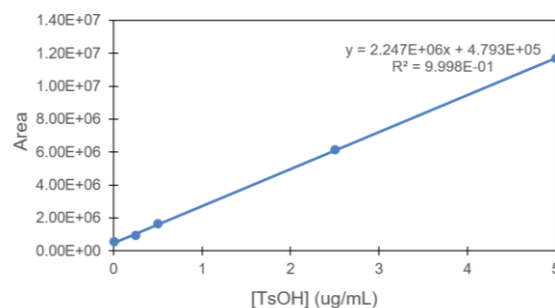


Figure S-10. The working curve of TsOH

Then, the rate of hydrolysis of TsCl was studied by monitoring the concentration of the product TsOH as a function of time.

Table S-4. The concentration of the product TsOH

Time (min)	Area	[TsOH] _t ($\mu\text{g/mL}$)
0	9.49E+05	0.21
10	2.47E+06	0.89
20	3.76E+06	1.46
30	5.95E+06	2.43
40	6.09E+06	2.50
50	7.15E+06	2.97

According to the initial concentration of TsCl, the corresponding degradation concentration of TsCl over time was calculated.

$$[\text{TsCl}]_t = [\text{TsCl}]_{t=0} - [\text{TsOH}]_t$$

Table S-5. The degradation concentration of TsCl

Time (min)	[TsOH] _t ($\mu\text{g/mL}$)	[TsCl] _t ($\mu\text{g/mL}$)	In[TsCl] _t
0.00	0.21	47.44	3.859486
10.00	0.89	46.76	3.845115
20.00	1.46	46.19	3.832763
30.00	2.43	45.22	3.811436
40.00	2.50	45.15	3.810057
50.00	2.97	44.68	3.799555

According to pseudo-first-order kinetic equation, we make a plot of ln[TsCl]_t as a function of time:

$$\ln[\text{TsCl}]_t = -1.2176 \times 10^{-3} \times t + 3.8568 \quad (\text{R}^2 = 0.9619) \quad (\text{eq 2})$$

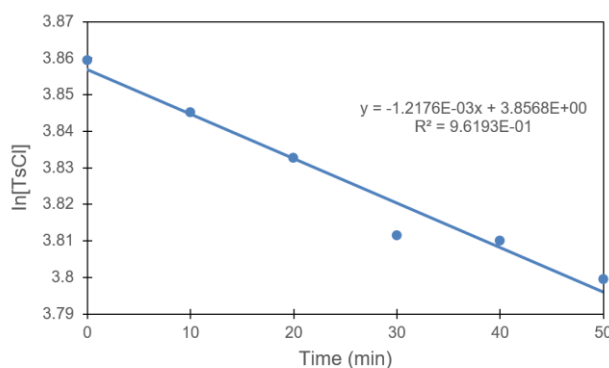


Figure S-11. A plot of ln[TsCl] as a function of time

The rate constant of the reaction:

$$k = 1.22 \times 10^{-3} \text{ min}^{-1}$$

X. Computational Methods

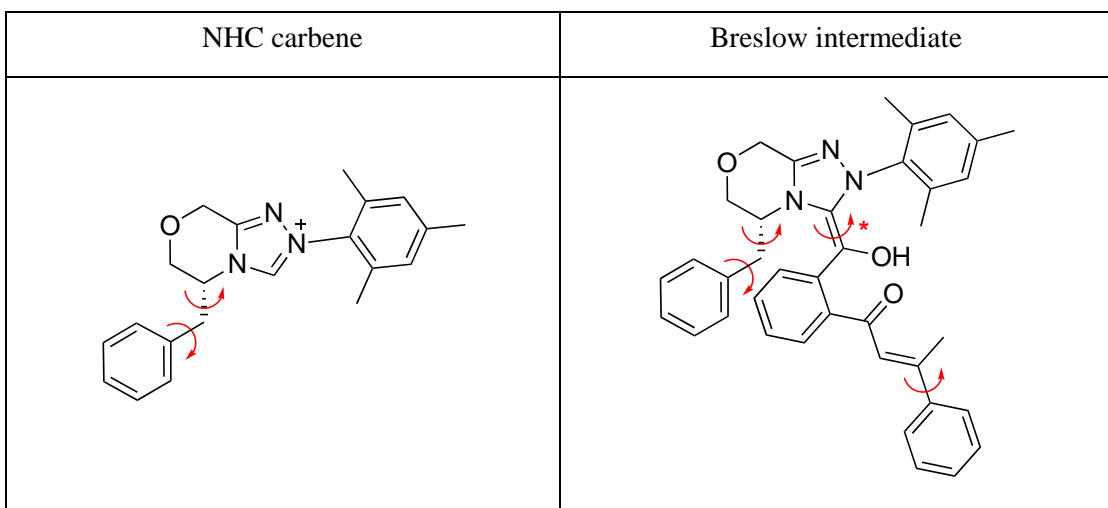
Geometry optimizations for conformational sampling in the gas phase were initially carried out using GFN2-xTB⁷ extended semiempirical tight-binding method in the *xtb* program^{8,9} from Grimme's group. The resulting cluster structures were further optimized using global hybrid functional M06-2X¹⁰ with Karlsruhe-family double- ζ valence def2-SVP^{11,12} basis set for all atoms as implemented in *Gaussian 16* rev. B.01.¹³ Single point (SP) corrections were performed using M06-2X functional and def2-TZVP¹¹ basis set for all atoms. Minima and transition structures on the potential energy surface (PES) were confirmed as such by harmonic frequency analysis, showing respectively zero and one imaginary frequency. The implicit SMD continuum solvation model¹⁴ for toluene solvent was used to account for the effect of solvent on the potential energy surface. Gibbs energies were evaluated at 30°C, which was used in the experiments, using a quasi-RRHO treatment of vibrational entropies.¹⁵ Vibrational entropies of frequencies below 100 cm⁻¹ were obtained according to a free rotor description, using a smooth damping function to interpolate between the two limiting descriptions.¹⁶ The free energies were further corrected using standard concentration of 1 mol/L for gas-phase-to-solvent correction.

For species involving open-shell characteristics, including radical ions in the redox potential calculations and closed-shell diradicaloid species in diradical coupling, we performed above-mentioned DFT methodologies using the unrestricted formalism of Kohn-Sham theory (UKS). Wavefunction stability in these cases were checked using Gaussian keyword “*stable=opt, guess=mix*”. The eigenvalues of the spin operator S^2 after annihilation of spin contamination were checked to ensure that they comply with the expected value of $S(S+I) = 0.75$ for a doublet wavefunction and $S(S+I) = 0$ for closed shell diradical, indicating that spin contamination is not a problem for the present methodology.

Non-covalent interactions (NCIs) were analyzed using NCIPILOT¹⁷ calculations. The *.wfn* files for NCIPILOT were generated at M06-2X/def2-SVP level of theory. NCI indices calculated with NCIPILOT were visualized at a gradient isosurface value of $s = 0.5$ au. These are colored according to the sign of the second eigenvalue (λ_2) of the Laplacian of the density ($\nabla^2\rho$) over the range of -0.1 (blue = attractive) to +0.1 (red = repulsive). Molecular orbitals are visualized using an isosurface value of 0.05 au throughout. All molecular structures and molecular orbitals were visualized using *PyMOL* software.¹⁸

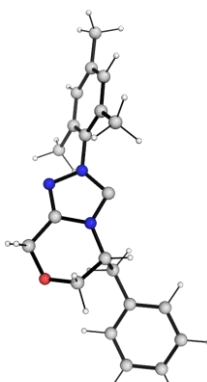
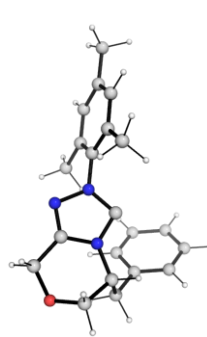
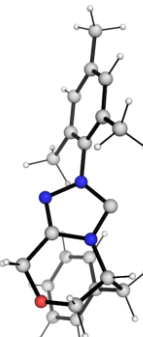
1. Conformational considerations

We determined the most stable form of the NHC carbene and the covalently formed Breslow intermediate (enol azolium) by performing a thorough conformational sampling. We generated a set of rotamers by performing 5-fold rotations about the key dihedral angles (in red) as shown in the Chemdraw structure in Scheme S-1.



Scheme S-1. Chemdraw structures of NHC carbene and azolium-enolate intermediate for which conformational samplings were performed by rotamer generation along bonds indicated by red arrows. For the latter structure, the rotation along the C=C bond (indicated by asterisk) is to account for all possible conformers that can arise from the initial NHC attack on either face of the aldehyde.

A total of 25 rotamers for NHC and 625 rotamers for the Breslow intermediate were generated and then cleaned by removing those species having overlapping atoms within 0.5 Å radius. These were performed using the script in the study of conformational effects on physical-organic descriptors by Brethomé *et al.*¹⁹ The resulting rotamers were subject to geometry optimization using GFN2-xTB method. The xTB-optimized structures were then clustered using the clustering_traj.py²⁰ with an RMSD cutoff of 1.0 Å (excluding H atoms) to give distinct conformers that were further optimized at DFT M06-2X/def2-SVP level. The Gibbs energies of the resulting structures were corrected using single-point M06-2x/def2-TZVP in toluene solvent using SMD implicit solvation model. Their DFT-optimized structures and relative solvent-corrected Gibbs energies are given in Figure S-12.

NHC carbene conformers		
NHC-c1	NHC-c2	NHC-c3
$\Delta G = 0.0$	2.6	2.6
		

NHC-c4	NHC-c5	NHC-c6
$\Delta G = 3.3$	3.6	4.5
Breslow intermediate I conformers		
I-c1	I-c2	I-c3
$\Delta G = 3.1$	4.6	5.0
I-c4	I-c5	I-c6
$\Delta G = 6.4$	6.7	8.0
I-c7	I-c8	I-c9
$\Delta G = 8.8$	9.0	9.1

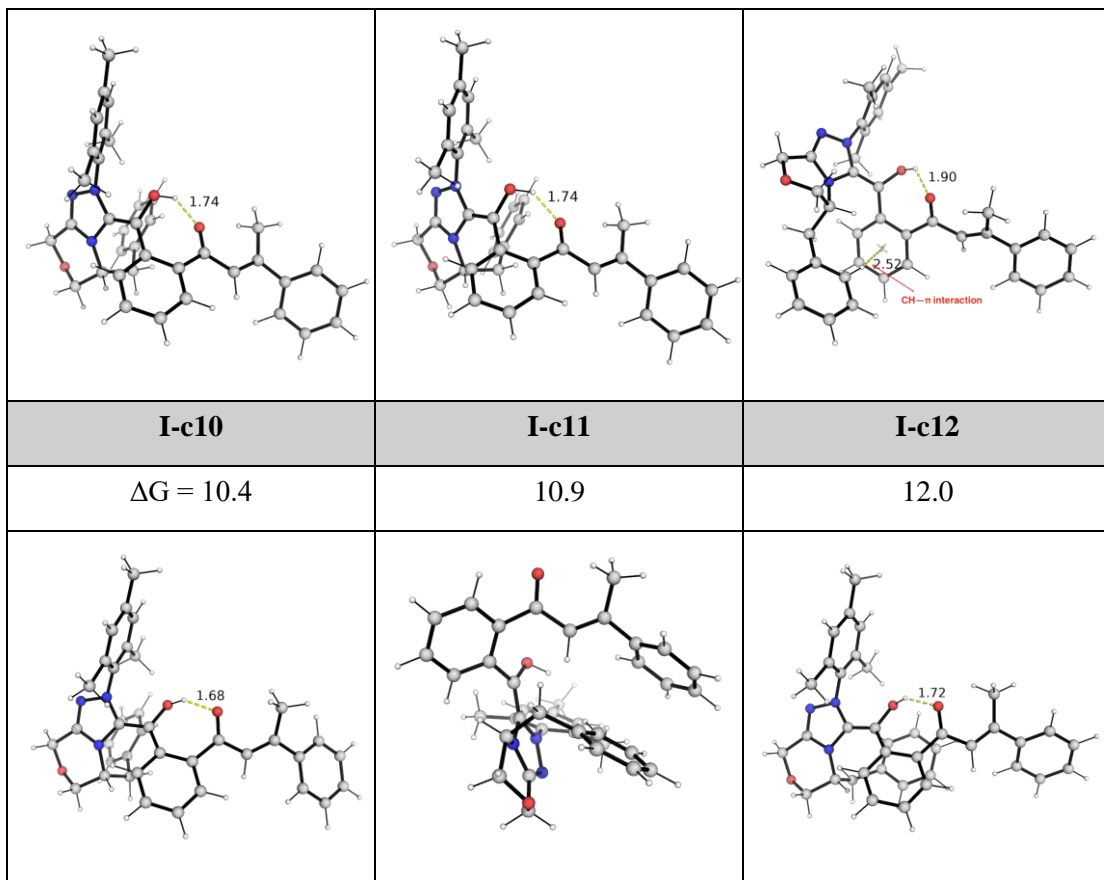


Figure S-12. DFT optimized conformer structures of NHC catalyst and Breslow intermediate **I**. Relative Gibbs energies are calculated at SMD (toluene)-M06-2X/def2-TZVP//M06-2X/def2-SVP level of theory and taken relative to the lowest energy conformer of the NHC carbene. For Breslow intermediate, the energies are taken relative to the sum of the lowest energy conformer of the NHC carbene and the enone aryl aldehyde substrate **1a**. Their units are given in kcal mol⁻¹.

2. Stereo-determining transition state (TS) structures

We compare the factors influencing the energetic differences between the stereo-determining TSs, **Re-TS5** and **Si-TS5**. Figure S-13 shows their DFT-optimized structures, frontier molecular orbitals (FMOs) and non-covalent interaction (NCI) plots. The HOMO and LUMO structures for both TSs are similar, indicating similar electronic influences. **Re-TS5** has a lower activation barrier due to the favorable NCIs between the C-H bonds on the aryl ring of the NHC and the O-atoms of Ts⁻ anion, which stabilize the transition state. These CH--O NCIs are absent in **Si-TS5**.

	Re-TS5	Si-TS5
ΔG^\ddagger	12.6 kcal mol ⁻¹	14.3 kcal mol ⁻¹

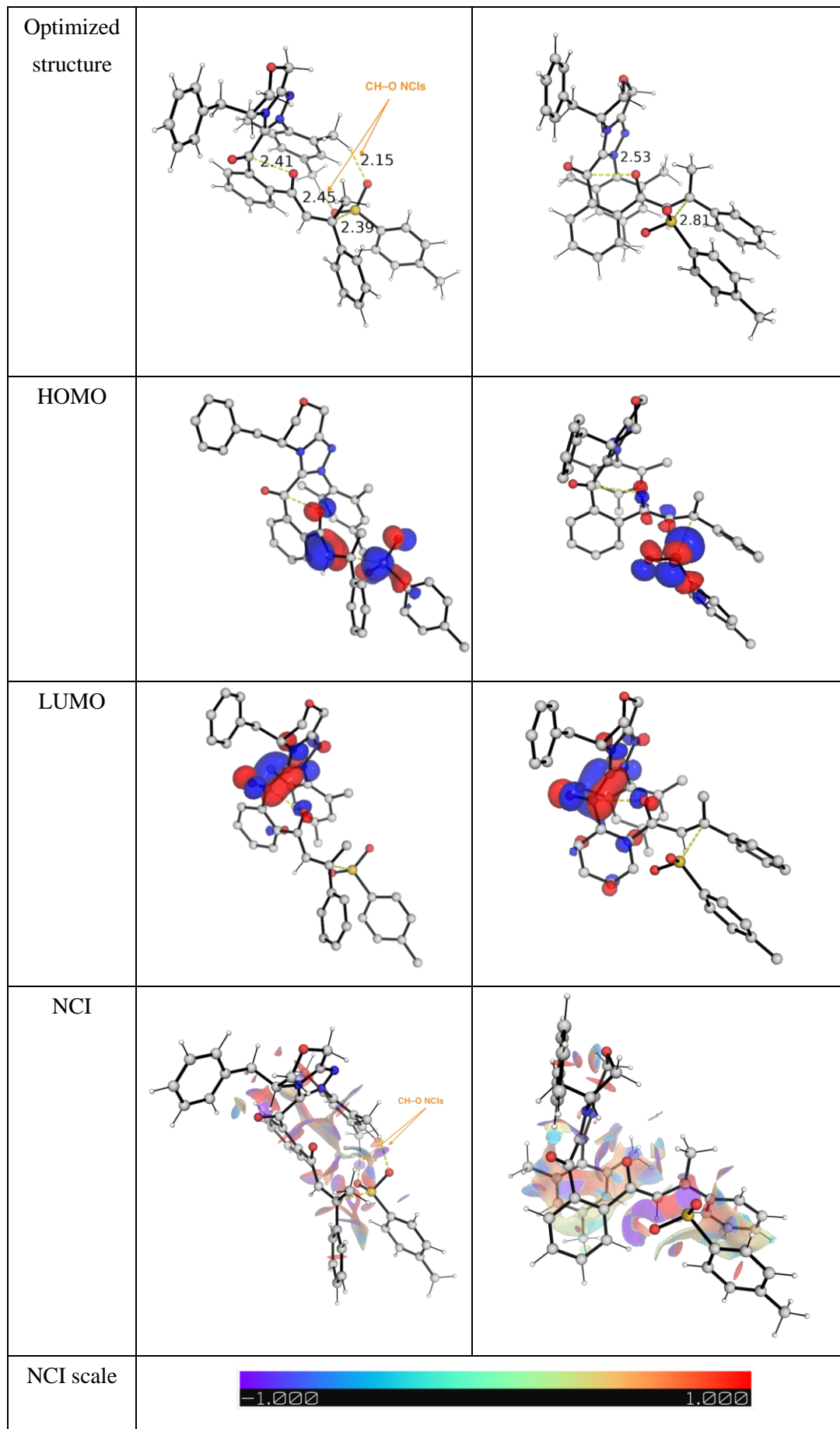
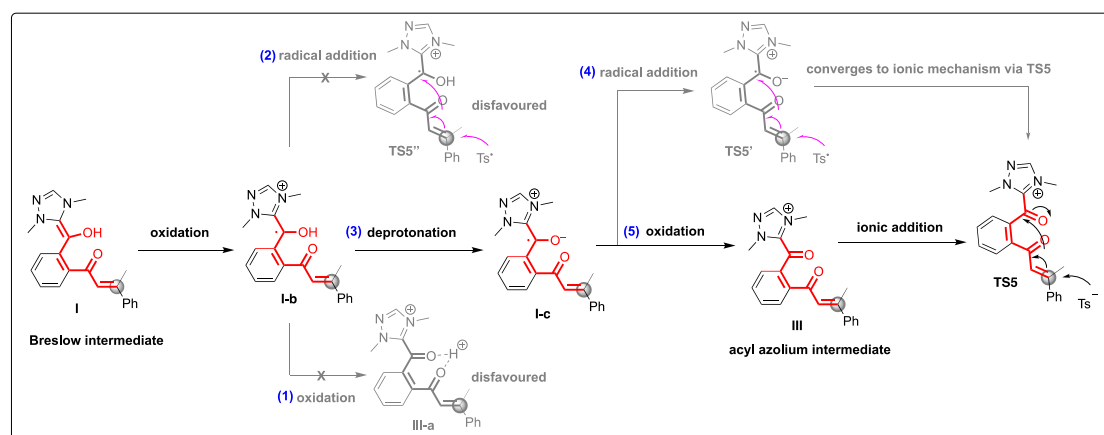


Figure S-13. Optimized TS structures, their FMOs (isosurface value = 0.05 au) and NCI plots for the stereo-determining transition states (**TS5s**) for the addition of Ts^- anion to acyl azolium intermediate **III** *via* ionic mechanism. Key bond distances are given in Å. Activation barriers are given in kcal mol⁻¹.

3. Redox chemistry/Radical mechanism

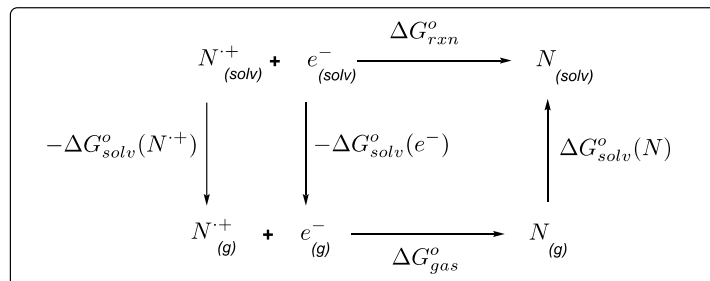
The alternative mechanism of the reaction *via* one-electron redox processes were investigated computationally. We considered the reaction pathways outlined in Scheme S-2. The Breslow intermediate **I** could undergo a single-electron oxidation to give **I-b**, which could undergo 3 possibilities: 1) further, second single-electron oxidation to give **III-a**; 2) direct radical addition with tosyl radical Ts^\bullet ; 3) deprotonation to give **I-c** followed by either (4) radical addition with Ts^\bullet or (5) further oxidation and subsequent addition by Ts^- *via* ionic mechanism. We carried out computational redox potential calculations to determine the feasibility of the catalytic transformation *via* redox chemistry.



Scheme S-2. Possible redox chemistry reaction pathways for Breslow intermediate **I**.

3.1 Computational redox potential calculations

To compute the electrochemical redox potentials of the species involved in the reaction, we applied the thermodynamic cycle as shown in Scheme S-3.^{21,22} We aim to calculate the Gibbs energy of reaction in the solvent phase, ΔG_{rxn}^o , using the structures we have optimized in the gas phase at M06-2X/def2-SVP level of theory. M06-2X functional has been shown to give good agreement between experimental and computed redox potentials.^{23,24}



Scheme S-3. Computational redox potential for the reduction of a radical cation to its neutral form *via* thermodynamic cycle.

In our calculations, the gas phase energy change, ΔG_{gas}^o , is further refined by calculating the single point energy in gas phase at a M06-2X/def2-TZVP for improved accuracy.²¹ The reduction potentials calculated here are *adiabatic* reduction potentials (ARP) since the energy is taken from each optimised species, i.e.,

$$\text{ARP} = E(\text{optimised neutral}) - E(\text{optimised radical cation}). \quad (1)$$

We then have

$$\Delta G_{rxn}^o = -\Delta G_{solv}^o(N^{•+}) - \Delta G_{solv}^o(e^-) + \Delta G_{gas}^o(N^{•+}) + \Delta G_{solv}^o(N) \quad (2)$$

The reduction potential of the reaction is then given by

$$E_{cell} = -\frac{\Delta G_{rxn}^o}{nF} - E_{SHE} \quad (3)$$

where the standard hydrogen electrode (SHE) redox value is taken as 4.28V in SMD model.^{21,22,25} We need not consider the free energy of solvation of the electron as their contribution cancels out when we consider the full reaction against experimentally measured values.²² The computed redox potentials for the chemical reactions are given in Table S-6.

Reaction	Oxidation	E_{ox}^o / V
O1		-0.193
O2		-1.958

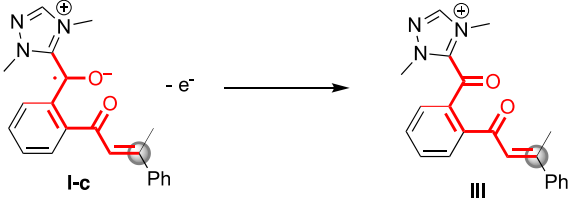
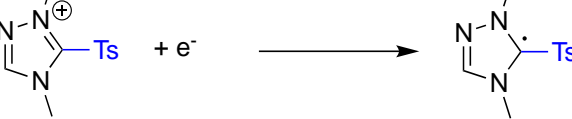
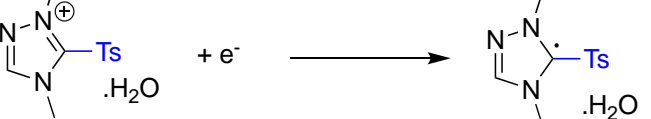
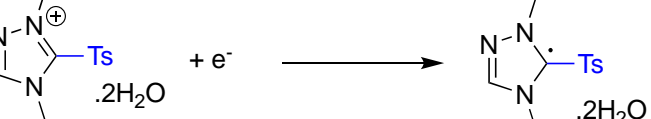
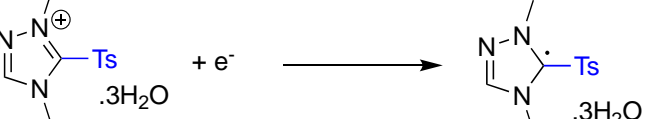
O3		+0.171
Reaction	Reduction	E_{red}^o / V
R1	$TsOH + e^- \longrightarrow [TsOH]^{..-}$	-3.039
R2	$TsOH \cdot H_2O + e^- \longrightarrow [TsOH \cdot H_2O]^{..-}$	-3.139
R3	$TsOH \cdot 3H_2O + e^- \longrightarrow [TsOH \cdot 3H_2O]^{..-}$	-2.793
R4	$TsCl + e^- \longrightarrow [TsCl]^{..-}$	-1.533
R5	$Ts^{\cdot} + e^- \longrightarrow Ts^-$	-0.583
R6		-0.418
R7		-0.392
R8		-0.285
R9		-0.642
R10		-1.206

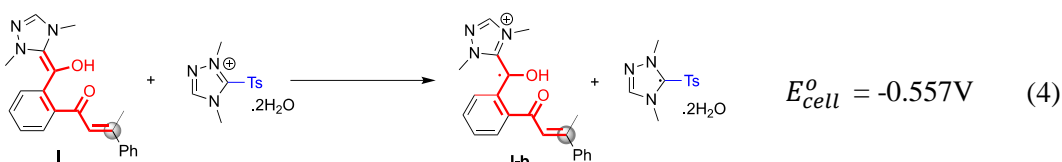
Table S-6. Computed redox potentials for the possible chemical transformations.

First redox event

From the table, the most likely oxidizing agent to oxidize Breslow intermediate **I** to intermediate **I-b** (reaction **O1**, $E_{ox}^o = -0.139$ V) is the $[\text{NHC-Ts}]^+$ complex that was detected experimentally. The reduction of $[\text{NHC-Ts}]^+$ complex to $[\text{NHC-Ts}]^\cdot$ can be enhanced in the presence of water, the reduction potential becomes less negative from -0.418 V without water (reaction **R6**) to -0.285 V with two water molecules (reaction **R8**).

The use of other species as oxidizing agents, such as TsOH (reactions **R1**, **R2** and **R3**) or TsCl (reaction **R4**) have more negative and unfavorable redox potentials than the reduction of $[\text{NHC-Ts}.2\text{H}_2\text{O}]^+$ complex.

The overall potential first redox transformation is thus:

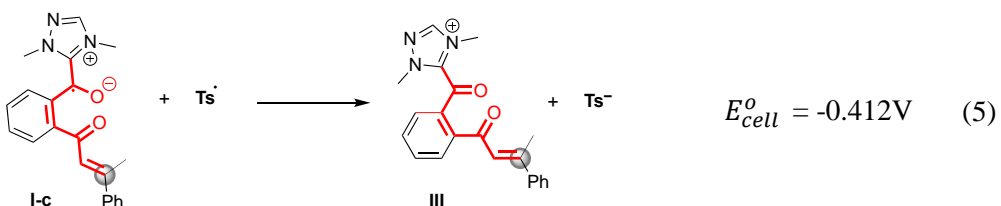


with an overall E_{cell}^o of -0.557 V, this implies an uphill electron transfer barrier of about 12.8 kcal mol^{-1} .

Second redox event

The reduced $[\text{NHC-Ts}.2\text{H}_2\text{O}]^\cdot$ complex can dissociate to give Ts^\cdot radical, which can be reduced to Ts^- anion with $E_{red}^o = -0.583$ V (reaction **R5**, Table S-6).

The direct oxidation (loss of an electron) of radical cationic intermediate **I-b** to **III-a** has a large unfavorable redox potential of $E_{ox}^o = -1.958$ V (reaction **O2**, Table S-6). Thus, this rules out the pathway (1) in Scheme S-2. In the basic reaction condition, intermediate **I-b** can easily lose a proton to give intermediate **I-c** (pathway (2) in Scheme S-2), which can be oxidized to close-shell intermediate **III** much more easily, with $E_{ox}^o = +0.171$ V (reaction **O3**, Table S-6). This gives overall second redox transformation as



with an overall E_{cell}^o of -0.412 V. This implies an uphill electron transfer barrier of about 9.5 kcal mol^{-1} .

3.2 Energy profile for redox chemistry

From the computational redox potential calculations, the reaction proceeding *via* redox events will have the Gibbs energy profile as shown in Figure S-14. The first redox event between $[\text{NHC-Ts}]^+.2\text{H}_2\text{O}$

complex and Breslow intermediate **I** will have an activation barrier of at least 11.0 kcal mol⁻¹ (with a small barrier for electron transfer²⁴). However, in the presence of both carbonate and TsCl, intermediate **I** will undergo a carbonate-assisted deprotonation of the OH group, forming an alkoxy group that gets tosylated with TsCl (as described in the main text). As such, we anticipate that the Breslow intermediate **I** will undergo tosylation readily with TsCl before it can get oxidized to intermediate **I-b** (Figure 2 in the main text).

For completeness, we investigated the mechanism for the radical coupling between the radical cationic intermediate **I-b** and Ts[·] radical (pathway (2) in Scheme S-2). From the reactant complex between **I-b** and Ts[·] radical (**INT1''**), the barrier for the radical addition to the (*Re*)-face of intermediate **I-b** (**Re-TS5''**) is 8.7 kcal mol⁻¹ and the barrier for the radical addition to the (*Si*)-face of intermediate **I-b** (**Si-TS5''**) is 10.3 kcal mol⁻¹. Due to the reversibility of the formation of intermediate **I-b** and Ts[·] radical, the energetic span for this reaction pathway is at least 18.1 kcal mol⁻¹ (from the Breslow intermediate **I**). This is much less favorable than the main reaction pathway discussed in the main text.

Alternatively, species **I-b** can lose a proton to give species **I-c** (pathway (3), Scheme S-2), which can undergo redox event with Ts[·] radical (pathway (5), Scheme S-2) to give thermodynamically uphill acyl azonium intermediate **III** and Ts⁻ anion. The acyl azonium intermediate formed then undergoes ionic mechanism as discussed in the main text (Figure 2 in the main text).

The alternative mechanism from species **I-c** is its direct reaction with Ts[·] radical (pathway (4), Scheme S-2). However, the TS search using unrestricted closed-shell diradical formalism (on the singlet PES) converged to the ionic pathway in which Ts⁻ anion adds to the acyl azonium intermediate **III** (main mechanism in the main text). The unrestricted openshell diradical TS search (on the triplet PES) between species **I-c** and Ts[·] radical yielded ³**Si-TS5'** with a barrier of 17.4 kcal mol⁻¹ and ³**Re-TS5'** with a barrier of 20.0 kcal mol⁻¹ (Figure S-14) and these are less kinetically favorable.

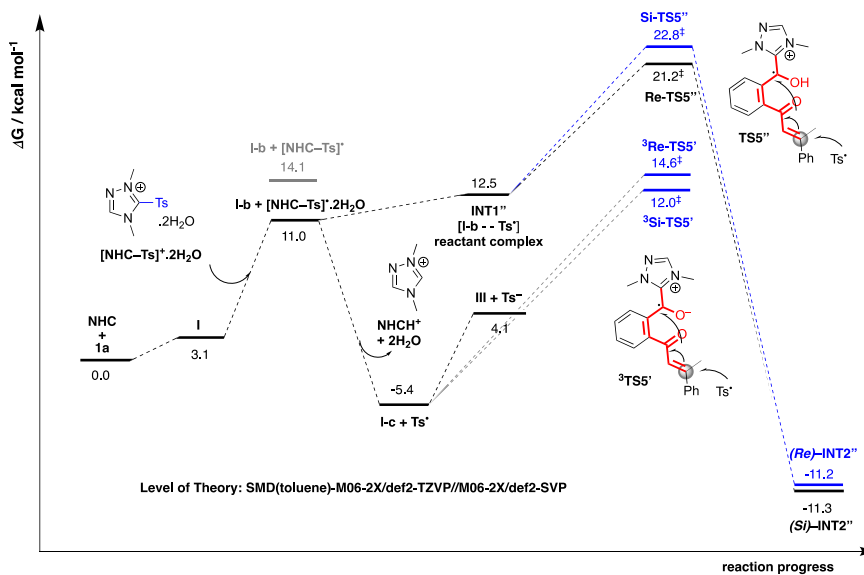


Figure S-14. Gibbs free energy profile calculated at SMD(toluene)-M06-2X/def2-TZVP//M06-2X/def2-SVP level of theory for redox chemistry.

4. Ionic mechanism

4.1 Addition of NHC to enone aryl aldehyde substrate

The transition state for the addition of NHC to either the (*Re*)- or the (*Si*)-face of aldehyde moiety of the substrate was found computationally. The DFT optimized structures are given in Figure S-15.

	<i>Re</i> -TS1	<i>Si</i> -TS1
ΔG^\ddagger	20.6 kcal mol ⁻¹	25.0 kcal mol ⁻¹
Optimized structure		

Figure S-15. DFT optimized structures for the addition of NHC to aldehyde substrate.

4.2 Formation of Breslow intermediate I

Due to the highly (*Re*)-face selective addition of NHC, for subsequent transformations, we follow the mechanistic pathways from the reaction product resulting from (*Re*)-face addition. In accordance with previous reports,^{26,27} a protonated base assists in the formation of the Breslow intermediate. Herein, we used hydrogen carbonate in the transition state search and the DFT optimized structures and their associated energy barriers are shown in Figure S-16.

S-TS2	S-TS2-c2	S-TS2-c3
$\Delta G^\ddagger = 22.4$ kcal mol ⁻¹	37.0 kcal mol ⁻¹	42.1 kcal mol ⁻¹

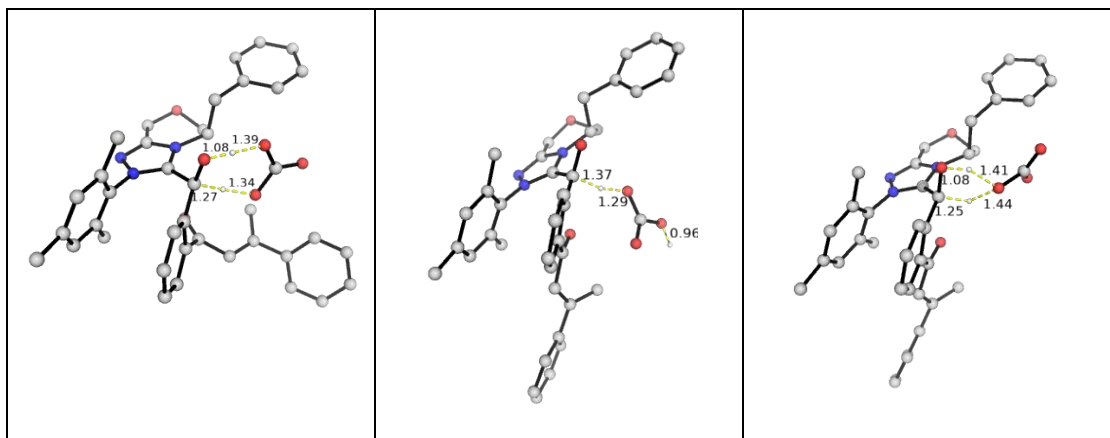


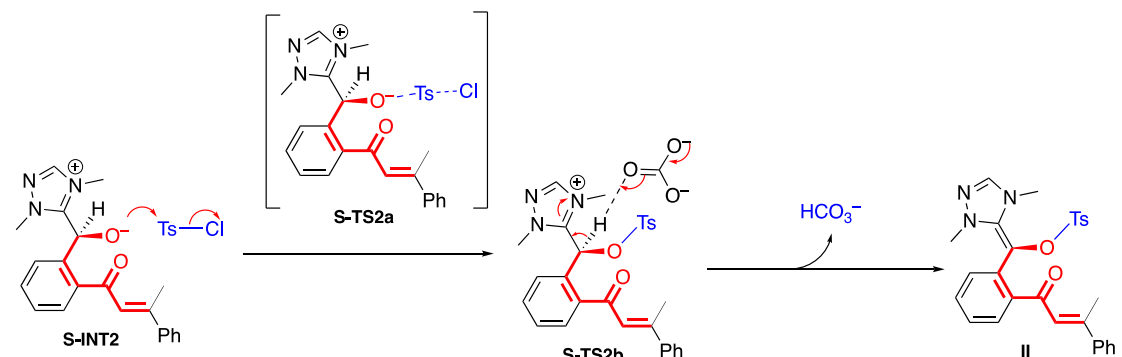
Figure S-16. DFT optimized structures for the hydrogen carbonate assisted formation of Breslow intermediate from NHC addition product.

We see that the concerted deprotonation and reprotonation by hydrogen carbonate *via* a highly ordered 7-membered ring transition state **S-TS2** has the lowest activation barrier of 22.4 kcal mol⁻¹, whereas the direct deprotonation *via* **S-TS2-c2** and the deprotonation by the same carboxyl oxygen *via* **S-TS2-c3** with a 5-membered ring TS both have much higher barriers at 37.0 and 42.1 kcal mol⁻¹ respectively.

4.3 Alternative mechanism for the direct tosylation of NHC-adduct oxyanion without the formation of Breslow intermediate I

We computationally investigated the mechanistic alternative for the direct formation of intermediate **II** by direct tosylation of NHC-adduct, without the formation of Breslow intermediate **I** (Scheme S-4).

We successfully located and verified the transition state for the direct tosylation at the oxyanion oxygen atom (**S-TS2a**). The solvent-corrected Gibbs energy profile is shown in Figure S-17.



Scheme S-4. Alternative mechanism for the formation of intermediate **II** *via* direct tosylation of NHC adduct.

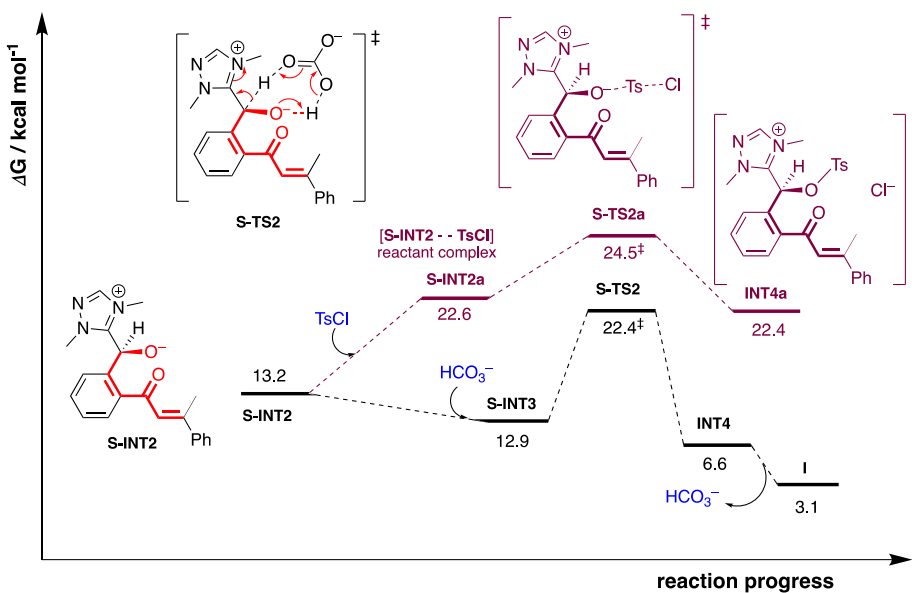


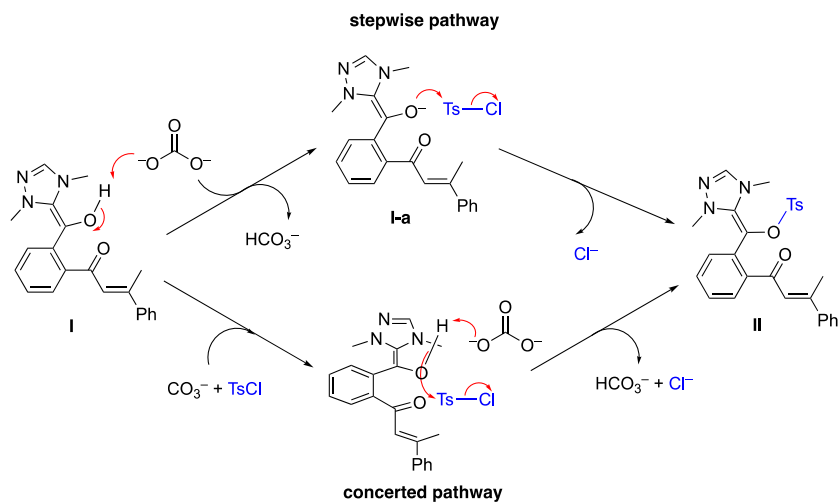
Figure S-17. Gibbs free energy profile for the direct tosylation of oxyanion from NHC adduct (**S-TS2a**) and its comparison to the transition state for the base-assisted Breslow intermediate formation (**S-TS2**).

We see that the direct tosylation of the oxyanion oxygen (**S-TS2a**) has a higher barrier than the base-assisted formation of Breslow intermediate **I** via **S-TS2**. This barrier difference $\Delta\Delta G^\ddagger$ of 2.1 kcal mol⁻¹ translates to about 33:1 kinetic favorability for **S-TS2** over **S-TS2a**, using simple transition state theory at the reaction temperature. Similar mechanism to what we proposed in our manuscript for base-assisted Breslow intermediate formation in carbene organocatalysis have been reported by Donghui Wei, Yu Lan and co-workers.^{26,27}

In addition and more importantly, intermediates **I** and **I-a** have been successfully detected experimentally, for the first time, using high-resolution mass spectroscopy (HRMS), under positive ion and negative ion mode, respectively. These intermediates would not have been formed via this mechanistic alternative of direct tosylation of NHC-adduct. This provides unequivocal evidence for the formation of the Breslow intermediate and is in direct support of the mechanism we proposed in the main text.

4.4 Conversion of Breslow intermediate **I** to intermediate **II**

We explore both the concerted pathway and the stepwise pathway for the conversion of intermediate **I** to intermediate **II** as shown in Scheme S-5.



Scheme S-5. Stepwise vs concerted mechanistic pathway for the conversion of intermediate **I** to intermediate **II**.

In the stepwise pathway, carbonate anion deprotonates the alcohol group of the Breslow intermediate **I**, giving the alkoxide **I-a**, which subsequently undergoes tosylation with tosyl chloride to give tosylated intermediate **II**. We found that the deprotonation of intermediate **I** by carbonate anion is barrierless, as can be seen from the geometry optimization shown in Figure S-18. From an initial guess where the carbonate is placed far away from the NHC adduct (O(carbonate)-H(hydroxyl) distance of 3.5 Å, structure **1**, Figure S-18), the geometry optimization gave the deprotonated product (structure **81**, Figure S-18) directly, indicating that no barriers exist for the deprotonation of hydroxyl group of NHC adduct by carbonate anion.

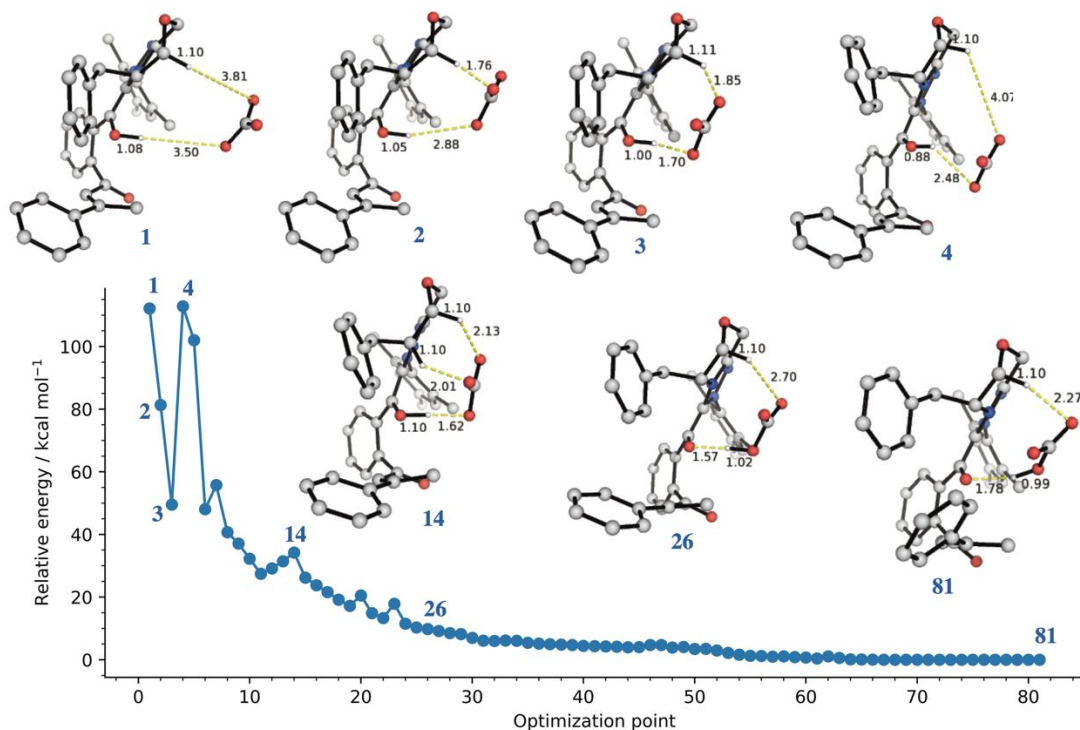
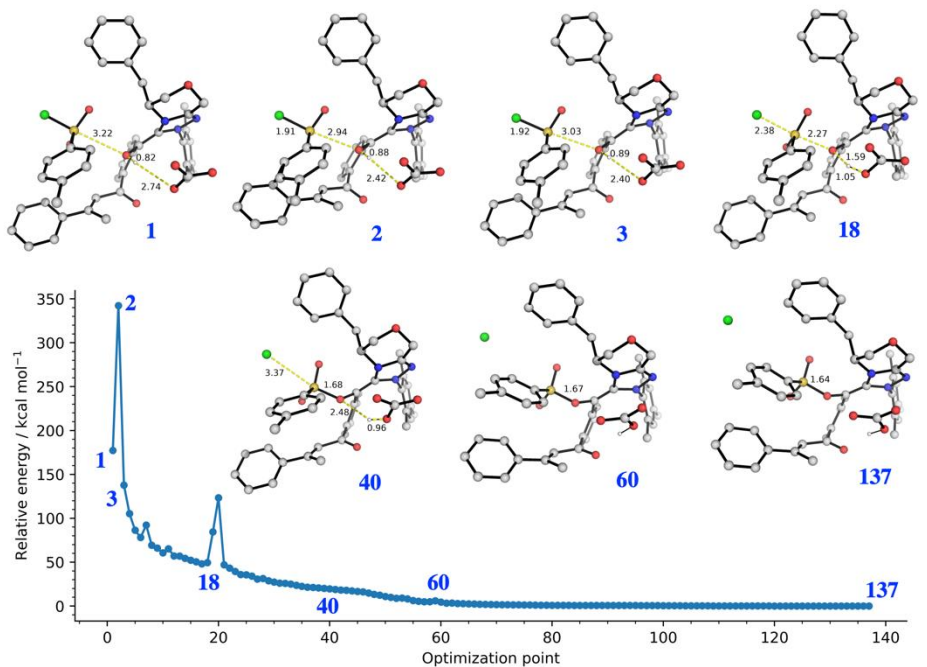


Figure S-18. Geometry optimization of carbonate anion and the Breslow intermediate **I** starting from guess structure **1**. Shown are selected structures along the optimization. Structure **81** is the DFT optimized structure. Selected bond distances are given in Å.

In the concerted pathway, carbonate anion deprotonates the alcohol group of the Breslow intermediate while the deprotonated alkoxide attacks the sulfur center of TsCl in an S_N2 mechanism as chloride leaves, much similar to a general base catalysis. The direct TS search did not yield any transition structure. The optimization of initial guess structure **1** in Figure S-19a) gives the tosylated intermediate **II** directly. However, with a larger O (Breslow intermediate)-S distance as in guess structure **1'** in Figure S-19b, the direct optimization did not yield the tosylated intermediate **II** directly, although spontaneous deprotonation of the alcohol group by carbonate is still observed. This suggests that the conversion of intermediate **I** to intermediate **II** is likely stepwise, with firstly a barrierless deprotonation of OH group of **I** followed by subsequent tosylation of the alkoxide with TsCl.

a) Optimization from guess structure 1



b) Optimization from guess structure 1'

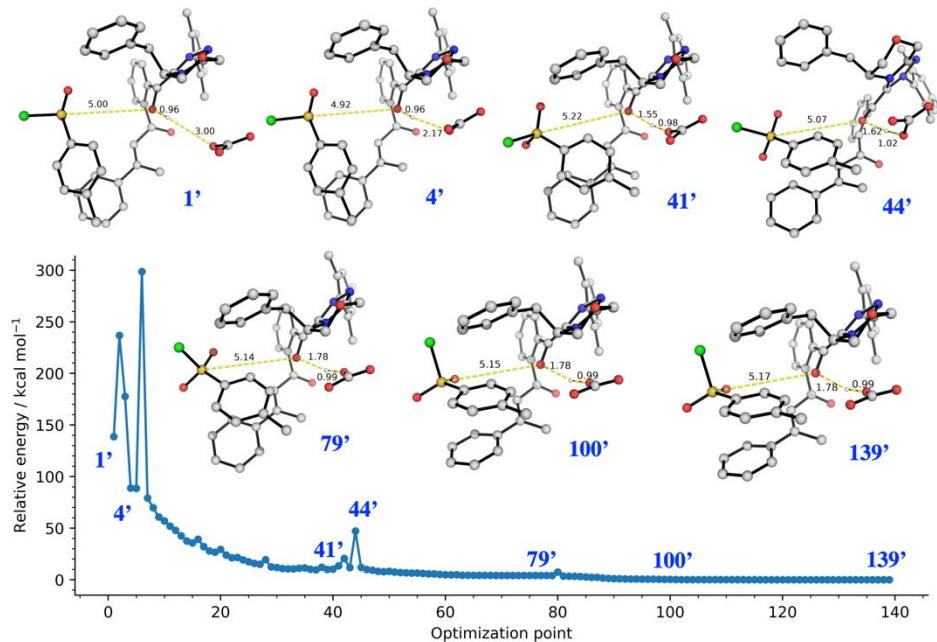
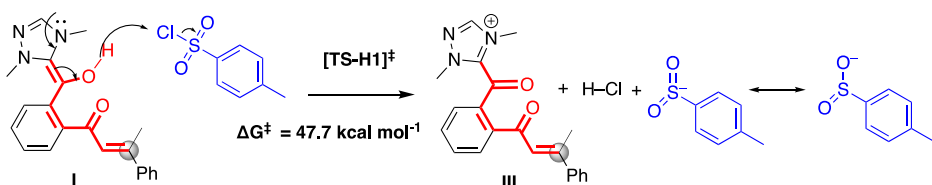


Figure S-19. Geometry optimizations of concerted carbonate anion-assisted deprotonation and tosylation of the Breslow intermediate **I** starting from guess structure **1** (a; top panel) and guess structure **1'** (b; bottom panel). Shown are selected structures along the optimization. Structures **137** and **139** are the DFT optimized structures. Selected bond distances are given in Å.

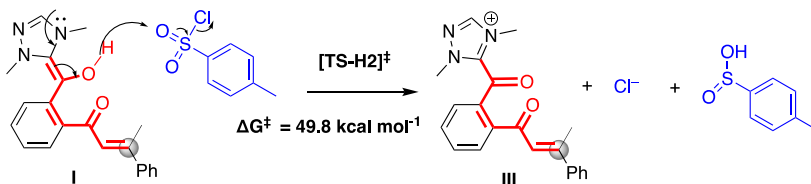
4.5 Alternative mechanism for the generation of Ts^- anion *via* hydride transfer

The alternative mechanism for the generation of tosyl anion Ts^- *via* hydride transfer from the Breslow intermediate **I** is also considered (Scheme S-6). These TSs (hydride transfer to either the Cl-atom or the O-atom of TsCl), shown in Figure S-20, have very high barriers ($47.7 \text{ kcal mol}^{-1}$ and $49.8 \text{ kcal mol}^{-1}$, respectively) and are thus highly disfavored.

a) hydride transfer to Cl-atom of TsCl



b) hydride transfer to O-atom of TsCl



Scheme S-6. Possible reaction pathways for the generation of tosyl anion *via* hydride transfer.

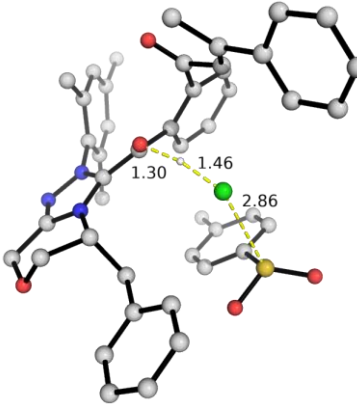
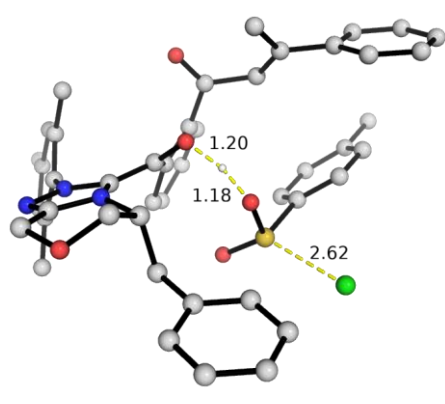
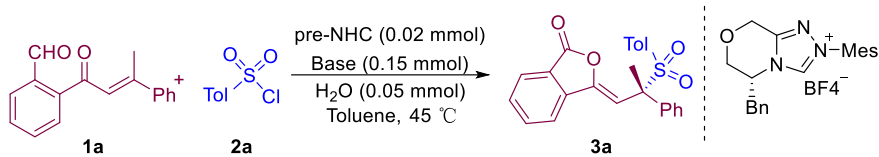
TS-H1	TS-H2
$\Delta G^{\ddagger} = 47.7 \text{ kcal mol}^{-1}$	$49.8 \text{ kcal mol}^{-1}$
	

Figure S-20. DFT optimized structures for the generation of Ts^- anion *via* hydride transfer.

4.6. The roles of bases in key steps were further studies *via* experiments and DFT calculation

With an optimal reaction condition in hand, we tested the effect of bases other than carbonate due to the central role in the mechanism as **INT5**. We observe that the identity of the base does not drastically affect the ee values. This suggests that the base does not participate in the stereo-determining step and is consistent with our computed mechanism showing that the stereo-determining step only involves the addition of Ts^- anion to the acyl azolium intermediate, without any base participation.



Bases	Yield (%) ^a	Ee (%) ^b
DBU	21	98
Et ₃ N	15	98
DABCO	nr	nr
K ₃ PO ₄	34	94
KOAc	< 10	98
t-BuOK	22	90

Unless otherwise specified, the reactions were carried out using **1a** (0.1 mmol), **2a** (0.12 mmol), pre-NHC (0.02 mmol), base (0.15 mmol), Toluene (2.0 mL) and H₂O (0.05 mmol) at 45 °C for 4 h. ^aIsolated yield of **3a**. ^bThe ee values were determined via HPLC on chiral stationary phase. DBU = 1,8-Diazabicyclo[5.4.0]undec-7-ene. Et₃N = Triethylamine. DABCO = 1,4-Diazabicyclo[2.2.2]octane; triethylenediamine. KOAc = Potassium Acetate. t-BuOK = Potassium tert-butoxide. nr = no reaction.

The roles of the base in our reaction are three folds: 1) to deprotonate the NHC pre-catalyst to form the NHC singlet carbene active catalyst; 2) to participate in the base- (or its conjugate acid-) assisted formation of Breslow intermediate from NHC-aldehyde adduct (**S-TS2** in our reaction); and 3) to participate in the deprotonation of Breslow intermediate to form its enolate equivalent which subsequently undergoes tosylation to give intermediate **II**.

Preliminary DFT studies were carried out to investigate how the base may affect the yield of the present transformation. For bases DBU, Et₃N and DABCO, thermodynamics calculations showed that the complex formation between the base and the Breslow intermediate **I** is uphill by more than 10 kcal mol⁻¹ (DBU 11.6 kcal mol⁻¹, Et₃N 11.4 kcal mol⁻¹ and DABCO 10.6 kcal mol⁻¹). In addition, the geometry optimization using deprotonated product (**I-a** and HNR₃⁺) as the initial guess structure (with O-H bond distance of 2 Å and H-N distance of 1 Å, Figure S-21a below) yields the Breslow intermediate **I** and the neutral amine base. This suggests that the deprotonation of Breslow intermediate by these nitrogenous amines is highly reversible, with equilibrium lying to the Breslow intermediate **I** (Figure S-21b below). Thus, no barrierless deprotonation at this step by these bases are possible, explaining the poor yields observed experimentally for these bases.

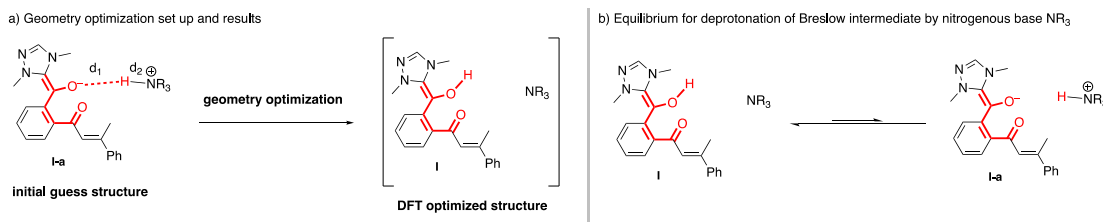


Figure S-21. DFT for the deprotonation of Breslow intermediate

For strong base tBuOK, although the barrierless deprotonation of Breslow intermediate **I** is observed computationally (as expected, as t-BuO⁻ is a much stronger base than CO₃²⁻), however, its conjugate acid t-BuOH is very weak. The participation of tBuOH in the Breslow intermediate formation (as compared

to HCO_3^-) is highly disfavored. The computed Gibbs energy for this process is shown in the Figure below:

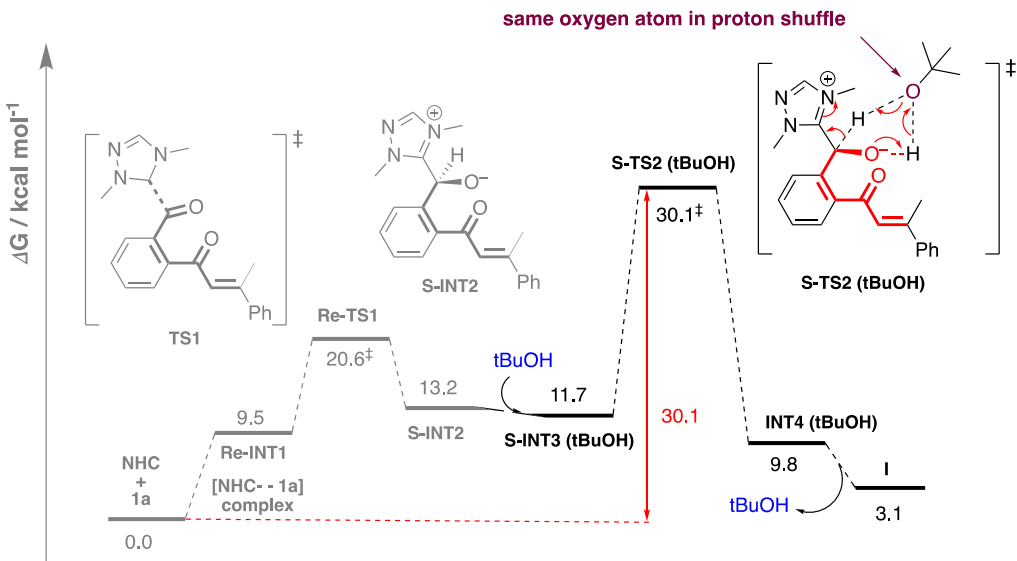


Figure S-22. Gibbs energy profile for tBuOK-assisted to generate Breslow intermediate.

This process is highly disfavored for two reasons: 1) this weak conjugate acid makes the breaking of O-H bond difficult, thus making it a poor proton shuffler, and 2) the involvement of the same oxygen atom in the cyclic transition state (**S-TS2(tBuOH)**) is less favored than if two *different* O atoms are involved, as in the case of hydrogen carbonate in **S-TS2**. This effect is similarly observed when only one oxygen atom of hydrogen carbonate was used (**S-TS2-c3**, Figure S-23), as demonstrated in Figure S-23.

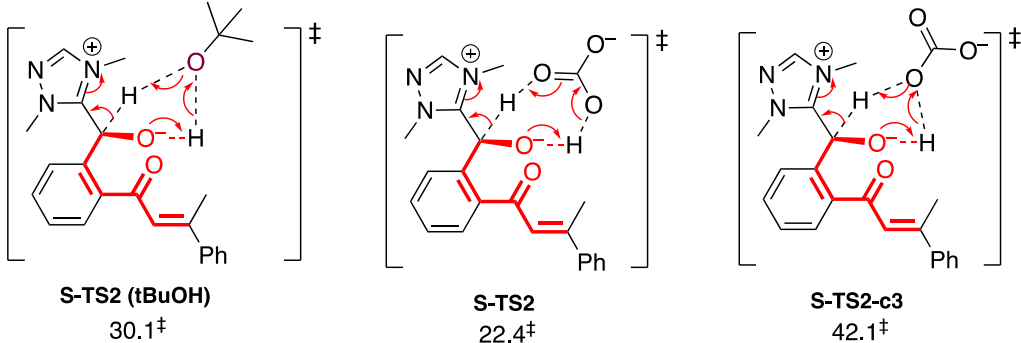


Figure S-23. The barrier of the proton transfer to form Breslow intermediate with different bases

For acetate and phosphate bases, preliminary DFT calculations suggested that the poor yields may not be due to their poor participation in the deprotonation base-assisted formation of Breslow intermediate (role 2) and in the deprotonation of Breslow intermediate to form its enolate equivalent (role 3). They may be less efficient than carbonate in generating the active NHC from the triazolium pre-catalyst (role 1). Additional detailed investigations on the roles of bases affecting various steps in this reaction are currently underway in our laboratory.

5. Optimized structures and absolute energies, zero-point energies

Geometries of all optimized structures (in .xyz format with their associated energy in Hartrees) are included in a separate folder named *final_xyz_structures*. All these data have been uploaded to zenodo.org (DOI: 10.5281/zenodo.5889602).

Absolute values (in Hartrees) for SCF energy, zero-point vibrational energy (ZPE), enthalpy and quasi-harmonic Gibbs free energy (at 303.15K) for M06-2X/def2-SVP optimized structures are given below. Single point corrections in SMD (toluene) using M06-2X/def2-TZVP functional are also included.

Structure	E/au	ZPE/a u	H/au	T.S/au	qh-G/au	SP M06- 2X/def2TZV P
1a	-805.731571	0.264746	-805.448951	0.061849	-805.50766	-806.6467343
TsCl	-1278.93909	0.130338	-1278.796842	0.048432	-1278.84314	-1279.780193
TsCl_ra	-1278.993608	0.127551	-1278.853314	0.05113	-1278.902266	-1279.87654
nhc_Ts	-1871.02858	0.537212	-1870.457171	0.099698	-1870.548503	-1872.912768
nhc_Ts_rad						
ical	-1871.203581	0.534835	-1870.634459	0.099121	-1870.726137	-1873.052055
nhc_Ts_ra	-1871.275795	0.532019	-1870.708819	0.101826	-1870.801709	-1873.161667
nhc_Ts_H2						
O	-1947.368323	0.561012	-1946.769325	0.108232	-1946.868262	-1949.347453
nhc_Ts_H2						
O_radical	-1947.544244	0.559813	-1946.946995	0.105758	-1947.044595	-1949.489907
nhc_Ts_2H						
2O	-2023.710935	0.586096	-2023.083687	0.115341	-2023.188743	-2025.78802
nhc_Ts_2H						
2O_radical	-2023.890783	0.58595	-2023.264598	0.113372	-2023.367889	-2025.935547
nhc_Ts_3H						
2O	-2100.083072	0.613317	-2099.426778	0.116807	-2099.534141	-2102.246185
nhc_Ts_3H						
2O_radical	-2100.248116	0.612463	-2099.593572	0.11557	-2099.699872	-2102.37919
Cl_anion	-460.067961	0	-460.065561	0.014629	-460.08019	-460.3216879
TsOH	-894.635635	0.14394	-894.479849	0.047287	-894.525367	-895.4191102
TsOH_ra	-894.634368	0.139603	-894.482428	0.048457	-894.529396	-895.4594056
Ts Radical	-818.86639	0.127222	-818.728557	0.044992	-818.7722	-819.5386707
Ts_anion	-818.947812	0.125716	-818.811366	0.044683	-818.854594	-819.6735503
TsO_anion	-894.105011	0.131823	-893.9619	0.047101	-894.006785	-894.9462024

TsOH_H2

O	-970.989144	0.169728	-970.805205	0.052282	-970.855403	-971.8671387
----------	-------------	----------	-------------	----------	-------------	--------------

TsOH_H2

O_ra	-970.986143	0.165612	-970.80555	0.055096	-970.858114	-971.9033566
-------------	-------------	----------	------------	----------	-------------	--------------

OH_anion	-75.63046	0.008034	-75.619066	0.016888	-75.635954	-75.84411311
-----------------	-----------	----------	------------	----------	------------	--------------

H2O	-76.323214	0.021594	-76.297776	0.018768	-76.316544	-76.43033506
------------	------------	----------	------------	----------	------------	--------------

H2O_ra	-76.186163	0.015457	-76.166853	0.01964	-76.186493	-76.3927995
---------------	------------	----------	------------	---------	------------	-------------

nhc_Ts_Cl	-2331.271845	0.536888	-2330.698776	0.102937	-2330.793628	-2333.282309
------------------	--------------	----------	--------------	----------	--------------	--------------

nhc_Ts	-1871.02858	0.537212	-1870.457171	0.099698	-1870.548503	-1872.912768
---------------	-------------	----------	--------------	----------	--------------	--------------

HCl	-460.637287	0.006845	-460.627083	0.018515	-460.645598	-460.8017807
------------	-------------	----------	-------------	----------	-------------	--------------

carbonate	-263.302341	0.014746	-263.28342	0.027119	-263.310539	-263.8833848
------------------	-------------	----------	------------	----------	-------------	--------------

hydrogen_c

arbonate	-264.138182	0.027396	-264.106287	0.027639	-264.133927	-264.5283622
-----------------	-------------	----------	-------------	----------	-------------	--------------

nhc	-1052.302221	0.405021	-1051.873311	0.07661	-1051.944345	-1053.495727
------------	--------------	----------	--------------	---------	--------------	--------------

nhc_c2	-1052.299223	0.404748	-1051.870571	0.077106	-1051.941742	-1053.491192
---------------	--------------	----------	--------------	----------	--------------	--------------

nhc_c3	-1052.302507	0.405081	-1051.873684	0.07537	-1051.943925	-1053.492206
---------------	--------------	----------	--------------	---------	--------------	--------------

nhc_c4	-1052.302507	0.405079	-1051.874389	0.073459	-1051.942856	-1053.492205
---------------	--------------	----------	--------------	----------	--------------	--------------

nhc_c5	-1052.299224	0.404724	-1051.871534	0.073108	-1051.940158	-1053.491192
---------------	--------------	----------	--------------	----------	--------------	--------------

nhc_c6	-1052.296896	0.404965	-1051.867954	0.077201	-1051.939352	-1053.488265
---------------	--------------	----------	--------------	----------	--------------	--------------

I	-1858.083221	0.673815	-1857.368329	0.114792	-1857.472897	-1860.166086
----------	--------------	----------	--------------	----------	--------------	--------------

I_c2	-1858.080924	0.673949	-1857.366012	0.112797	-1857.469602	-1860.16462371
-------------	--------------	----------	--------------	----------	--------------	----------------

I_c3	-1858.081426	0.673989	-1857.366573	0.113228	-1857.470434	-1860.163654
-------------	--------------	----------	--------------	----------	--------------	--------------

I_c4	-1858.083438	0.674298	-1857.368338	0.112824	-1857.471829	-1860.162042
-------------	--------------	----------	--------------	----------	--------------	--------------

I_c5	-1858.081099	0.673631	-1857.366426	0.11364	-1857.470502	-1860.160624
-------------	--------------	----------	--------------	---------	--------------	--------------

I_c6	-1858.082899	0.674345	-1857.369009	0.109949	-1857.469742	-1860.161073
-------------	--------------	----------	--------------	----------	--------------	--------------

I_c7	-1858.075809	0.674113	-1857.360794	0.11577	-1857.465597	-1860.156817
-------------	--------------	----------	--------------	---------	--------------	--------------

I_c8	-1858.075811	0.674099	-1857.360812	0.115171	-1857.465321	-1860.156786
-------------	--------------	----------	--------------	----------	--------------	--------------

I_c9	-1858.068459	0.673244	-1857.353826	0.116596	-1857.459391	-1860.155234
-------------	--------------	----------	--------------	----------	--------------	--------------

I_c10	-1858.071621	0.67365	-1857.356879	0.116173	-1857.462137	-1860.15352
--------------	--------------	---------	--------------	----------	--------------	-------------

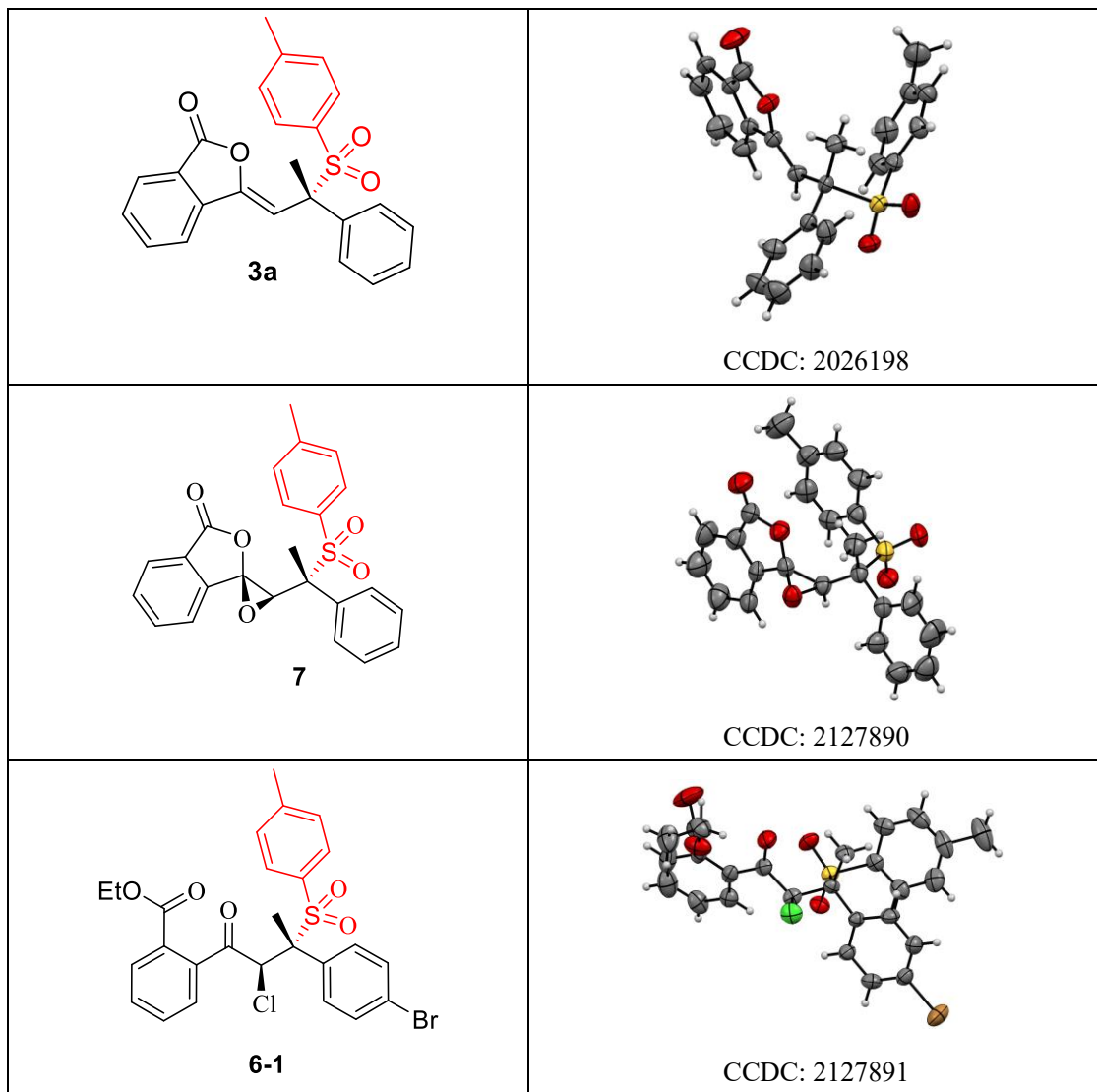
I_c11	-1858.073802	0.673086	-1857.360632	0.109844	-1857.461688	-1860.155467
I_c12	-1858.070678	0.673078	-1857.356499	0.113576	-1857.460417	-1860.151747
I-a	-1857.520507	0.659356	-1856.82045	0.111287	-1856.923182	-1859.637919
I-b	-1857.88792	0.673842	-1857.173141	0.116088	-1857.278542	-1860.000776
I-c	-1857.480264	0.662457	-1856.777271	0.112875	-1856.880898	-1859.562497
II	-2676.395295	0.793284	-2675.550977	0.135208	-2675.674058	-2679.142703
III	-1857.301007	0.663773	-1856.596672	0.111864	-1856.699773	-1859.413372
Re-INT1	-1858.067215	0.672244	-1857.353241	0.11406	-1857.458385	-1860.154344
Re-TS1	-1858.055137	0.673349	-1857.34154	0.111225	-1857.443812	-1860.139225
Re-INT1	-1858.067215	0.672244	-1857.353241	0.11406	-1857.458385	-1860.154344
Re-TS1	-1858.055137	0.673349	-1857.34154	0.111225	-1857.443812	-1860.139225
S-INT2	-1858.068099	0.674912	-1857.353043	0.110413	-1857.454935	-1860.152731
S-INT3	-2122.267003	0.703169	-2121.518957	0.119588	-2121.629799	-2124.70143
S-TS2	-2122.251111	0.697627	-2121.50934	0.117779	-2121.618527	-2124.681709
S-TS2-c2	-2122.224055	0.697653	-2121.481617	0.120884	-2121.592534	-2124.65731
S-TS2-c3	-2122.201492	0.697344	-2121.459731	0.12073	-2121.570381	-2124.648806
INT4	-2122.284598	0.702351	-2121.536663	0.122756	-2121.649352	-2124.709483
INT5	-2121.625306	0.688215	-2120.891894	0.12038	-2121.003293	-2124.14523
INT6	-3136.482731	0.790578	-3135.638768	0.14171	-3135.766658	-3139.420557
TS-3	-3136.474582	0.790529	-3135.631467	0.13803	-3135.757333	-3139.406645
INT7	-3136.522091	0.793366	-3135.675632	0.139579	-3135.802889	-3139.473786
TS4	-2676.366913	0.790691	-2675.525077	0.135519	-2675.648465	-2679.103741
INT8	-2676.409815	0.791888	-2675.566926	0.133943	-2675.689746	-2679.138278
INT9	-2676.407169	0.792905	-2675.563096	0.135924	-2675.686924	-2679.14758
INT9''	-2676.780787	0.802193	-2675.926033	0.143592	-2676.053991	-2679.549241
Re-TS5	-2676.387713	0.792285	-2675.545029	0.133419	-2675.666927	-2679.128092
Re-TS5'	-2676.387714	0.792304	-2675.545023	0.133364	-2675.666885	-2679.128093
Re-TS5''	-2676.770573	0.802113	-2675.917207	0.138241	-2676.041615	-2679.537628

<i>Re</i>-TS5"-c2	-2676.766138	0.802153	-2675.912836	0.1389	-2676.037517	-2679.535744
S-INT10	-2676.411065	0.794989	-2675.566321	0.131575	-2675.686622	-2679.155511
S-INT10"	-2676.778404	0.804097	-2675.923099	0.137086	-2676.046915	-2679.547719
S-INT11	-2676.419531	0.79364	-2675.575151	0.135316	-2675.69788	-2679.165517
<i>Si</i>-TS5	-2676.370061	0.790975	-2675.527968	0.13826	-2675.652356	-2679.122369
<i>Si</i>-TS5'	-2676.377433	0.791921	-2675.53469	0.137874	-2675.6584	-2679.124027
<i>Si</i>-TS5"	-2676.766808	0.801962	-2675.914489	0.136927	-2676.037545	-2679.535269
<i>Si</i>-TS5"-c2	-2676.769773	0.802392	-2675.916305	0.137717	-2676.040343	-2679.535208
S-INT2a	-3137.033554	0.806411	-3136.174327	0.138863	-3136.300897	-3139.941611
S-TS2a	-3137.035574	0.80665	-3136.177082	0.135947	-3136.301489	-3139.939997
INT4a	-3137.036698	0.807935	-3136.176425	0.137257	-3136.301926	-3139.943986

XI. Stereochemistry determination *via* X-ray crystallographic analysis:

The absolute stereochemistry was determined by the X-ray diffraction. This crystal was deposited in the Cambridge Crystallographic Data Centre.

[www.ccdc.cam.ac.uk/data request/cif](http://www.ccdc.cam.ac.uk/data_request/cif)



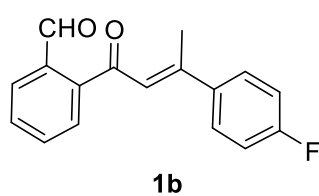
XII. References

- (1) Li, J. L.; Sahoo, B.; Daniliuc, C. G.; Glorius, F. Conjugate umpolung of β,β -disubstituted enals by dual catalysis with an *N*-heterocyclic carbene and a Bronsted acid: facile construction of contiguous quaternary stereocenters. *Angew Chem., Int. Ed.* **2014**, *53*, 10515-9.
- (2) Mo, J.; Chen, X.; Chi, Y. R., Oxidative gamma-addition of enals to trifluoromethyl ketones: enantioselectivity control *via* Lewis acid/*N*-heterocyclic carbene cooperative catalysis. *J. Am. Chem. Soc.* **2012**, *134*, 8810-3.
- (3) Yang, H.; Sun, J.; Gu, W.; Tang, W. Enantioselective Cross-Coupling for Axially Chiral Tetra-ortho-Substituted Biaryls and Asymmetric Synthesis of Gossypol. *J. Am. Chem. Soc.* **2020**, *142*, 8036-8043.
- (4) Satpathi, B.; Ramasastry, S. S. Morita-Baylis-Hillman Reaction of β,β -Disubstituted Enones: An Enantioselective Organocatalytic Approach for the Synthesis of Cyclopenta[*b*]Annulated Arenes and Heteroarenes. *Angew. Chem., Int. Ed.* **2016**, *55*, 1777-1781.
- (5) Ghosh, A.; Patra, A.; Mukherjee, S.; Biju, A. T. Synthesis of 2-Aryl Naphthoquinones by the Cross-Dehydrogenative Coupling Involving an NHC-Catalyzed *endo*-Stetter Reaction. *J. Org. Chem.* **2019**, *84*, 1103-1110.
- (6) Mishra, U. K.; Patel, K.; Ramasastry, S. S. V. Synthesis of Cyclopropanoids *via* Substrate-Based Cyclization Pathways. *Org. Lett.* **2019**, *21*, 175-179.
- (7) Bannwarth, C.; Ehlert, S.; Grimme, S. GFN2-XTB - an Accurate and Broadly Parametrized Self-Consistent Tight-Binding Quantum Chemical Method with Multipole Electrostatics and Density-Dependent Dispersion Contributions. *J. Chem. Theory Comput.* **2019**, *15*, 1652-1671.
- (8) Grimme, S.; Bannwarth, C.; Shushkov, P. A Robust and Accurate Tight-Binding Quantum Chemical Method for Structures, Vibrational Frequencies, and Noncovalent Interactions of Large Molecular Systems Parametrized for All Spd-Block Elements ($Z = 1\text{-}86$). *J. Chem. Theory Comput.* **2017**, *13*, 1989-2009.
- (9) Bannwarth, C.; Caldeweyher, E.; Ehlert, S.; Hansen, A.; Pracht, P.; Seibert, J.; Spicher, S.; Grimme, S. Extended <sc>tight-binding</Sc> Quantum Chemistry Methods. *WIREs Comput. Mol. Sci.* **2020**.
- (10) Zhao, Y.; Truhlar, D. G. The M06 Suite of Density Functionals for Main Group Thermochemistry, Thermochemical Kinetics, Noncovalent Interactions, Excited States, and Transition Elements: Two New Functionals and Systematic Testing of Four M06-Class Functionals and 12 Other Function. *Theor. Chem. Acc.* **2008**, *120*, 215-241.
- (11) Weigend, F.; Ahlrichs, R. Balanced Basis Sets of Split Valence, Triple Zeta Valence and Quadruple Zeta Valence Quality for H to Rn: Design and Assessment of Accuracy. *Phys. Chem. Chem. Phys.* **2005**, *7*, 3297-3305.
- (12) Weigend, F. Accurate Coulomb-Fitting Basis Sets for H to Rn. *Phys. Chem. Chem. Phys.* **2006**, *8*, 1057-1065.
- (13) Frisch, M. J.; Trucks, G. W.; Schlegel, H. B.; Scuseria, G. E.; Robb, M. A.; Cheeseman, J. R.;

- Scalmani, G.; Barone, V.; Mennucci, B.; Petersson, G. A.; Nakatsuji, H.; Caricato, M.; Li, X.; Hratchian, H. P.; Izmaylov, A. F.; Bloino, J.; Zheng, G.; Sonnenberg, J. L.; Hada, M.; Ehara, M.; Toyota, K.; Fukuda, R.; Hasegawa, J.; Ishida, M.; Nakajima, T.; Honda, Y.; Kitao, O.; Nakai, H.; Vreven, T.; Montgomery, J. A., Jr.; Peralta, J. E.; Ogliaro, F.; Bearpark, M.; Heyd, J. J.; Brothers, E.; Kudin, K. N.; Staroverov, V. N.; Keith, T.; Kobayashi, R.; Normand, J.; Raghavachari, K.; Rendell, A.; Burant, J. C.; Iyengar, S. S.; Tomasi, J.; Cossi, M.; Rega, N.; Millam, J. M.; Klene, M.; Knox, J. E.; Cross, J. B.; Bakken, V.; Adamo, C.; Jaramillo, J.; Gomperts, R.; Stratmann, R. E.; Yazyev, O.; Austin, A. J.; Cammi, R.; Pomelli, C.; Ochterski, J. W.; Martin, R. L.; Morokuma, K.; Krzewski, V. G.; Voth, G. A.; Salvador, P.; Dannenberg, J. J.; Dapprich, S.; Daniels, A. D.; Farkas, O.; Foresman, J. B.; Ortiz, J. V.; Cioslowski, J.; Fox, D. J. Gaussian 16, rev. A.03.; Gaussian, Inc.: Wallingford, CT, 2016.
- (14) Marenich, A. V.; Cramer, C. J.; Truhlar, D. G. Universal Solvation Model Based on Solute Electron Density and on a Continuum Model of the Solvent Defined by the Bulk Dielectric Constant and Atomic Surface Tensions. *J. Phys. Chem. B.* **2009**, *113*, 6378-6396.
- (15) Funes-Ardoiz, I.; Paton, R. S. GoodVibes v1.0.1 <http://doi.org/10.5281/zenodo.56091>.
- (16) Grimme, S. Supramolecular Binding Thermodynamics by Dispersion-Corrected Density Functional Theory. *Chem. Eur. J.* **2012**, *18*, 9955-9964.
- (17) Contreras-García, J.; Johnson, E. R.; Keinan, S.; Chaudret, R.; Piquemal, J. P.; Beratan, D. N.; Yang, W. NCIPILOT: A Program for Plotting Noncovalent Interaction Regions. *J. Chem. Theory Comput.* **2011**, *7*, 625-632.
- (18) Schrödinger, L. The PyMOL Molecular Graphics Development Component, Version 1.8; 2015.
- (19) Brethomé, A. V.; Fletcher, S. P.; Paton, R. S. Conformational Effects on Physical-Organic Descriptors: The Case of Sterimol Steric Parameters. *ACS Catal.* **2019**, *9*, 2313-2323.
- (20) Cezar, H. M. Clustering Traj <https://github.com/hmcezar/clustering-traj>.
- (21) Ho, J. Are Thermodynamic Cycles Necessary for Continuum Solvent Calculation of PK a s and Reduction Potentials? *Phys. Chem. Chem. Phys.* **2015**, *17*, 2859-2868.
- (22) Marenich, A. V.; Ho, J.; Coote, M. L.; Cramer, C. J.; Truhlar, D. G. Computational Electrochemistry: Prediction of Liquid-Phase Reduction Potentials. *Phys. Chem. Chem. Phys.* **2014**, *16*, 15068-15106.
- (23) Roth, H. G.; Romero, N. A.; Nicewicz, D. A. Experimental and Calculated Electrochemical Potentials of Common Organic Molecules for Applications to Single-Electron Redox Chemistry. *Synlett* **2016**, *27*, 714-723.
- (24) Zhang, X.; Paton, R. S. Stereoretention in Styrene Heterodimerisation Promoted by One-Electron Oxidants. *Chem. Sci.* **2020**, *11*, 9309-9324.
- (25) Isse, A. A.; Gennaro, A. Absolute Potential of the Standard Hydrogen Electrode and the Problem of Interconversion of Potentials in Different Solvents. *J. Phys. Chem. B.* **2010**, *114*, 7894-7899.
- (26) Zhang, M.; Wang, Y.; Li, S. J.; Wang, X.; Shi, Q.; Li, X.; Qu, L. B.; Wei, D.; Lan, Y. Multiple Functional Organocatalyst-Promoted Inert C-C Activation: Mechanism and Origin

- of Selectivities. *ACS Catal.* **2021**, *11*, 3443-3454.
- (27) Zhang, M.; Wang, X.; Yang, T.; Qiao, Y.; Wei, D. Theoretical Model for *N*-Heterocyclic Carbene-Catalyzed Decarboxylation Reactions. *Org. Chem. Front.* **2021**, *8*, 3268-3273.

XIII. Characterization of substrates and products



(E)-2-(3-(4-fluorophenyl)but-2-enoyl)benzaldehyde

White solid, 37% yield, 1.2 g, m.p. 102-103 °C.

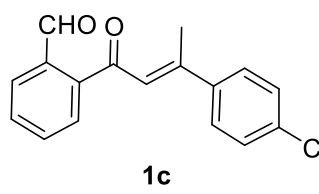
¹H NMR (400 MHz, CDCl₃) δ 10.27 (s, 1H), 7.99 – 7.93 (m, 1H), 7.76 – 7.70 (m, 1H), 7.69 – 7.59 (m, 2H), 7.57 – 7.50 (m, 2H), 7.14 – 7.05 (m, 2H), 6.94 (d, *J* = 1.2 Hz, 1H), 2.65 (d, *J* = 1.2 Hz, 3H).

¹³C NMR (101 MHz, CDCl₃) δ 193.2, 191.6, 163.6 (d, *J* = 250.5 Hz), 155.9, 143.5, 138.2 (d, *J* = 3.1 Hz), 135.8, 133.1, 131.2, 129.1, 128.5 (d, *J* = 8.5 Hz), 128.1, 123.2, 115.7 (d, *J* = 21.5 Hz), 19.0.

¹⁹F NMR (377 MHz, CDCl₃) δ -111.2.

IR (thin film): ν_{max} (cm⁻¹) = 2988, 2972, 2901, 1690, 1645, 1598, 1582, 1508, 1395, 1222, 1049, 832, 781, 752.

HRMS (ESI, m/z): Mass calcd. for C₁₇H₁₄FO₂⁺ [M+H]⁺, 269.0972; found 269.0972.



(E)-2-(3-(4-chlorophenyl)but-2-enoyl)benzaldehyde

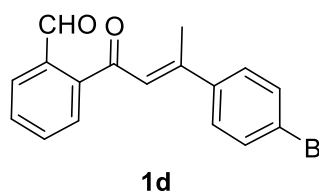
Light yellow solid, 32% yield, 1.0 g, m.p. 83-84 °C.

¹H NMR (400 MHz, CDCl₃) δ 10.27 (s, 1H), 8.00 – 7.93 (m, 1H), 7.74 – 7.69 (m, 1H), 7.69 – 7.59 (m, 2H), 7.52 – 7.46 (m, 2H), 7.41 – 7.35 (m, 2H), 6.95 (d, *J* = 1.2 Hz, 1H), 2.64 (d, *J* = 1.2 Hz, 3H).

¹³C NMR (101 MHz, CDCl₃) δ 193.2, 191.6, 155.6, 143.4, 140.5, 135.9, 135.6, 133.1, 131.2, 129.2, 128.9, 128.1, 127.9, 123.5, 18.8.

IR (thin film): ν_{max} (cm⁻¹) = 2988, 2972, 2901, 1688, 1648, 1582, 1560, 1395, 1218, 1048, 824, 776, 743.

HRMS (ESI, m/z): Mass calcd. for C₁₇H₁₄ClO₂⁺ [M+H]⁺, 285.0676; found 285.0676.



(E)-2-(3-(4-bromophenyl)but-2-enoyl)benzaldehyde

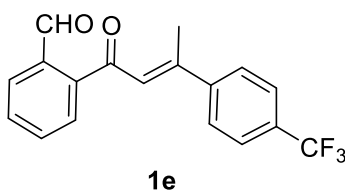
White solid, 14% yield, 0.4 g, m.p. 91-92 °C.

¹H NMR (400 MHz, CDCl₃) δ 10.26 (s, 1H), 7.98 – 7.89 (m, 1H), 7.73 – 7.60 (m, 3H), 7.54 (d, *J* = 8.6 Hz, 2H), 7.42 (d, *J* = 8.6 Hz, 2H), 6.95 (d, *J* = 0.7 Hz, 1H), 2.63 (d, *J* = 0.7 Hz, 3H).

¹³C NMR (101 MHz, CDCl₃) δ 193.2, 191.6, 155.7, 143.3, 141.0, 135.8, 133.1, 131.8, 131.2, 129.2, 128.1, 128.1, 123.9, 123.5, 18.8.

IR (thin film): ν_{max} (cm⁻¹) = 2988, 2972, 2901, 1688, 1650, 1581, 1558, 1395, 1218, 1048, 826, 821, 777, 745.

HRMS (ESI, m/z): Mass calcd. for C₁₇H₁₄BrO₂⁺ [M+H]⁺, 329.0171; found 329.0170.



(*E*)-2-(3-(4-(trifluoromethyl)phenyl)but-2-enoyl)benzaldehyde

Light yellow solid, 20% yield, 0.6 g, m.p. 59–60 °C.

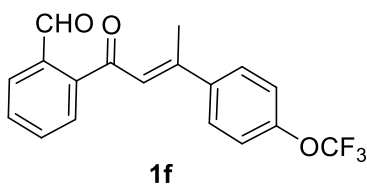
¹H NMR (400 MHz, CDCl₃) δ 10.27 (s, 1H), 7.97 – 7.93 (m, 1H), 7.75 – 7.70 (m, 1H), 7.70 – 7.60 (m, 6H), 6.97 (d, *J* = 1.2 Hz, 1H), 2.66 (d, *J* = 1.2 Hz, 3H).

¹³C NMR (101 MHz, CDCl₃) δ 193.2, 191.6, 155.1, 145.8 (d, *J* = 1.1 Hz), 143.0, 135.9, 133.1, 131.4, 131.2 (d, *J* = 30.8 Hz), 129.5, 128.2, 126.9, 125.6 (q, *J* = 3.7 Hz), 124.8, 123.8 (q, *J* = 273.7 Hz), 18.9.

¹⁹F NMR (377 MHz, CDCl₃) δ -62.7.

IR (thin film): ν_{max} (cm⁻¹) = 2988, 2972, 2901, 1691, 1653, 1601, 1571, 1408, 1323, 1078, 1066, 844, 835, 778, 731

HRMS (ESI, m/z): Mass calcd. for C₁₈H₁₄F₃O₂⁺ [M+H]⁺, 319.0940; found 319.0935.



(*E*)-2-(3-(4-(trifluoromethoxy)phenyl)but-2-enoyl)benzaldehyde

Yellow solid, 18% yield, 0.5 g, m.p. 40–41 °C.

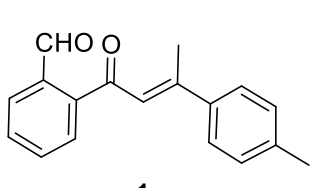
¹H NMR (400 MHz, CDCl₃) δ 10.27 (s, 1H), 7.98 – 7.93 (m, 1H), 7.74 – 7.70 (m, 1H), 7.69 – 7.61 (m, 2H), 7.61 – 7.55 (m, 2H), 7.28 – 7.23 (m, 2H), 6.95 (d, *J* = 1.2 Hz, 1H), 2.65 (d, *J* = 1.2 Hz, 3H).

¹³C NMR (101 MHz, CDCl₃) δ 193.2, 191.6, 155.3, 150.0 (d, *J* = 1.5 Hz), 143.2, 140.7, 135.9, 133.1, 131.3, 129.3, 128.2, 128.1, 123.9, 120.9, 120.4 (q, *J* = 257.9 Hz), 18.9.

¹⁹F NMR (377 MHz, CDCl₃) δ -57.7.

IR (thin film): ν_{max} (cm⁻¹) = 2988, 2972, 2901, 1717, 1696, 1595, 1577, 1509, 1251, 1207, 1154, 847, 812, 760, 667.

HRMS (ESI, m/z): Mass calcd. for C₁₈H₁₄F₃O₃⁺ [M+H]⁺, 335.0889; found 335.0886.



(*E*)-2-(3-(4-(p-tolyl)phenyl)but-2-enoyl)benzaldehyde

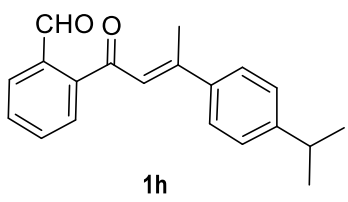
White solid, 21% yield, 0.7 g, m.p. 61–62 °C.

¹H NMR (400 MHz, CDCl₃) δ 10.28 (s, 1H), 7.95 (dd, *J* = 7.4, 1.4 Hz, 1H), 7.73 (dd, *J* = 7.4, 1.4 Hz, 1H), 7.67 – 7.56 (m, 2H), 7.47 (d, *J* = 8.0 Hz, 2H), 7.22 (d, *J* = 8.0 Hz, 2H), 7.00 (d, *J* = 1.1 Hz, 1H), 2.65 (d, *J* = 1.1 Hz, 3H), 2.38 (s, 3H).

¹³C NMR (101 MHz, CDCl₃) δ 193.2, 191.8, 157.5, 143.8, 140.0, 139.1, 135.9, 133.0, 131.1, 129.4, 128.8, 128.2, 126.5, 122.5, 21.3, 18.8.

IR (thin film): ν_{max} (cm⁻¹) = 2988, 2972, 2901, 1686, 1638, 1559, 1542, 1395, 1251, 1067, 893, 870, 814, 776, 731.

HRMS (ESI, m/z): Mass calcd. for C₁₈H₁₇O₂⁺ [M+H]⁺, 265.1223; found 265.1221.



(E)-2-(3-(4-isopropylphenyl)but-2-enoyl)benzaldehyde

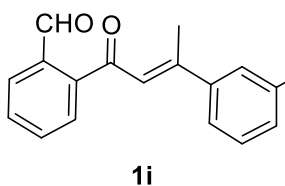
Yellow oil, 32% yield, 1.0 g.

¹H NMR (400 MHz, CDCl₃) δ 10.29 (s, 1H), 7.98 – 7.91 (m, 1H), 7.77 – 7.71 (m, 1H), 7.67 – 7.57 (m, 2H), 7.55 – 7.44 (m, 2H), 7.30 – 7.22 (m, 2H), 7.00 (d, *J* = 1.2 Hz, 1H), 2.95 (dt, *J* = 13.8, 6.9 Hz, 1H), 2.66 (d, *J* = 1.2 Hz, 3H), 1.27 (d, *J* = 6.9 Hz, 6H).

¹³C NMR (101 MHz, CDCl₃) δ 193.2, 191.7, 157.5, 150.9, 143.8, 139.5, 135.9, 133.0, 131.1, 128.8, 128.2, 126.8, 126.6, 122.6, 33.9, 23.8, 18.8.

IR (thin film): ν_{max} (cm⁻¹) = 2987, 2960, 2923, 2901, 1784, 1734, 1695, 1651, 1584, 1559, 1509, 1213, 1193, 1067, 1047, 829, 775, 750.

HRMS (ESI, m/z): Mass calcd. for C₂₀H₂₁O₂⁺ [M+H]⁺, 293.1536; found 293.1537.



(E)-2-(3-(3-fluorophenyl)but-2-enoyl)benzaldehyde

White solid, 31% yield, 1.0 g, m.p. 100-101 °C.

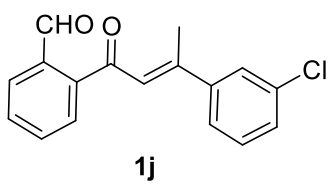
¹H NMR (400 MHz, CDCl₃) δ 10.27 (s, 1H), 7.99 – 7.94 (m, 1H), 7.75 – 7.70 (m, 1H), 7.70 – 7.59 (m, 2H), 7.41 – 7.30 (m, 2H), 7.28 – 7.20 (m, 1H), 7.14 – 7.06 (m, 1H), 6.97 (d, *J* = 1.2 Hz, 1H), 2.63 (d, *J* = 1.2 Hz, 3H).

¹³C NMR (101 MHz, CDCl₃) δ 193.2, 191.6, 162.8 (d, *J* = 246.9 Hz), 155.4 (d, *J* = 2.2 Hz), 144.4 (d, *J* = 7.3 Hz), 143.2, 135.9, 133.1, 131.3, 130.2 (d, *J* = 8.2 Hz), 129.3, 128.2, 124.0, 122.2 (d, *J* = 2.8 Hz), 116.3 (d, *J* = 21.2 Hz), 113.6 (d, *J* = 22.5 Hz), 18.8.

¹⁹F NMR (377 MHz, CDCl₃) δ -112.3.

IR (thin film): ν_{max} (cm⁻¹) = 2988, 2972, 2901, 1688, 1646, 1577, 1483, 1395, 1231, 1067, 1049, 880, 770, 752, 728, 688, 662.

HRMS (ESI, m/z): Mass calcd. for C₁₇H₁₄FO₂⁺ [M+H]⁺, 269.0972; found 269.0971.



(E)-2-(3-(3-chlorophenyl)but-2-enoyl)benzaldehyde

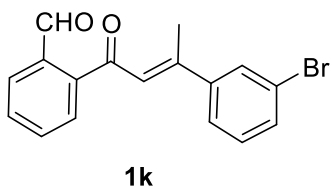
White solid, 18% yield, 0.5 g, m.p. 76-77 °C.

¹H NMR (400 MHz, CDCl₃) δ 10.27 (s, 1H), 8.00 – 7.91 (m, 1H), 7.75 – 7.69 (m, 1H), 7.70 – 7.59 (m, 2H), 7.52 (t, *J* = 1.7 Hz, 1H), 7.43 (dt, *J* = 7.2, 1.7 Hz, 1H), 7.41 – 7.31 (m, 2H), 6.95 (d, *J* = 1.2 Hz, 1H), 2.63 (d, *J* = 1.2 Hz, 3H).

¹³C NMR (101 MHz, CDCl₃) δ 193.2, 191.6, 155.3, 144.0, 143.2, 135.9, 134.7, 133.1, 131.3, 129.9, 129.4, 129.3, 128.2, 126.7, 124.7, 124.1, 18.8.

IR (thin film): ν_{max} (cm⁻¹) = 3057, 2988, 2972, 2901, 1691, 1646, 1585, 1472, 1372, 1278, 1044, 808, 770, 748, 687, 661.

HRMS (ESI, m/z): Mass calcd. for C₁₇H₁₄ClO₂⁺ [M+H]⁺, 285.0676; found 285.0677.



(E)-2-(3-(3-bromophenyl)but-2-enoyl)benzaldehyde

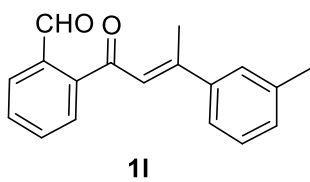
Yellow solid, 24% yield, 0.7 g, m.p. 69-70 °C.

¹H NMR (400 MHz, CDCl₃) δ 10.27 (s, 1H), 7.99 – 7.93 (m, 1H), 7.75 – 7.70 (m, 1H), 7.70 – 7.60 (m, 3H), 7.53 (ddd, *J* = 7.9, 1.8, 0.9 Hz, 1H), 7.47 (ddd, *J* = 7.9, 1.6, 1.0 Hz, 1H), 7.29 (t, *J* = 7.9 Hz, 1H), 6.94 (d, *J* = 1.2 Hz, 1H), 2.63 (d, *J* = 1.2 Hz, 3H).

¹³C NMR (101 MHz, CDCl₃) δ 193.2, 191.6, 155.3, 144.3, 143.2, 135.9, 133.1, 132.4, 131.3, 130.2, 129.6, 129.3, 128.2, 125.2, 124.1, 122.8, 18.9.

IR (thin film): ν_{max} (cm⁻¹) = 2988, 2972, 2901, 1688, 1650, 1581, 1561, 1372, 1278, 1044, 808, 821, 772, 750.

HRMS (ESI, m/z): Mass calcd. for C₁₇H₁₄BrO₂⁺ [M+H]⁺, 329.0171; found 329.0169.



(E)-2-(3-(m-tolyl)but-2-enoyl)benzaldehyde

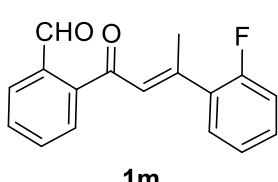
White solid, 42% yield, 1.4 g, m.p. 62-63 °C.

¹H NMR (400 MHz, CDCl₃) δ 10.29 (s, 1H), 7.96 (dd, *J* = 7.4, 1.5 Hz, 1H), 7.74 (dd, *J* = 7.5, 1.3 Hz, 1H), 7.69 – 7.58 (m, 2H), 7.37 – 7.34 (m, 2H), 7.30 (t, *J* = 7.4 Hz, 1H), 7.23 (d, *J* = 7.4 Hz, 1H), 6.98 (d, *J* = 1.2 Hz, 1H), 2.66 (d, *J* = 1.2 Hz, 3H), 2.40 (s, 3H).

¹³C NMR (101 MHz, CDCl₃) δ 193.2, 191.7, 157.7, 143.7, 142.2, 138.3, 135.9, 133.0, 131.1, 130.4, 128.9, 128.6, 128.2, 127.2, 123.7, 123.1, 21.5, 19.0.

IR (thin film): ν_{max} (cm⁻¹) = 2988, 2972, 2901, 1693, 1644, 1568, 1395, 1230, 1044, 867, 825, 767, 755, 688.

HRMS (ESI, m/z): Mass calcd. for C₁₈H₁₇O₂⁺ [M+H]⁺, 265.1223; found 265.1222.



(E)-2-(3-(2-fluorophenyl)but-2-enoyl)benzaldehyde

Yellow solid, 24% yield, 0.8 g, m.p. 40-41 °C.

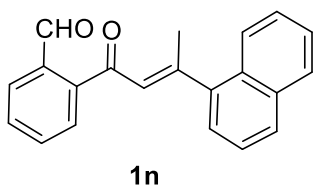
¹H NMR (400 MHz, CDCl₃) δ 10.29 (s, 1H), 7.99 – 7.91 (m, 1H), 7.79 – 7.72 (m, 1H), 7.69 – 7.58 (m, 2H), 7.36 (m, 2H), 7.18 (td, *J* = 7.5, 1.1 Hz, 1H), 7.12 (m, 1H), 6.93 – 6.84 (m, 1H), 2.60 (t, *J* = 1.5 Hz, 3H).

¹³C NMR (101 MHz, CDCl₃) δ 193.1, 191.7, 159.6 (d, *J* = 249.9 Hz), 153.0, 143.0, 136.1, 133.0, 131.4, 130.8 (d, *J* = 12.9 Hz), 130.5 (d, *J* = 8.4 Hz), 129.3 (d, *J* = 3.1 Hz), 129.0, 128.4, 126.4 (d, *J* = 3.5 Hz), 124.3 (d, *J* = 3.6 Hz), 116.3 (d, *J* = 22.7 Hz), 20.3 (d, *J* = 3.1 Hz).

¹⁹F NMR (377 MHz, CDCl₃) δ -113.9.

IR (thin film): ν_{max} (cm⁻¹) = 2988, 2972, 2901, 1691, 1648, 1592, 1571, 1488, 1448, 1220, 1047, 826, 755, 694, 665.

HRMS (ESI, m/z): Mass calcd. for C₁₇H₁₄FO₂⁺ [M+H]⁺, 269.0972; found 269.0972.



(E)-2-(3-(naphthalen-1-yl)but-2-enoyl)benzaldehyde

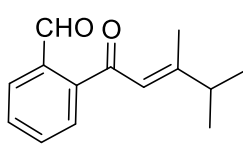
Yellow solid, 52% yield, 1.6 g, m.p. 88–89 °C.

¹H NMR (400 MHz, CDCl₃) δ 10.31 (s, 1H), 8.04 (s, 1H), 7.96 (d, *J* = 7.2 Hz, 1H), 7.87 (m, 3H), 7.77 (d, *J* = 7.3 Hz, 1H), 7.69 – 7.58 (m, 3H), 7.52 (dd, *J* = 6.1, 3.2 Hz, 2H), 7.14 (s, 1H), 2.77 (s, 3H).

¹³C NMR (101 MHz, CDCl₃) δ 193.2, 191.7, 157.1, 143.7, 139.3, 135.9, 133.8, 133.1, 133.1, 131.2, 129.0, 128.6, 128.4, 128.2, 127.6, 127.1, 126.7, 126.6, 123.9, 123.6, 19.0.

IR (thin film): ν_{max} (cm⁻¹) = 2988, 2972, 2901, 1684, 1668, 1640, 1561, 1395, 1235, 1058, 879, 858, 778, 755, 746.

HRMS (ESI, m/z): Mass calcd. for C₂₁H₁₇O₂⁺ [M+H]⁺, 301.1223; found 301.1226.



(E)-2-(3,4-dimethylpent-2-enoyl)benzaldehyde

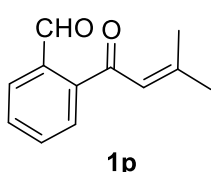
White oil, 52% yield, 2.0 g.

¹H NMR (400 MHz, CDCl₃) δ 10.23 (s, 1H), 8.00 – 7.84 (m, 1H), 7.69 – 7.66 (m, 1H), 7.65 – 7.61 (m, 1H), 7.60 – 7.55 (m, 1H), 6.59 (s, 1H), 2.48 (m, 1H), 2.21 (d, *J* = 1.1 Hz, 3H), 1.14 (d, *J* = 6.9 Hz, 6H).

¹³C NMR (101 MHz, CDCl₃) δ 193.4, 191.7, 168.2, 143.7, 135.8, 132.9, 130.9, 128.5, 128.1, 120.3, 38.7, 20.9, 17.5.

IR (thin film): ν_{max} (cm⁻¹) = 2987, 2969, 2901, 1695, 1655, 1594, 1573, 1395, 1242, 1067, 858, 780, 745, 662.

HRMS (ESI, m/z): Mass calcd. for C₁₄H₁₆NaO₂⁺ [M+Na]⁺, 239.1043; found 239.1041.



2-(3-methylbut-2-enoyl)benzaldehyde

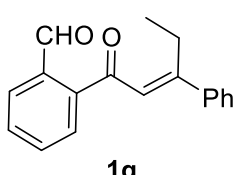
White oil, 25% yield, 1.1 g.

¹H NMR (400 MHz, CDCl₃) δ 10.22 (s, 1H), 7.96 – 7.86 (m, 1H), 7.70 – 7.54 (m, 3H), 6.58 (dt, *J* = 2.4, 1.1 Hz, 1H), 2.25 (d, *J* = 1.1 Hz, 3H), 2.03 (d, *J* = 1.2 Hz, 3H).

¹³C NMR (101 MHz, CDCl₃) δ 192.9, 191.7, 159.4, 143.6, 135.8, 132.9, 130.9, 128.7, 128.1, 123.0, 28.1, 21.3.

IR (thin film): ν_{max} (cm⁻¹) = 2987, 2972, 2901, 1694, 1656, 1603, 1593, 1572, 1380, 1246, 1067, 1013, 861, 815, 771, 745, 665.

HRMS (ESI, m/z): Mass calcd. for C₁₂H₁₂NaO₂⁺ [M+Na]⁺, 211.0730; found 211.0733.



(E)-2-(3-phenylpent-2-enoyl)benzaldehyde

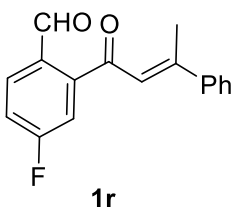
White oil, 30% yield, 1.2 g.

¹H NMR (400 MHz, CDCl₃) δ 10.29 (s, 1H), 7.95 (dd, *J* = 7.2, 1.6 Hz, 1H), 7.74 (dd, *J* = 7.1, 1.6 Hz, 1H), 7.68 – 7.58 (m, 2H), 7.56 – 7.50 (m, 2H), 7.43 – 7.38 (m, 3H), 6.88 (s, 1H), 3.15 (q, *J* = 7.5 Hz, 2H), 1.16 (t, *J* = 7.5 Hz, 3H).

¹³C NMR (101 MHz, CDCl₃) δ 192.8, 191.8, 163.8, 143.6, 141.0, 136.0, 133.0, 131.2, 129.5, 128.9, 128.7, 128.3, 126.9, 122.9, 25.0, 13.5.

IR (thin film): ν_{max} (cm⁻¹) = 3509, 2987, 2972, 2933, 2901, 1695, 1651, 1586, 1570, 1445, 1212, 1067, 1047, 870, 762, 696, 672.

HRMS (ESI, m/z): Mass calcd. for C₁₈H₁₆NaO₂⁺ [M+Na]⁺, 287.1043; found 287.1043.



(E)-4-fluoro-2-(3-phenylbut-2-enoyl)benzaldehyde

Yellow solid, 31% yield, 1.0 g, m.p. 40-41°C.

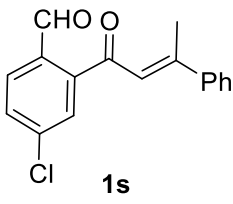
¹H NMR (400 MHz, CDCl₃) δ 10.18 (s, 1H), 7.98 (dd, *J* = 8.6, 5.5 Hz, 1H), 7.57 – 7.52 (m, 2H), 7.42 – 7.38 (m, 3H), 7.36 (dd, *J* = 8.6, 2.5 Hz, 1H), 7.26 (td, *J* = 8.2, 2.5 Hz, 1H), 6.91 (d, *J* = 1.2 Hz, 1H), 2.67 (d, *J* = 1.2 Hz, 3H).

¹³C NMR (101 MHz, CDCl₃) δ 191.7 (d, *J* = 1.3 Hz), 189.9, 165.1 (d, *J* = 257.6 Hz), 158.5, 146.5 (d, *J* = 7.2 Hz), 141.9, 131.9 (d, *J* = 9.3 Hz), 131.9, 129.9, 128.7, 126.6, 122.7, 118.0 (d, *J* = 21.8 Hz), 115.3 (d, *J* = 23.2 Hz), 19.0.

¹⁹F NMR (377 MHz, CDCl₃) δ -102.9.

IR (thin film): ν_{max} (cm⁻¹) = 2988, 2972, 2901, 2498, 1692, 1654, 1572, 1489, 1237, 1067, 914, 867, 833, 762, 696.

HRMS (ESI, m/z): Mass calcd. for C₁₇H₁₄FO₂⁺ [M+H]⁺, 269.0972; found 269.0973.



(E)-4-chloro-2-(3-phenylbut-2-enoyl)benzaldehyde

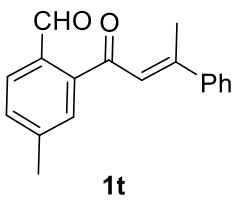
Light yellow solid, 30% yield, 0.9 g, m.p. 76-77 °C.

¹H NMR (400 MHz, CDCl₃) δ 10.22 (s, 1H), 7.92 (d, *J* = 8.3 Hz, 1H), 7.68 (d, *J* = 2.0 Hz, 1H), 7.60 – 7.53 (m, 3H), 7.46 – 7.40 (m, 3H), 6.92 (d, *J* = 1.2 Hz, 1H), 2.69 (d, *J* = 1.2 Hz, 3H).

¹³C NMR (101 MHz, CDCl₃) δ 191.7, 190.3, 158.8, 145.1, 141.9, 139.6, 133.8, 131.1, 130.5, 129.9, 128.7, 128.2, 126.6, 122.7, 19.1.

IR (thin film): ν_{max} (cm⁻¹) = 2988, 2972, 2901, 1701, 1649, 1584, 1561, 1542, 1395, 1211, 1067, 893, 865, 829, 770, 746, 698.

HRMS (ESI, m/z): Mass calcd. for C₁₇H₁₄ClO₂⁺ [M+H]⁺, 285.0676; found 285.0678.



(E)-4-methyl-2-(3-phenylbut-2-enoyl)benzaldehyde

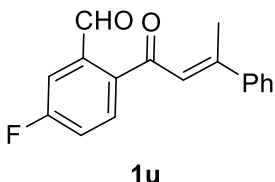
Yellow solid, 18% yield, 0.6 g, m.p. 40-41 °C.

¹H NMR (400 MHz, CDCl₃) δ 10.22 (s, 1H), 7.87 (d, *J* = 7.9 Hz, 1H), 7.58 – 7.52 (m, 2H), 7.48 (s, 1H), 7.44 – 7.37 (m, 4H), 6.94 (d, *J* = 1.2 Hz, 1H), 2.66 (d, *J* = 1.2 Hz, 3H), 2.47 (s, 3H).

¹³C NMR (101 MHz, CDCl₃) δ 193.7, 191.3, 156.9, 144.3, 144.0, 142.2, 133.2, 131.6, 129.6, 129.2, 128.7, 128.6, 126.6, 123.7, 21.7, 18.9.

IR (thin film): ν_{max} (cm^{-1}) = 2987, 2972, 2901, 1771, 1717, 1687, 1653, 1590, 1570, 1446, 1269, 1236, 1168, 1046, 828, 760, 696.

HRMS (ESI, m/z): Mass calcd. for $\text{C}_{18}\text{H}_{17}\text{O}_2^+$ [M+H]⁺, 265.1223; found 265.1219.



(E)-5-fluoro-2-(3-phenylbut-2-enoyl)benzaldehyde

White solid, 31% yield, 1.0 g, m.p. 97-98 °C.

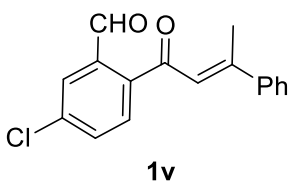
¹H NMR (400 MHz, CDCl₃) δ 10.28 (d, J = 2.6 Hz, 1H), 7.82 (dd, J = 8.5, 5.1 Hz, 1H), 7.63 (dd, J = 8.7, 2.7 Hz, 1H), 7.56 (m, 2H), 7.46 – 7.40 (m, 3H), 7.36 – 7.29 (m, 1H), 7.00 (d, J = 1.2 Hz, 1H), 2.66 (d, J = 1.2 Hz, 3H).

¹³C NMR (101 MHz, CDCl₃) δ 191.5, 190.4 (d, J = 1.1 Hz), 164.1 (d, J = 255.0 Hz), 158.2, 142.1, 139.5 (d, J = 3.6 Hz), 139.1 (d, J = 6.8 Hz), 131.0 (d, J = 8.3 Hz), 129.7, 128.7, 126.5, 122.8, 119.6 (d, J = 21.9 Hz), 115.5 (d, J = 22.8 Hz), 19.1.

¹⁹F NMR (377 MHz, CDCl₃) δ -106.1.

IR (thin film): ν_{max} (cm^{-1}) = 2988, 2972, 2901, 1687, 1644, 1584, 1570, 1492, 1229, 1046, 886, 845, 767, 744, 687.

HRMS (ESI, m/z): Mass calcd. for $\text{C}_{17}\text{H}_{14}\text{FO}_2^+$ [M+H]⁺, 269.0972; found 269.0973.



(E)-5-chloro-2-(3-phenylbut-2-enoyl)benzaldehyde

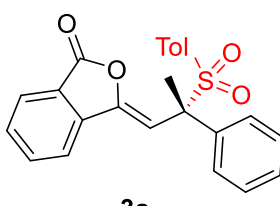
Light yellow solid, 41% yield, 1.3 g, m.p. 124-125 °C.

¹H NMR (400 MHz, CDCl₃) δ 10.25 (s, 1H), 7.91 (d, J = 2.1 Hz, 1H), 7.72 (d, J = 8.2 Hz, 1H), 7.60 (dd, J = 8.2, 2.2 Hz, 1H), 7.58 – 7.52 (m, 2H), 7.43 (m, 3H), 6.98 (d, J = 1.2 Hz, 1H), 2.67 (d, J = 1.2 Hz, 3H).

¹³C NMR (101 MHz, CDCl₃) δ 191.7, 190.4, 158.5, 142.0, 141.5, 137.9, 137.7, 132.7, 129.8, 129.8, 128.8, 128.7, 126.6, 122.6, 19.1.

IR (thin film): ν_{max} (cm^{-1}) = 3078, 3062, 2988, 2901, 1687, 1643, 1582, 1561, 1494, 1380, 1191, 1081, 1046, 906, 894, 844, 745, 690, 678.

HRMS (ESI, m/z): Mass calcd. for $\text{C}_{17}\text{H}_{14}\text{ClO}_2^+$ [M+H]⁺, 285.0676; found 285.0679.



(S,Z)-3-(2-phenyl-2-tosylpropylidene)isobenzofuran-1(3H)-one

White solid, 90% yield, 36.4 mg, m.p. 128-129 °C.

$[\alpha]_D^{25} = -62.1$ (c = 0.5 in CHCl₃).

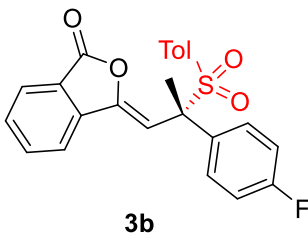
¹H NMR (400 MHz, CDCl₃) δ 7.85 (d, J = 8.5 Hz, 2H), 7.79 – 7.73 (m, 1H), 7.58 (td, J = 7.7, 0.7 Hz, 1H), 7.43 – 7.40 (m, 2H), 7.34 – 7.30 (m, 3H), 7.28 – 7.23 (m, 2H), 7.14 (d, J = 8.0 Hz, 2H), 6.61 (s, 1H), 2.38 (s, 3H), 2.18 (s, 3H).

¹³C NMR (101 MHz, CDCl₃) δ 165.9, 147.4, 145.0, 139.5, 136.3, 134.8, 131.4, 130.6, 130.5, 129.0, 128.9, 128.7, 128.0, 125.4, 123.6, 120.4, 104.7, 70.7, 21.6, 20.7.

IR (thin film): ν_{max} (cm^{-1}) = 2988, 2972, 2901, 2361, 2325, 1690, 1645, 1598, 1582, 1508, 1395, 1222, 1049, 832, 781, 752.

HRMS (ESI, m/z): Mass calcd. for $\text{C}_{24}\text{H}_{20}\text{NaO}_4\text{S}^+$ $[\text{M}+\text{Na}]^+$, 427.0974; found 427.0972.

HPLC analysis (Chiralcel IA; 25 °C, IPA/Hexane = 10/90, 0.3 mL/min, 254 nm), $Rt_1(\text{major}) = 15.2 \text{ min}$, $Rt_2(\text{minor}) = 12.9 \text{ min}$; ee = 98%).



(*S,Z*)-3-(2-(4-fluorophenyl)-2-tosylpropylidene)isobenzofuran-1(3*H*)-one

1(3*H*)-one

White solid, 91% yield, 38.4 mg, m.p. 134–135 °C.

$[\alpha]_D^{25} = -66.0$ ($c = 0.5$ in CHCl_3).

$^1\text{H NMR}$ (400 MHz, CDCl_3) δ 7.85 (dd, $J = 7.7, 6.1 \text{ Hz}$, 2H), 7.81 – 7.74 (m, 1H), 7.64 – 7.54 (m, 1H), 7.41 – 7.31 (m, 4H), 7.18 (d, $J = 8.0 \text{ Hz}$, 2H), 6.96 (t, $J = 8.7 \text{ Hz}$, 2H), 6.58 (s, 1H), 2.40 (s, 3H), 2.15 (s, 3H).

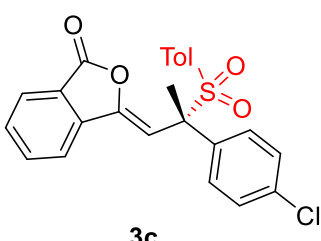
$^{13}\text{C NMR}$ (101 MHz, CDCl_3) δ 165.8, 162.8 (d, $J = 249.1 \text{ Hz}$), 147.5, 145.2, 139.4, 134.8, 132.2 (d, $J = 3.5 \text{ Hz}$), 131.2, 130.9 (d, $J = 8.3 \text{ Hz}$), 130.7, 130.5, 129.1, 125.5, 123.6, 120.4, 115.0 (d, $J = 21.6 \text{ Hz}$), 104.5, 70.1, 21.6, 20.9.

$^{19}\text{F NMR}$ (377 MHz, CDCl_3) δ -112.7.

IR (thin film): ν_{max} (cm^{-1}) = 2988, 2971, 2901, 2362, 2324, 1788, 1672, 1596, 1510, 1472, 1290, 1265, 1235, 1050, 980, 820, 767, 734, 711, 689, 651.

HRMS (ESI, m/z): Mass calcd. for $\text{C}_{24}\text{H}_{19}\text{FNaO}_4\text{S}^+$ $[\text{M}+\text{Na}]^+$, 445.0880; found 445.0875

HPLC analysis (Chiralcel IA; 25 °C, IPA/Hexane = 10/90, 0.3 mL/min, 254 nm), $Rt_1(\text{major}) = 16.2 \text{ min}$, $Rt_2(\text{minor}) = 13.6 \text{ min}$; ee = 98%).



(*S,Z*)-3-(2-(4-chlorophenyl)-2-tosylpropylidene)isobenzofuran-1(3*H*)-one

1(3*H*)-one

Yellow solid, 82% yield, 35.9 mg, m.p. 128–129 °C.

$[\alpha]_D^{25} = -48.8$ ($c = 0.5$ in CHCl_3).

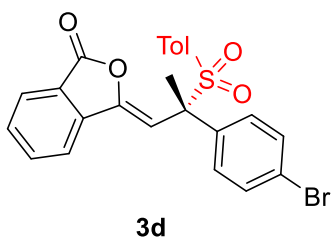
$^1\text{H NMR}$ (400 MHz, CDCl_3) δ 7.85 (dd, $J = 8.6, 7.9 \text{ Hz}$, 2H), 7.77 (td, $J = 7.6, 0.9 \text{ Hz}$, 1H), 7.60 (td, $J = 7.6, 0.7 \text{ Hz}$, 1H), 7.33 (m, 4H), 7.26 – 7.22 (m, 2H), 7.19 (d, $J = 8.1 \text{ Hz}$, 2H), 6.56 (s, 1H), 2.40 (s, 3H), 2.13 (s, 3H).

$^{13}\text{C NMR}$ (101 MHz, CDCl_3) δ 165.8, 147.6, 145.3, 139.3, 134.9, 134.9, 134.8, 131.1, 130.7, 130.5, 130.4, 129.2, 128.2, 125.5, 123.6, 120.4, 104.3, 70.2, 21.6, 20.8.

IR (thin film): ν_{max} (cm^{-1}) = 2988, 2971, 2901, 2362, 2331, 1785, 1672, 1595, 1494, 1472, 1290, 1140, 1051, 978, 819, 767, 712, 704, 690.

HRMS (ESI, m/z): Mass calcd. for $\text{C}_{24}\text{H}_{19}\text{ClNaO}_4\text{S}^+$ $[\text{M}+\text{Na}]^+$, 461.0584; found 461.0582.

HPLC analysis (Chiralcel IA; 25 °C, IPA/Hexane = 15/85, 0.5 mL/min, 254 nm), $Rt_1(\text{major}) = 37.4 \text{ min}$, $Rt_2(\text{minor}) = 30.5 \text{ min}$; ee = 97%).



(*S,Z*)-3-(2-(4-bromophenyl)-2-tosylpropylidene)isobenzofuran-1(3H)-one

White solid, 86% yield, 41.6 mg, m.p. 126-127 °C.

$[\alpha]_D^{25} = -33.2$ (c = 0.5 in CHCl₃).

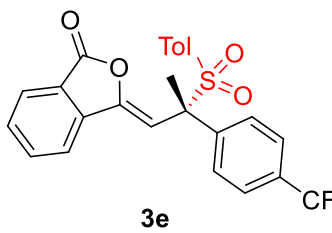
¹H NMR (400 MHz, CDCl₃) δ 7.90 – 7.81 (m, 2H), 7.77 (td, *J* = 7.6, 1.0 Hz, 1H), 7.60 (m, 1H), 7.43 – 7.37 (m, 2H), 7.35 (d, *J* = 8.3 Hz, 2H), 7.31 – 7.27 (m, 1H), 7.26 (d, *J* = 2.7 Hz, 1H), 7.19 (d, *J* = 8.0 Hz, 2H), 6.56 (s, 1H), 2.40 (s, 3H), 2.13 (s, 3H).

¹³C NMR (101 MHz, CDCl₃) δ 165.7, 147.6, 145.3, 139.3, 135.5, 134.8, 131.1, 131.1, 130.7, 130.5, 129.2, 125.5, 123.6, 123.2, 120.4, 104.2, 70.2, 21.6, 20.8.

IR (thin film): ν_{max} (cm⁻¹) = 2987, 2972, 2901, 2362, 2343, 1783, 1672, 1593, 1472, 1286, 1136, 1053, 982, 817, 768, 713, 701, 690, 682, 655.

HRMS (ESI, m/z): Mass calcd. for C₂₄H₁₉BrNaO₄S⁺ [M+Na]⁺, 505.0079; found 505.0075.

HPLC analysis (Chiralcel IA; 25 °C, IPA/Hexane = 10/90, 0.3 mL/min, 254 nm), Rt₁(minor) = 18.3 min, Rt₂(major) = 14.8 min; ee = 98%).



(*S,Z*)-3-(2-tosyl-2-(4-(trifluoromethyl)phenyl)propylidene)isobenzofuran-1(3H)-one

Yellow solid, 81% yield, 38.2 mg, m.p. 139-140 °C.

$[\alpha]_D^{25} = -30.2$ (c = 0.5 in CHCl₃).

¹H NMR (400 MHz, CDCl₃) δ 7.89 – 7.84 (m, 2H), 7.81 – 7.75 (m, 1H), 7.64 – 7.58 (m, 1H), 7.57 – 7.50 (m, 4H), 7.34 (d, *J* = 8.3 Hz, 2H), 7.18 (d, *J* = 8.1 Hz, 2H), 6.59 (s, 1H), 2.40 (s, 3H), 2.18 (s, 3H).

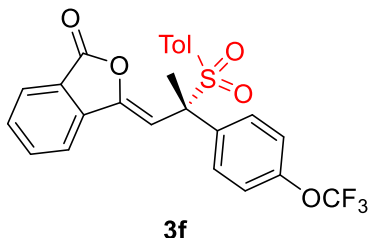
¹³C NMR (101 MHz, CDCl₃) δ 165.6, 147.8, 145.5, 140.5 (d, *J* = 1.0 Hz), 139.2, 134.9, 131.0, 130.8, 130.7 (d, *J* = 30.8 Hz), 130.5, 129.4, 129.2, 125.6, 124.9 (q, *J* = 3.6 Hz), 123.8 (q, *J* = 272.1 Hz), 123.6, 120.4, 104.0, 70.4, 21.6, 20.9.

¹⁹F NMR (377 MHz, CDCl₃) δ -62.7.

IR (thin film): ν_{max} (cm⁻¹) = 2988, 2972, 2901, 2361, 2343, 1779, 1682, 1619, 1596, 1327, 1289, 1114, 1074, 980, 840, 815, 770, 713, 687, 659.

HRMS (ESI, m/z): Mass calcd. for C₂₅H₁₉F₃NaO₄S⁺ [M+Na]⁺, 495.0848; found 495.0845.

HPLC analysis (Chiralcel IA; 25 °C, IPA/Hexane = 15/85, 0.5 mL/min, 254 nm), Rt₁(major) = 28.4 min, Rt₂(minor) = 24.8 min; ee = 95%).



(*S,Z*)-3-(2-tosyl-2-(4-(trifluoromethoxy)phenyl)propylidene)isobenzofuran-1(3H)-one

Yellow solid, 92% yield, 44.9 mg, m.p. 113-114 °C.

$[\alpha]_D^{25} = -39.3$ (c = 0.5 in CHCl₃).

¹H NMR (400 MHz, CDCl₃) δ 7.86 (dd, *J* = 7.1, 6.1 Hz, 2H), 7.80 – 7.74 (m, 1H), 7.63 – 7.56 (m, 1H), 7.47 – 7.40 (m, 2H), 7.32 (d, *J* = 8.3 Hz, 2H), 7.16 (d, *J* = 8.1 Hz, 2H), 7.11 (d, *J* = 8.2 Hz, 2H), 6.58 (s, 1H), 2.40 (s, 3H), 2.16 (s, 3H).

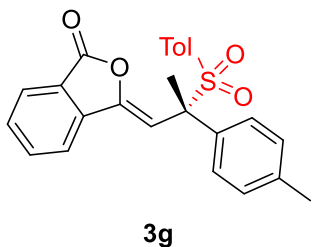
¹³C NMR (101 MHz, CDCl₃) δ 165.7, 149.4 (d, *J* = 1.6 Hz), 147.7, 145.3, 139.3, 135.1, 134.8, 131.1, 130.8, 130.6, 130.4, 129.1, 125.5, 123.6, 120.4, 120.3 (q, *J* = 258.5 Hz), 120.2, 104.1, 70.2, 21.6, 20.8.

¹⁹F NMR (377 MHz, CDCl₃) δ -57.7.

IR (thin film): ν_{max} (cm⁻¹) = 2988, 2972, 2901, 2361, 2343, 1787, 1680, 1595, 1509, 1473, 1288, 1256, 1140, 981, 821, 772, 692, 655.

HRMS (ESI, m/z): Mass calcd. for C₂₅H₁₉F₃NaO₅S⁺ [M+Na]⁺, 511.0797; found 511.0800.

HPLC analysis (Chiralcel IA; 25 °C, IPA/Hexane = 15/85, 0.5 mL/min, 254 nm), Rt₁(major) = 36.8 min, Rt₂(minor) = 31.6 min; ee = 97%.



(S,Z)-3-(2-(*p*-tolyl)-2-tosylpropylidene)isobenzofuran-1(3*H*)-one

Yellow solid, 95% yield, 39.7 mg, m.p. 134–135 °C.

$[\alpha]_D^{25} = -14.2$ (*c* = 0.5 in CHCl₃).

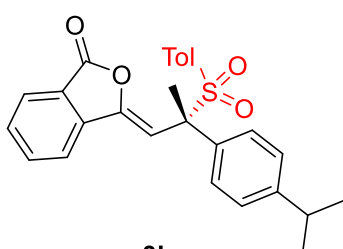
¹H NMR (400 MHz, CDCl₃) δ 7.88 – 7.81 (m, 2H), 7.76 (t, *J* = 7.6 Hz, 1H), 7.58 (t, *J* = 7.5 Hz, 1H), 7.35 (d, *J* = 8.2 Hz, 2H), 7.30 (d, *J* = 8.3 Hz, 2H), 7.16 (d, *J* = 8.1 Hz, 2H), 7.08 (d, *J* = 8.1 Hz, 2H), 6.59 (s, 1H), 2.39 (s, 3H), 2.34 (s, 3H), 2.15 (s, 3H).

¹³C NMR (101 MHz, CDCl₃) δ 166.0, 147.3, 144.9, 139.6, 138.6, 134.7, 133.2, 131.6, 130.6, 130.5, 129.0, 128.8, 128.7, 125.4, 123.6, 120.3, 104.9, 70.5, 21.6, 21.1, 20.7.

IR (thin film): ν_{max} (cm⁻¹) = 2988, 2972, 2901, 2361, 2343, 1785, 1750, 1671, 1597, 1473, 1284, 1144, 1067, 1052, 975, 815, 767, 718, 693, 665, 651.

HRMS (ESI, m/z): Mass calcd. for C₂₅H₂₂NaO₄S⁺ [M+Na]⁺, 441.1131; found 441.1126.

UPLC analysis (Chiralcel IA; 25 °C, IPA/Hexane = 10/90, 0.3 mL/min, 254 nm), Rt₁(major) = 17.4 min, Rt₂(minor) = 14.1 min; ee = 97%.



(S,Z)-3-(2-(4-isopropylphenyl)-2-tosylpropylidene)isobenzofuran-1(3*H*)-one

Light yellow oil, 91% yield, 40.6 mg.

$[\alpha]_D^{25} = -28.2$ (*c* = 0.5 in CHCl₃).

¹H NMR (400 MHz, CDCl₃) δ 7.87 – 7.83 (m, 2H), 7.76 (td, *J* = 7.7, 0.9 Hz, 1H), 7.61 – 7.55 (m, 1H), 7.36 – 7.30 (m, 4H), 7.14 – 7.10 (m, 4H), 6.60 (s, 1H), 2.89 (dt, *J* = 13.8, 6.9 Hz, 1H), 2.38 (s, 3H), 2.17 (s, 3H), 1.24 (dd, *J* = 6.9, 1.4 Hz, 6H).

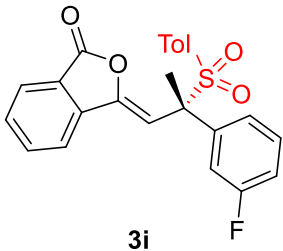
¹³C NMR (101 MHz, CDCl₃) δ 166.0, 149.6, 147.3, 144.8, 139.6, 134.7, 133.5, 131.7, 130.5, 130.5, 128.9, 128.8, 126.1, 125.4, 123.6, 120.3, 104.8, 70.6, 33.7, 23.9, 21.6, 20.6.

IR (thin film): ν_{max} (cm^{-1}) = 2958, 2922, 2361, 2343, 1784, 1717, 1699, 1654, 1596, 1458, 1285, 1262, 1141, 1066, 815, 759, 714, 690, 669, 651.

HRMS (ESI, m/z): Mass calcd. for $\text{C}_{27}\text{H}_{26}\text{NaO}_4\text{S}^+ [\text{M}+\text{Na}]^+$, 469.1444; found 469.1439.

HPLC analysis (Chiralcel IA; 25 °C, IPA/Hexane = 10/90, 0.3 mL/min, 254 nm), $\text{Rt}_1(\text{major}) = 12.5 \text{ min}$, $\text{Rt}_2(\text{minor}) = 10.6 \text{ min}$; ee = 95%).

(*S,Z*)-3-(2-(3-fluorophenyl)-2-tosylpropylidene)isobenzofuran-1(3*H*)-one



White solid, 96% yield, 40.5 mg, m.p. 139–140 °C.

$[\alpha]_D^{25} = -50.6$ (c = 0.5 in CHCl_3).

$^1\text{H NMR}$ (400 MHz, CDCl_3) δ 7.86 (dd, $J = 7.2, 6.2 \text{ Hz}$, 2H), 7.78 (td, $J = 7.8, 0.9 \text{ Hz}$, 1H), 7.60 (td, $J = 7.7, 0.7 \text{ Hz}$, 1H), 7.35 (d, $J = 8.3 \text{ Hz}$, 2H), 7.26 – 7.15 (m, 4H), 7.14 – 7.09 (m, 1H), 7.07 – 6.99 (m, 1H), 6.55 (s, 1H), 2.40 (s, 3H), 2.15 (s, 3H).

$^{13}\text{C NMR}$ (101 MHz, CDCl_3) δ 165.8, 162.2 (d, $J = 245.8 \text{ Hz}$), 147.7, 145.3, 139.3, 138.9 (d, $J = 7.2 \text{ Hz}$), 134.8, 131.1, 130.7, 130.5, 129.4 (d, $J = 8.1 \text{ Hz}$), 129.1, 125.5, 124.7 (d, $J = 2.9 \text{ Hz}$), 123.6, 120.4, 116.3 (d, $J = 23.3 \text{ Hz}$), 115.7 (d, $J = 21.0 \text{ Hz}$), 104.1, 70.3, 21.6, 20.8.

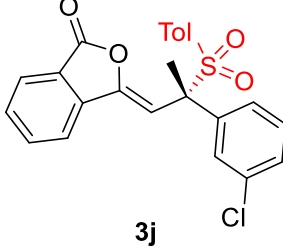
$^{19}\text{F NMR}$ (377 MHz, CDCl_3) δ -112.5.

IR (thin film): ν_{max} (cm^{-1}) = 2988, 2972, 2901, 2361, 2343, 1798, 1680, 1589, 1473, 1436, 1301, 1145, 1050, 984, 824, 799, 770, 709, 690, 672, 658.

HRMS (ESI, m/z): Mass calcd. for $\text{C}_{24}\text{H}_{19}\text{FNaO}_4\text{S}^+ [\text{M}+\text{Na}]^+$, 445.0880; found 445.0878.

HPLC analysis (Chiralcel IA; 25 °C, IPA/Hexane = 15/85, 0.5 mL/min, 254 nm), $\text{Rt}_1(\text{major}) = 44.7 \text{ min}$, $\text{Rt}_2(\text{minor}) = 40.7 \text{ min}$; ee = 97%).

(*S,Z*)-3-(2-(3-chlorophenyl)-2-tosylpropylidene)isobenzofuran-1(3*H*)-one



Yellow solid, 83% yield, 36.4 mg, m.p. 136–137 °C.

$[\alpha]_D^{25} = -46.8$ (c = 0.5 in CHCl_3).

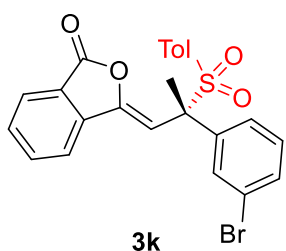
$^1\text{H NMR}$ (400 MHz, CDCl_3) δ 7.86 (dd, $J = 7.8, 4.0 \text{ Hz}$, 2H), 7.78 (td, $J = 7.7, 0.8 \text{ Hz}$, 1H), 7.60 (td, $J = 7.6, 0.7 \text{ Hz}$, 1H), 7.38 – 7.28 (m, 5H), 7.24 – 7.16 (m, 3H), 6.55 (s, 1H), 2.40 (s, 3H), 2.15 (s, 3H).

$^{13}\text{C NMR}$ (101 MHz, CDCl_3) δ 165.8, 147.7, 145.4, 139.3, 138.5, 134.8, 134.0, 131.0, 130.8, 130.5, 129.2, 129.2, 128.8, 127.2, 125.5, 123.6, 120.5, 104.0, 70.4, 21.6, 20.8.

IR (thin film): ν_{max} (cm^{-1}) = 2988, 2972, 2901, 2361, 2343, 1793, 1678, 1594, 1472, 1300, 1291, 1146, 1049, 982, 822, 769, 708, 690, 668, 655.

HRMS (ESI, m/z): Mass calcd. for $\text{C}_{24}\text{H}_{19}\text{ClNaO}_4\text{S}^+ [\text{M}+\text{Na}]^+$, 461.0584; found 461.0580.

HPLC analysis (Chiralcel IA; 25 °C, IPA/Hexane = 15/85, 0.5 mL/min, 254 nm), $\text{Rt}_1(\text{major}) = 32.3 \text{ min}$, $\text{Rt}_2(\text{minor}) = 30.1 \text{ min}$; ee = 98%).



(*S,Z*)-3-(2-(3-bromophenyl)-2-tosylpropylidene)isobenzofuran-1(3*H*)-one

Yellow solid, 89% yield, 43.0 mg, m.p. 136–137 °C.

$[\alpha]_D^{25} = -32.2$ (c = 0.5 in CHCl₃).

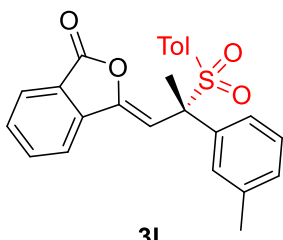
¹H NMR (400 MHz, CDCl₃) δ 7.86 (dd, *J* = 7.8, 3.6 Hz, 2H), 7.78 (td, *J* = 7.8, 0.8 Hz, 1H), 7.60 (td, *J* = 7.8, 0.7 Hz, 1H), 7.49 – 7.43 (m, 1H), 7.41 (t, *J* = 1.7 Hz, 1H), 7.40 – 7.32 (m, 3H), 7.22 – 7.12 (m, 3H), 6.55 (s, 1H), 2.41 (s, 3H), 2.14 (s, 3H).

¹³C NMR (101 MHz, CDCl₃) δ 165.8, 147.7, 145.4, 139.3, 138.7, 134.8, 132.0, 131.8, 131.0, 130.8, 130.5, 129.5, 129.2, 127.7, 125.5, 123.6, 122.1, 120.5, 104.0, 70.4, 21.6, 20.7.

IR (thin film): ν_{max} (cm⁻¹) = 2988, 2972, 2901, 2361, 2343, 1794, 1675, 1596, 1560, 1474, 1290, 1143, 1079, 1060, 970, 758, 752, 688, 672.

HRMS (ESI, m/z): Mass calcd. for C₂₄H₁₉BrNaO₄S⁺ [M+Na]⁺, 505.0079; found 505.0077.

HPLC analysis (Chiralcel IA; 25 °C, IPA/Hexane = 15/85, 0.5 mL/min, 254 nm), Rt₁(major) = 47.7 min, Rt₂(minor) = 45.2 min; ee = 96%).



(*S,Z*)-3-(2-(*m*-tolyl)-2-tosylpropylidene)isobenzofuran-1(3*H*)-one

White solid, 92% yield, 38.5 mg, m.p. 128–129 °C.

$[\alpha]_D^{25} = -55.0$ (c = 0.5 in CHCl₃).

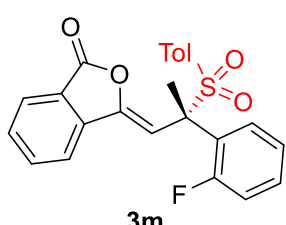
¹H NMR (400 MHz, CDCl₃) δ 7.86 (d, *J* = 7.9 Hz, 2H), 7.77 (t, *J* = 7.6 Hz, 1H), 7.58 (t, *J* = 7.5 Hz, 1H), 7.34 (d, *J* = 8.3 Hz, 2H), 7.22 – 7.18 (m, 2H), 7.17 – 7.10 (m, 4H), 6.60 (s, 1H), 2.39 (s, 3H), 2.28 (s, 3H), 2.17 (s, 3H).

¹³C NMR (101 MHz, CDCl₃) δ 166.0, 147.3, 144.9, 139.6, 137.5, 136.2, 134.7, 131.5, 130.6, 129.6, 129.4, 128.9, 127.9, 126.1, 125.4, 123.6, 120.4, 104.9, 70.7, 21.6, 21.5, 20.7.

IR (thin film): ν_{max} (cm⁻¹) = 2988, 2972, 2901, 2360, 2343, 1793, 1684, 1542, 1395, 1288, 1068, 1049, 975, 873, 820, 764, 687, 677.

HRMS (ESI, m/z): Mass calcd. for C₂₅H₂₂NaO₄S⁺ [M+Na]⁺, 441.1131; found 441.1128.

UPLC analysis (Chiralcel IA; 25 °C, IPA/Hexane = 10/90, 0.3 mL/min, 254 nm), Rt₁(major) = 13.3 min, Rt₂(minor) = 11.9 min; ee = 98%).



(*S,Z*)-3-(2-(2-fluorophenyl)-2-tosylpropylidene)isobenzofuran-1(3*H*)-one

White solid, 62% yield, 26.1 mg, m.p. 126–127 °C.

$[\alpha]_D^{25} = -41.2$ (c = 0.5 in CHCl₃).

¹H NMR (400 MHz, CDCl₃) δ 7.84 (dd, *J* = 8.7, 1.0 Hz, 2H), 7.79 – 7.71 (m, 1H), 7.61 – 7.53 (m, 1H), 7.41 – 7.28 (m, 4H), 7.19 (d, *J* = 8.1 Hz, 2H), 7.07 (td, *J* = 7.8, 1.2 Hz, 1H), 6.89 (ddd, *J* = 12.3, 8.1, 1.1 Hz, 1H), 6.70 (d, *J* = 3.5 Hz, 1H), 2.41 (s, 3H), 2.21 (d, *J* = 1.7 Hz, 3H).

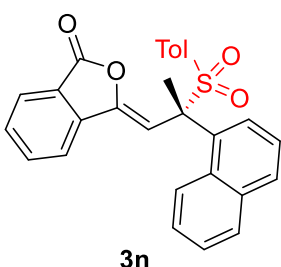
¹³C NMR (101 MHz, CDCl₃) δ 166.0, 161.7 (d, *J* = 253.1 Hz), 146.6 (d, *J* = 3.3 Hz), 145.2, 139.5, 134.7, 131.4, 131.1 (d, *J* = 2.6 Hz), 130.9 (d, *J* = 9.1 Hz), 130.5, 130.4, 129.1, 125.4, 123.8 (d, *J* = 3.4 Hz), 123.6, 123.4 (d, *J* = 8.8 Hz), 120.4, 116.6 (d, *J* = 24.2 Hz), 105.1 (d, *J* = 2.8 Hz), 69.3 (d, *J* = 2.7 Hz), 21.7, 21.6.

¹⁹F NMR (377 MHz, CDCl₃) δ -104.6.

IR (thin film): ν_{max} (cm⁻¹) = 2988, 2972, 2901, 2361, 2343, 1776, 1686, 1596, 1451, 1287, 1141, 1060, 982, 758, 692, 677, 651.

HRMS (ESI, m/z): Mass calcd. for C₂₄H₁₉FNaO₄S⁺ [M+Na]⁺, 445.0880; found 445.0876.

UPLC analysis (Chiralcel IA; 25 °C, IPA/Hexane = 5/95, 0.3 mL/min, 254 nm), Rt₁(major) = 22.5 min, Rt₂(minor) = 19.0 min; ee = 97%).



(*S,Z*)-3-(2-(naphthalen-1-yl)-2-tosylpropylidene)isobenzofuran-1(3*H*)-one

Yellow solid, 90% yield, 40.9 mg, m.p. 129-130 °C.

[*a*D]²⁵ = -40.3 (c = 0.5 in CHCl₃).

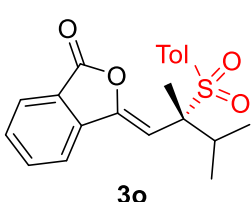
¹H NMR (400 MHz, CDCl₃) δ 7.89 (d, *J* = 7.8 Hz, 1H), 7.84 (d, *J* = 7.7 Hz, 1H), 7.83 – 7.73 (m, 1H), 7.71 (d, *J* = 7.9 Hz, 1H), 7.64 – 7.55 (m, 2H), 7.53 – 7.43 (m, 2H), 7.30 (d, *J* = 8.3 Hz, 2H), 7.07 (d, *J* = 8.0 Hz, 2H), 6.71 (s, 1H), 2.34 (s, 3H), 2.28 (s, 3H).

¹³C NMR (101 MHz, CDCl₃) δ 165.9, 147.6, 145.0, 139.5, 134.8, 133.8, 133.0, 132.6, 131.3, 130.6, 130.5, 129.0, 128.6, 128.5, 127.6, 127.4, 126.8, 126.4, 126.2, 125.5, 123.6, 120.4, 104.7, 70.9, 21.6, 21.0.

IR (thin film): ν_{max} (cm⁻¹) = 2988, 2972, 2901, 2361, 2343, 1790, 1672, 1595, 1473, 1301, 1144, 1047, 970, 816, 757, 690, 660.

HRMS (ESI, m/z): Mass calcd. for C₂₈H₂₂NaO₄S⁺ [M+Na]⁺, 477.1131; found 477.1130.

UPLC analysis (Chiralcel IA; 25 °C, IPA/Hexane = 15/85, 0.5 mL/min, 254 nm), Rt₁(major) = 72.8 min, Rt₂(minor) = 56.7 min; ee = 93%).



(*R,Z*)-3-(2,3-dimethyl-2-tosylbutylidene)isobenzofuran-1(3*H*)-one

Yellow solid, 82% yield, 30.3 mg, m.p. 126-127 °C.

[*a*D]²⁵ = 15.6 (c = 0.3 in CHCl₃).

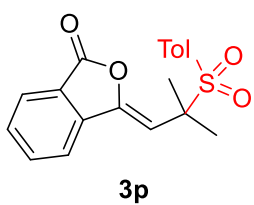
¹H NMR (400 MHz, CDCl₃) δ 7.83 (d, *J* = 7.7 Hz, 1H), 7.78 – 7.71 (m, 2H), 7.63 (d, *J* = 8.3 Hz, 2H), 7.58 (m, 1H), 7.12 (d, *J* = 8.3 Hz, 2H), 5.65 (s, 1H), 2.73 (dt, *J* = 13.6, 6.8 Hz, 1H), 2.33 (s, 3H), 1.71 (s, 3H), 1.26 (d, *J* = 6.7 Hz, 3H), 1.12 (d, *J* = 6.9 Hz, 3H).

¹³C NMR (101 MHz, CDCl₃) δ 165.8, 148.3, 144.7, 139.5, 134.7, 133.4, 130.6, 130.1, 128.9, 125.3, 123.2, 120.1, 105.2, 71.9, 33.4, 21.4, 19.7, 18.3, 15.3.

IR (thin film): ν_{max} (cm⁻¹) = 2971, 2955, 2912, 2880, 2361, 2343, 1783, 1675, 1596, 1472, 1283, 1267, 1081, 1072, 980, 769, 713, 694, 655.

HRMS (ESI, m/z): Mass calcd. for C₂₁H₂₂NaO₄S⁺ [M+Na]⁺, 393.1131; found 393.1126.

UPLC analysis (Chiralcel IA; 25 °C, IPA/Hexane = 10/90, 0.3 mL/min, 254 nm), Rt₁(major) = 9.9 min, Rt₂(minor) = 8.8 min; ee = 72%.



(Z)-3-(2-methyl-2-tosylpropylidene)isobenzofuran-1(3H)-one

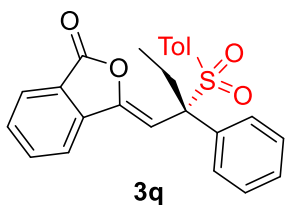
White solid, 82% yield, 28.0 mg, m.p. 138–139 °C.

¹H NMR (400 MHz, CDCl₃) δ 7.86 (d, *J* = 7.7 Hz, 1H), 7.78 – 7.72 (m, 2H), 7.71 – 7.68 (m, 2H), 7.59 (ddd, *J* = 8.1, 6.8, 1.5 Hz, 1H), 7.23 (d, *J* = 8.0 Hz, 2H), 5.72 (s, 1H), 2.40 (s, 3H), 1.75 (s, 6H).

¹³C NMR (101 MHz, CDCl₃) δ 165.8, 147.6, 145.1, 139.5, 134.7, 131.9, 130.68, 130.3, 129.2, 125.4, 123.4, 120.3, 105.0, 64.6, 22.6, 21.6.

IR (thin film): ν_{max} (cm⁻¹) = 2987, 2972, 2901, 1793, 1671, 1596, 1472, 1451, 1395, 1076, 1068, 893, 771, 713, 691, 681.

HRMS (ESI, m/z): Mass calcd. for C₁₉H₁₈NaO₄S⁺ [M+Na]⁺, 365.0818; found 365.0817.



(S,Z)-3-(2-phenyl-2-tosylbutylidene)isobenzofuran-1(3H)-one

White solid, 82% yield, 35.0 mg, m.p. 123–124 °C.

[α]_D²⁵ = -84.5 (c = 0.3 in CHCl₃).

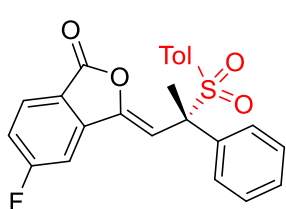
¹H NMR (400 MHz, CDCl₃) δ 7.90 – 7.84 (m, 2H), 7.81 – 7.75 (m, 1H), 7.66 – 7.56 (m, 1H), 7.49 – 7.43 (m, 2H), 7.39 – 7.27 (m, 5H), 7.08 (d, *J* = 8.0 Hz, 2H), 6.27 (s, 1H), 2.82 (dq, *J* = 14.5, 7.3 Hz, 1H), 2.64 (dq, *J* = 14.5, 7.3 Hz, 1H), 2.35 (s, 3H), 0.94 (t, *J* = 7.3 Hz, 3H).

¹³C NMR (101 MHz, CDCl₃) δ 165.8, 147.9, 144.8, 139.6, 134.7, 133.8, 132.2, 130.7, 130.4, 129.6, 128.8, 128.6, 128.0, 125.4, 123.6, 120.3, 101.7, 25.8, 21.5, 9.3.

IR (thin film): ν_{max} (cm⁻¹) = 2987, 2942, 2901, 2885, 2360, 2343, 1780, 1672, 1597, 1472, 1284, 1139, 973, 808, 764, 705, 691, 653.

HRMS (ESI, m/z): Mass calcd. for C₂₅H₂₂NaO₄S⁺ [M+Na]⁺, 441.1131; found 441.1130.

UPLC analysis (Chiralcel IB; 25 °C, IPA/Hexane = 10/90, 0.3 mL/min, 254 nm), Rt₁(major) = 10.7 min, Rt₂(minor) = 12.1 min; ee = 97%.



(S,Z)-5-fluoro-3-(2-phenyl-2-tosylpropylidene)isobenzofuran-1(3H)-one

White solid, 85% yield, 35.9 mg, m.p. 137–138 °C.

[α]_D²⁵ = -67.1 (c = 0.5 in CHCl₃).

¹H NMR (400 MHz, CDCl₃) δ 7.85 (dd, *J* = 8.4, 4.7 Hz, 1H), 7.50 (dd, *J* = 7.8, 2.1 Hz, 1H), 7.41 – 7.36 (m, 2H), 7.35 – 7.23 (m, 6H), 7.15 (d, *J* = 8.2 Hz, 2H), 6.59 (s, 1H), 2.39 (s, 3H), 2.16 (s, 3H).

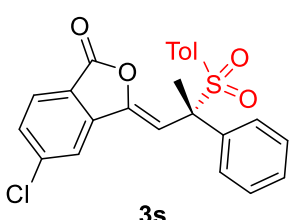
¹³C NMR (101 MHz, CDCl₃) δ 166.9 (d, *J* = 257.2 Hz), 164.7, 146.4 (d, *J* = 4.1 Hz), 145.0, 142.1 (d, *J* = 10.9 Hz), 136.1, 131.2, 130.5, 129.0, 128.9, 128.7, 128.0, 127.9 (d, *J* = 10.6 Hz), 119.8 (d, *J* = 1.5 Hz), 119.0 (d, *J* = 24.4 Hz), 107.4 (d, *J* = 25.1 Hz), 106.1, 70.6, 21.6, 20.5.

¹⁹F NMR (377 MHz, CDCl₃) δ -100.9.

IR (thin film): ν_{max} (cm⁻¹) = 2988, 2901, 2361, 2343, 1775, 1735, 1672, 1601, 1478, 1448, 1289, 1141, 1051, 988, 771, 703, 689, 668, 651.

HRMS (ESI, m/z): Mass calcd. for C₂₄H₁₉FNaO₄S⁺ [M+Na]⁺, 445.0880; found 445.0883.

UPLC analysis (Chiralcel IB; 25 °C, IPA/Hexane = 10/90, 0.3 mL/min, 254 nm), Rt₁(major) = 13.1 min, Rt₂(minor) = 11.1 min; ee = 98%).



(S,Z)-5-chloro-3-(2-phenyl-2-tosylpropylidene)isobenzofuran-1(3H)-one

White solid, 91% yield, 39.9 mg, m.p. 134–135 °C.

[α]_D²⁵ = -86.9 (c = 0.5 in CHCl₃).

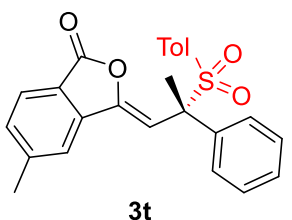
¹H NMR (400 MHz, CDCl₃) δ 7.83 (d, *J* = 1.2 Hz, 1H), 7.78 (d, *J* = 8.2 Hz, 1H), 7.55 (dd, *J* = 8.2, 1.6 Hz, 1H), 7.41 – 7.35 (m, 2H), 7.33 – 7.23 (m, 5H), 7.15 (d, *J* = 8.1 Hz, 2H), 6.61 (s, 1H), 2.39 (s, 3H), 2.16 (s, 3H).

¹³C NMR (101 MHz, CDCl₃) δ 164.8, 146.2, 145.0, 141.7, 141.0, 136.1, 131.2, 131.2, 130.5, 129.0, 128.9, 128.7, 128.1, 126.6, 122.0, 120.7, 106.2, 70.6, 21.6, 20.5.

IR (thin film): ν_{max} (cm⁻¹) = 2988, 2972, 2901, 2361, 2343, 1774, 1291, 1142, 1068, 1052, 982, 891, 778, 688, 680, 651.

HRMS (ESI, m/z): Mass calcd. for C₂₄H₁₉ClNaO₄S⁺ [M+Na]⁺, 461.0584; found 461.0588.

UPLC analysis (Chiralcel IA; 25 °C, IPA/Hexane = 15/85, 0.3 mL/min, 254 nm), Rt₁(major) = 7.2 min, Rt₂(minor) = 6.6 min; ee = 97%).



(S,Z)-5-methyl-3-(2-phenyl-2-tosylpropylidene)isobenzofuran-1(3H)-one

White solid, 79% yield, 33.0 mg, m.p. 126–127 °C.

[α]_D²⁵ = -61.5 (c = 0.5 in CHCl₃).

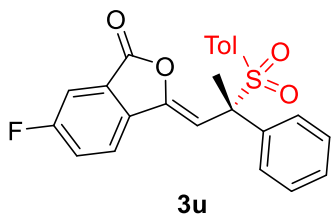
¹H NMR (400 MHz, CDCl₃) δ 7.72 (d, *J* = 7.9 Hz, 1H), 7.64 (s, 1H), 7.44 – 7.36 (m, 3H), 7.35 – 7.29 (m, 3H), 7.26 (t, *J* = 7.3 Hz, 2H), 7.14 (d, *J* = 8.1 Hz, 2H), 6.57 (s, 1H), 2.56 (s, 3H), 2.38 (s, 3H), 2.16 (s, 3H).

¹³C NMR (101 MHz, CDCl₃) δ 166.0, 147.5, 146.1, 144.9, 140.0, 136.4, 131.9, 131.5, 130.5, 129.0, 128.9, 128.6, 128.0, 125.2, 121.2, 120.5, 104.2, 70.7, 22.2, 21.6, 20.7.

IR (thin film): ν_{max} (cm⁻¹) = 2988, 2972, 2901, 1790, 1682, 1595, 1473, 1300, 1292, 1267, 1144, 1068, 1049, 982, 823, 770, 691, 676, 654.

HRMS (ESI, m/z): Mass calcd. for C₂₅H₂₂NaO₄S⁺ [M+Na]⁺, 441.1131; found 441.1127.

UPLC analysis (Chiralcel IA; 25 °C, IPA/Hexane = 10/90, 0.3 mL/min, 254 nm), Rt₁(major) = 13.1 min, Rt₂(minor) = 12.0 min; ee = 98%).



(*S,Z*)-6-fluoro-3-(2-phenyl-2-tosylpropylidene)isobenzofuran-1(3*H*)-one

White solid, 89% yield, 37.6 mg, m.p. 122-123 °C.

$[\alpha]_D^{25} = -57.4$ (c = 0.5 in CHCl₃).

¹H NMR (400 MHz, CDCl₃) δ 7.86 – 7.80 (m, 1H), 7.48 (ddd, *J* = 10.8, 7.7, 2.4 Hz, 2H), 7.39 (dd, *J* = 5.3, 3.3 Hz, 2H), 7.34 – 7.21 (m, 5H), 7.14 (d, *J* = 8.1 Hz, 2H), 6.58 (s, 1H), 2.38 (s, 3H), 2.16 (s, 3H).

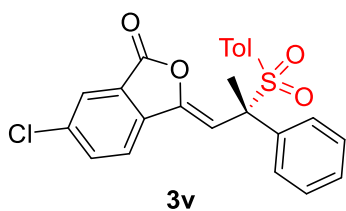
¹³C NMR (101 MHz, CDCl₃) δ 164.7 (d, *J* = 4.1 Hz), 163.9 (d, *J* = 253.0 Hz), 146.7, 145.0, 136.3, 135.5 (d, *J* = 2.2 Hz), 131.3, 130.5, 129.0, 128.9, 128.7, 128.0, 125.6 (d, *J* = 9.4 Hz), 123.0 (d, *J* = 24.6 Hz), 122.5 (d, *J* = 8.8 Hz), 111.7 (d, *J* = 24.3 Hz), 104.9 (d, *J* = 2.1 Hz), 70.7, 21.6, 20.7.

¹⁹F NMR (377 MHz, CDCl₃) δ -107.6.

IR (thin film): ν_{max} (cm⁻¹) = 2988, 2972, 2901, 2361, 2343, 1774, 1683, 1598, 1482, 1293, 1279, 1266, 1145, 1067, 1052, 999, 852, 812, 771, 711, 693.

HRMS (ESI, m/z): Mass calcd. for C₂₄H₁₉FNaO₄S⁺ [M+Na]⁺, 445.0880; found 445.0881.

UPLC analysis (Chiralcel IB; 25 °C, IPA/Hexane = 10/90, 0.3 mL/min, 254 nm), Rt₁(major) = 17.3 min, Rt₂(minor) = 12.5 min; ee = 98%).



(*S,Z*)-6-chloro-3-(2-phenyl-2-tosylpropylidene)isobenzofuran-1(3*H*)-one

White solid, 86% yield, 37.7 mg, m.p. 98-99 °C.

$[\alpha]_D^{25} = -62.9$ (c = 0.5 in CHCl₃).

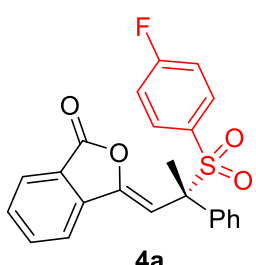
¹H NMR (400 MHz, CDCl₃) δ 7.80 (dd, *J* = 9.6, 5.0 Hz, 2H), 7.72 (dd, *J* = 8.3, 1.8 Hz, 1H), 7.44 – 7.36 (m, 2H), 7.35 – 7.22 (m, 5H), 7.14 (d, *J* = 8.1 Hz, 2H), 6.62 (s, 1H), 2.39 (s, 3H), 2.15 (s, 3H).

¹³C NMR (101 MHz, CDCl₃) δ 164.5, 146.7, 145.0, 137.7, 136.9, 136.2, 135.1, 131.2, 130.5, 129.0, 128.9, 128.7, 128.0, 125.3, 125.2, 121.7, 105.7, 70.7, 21.6, 20.6.

IR (thin film): ν_{max} (cm⁻¹) = 2988, 2972, 2901, 2361, 2343, 1793, 1685, 1458, 1395, 1289, 1248, 1140, 1067, 898, 882, 777, 711, 692, 681, 671.

HRMS (ESI, m/z): Mass calcd. for C₂₄H₁₉ClNaO₄S⁺ [M+Na]⁺, 461.0584; found 461.0581.

UPLC analysis (Chiralcel IA; 25 °C, IPA/Hexane = 10/90, 0.3 mL/min, 254 nm), Rt₁(major) = 19.2 min, Rt₂(minor) = 22.1 min; ee = 97%).



(*S,Z*)-3-((4-fluorophenyl)sulfonyl)-2-phenylpropylidene)isobenzofuran-1(3*H*)-one

White solid, 85% yield, 34.7 mg, m.p. 119-120 °C.

$[\alpha]_D^{25} = -59.2$ (c = 0.5 in CHCl₃).

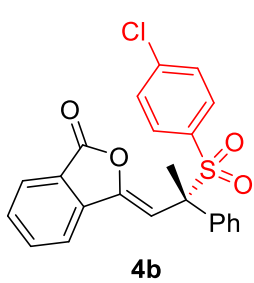
¹H NMR (400 MHz, CDCl₃) δ 7.86 (dd, *J* = 7.8, 4.3 Hz, 2H), 7.77 (td, *J* = 7.9, 0.8 Hz, 1H), 7.59 (td, *J* = 7.6, 0.6 Hz, 1H), 7.46 – 7.37 (m, 4H), 7.36 – 7.24 (m, 3H), 7.06 – 6.99 (m, 2H), 6.59 (s, 1H), 2.19 (s, 3H).

¹³C NMR (101 MHz, CDCl₃) δ 165.9 (d, *J* = 257.3 Hz), 165.8, 147.6, 139.4, 136.1, 134.8, 133.2 (d, *J* = 9.8 Hz), 130.7, 130.3 (d, *J* = 3.3 Hz), 128.9, 128.1, 125.5, 123.6, 120.4, 115.7 (d, *J* = 22.5 Hz), 104.0, 70.9, 20.6.

IR (thin film): ν_{max} (cm⁻¹) = 2988, 2972, 2901, 2361, 2343, 1784, 1395, 1266, 1226, 1143, 1050, 983, 839, 767, 692, 681, 656.

HRMS (ESI, m/z): Mass calcd. for C₂₃H₁₇FNaO₄S⁺ [M+Na]⁺, 431.0723; found 431.0725.

HPLC analysis (Chiralcel IB; 25 °C, IPA/Hexane = 15/85, 0.5 mL/min, 254 nm), Rt₁(major) = 56.2 min, Rt₂(minor) = 47.9 min; ee = 97%.



(*S,Z*)-3-((4-chlorophenyl)sulfonyl)-2-phenylpropylidene)isobenzofuran-1(3*H*)-one

White solid, 69% yield, 29.3 mg, m.p. 121-122 °C.

[*a*]_D²⁵ = -71.3 (c = 0.5 in CHCl₃).

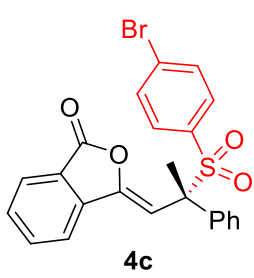
¹H NMR (400 MHz, CDCl₃) δ 7.86 (t, *J* = 7.3 Hz, 2H), 7.78 (dd, *J* = 11.3, 4.7 Hz, 1H), 7.64 – 7.55 (m, 1H), 7.40 (dd, *J* = 5.4, 3.4 Hz, 2H), 7.37 – 7.23 (m, 7H), 6.57 (s, 1H), 2.19 (s, 3H).

¹³C NMR (101 MHz, CDCl₃) δ 165.8, 147.7, 140.8, 139.4, 136.0, 134.8, 132.9, 131.8, 130.7, 128.9, 128.9, 128.7, 128.2, 125.5, 123.6, 120.4, 103.9, 71.0, 20.6.

IR (thin film): ν_{max} (cm⁻¹) = 2988, 2972, 2901, 2361, 2343, 1784, 1675, 1474, 1394, 1299, 1267, 1145, 1049, 975, 765, 752, 691, 676.

HRMS (ESI, m/z): Mass calcd. for C₂₃H₁₇ClNaO₄S⁺ [M+Na]⁺, 447.0428; found 447.0423.

HPLC analysis (Chiralcel IB; 25 °C, IPA/Hexane = 15/85, 0.5 mL/min, 254 nm), Rt₁ (minor) = 60.4 min, Rt₂(major) = 49.9 min; ee = 97%



(*S,Z*)-3-((4-bromophenyl)sulfonyl)-2-phenylpropylidene)isobenzofuran-1(3*H*)-one

White solid, 75% yield, 29.3 mg, m.p. 121-122 °C.

[*a*]_D²⁵ = -70.5 (c = 0.5 in CHCl₃).

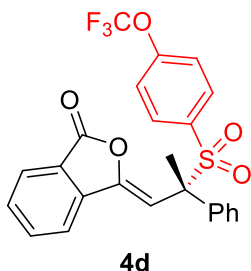
¹H NMR (400 MHz, CDCl₃) δ 7.86 (t, *J* = 7.5 Hz, 2H), 7.81 – 7.73 (m, 1H), 7.62 – 7.57 (m, 1H), 7.49 (d, *J* = 8.6 Hz, 2H), 7.43 – 7.39 (m, 2H), 7.37 – 7.31 (m, 1H), 7.27 (dd, *J* = 12.1, 8.2 Hz, 4H), 6.57 (s, 1H), 2.19 (s, 3H).

¹³C NMR (101 MHz, CDCl₃) δ 165.8, 147.7, 139.4, 136.0, 134.8, 133.5, 131.9, 131.7, 130.8, 129.5, 128.9, 128.9, 128.2, 125.5, 123.6, 120.4, 103.9, 71.0, 20.6.

IR (thin film): ν_{max} (cm⁻¹) = 2988, 2972, 2901, 2361, 2343, 1772, 1717, 1663, 1305, 1142, 1068, 1050, 818, 759, 740, 686.

HRMS (ESI, m/z): Mass calcd. for C₂₃H₁₇BrNaO₄S⁺ [M+Na]⁺, 490.9923; found 490.9921.

HPLC analysis (Chiralcel IB; 25 °C, IPA/Hexane = 15/85, 0.5 mL/min, 254 nm), Rt₁(major) = 62.4 min, Rt₂(minor) = 51.2 min; ee = 96%.



(*S,Z*)-3-(2-phenyl-2-((4-(trifluoromethoxy)phenyl)sulfonyl)propylidene)isobenzofuran-1(3*H*)-one

White solid, 57% yield, 27.8 mg, m.p. 108-109 °C.

$[\alpha]_D^{25} = -53.0$ (c = 0.5 in CHCl₃).

¹H NMR (400 MHz, CDCl₃) δ 7.88 – 7.84 (m, 2H), 7.78 (td, *J* = 7.8, 0.9 Hz, 1H), 7.60 (td, *J* = 7.7, 0.7 Hz, 1H), 7.48 – 7.43 (m, 2H), 7.42 – 7.38 (m, 2H), 7.36 – 7.31 (m, 1H), 7.30 – 7.24 (m, 2H), 7.16 (dd, *J* = 8.8, 0.7 Hz, 2H), 6.58 (s, 1H), 2.20 (s, 3H).

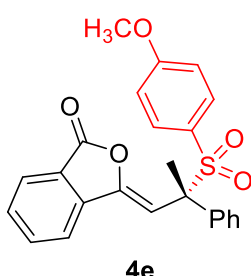
¹³C NMR (101 MHz, CDCl₃) δ 165.8, 153.1 (q, *J* = 1.5 Hz), 147.7, 139.4, 136.0, 134.8, 132.6, 130.8, 129.0, 128.9, 128.2, 125.5, 123.6, 120.4, 120.1 (q, *J* = 260.0 Hz), 119.9, 103.8, 71.1, 20.6.

¹⁹F NMR (377 MHz, CDCl₃) δ -57.7.

IR (thin film): ν_{max} (cm⁻¹) = 2988, 2972, 2901, 2361, 2343, 1790, 1664, 1250, 1230, 1142, 1067, 1052, 981, 770, 757, 707, 700, 685.

HRMS (ESI, m/z): Mass calcd. for C₂₃H₁₇FNaO₄S⁺ [M+Na]⁺, 431.0723; found 431.0723.

UPLC analysis (Chiralcel IB; 25 °C, IPA/Hexane = 10/90, 0.3 mL/min, 254 nm), Rt₁(major) = 9.7 min, Rt₂(minor) = 8.0 min; ee = 95%).



(*S,Z*)-3-(2-((4-methoxyphenyl)sulfonyl)-2-phenylpropylidene)isobenzofuran-1(3*H*)-one

Yellow solid, 86% yield, 36.1 mg, m.p. 127-128 °C.

$[\alpha]_D^{25} = -99.5$ (c = 0.5 in CHCl₃).

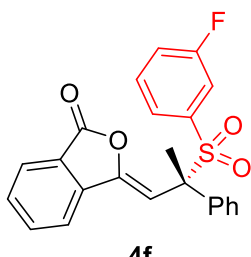
¹H NMR (400 MHz, CDCl₃) δ 7.85 (dd, *J* = 8.6, 0.8 Hz, 2H), 7.79 – 7.73 (m, 1H), 7.60 – 7.55 (m, 1H), 7.43 – 7.38 (m, 2H), 7.37 – 7.23 (m, 5H), 6.84 – 6.78 (m, 2H), 6.61 (s, 1H), 3.83 (s, 3H), 2.18 (s, 3H).

¹³C NMR (101 MHz, CDCl₃) δ 166.0, 163.9, 147.4, 139.5, 136.5, 134.7, 132.6, 130.6, 128.9, 128.6, 128.0, 125.7, 125.4, 123.6, 120.4, 113.6, 104.9, 70.7, 55.6, 20.7.

IR (thin film): ν_{max} (cm⁻¹) = 2988, 2972, 2901, 2361, 2343, 1774, 1670, 1593, 1497, 1291, 1267, 1139, 1053, 983, 838, 768, 694.

HRMS (ESI, m/z): Mass calcd. for C₂₄H₂₀NaO₅S⁺ [M+Na]⁺, 443.0923; found 443.0922.

UPLC analysis (Chiralcel IB; 25 °C, IPA/Hexane = 10/90, 0.3 mL/min, 254 nm), Rt₁ (major) = 19.6 min, Rt₂(minor) = 16.7 min; ee = 97%).



(*S,Z*)-3-(2-((3-fluorophenyl)sulfonyl)-2-phenylpropylidene)isobenzofuran-1(3*H*)-one

Yellow solid, 71% yield, 28.9 mg, m.p. 108-109 °C.

$[\alpha]_D^{25} = -59.8$ (c = 0.5 in CHCl₃).

¹H NMR (400 MHz, CDCl₃) δ 7.89 – 7.83 (m, 2H), 7.81 – 7.74 (m, 1H), 7.63 – 7.57 (m, 1H), 7.41 (dd, *J* = 5.4, 3.3 Hz, 2H), 7.38 – 7.32 (m, 2H), 7.30 – 7.22 (m, 4H), 7.14 – 7.08 (m, 1H), 6.58 (s, 1H), 2.21 (s, 3H).

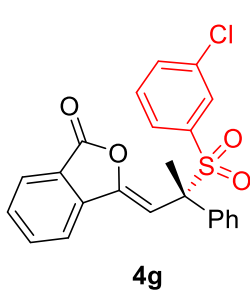
¹³C NMR (101 MHz, CDCl₃) δ 165.8, 161.8 (d, *J* = 252.0 Hz), 147.7, 139.4, 136.5 (d, *J* = 6.5 Hz), 135.9, 134.8, 130.8, 130.0 (d, *J* = 7.6 Hz), 129.0, 128.9, 128.2, 126.3 (d, *J* = 3.3 Hz), 125.5, 123.6, 121.1 (d, *J* = 21.2 Hz), 120.4, 117.8 (d, *J* = 24.3 Hz), 103.8, 71.2, 20.6.

¹⁹F NMR (377 MHz, CDCl₃) δ -110.3.

IR (thin film): ν_{max} (cm⁻¹) = 2988, 2972, 2901, 2361, 2343, 1792, 1671, 1395, 1067, 769, 758, 698, 689, 678.

HRMS (ESI, m/z): Mass calcd. for C₂₃H₁₇FNaO₄S⁺ [M+Na]⁺, 431.0723; found 431.0723.

UPLC analysis (Chiralcel IB; 25 °C, IPA/Hexane = 10/90, 0.3 mL/min, 254 nm), Rt₁(major) = 9.9 min, Rt₂(minor) = 9.2 min; ee = 95%).



(*S,Z*)-3-(2-((3-chlorophenyl)sulfonyl)-2-phenylpropylidene)isobenzofuran-1(3*H*)-one

Yellow solid, 48% yield, 20.3 mg, m.p. 123-124 °C.

[*α*]_D²⁵ = -23.4 (c = 0.2 in CHCl₃).

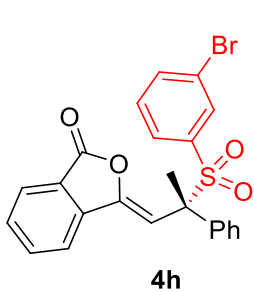
¹H NMR (400 MHz, CDCl₃) δ 7.88 – 7.85 (m, 2H), 7.81 – 7.76 (m, 1H), 7.62 – 7.58 (m, 1H), 7.53 (dt, *J* = 7.2, 1.9 Hz, 1H), 7.43 – 7.39 (m, 2H), 7.36 – 7.25 (m, 6H), 6.56 (s, 1H), 2.19 (s, 3H).

¹³C NMR (101 MHz, CDCl₃) δ 165.8, 147.8, 139.4, 136.1, 135.8, 134.8, 134.7, 133.9, 130.8, 130.5, 129.5, 129.0, 128.9, 128.5, 128.2, 125.5, 123.6, 120.4, 103.7, 71.3, 20.6.

IR (thin film): ν_{max} (cm⁻¹) = 2988, 2972, 2901, 2361, 2343, 1790, 1675, 1407, 1395, 1067, 1058, 979, 889, 757, 684, 671.

HRMS (ESI, m/z): Mass calcd. for C₂₃H₁₇ClNaO₄S⁺ [M+Na]⁺, 447.0428; found 447.0423.

UPLC analysis (Chiralcel IA 25 °C, IPA/Hexane = 10/90, 0.3 mL/min, 254 nm), Rt₁(major) = 11.6 min, Rt₂(minor) = 14.0 min; ee = 87%).



(*S,Z*)-3-(2-((3-bromophenyl)sulfonyl)-2-phenylpropylidene)isobenzofuran-1(3*H*)-one

Yellow solid, 37% yield, 17.3 mg, m.p. 121-122 °C.

[*α*]_D²⁵ = -23.4 (c = 0.2 in CHCl₃).

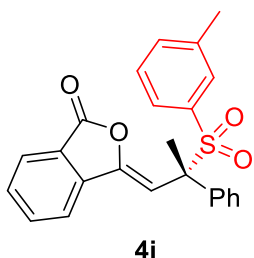
¹H NMR (400 MHz, CDCl₃) δ 7.89 – 7.85 (m, 2H), 7.82 – 7.75 (m, 1H), 7.68 (m, 1H), 7.64 – 7.57 (m, 1H), 7.47 (t, *J* = 1.7 Hz, 1H), 7.44 – 7.34 (m, 4H), 7.33 – 7.27 (m, 2H), 7.23 (d, *J* = 7.9 Hz, 1H), 6.56 (s, 1H), 2.19 (s, 3H).

¹³C NMR (101 MHz, CDCl₃) δ 165.8, 147.8, 139.4, 136.8, 136.3, 135.8, 134.8, 133.4, 130.8, 129.7, 129.1, 128.9, 128.9, 128.2, 125.5, 123.6, 122.5, 120.4, 103.7, 71.3, 20.6.

IR (thin film): ν_{max} (cm⁻¹) = 2988, 2972, 2901, 2360, 2343, 1791, 1674, 1289, 1147, 1067, 1049, 757, 697, 683, 668.

HRMS (ESI, m/z): Mass calcd. for C₂₃H₁₇BrNaO₄S⁺ [M+Na]⁺, 490.9923; found 490.9926.

UPLC analysis (Chiralcel IA; 25 °C, IPA/Hexane = 10/90, 0.3 mL/min, 254 nm), Rt₁(major) = 12.2 min, Rt₂(minor) = 10.4 min; ee = 92%).



(*S,Z*)-3-(2-phenyl-2-(m-tolylsulfonyl)propylidene)isobenzofuran-1(3*H*)-one

White solid, 88% yield, 35.5 mg, m.p. 126-128 °C.

$[\alpha]_D^{25} = -67.9$ (c = 0.5 in CHCl₃).

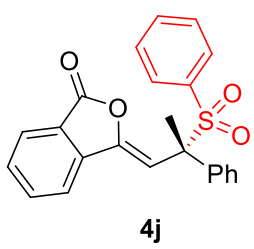
¹H NMR (400 MHz, CDCl₃) δ 7.85 (d, *J* = 8.5 Hz, 2H), 7.80 – 7.74 (m, 1H), 7.61 – 7.55 (m, 1H), 7.40 (dd, *J* = 5.4, 3.3 Hz, 2H), 7.37 – 7.22 (m, 6H), 7.12 (s, 1H), 6.62 (s, 1H), 2.24 (s, 3H), 2.18 (s, 3H).

¹³C NMR (101 MHz, CDCl₃) δ 165.9, 147.5, 139.5, 138.5, 136.3, 134.7, 134.6, 134.1, 131.1, 130.6, 129.0, 128.7, 128.1, 128.0, 127.6, 125.4, 123.6, 120.4, 104.6, 70.9, 20.9, 20.7.

IR (thin film): ν_{max} (cm⁻¹) = 2988, 2972, 2901, 2361, 2343, 1700, 1598, 1449, 1395, 1251, 1136, 881, 766, 689.

HRMS (ESI, m/z): Mass calcd. for C₂₄H₂₀NaO₄S⁺ [M+Na]⁺, 427.0974; found 427.0969.

UPLC analysis (Chiralcel IA; 25 °C, IPA/Hexane = 15/85, 0.5 mL/min, 254 nm), Rt₁(major) = 58.7 min, Rt₂(minor) = 52.3 min; ee = 98%.



(*S,Z*)-3-(2-phenyl-2-(phenylsulfonyl)propylidene)isobenzofuran-1(3*H*)-one

White solid, 77% yield, 30.0 mg, m.p. 109-110 °C.

$[\alpha]_D^{25} = -56.0$ (c = 0.5 in CHCl₃).

¹H NMR (400 MHz, CDCl₃) δ 7.86 (d, *J* = 8.6 Hz, 2H), 7.78 (dd, *J* = 11.2, 4.8 Hz, 1H), 7.62 – 7.50 (m, 2H), 7.44 (dd, *J* = 8.4, 1.2 Hz, 2H), 7.42 – 7.38

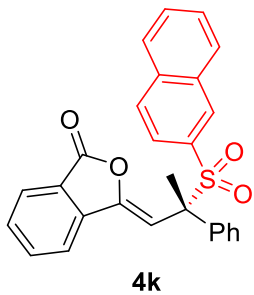
(m, 2H), 7.38 – 7.29 (m, 3H), 7.28 – 7.23 (m, 2H), 6.62 (s, 1H), 2.19 (s, 3H).

¹³C NMR (101 MHz, CDCl₃) δ 165.9, 147.5, 139.5, 136.2, 134.7, 134.4, 133.8, 130.6, 130.5, 128.9, 128.7, 128.3, 128.0, 125.5, 123.6, 120.4, 104.4, 70.8, 20.7.

IR (thin film): ν_{max} (cm⁻¹) = 2988, 2972, 2901, 2361, 2343, 1781, 1699, 1685, 1597, 1577, 1407, 1395, 1251, 1067, 881, 757, 722, 690.

HRMS (ESI, m/z): Mass calcd. for C₂₃H₁₈NaO₄S⁺ [M+Na]⁺, 413.0818; found 413.0814.

UPLC analysis (Chiralcel IA; 25 °C, IPA/Hexane = 10/90, 0.3 mL/min, 254 nm), Rt₁(major) = 14.1 min, Rt₂(minor) = 12.4 min; ee = 98%.



(*S,Z*)-3-(2-(naphthalen-2-ylsulfonyl)-2-phenylpropylidene)isobenzofuran-1(3*H*)-one

White solid, 82% yield, 36.1 mg, m.p. 128-129 °C.

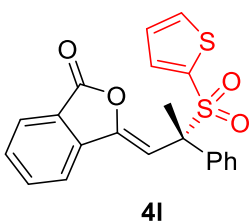
$[\alpha]_D^{25} = -69.4$ (c = 0.5 in CHCl₃).

¹H NMR (400 MHz, CDCl₃) δ 7.99 (s, 1H), 7.86 (dd, *J* = 11.4, 8.1 Hz, 3H), 7.78 (dd, *J* = 13.3, 5.2 Hz, 3H), 7.70 – 7.62 (m, 1H), 7.61 – 7.54 (m, 2H), 7.44 – 7.37 (m, 2H), 7.34 (dd, *J* = 11.8, 4.7 Hz, 2H), 7.23 (t, *J* = 7.6 Hz, 2H), 6.68 (s, 1H), 2.23 (s, 3H).

¹³C NMR (101 MHz, CDCl₃) δ 165.9, 147.6, 139.5, 136.3, 135.2, 134.7, 132.8, 131.6, 131.3, 130.6, 129.4, 129.3, 129.0, 128.8, 128.2, 128.1, 127.8, 127.5, 125.5, 124.9, 123.7, 120.4, 104.5, 71.1, 20.7.
IR (thin film): ν_{max} (cm⁻¹) = 2988, 2972, 2901, 1773, 1664, 1395, 1300, 1067, 1052, 986, 867, 754, 747, 702, 685, 651.

HRMS (ESI, m/z): Mass calcd. for C₂₇H₂₀NaO₄S⁺ [M+Na]⁺, 463.0974; found 463.0970.

UPLC analysis (Chiralcel IA; 25 °C, IPA/Hexane = 10/90, 0.3 mL/min, 254 nm), Rt₁(major) = 25.4 min, Rt₂(minor) = 20.1 min; ee = 94%).



(S,Z)-3-(2-phenyl-2-(thiophen-2-ylsulfonyl)propylidene)isobenzofuran-1(3H)-one

Light yellow oil, 27% yield, 10.7 mg.

[α]_D²⁵ = -7.2 (c = 0.5 in CHCl₃).

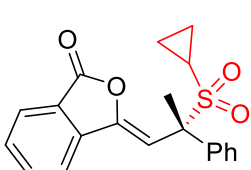
¹H NMR (400 MHz, CDCl₃) δ 7.87 (dd, J = 7.8, 4.5 Hz, 2H), 7.78 (dd, J = 11.1, 4.2 Hz, 1H), 7.65 (dd, J = 5.0, 1.3 Hz, 1H), 7.59 (dd, J = 11.3, 4.2 Hz, 1H), 7.52 – 7.44 (m, 2H), 7.37 – 7.24 (m, 4H), 7.03 (dd, J = 4.9, 3.9 Hz, 1H), 6.60 (s, 1H), 2.28 (s, 3H).

¹³C NMR (101 MHz, CDCl₃) δ 165.9, 147.6, 139.5, 136.6, 136.1, 135.2, 135.1, 134.8, 130.7, 128.9, 128.2, 127.3, 125.5, 123.7, 120.4, 104.3, 71.4, 29.7, 20.7.

IR (thin film): ν_{max} (cm⁻¹) = 2988, 2972, 2901, 1773, 1664, 1395, 1300, 1067, 1052, 754, 747, 702, 685.

HRMS (ESI, m/z): Mass calcd. for C₂₁H₁₆NaO₄S₂⁺ [M+Na]⁺, 419.0382; found 419.0375.

UPLC analysis (Chiralcel IA; 25 °C, IPA/Hexane = 10/90, 0.3 mL/min, 254 nm), Rt₁(major) = 17.1 min, Rt₂(minor) = 15.6 min; ee = 91%).



(S,Z)-3-(2-(cyclopropylsulfonyl)-2-phenylpropylidene)isobenzofuran-1(3H)-one

White oil, 53% yield, 18.7 mg.

[α]_D²⁵ = -8.4 (c = 0.5 in CHCl₃).

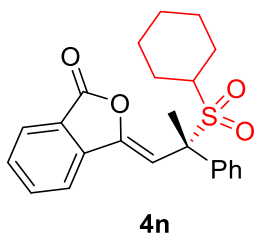
¹H NMR (400 MHz, CDCl₃) δ 7.88 (d, J = 7.7 Hz, 1H), 7.83 (d, J = 7.8 Hz, 1H), 7.76 (t, J = 7.5 Hz, 1H), 7.70 – 7.65 (m, 2H), 7.59 (t, J = 7.5 Hz, 1H), 7.41 – 7.34 (m, 3H), 6.53 (s, 1H), 2.34 (s, 3H), 2.20 – 2.13 (m, 1H), 1.17 – 0.81 (m, 4H).

¹³C NMR (101 MHz, CDCl₃) δ 166.0, 147.3, 139.5, 136.5, 134.8, 130.7, 128.8, 128.7, 128.4, 125.5, 123.7, 120.4, 104.8, 70.1, 25.2, 20.8, 5.1, 4.9.

IR (thin film): ν_{max} (cm⁻¹) = 2988, 2972, 2901, 1790, 1682, 1595, 1473, 1300, 1292, 1267, 1144, 1068, 1049, 982, 823, 770, 691, 676, 654.

HRMS (ESI, m/z): Mass calcd. for C₂₀H₁₈NaO₄S⁺ [M+Na]⁺, 377.0818; found 377.0814.

HPLC analysis (Chiralcel IB; 25 °C, IPA/Hexane = 15/85, 0.5 mL/min, 254 nm), Rt₁(major) = 73.6 min, Rt₂(minor) = 69.9 min; ee = 95%).



(*S,Z*)-3-(2-(cyclohexylsulfonyl)-2-phenylpropylidene)isobenzofuran-1(3*H*)-one

Yellow oil, 28% yield, 11.1 mg.

$[\alpha]_D^{25} = +7.5$ (*c* = 0.4 in CHCl₃).

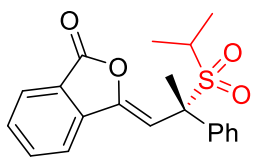
¹H NMR (400 MHz, CDCl₃) δ 7.88 (d, *J* = 7.7 Hz, 1H), 7.83 (d, *J* = 7.8 Hz, 1H), 7.76 (td, *J* = 7.7, 1.0 Hz, 1H), 7.68 – 7.62 (m, 2H), 7.59 (td, *J* = 7.6, 0.8 Hz, 1H), 7.39 – 7.35 (m, 3H), 6.55 (s, 1H), 2.92 (m, 1H), 2.28 (s, 3H), 1.79 (m, 4H), 1.55 – 1.43 (m, 2H), 1.17 – 1.03 (m, 4H).

¹³C NMR (101 MHz, CDCl₃) δ 165.9, 146.6, 139.5, 136.2, 134.8, 130.6, 128.8, 128.6, 128.5, 125.5, 123.7, 120.4, 105.7, 70.6, 58.7, 26.8, 26.5, 25.5, 25.4, 24.9, 20.9.

IR (thin film): ν_{\max} (cm⁻¹) = 2988, 2972, 2901, 1772, 1699, 1598, 1407, 1395, 1251, 1068, 1050, 893, 758, 695, 597, 524, 417.

HRMS (ESI, m/z): Mass calcd. for C₂₃H₂₄NaO₄S⁺ [M+Na]⁺, 419.1287; found 419.1284.

UPLC analysis (Chiralcel IE; 25 °C, IPA/Hexane = 20/80, 0.5 mL/min, 254 nm), Rt₁(major) = 34.6 min, Rt₂(minor) = 24.8 min; ee = 90%).



(*S,Z*)-3-(2-(isopropylsulfonyl)-2-phenylpropylidene)isobenzofuran-1(3*H*)-one

1(3*H*)-one

Yellow oil, 28% yield, 9.9 mg.

$[\alpha]_D^{25} = -1.8$ (*c* = 0.5 in CHCl₃).

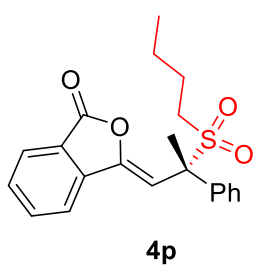
¹H NMR (400 MHz, CDCl₃) δ 7.86 (dd, *J* = 21.9, 7.8 Hz, 2H), 7.76 (td, *J* = 7.7, 0.9 Hz, 1H), 7.70 – 7.64 (m, 2H), 7.59 (td, *J* = 7.7, 0.8 Hz, 1H), 7.37 (dt, *J* = 6.4, 1.9 Hz, 3H), 6.55 (s, 1H), 3.30 – 3.13 (m, 1H), 2.30 (s, 3H), 1.24 (d, *J* = 6.9 Hz, 3H), 1.16 (d, *J* = 6.9 Hz, 3H).

¹³C NMR (101 MHz, CDCl₃) δ 165.9, 146.6, 139.5, 136.2, 134.8, 130.6, 128.9, 128.6, 128.5, 125.5, 123.7, 120.4, 105.6, 70.6, 50.7, 21.0, 17.1, 17.0.

IR (thin film): ν_{\max} (cm⁻¹) = 2987, 2972, 2901, 1763, 1707, 1598, 1449, 1251, 1067, 893, 881, 756, 693.

HRMS (ESI, m/z): Mass calcd. for C₂₀H₂₀NaO₄S⁺ [M+Na]⁺, 379.0974; found 379.0970.

UPLC analysis (Chiralcel IE; 25 °C, IPA/Hexane = 20/80, 0.5 mL/min, 254 nm), Rt₁(major) = 26.1 min, Rt₂(minor) = 21.0 min; ee = 94%).



(*S,Z*)-3-(2-(butylsulfonyl)-2-phenylpropylidene)isobenzofuran-1(3*H*)-one

White oil, 37% yield, 9.9 mg.

$[\alpha]_D^{25} = -21.8$ (*c* = 0.4 in CHCl₃).

¹H NMR (400 MHz, CDCl₃) δ 7.89 (d, *J* = 7.7 Hz, 1H), 7.85 (d, *J* = 7.8 Hz, 1H), 7.80 – 7.73 (m, 1H), 7.69 – 7.63 (m, 2H), 7.62 – 7.56 (m, 1H), 7.46 –

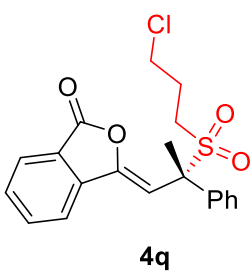
7.33 (m, 3H), 6.49 (s, 1H), 2.89 – 2.64 (m, 2H), 2.30 (s, 3H), 1.83 – 1.65 (m, 2H), 1.48 – 1.29 (m, 2H), 0.87 (t, J = 7.3 Hz, 3H).

^{13}C NMR (101 MHz, CDCl_3) δ 165.9, 147.5, 139.4, 136.2, 134.8, 130.7, 128.9, 128.6, 128.6, 125.5, 123.7, 120.5, 104.5, 69.7, 46.9, 22.9, 21.9, 20.6, 13.5.

IR (thin film): ν_{max} (cm^{-1}) = 2987, 2971, 2901, 1783, 1678, 1598, 1448, 1262, 1135, 1054, 976, 769, 693, 593, 510.

HRMS (ESI, m/z): Mass calcd. for $\text{C}_{21}\text{H}_{22}\text{NaO}_4\text{S}^+$ [M+Na] $^+$, 393.1131; found 393.1127.

UPLC analysis (Chiralcel IE; 25 °C, IPA/Hexane = 20/80, 0.5 mL/min, 254 nm), Rt_1 (major) = 22.8 min, Rt_2 (minor) = 18.9 min; ee = 98%).



(*S,Z*)-3-(2-((3-chloropropyl)sulfonyl)-2-phenylpropylidene)isobenzofuran-1(3*H*)-one

White oil, 20% yield, 7.8 mg.

$[\alpha]_D^{25} = +20.8$ ($c = 0.2$ in CHCl_3).

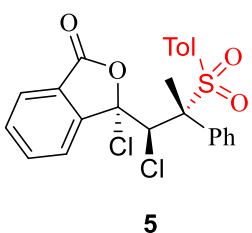
^1H NMR (400 MHz, CDCl_3) δ 7.87 (dd, J = 16.9, 7.8 Hz, 2H), 7.81 – 7.74 (m, 1H), 7.68 – 7.58 (m, 3H), 7.44 – 7.37 (m, 3H), 6.46 (s, 1H), 3.66 – 3.54 (m, 2H), 3.08 – 2.90 (m, 2H), 2.32 (s, 3H), 2.22 – 2.13 (m, 2H).

^{13}C NMR (101 MHz, CDCl_3) δ 165.8, 147.7, 139.3, 135.7, 134.8, 130.8, 129.1, 128.7, 128.6, 125.6, 123.7, 120.5, 103.9, 70.1, 44.5, 43.1, 24.5, 20.6.

IR (thin film): ν_{max} (cm^{-1}) = 2987, 2972, 2901, 1789, 1675, 1590, 1447, 1293, 1137, 1055, 979, 768, 701, 690, 597, 579, 512.

HRMS (ESI, m/z): Mass calcd. for $\text{C}_{20}\text{H}_{19}\text{ClNaO}_4\text{S}^+$ [M+Na] $^+$, 413.0584; found 413.0580.

UPLC analysis (Chiralcel IE; 25 °C, IPA/Hexane = 20/80, 0.5 mL/min, 254 nm), Rt_1 (major) = 29.0 min, Rt_2 (minor) = 22.9 min; ee = 94%).



(*S*)-3-chloro-3-((1*R*,2*R*)-1-chloro-2-phenyl-2-tosylpropyl)isobenzofuran-1(3*H*)-one

White oil, 63% yield, 29.8 mg.

$[\alpha]_D^{25} = -122.5$ ($c = 0.5$ in CHCl_3).

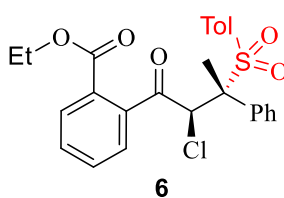
^1H NMR (400 MHz, CDCl_3) δ 8.03 (d, J = 7.9 Hz, 1H), 7.96 (d, J = 7.6 Hz, 1H), 7.79 (td, J = 7.7, 1.1 Hz, 1H), 7.66 (td, J = 7.6, 0.8 Hz, 1H), 7.42 (d, J = 7.3 Hz, 2H), 7.24 – 7.16 (m, 3H), 7.02 (d, J = 8.3 Hz, 2H), 6.90 (d, J = 8.1 Hz, 2H), 5.67 (s, 1H), 2.24 (s, 3H), 2.03 (s, 3H).

^{13}C NMR (101 MHz, CDCl_3) δ 166.0, 149.9, 144.1, 136.5, 134.7, 134.5, 131.3, 129.5, 128.7, 128.6, 128.2, 127.9, 125.7, 125.7, 124.3, 101.1, 74.9, 68.3, 21.4, 16.5.

IR (thin film): ν_{max} (cm^{-1}) = 2987, 2972, 2901, 1797, 1717, 1597, 1395, 1251, 1140, 1067, 753, 686, 639, 575, 517.

HRMS (ESI, m/z): Mass calcd. for $\text{C}_{24}\text{H}_{20}\text{Cl}_2\text{NaO}_4\text{S}^+$ [M+Na] $^+$, 497.0352; found 497.0352.

UPLC analysis (Chiralcel IA; 25 °C, IPA/Hexane = 10/90, 0.3 mL/min, 254 nm), Rt₁(major) = 14.3 min, Rt₂(minor) = 22.9 min; ee = 97%).



2-((2*S*,3*R*)-2-chloro-3-phenyl-3-tosylbutanoyl)-N,N-diethylbenzamide

White oil, 74% yield, 35.8 mg.

$[\alpha]_D^{25} = -113.4$ (c = 0.4 in CHCl₃).

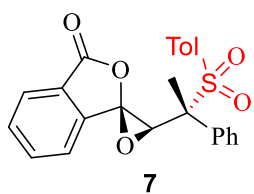
¹H NMR (400 MHz, CDCl₃) δ 8.03 (dd, *J* = 7.5, 1.3 Hz, 1H), 7.80 (dd, *J* = 7.3, 1.6 Hz, 1H), 7.67 – 7.56 (m, 2H), 7.54 (d, *J* = 7.2 Hz, 2H), 7.37 – 7.27 (m, 3H), 7.10 (d, *J* = 8.3 Hz, 2H), 7.02 (d, *J* = 8.2 Hz, 2H), 6.21 (s, 1H), 4.40 (m, 2H), 2.32 (s, 3H), 2.08 (s, 3H), 1.38 (t, *J* = 7.1 Hz, 3H).

¹³C NMR (101 MHz, CDCl₃) δ 194.0, 167.9, 144.8, 138.3, 134.9, 132.7, 132.6, 131.7, 131.0, 130.1, 129.9, 129.4, 128.9, 128.8, 128.5, 128.2, 73.6, 61.9, 60.1, 21.5, 16.1, 14.6.

IR (thin film): ν_{\max} (cm⁻¹) = 2987, 2901, 1781, 1706, 1596, 1447, 1395, 1264, 1140, 1058, 881, 753, 695, 636, 574, 519.

HRMS (ESI, m/z): Mass calcd. for C₂₈H₃₀ClNNaO₄S⁺ [M+Na]⁺, 507.1003; found 507.1001.

UPLC analysis (Chiralcel IE; 25 °C, IPA/Hexane = 50/50, 0.5 mL/min, 254 nm), Rt₁(major) = 19.9 min, Rt₂(minor) = 29.4 min; ee = 97%).



(1*S*,3*S*)-3'-((*R*)-1-phenyl-1-tosylethyl)-3H-spiro[isobenzofuran-1,2'-oxiran]-3-one

White solid, 62% yield, 26.0 mg, m.p. 118–119 °C.

$[\alpha]_D^{25} = -25.4$ (c = 0.4 in CHCl₃).

¹H NMR (400 MHz, CDCl₃) δ 7.87 (d, *J* = 7.6 Hz, 1H), 7.81 (td, *J* = 7.6, 1.0 Hz, 1H), 7.77 – 7.73 (m, 2H), 7.69 (td, *J* = 7.5, 0.8 Hz, 1H), 7.51 (d, *J* = 7.7 Hz, 1H), 7.45 – 7.41 (m, 3H), 7.37 (d, *J* = 8.3 Hz, 2H), 6.99 (d, *J* = 8.0 Hz, 2H), 4.63 (s, 1H), 2.34 (s, 3H), 1.89 (s, 3H).

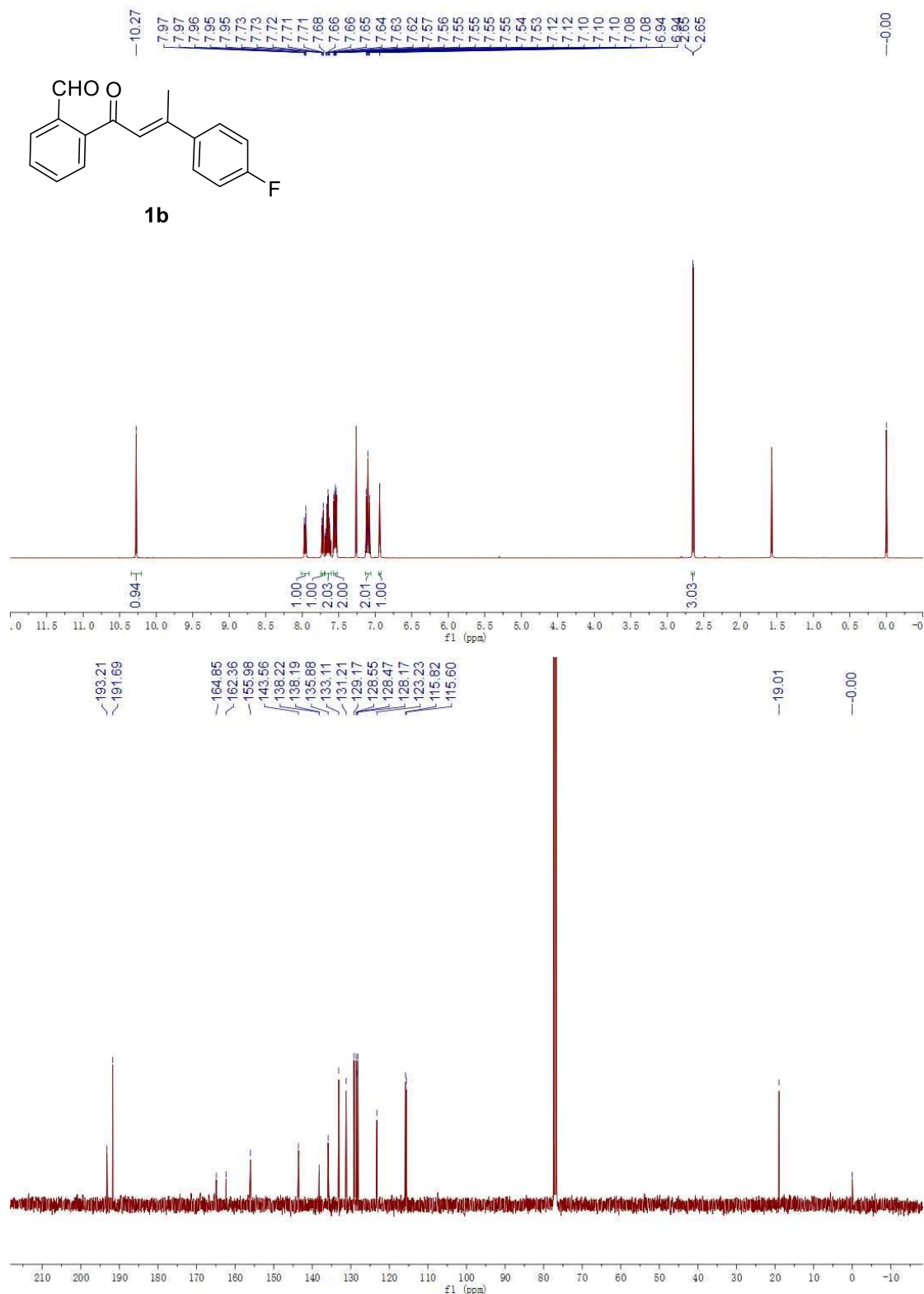
¹³C NMR (101 MHz, CDCl₃) δ 165.5, 145.4, 142.5, 135.1, 133.8, 132.3, 131.7, 130.0, 129.3, 129.0, 129.0, 128.4, 127.4, 125.3, 121.6, 89.1, 70.2, 63.2, 21.5, 17.7.

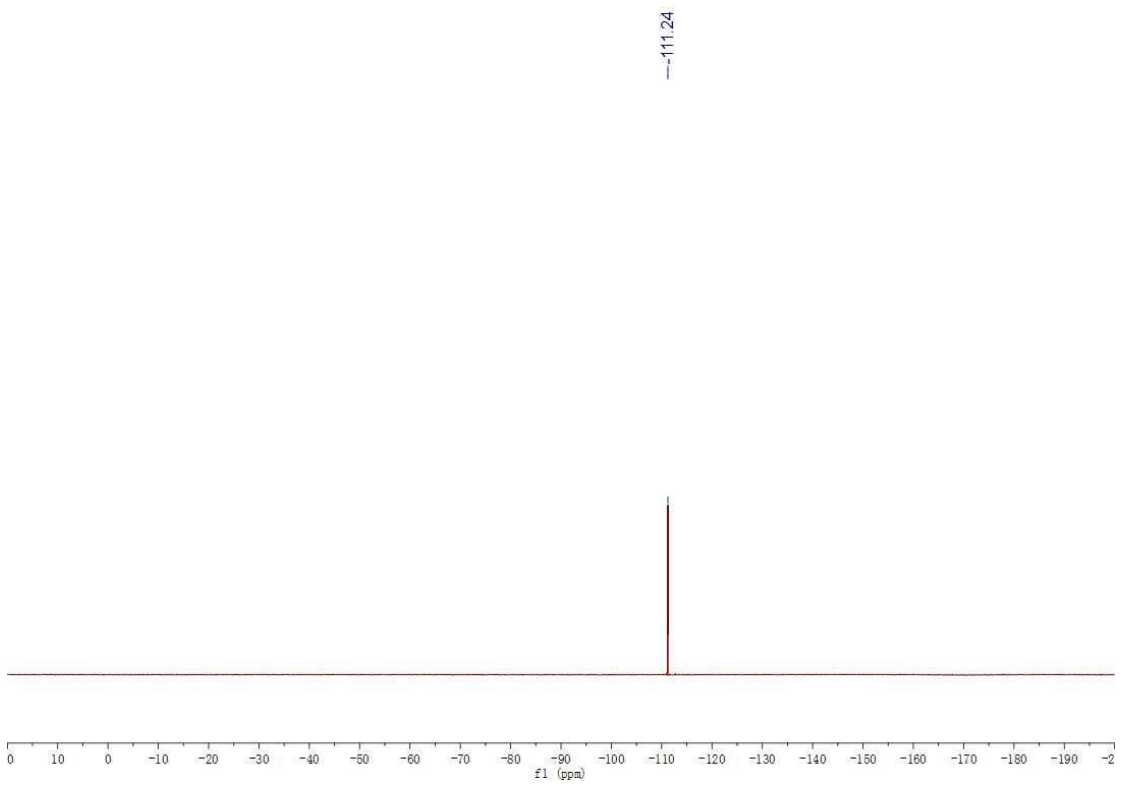
IR (thin film): ν_{\max} (cm⁻¹) = 2987, 2972, 2901, 1784, 1736, 1698, 1596, 1407, 1395, 1258, 1067, 1059, 893, 701, 690, 666, 654, 561, 534.

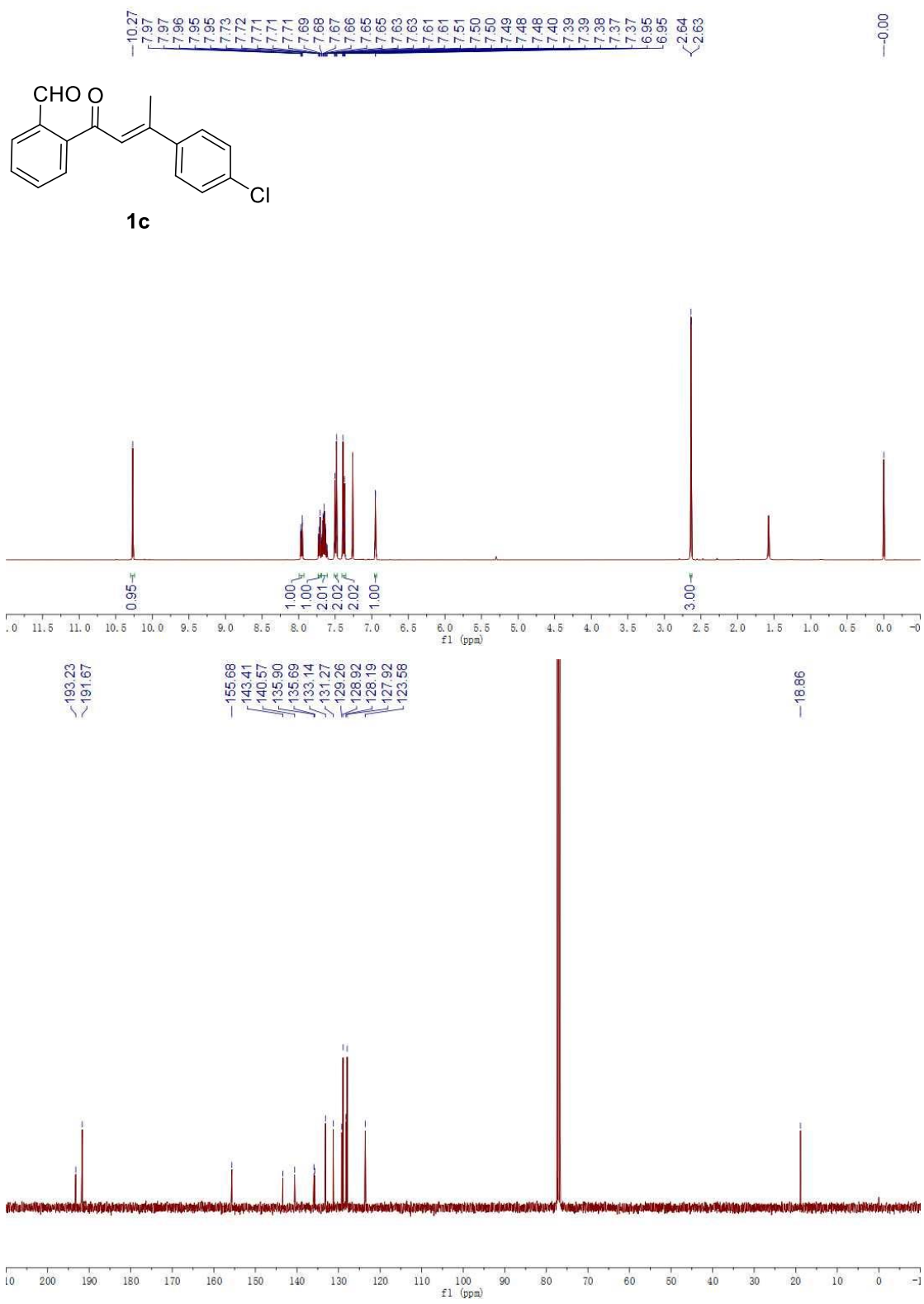
HRMS (ESI, m/z): Mass calcd. for C₂₄H₂₀NaO₅S⁺ [M+Na]⁺, 443.0924; found 443.0927.

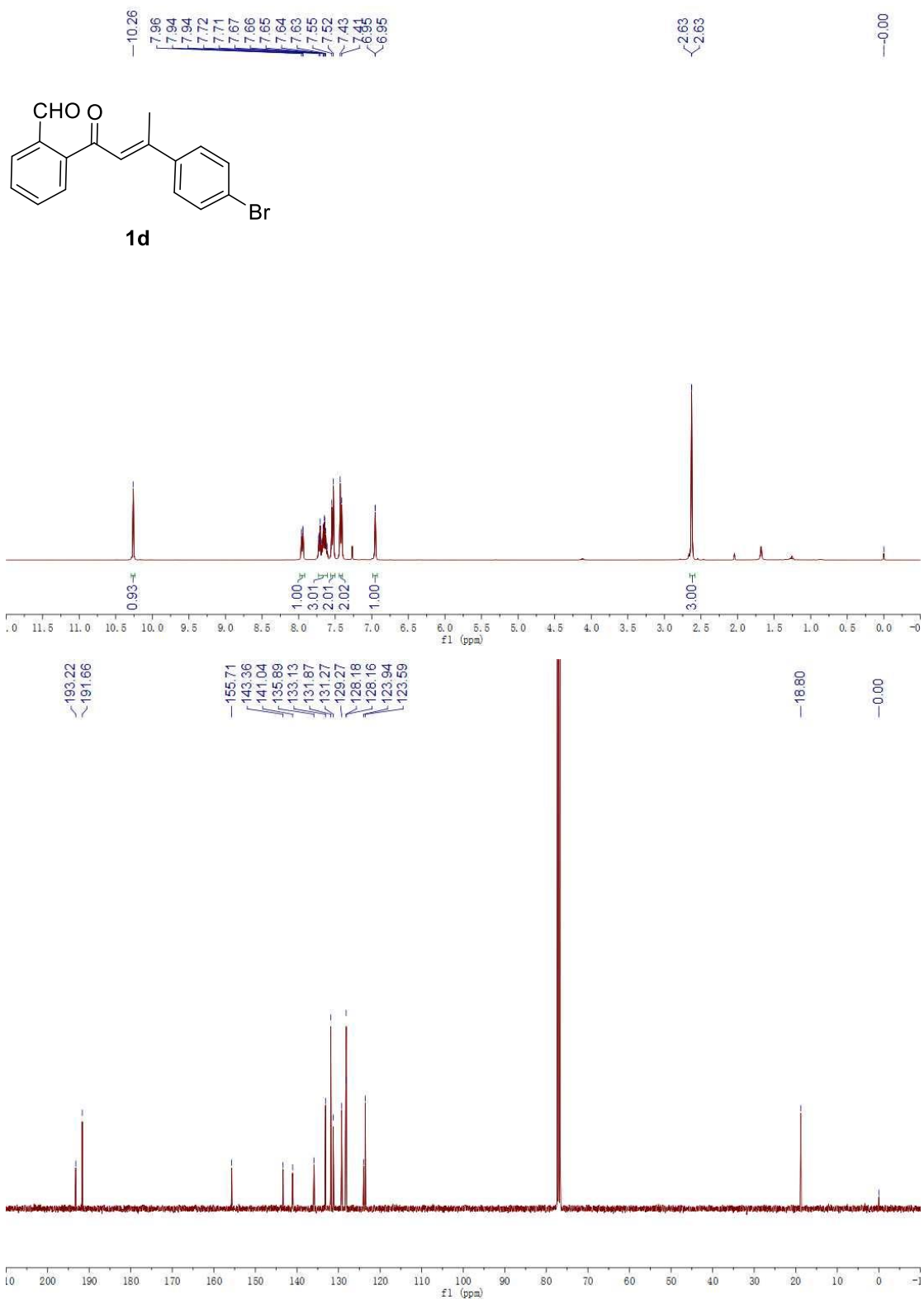
HPLC analysis (Chiralcel IA; 25 °C, IPA/Hexane = 10/90, 0.5 mL/min, 254 nm), Rt₁(major) = 61.9 min, Rt₂(minor) = 75.0 min; ee = 98%).

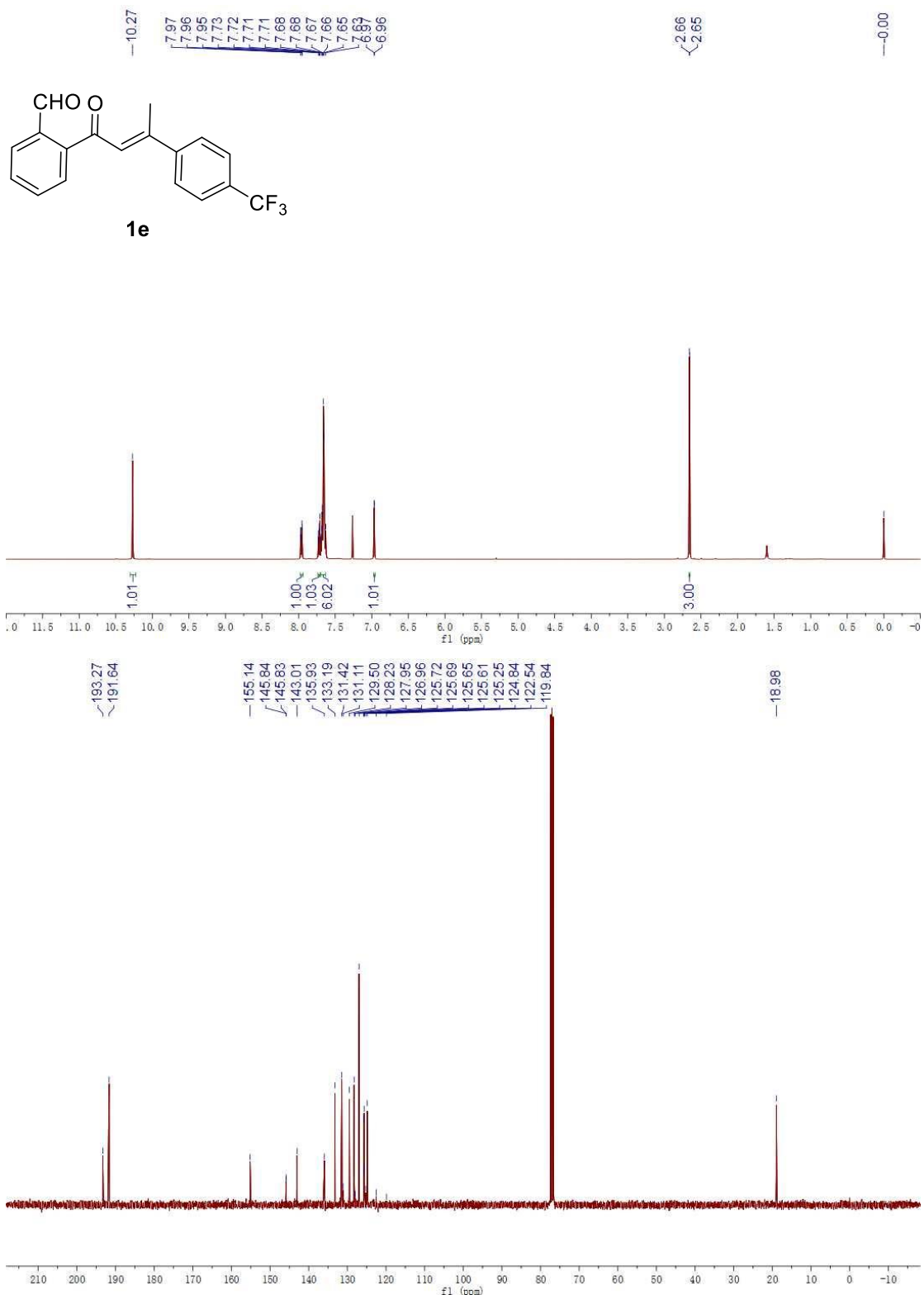
XIV. ^1H NMR, ^{13}C NMR, ^{19}F NMR and HPLC spectra

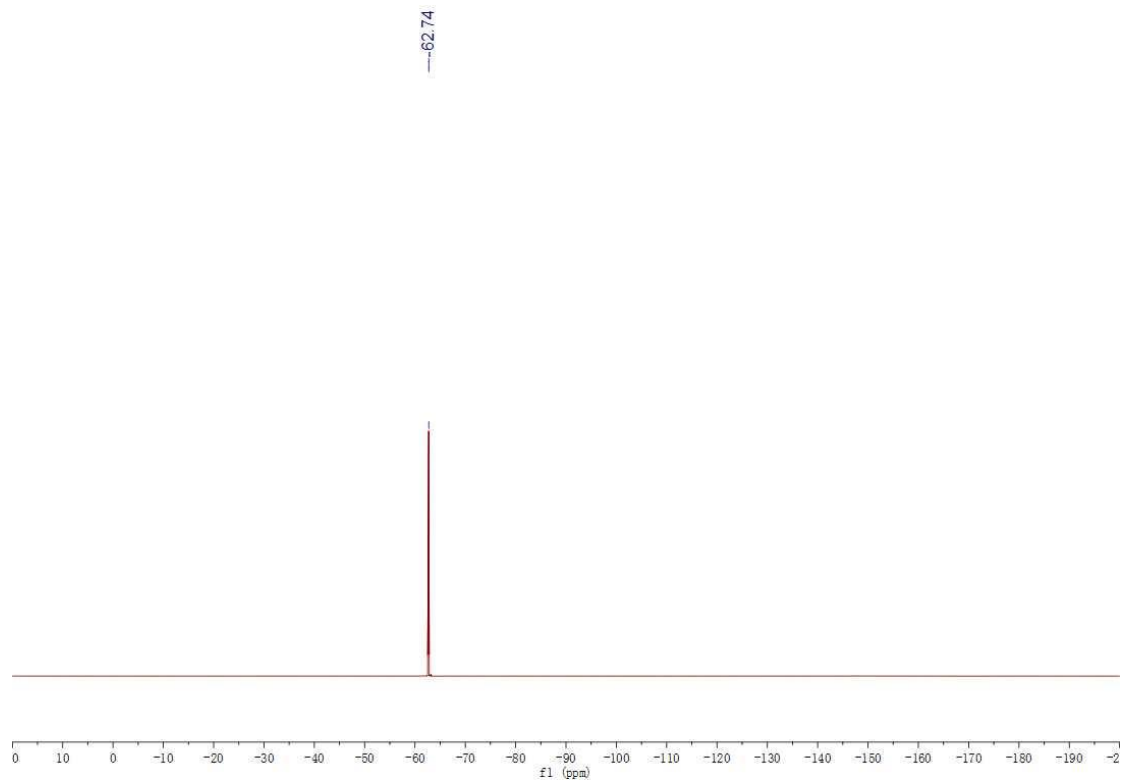


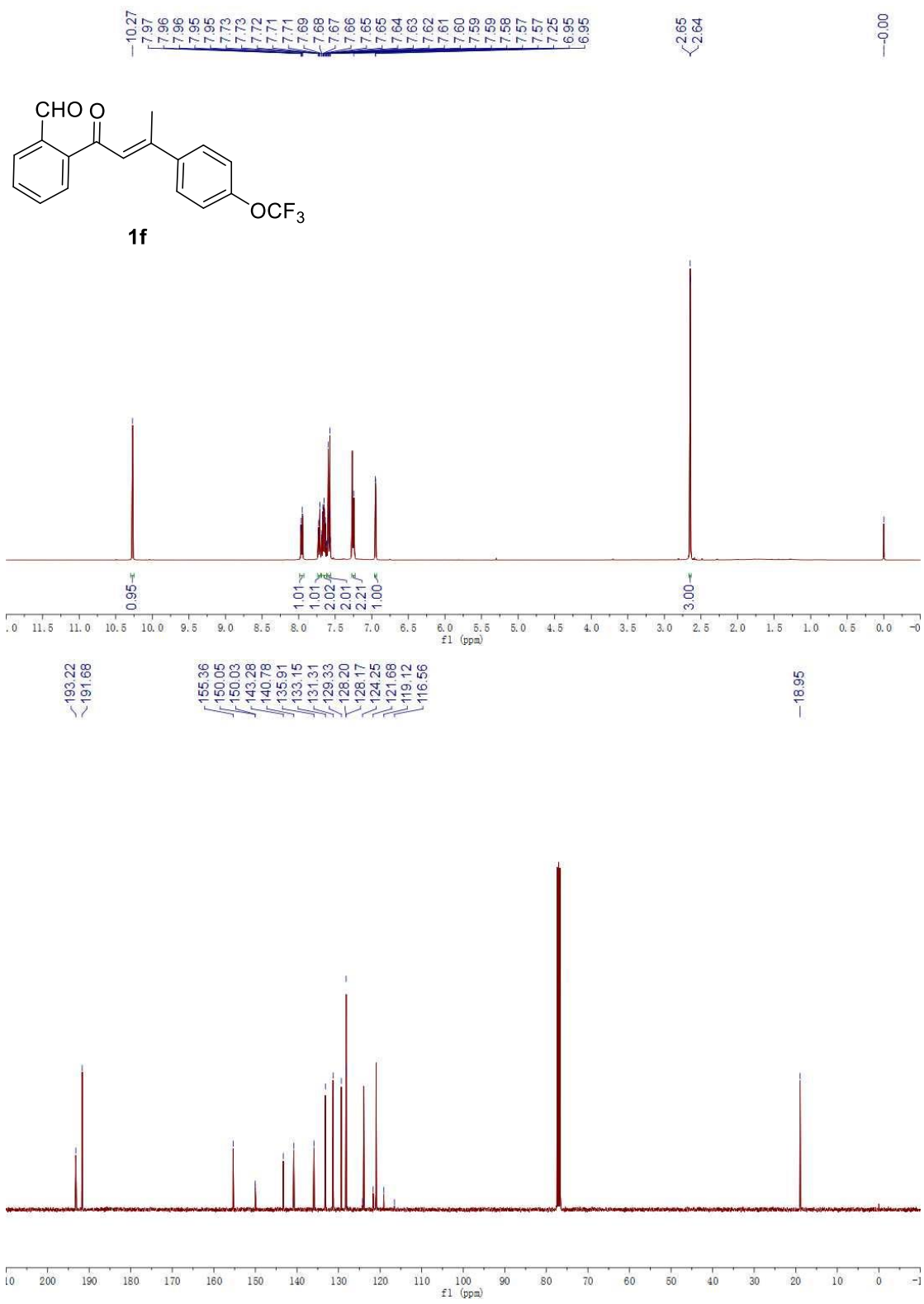


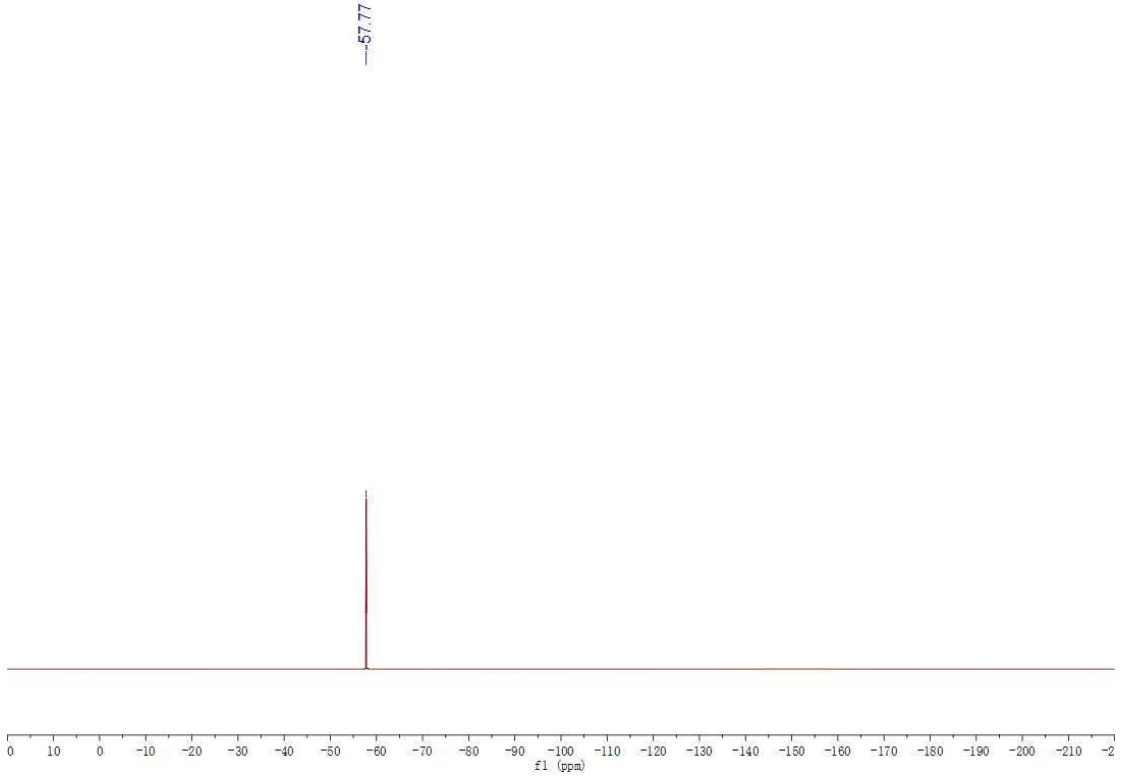


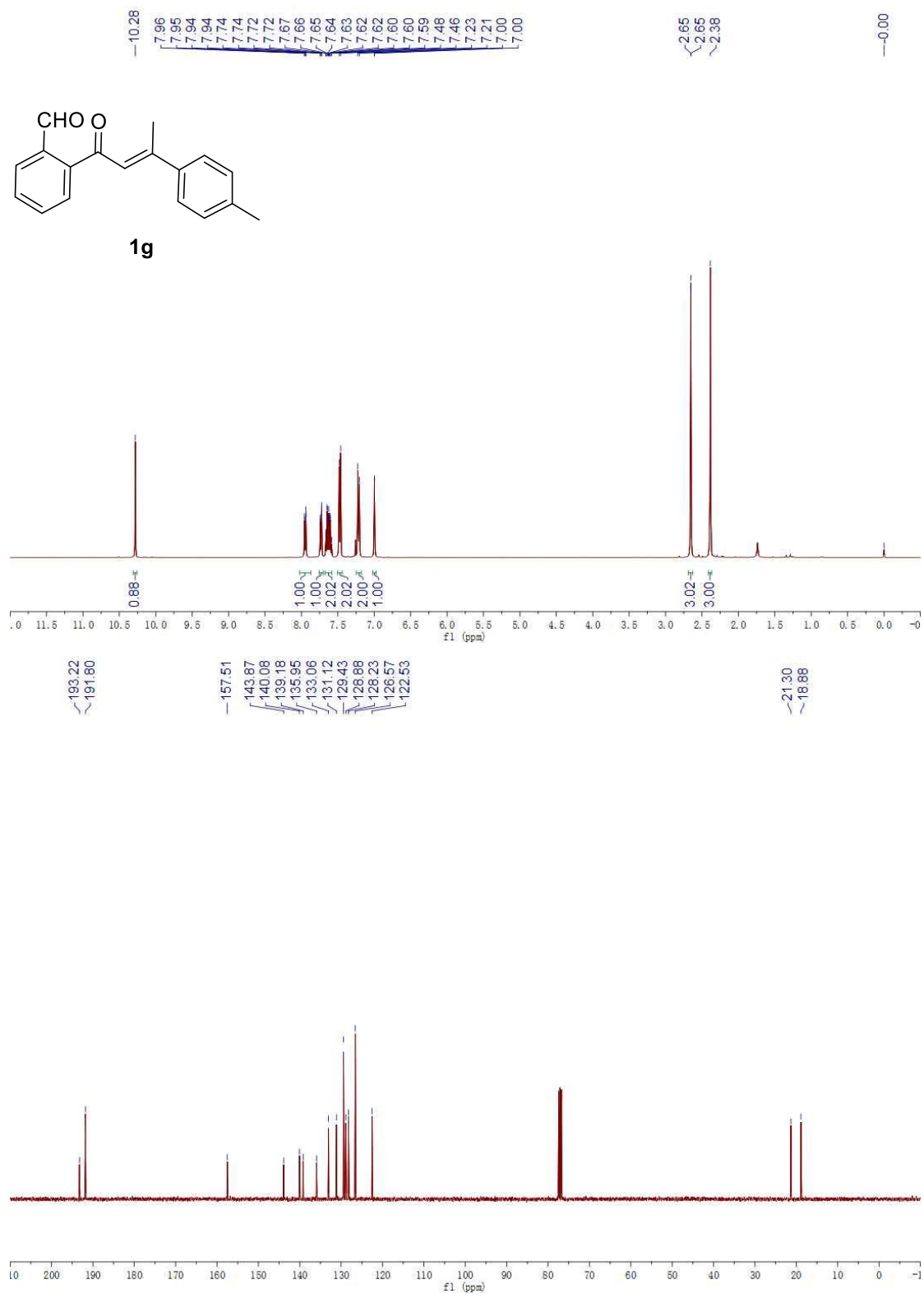


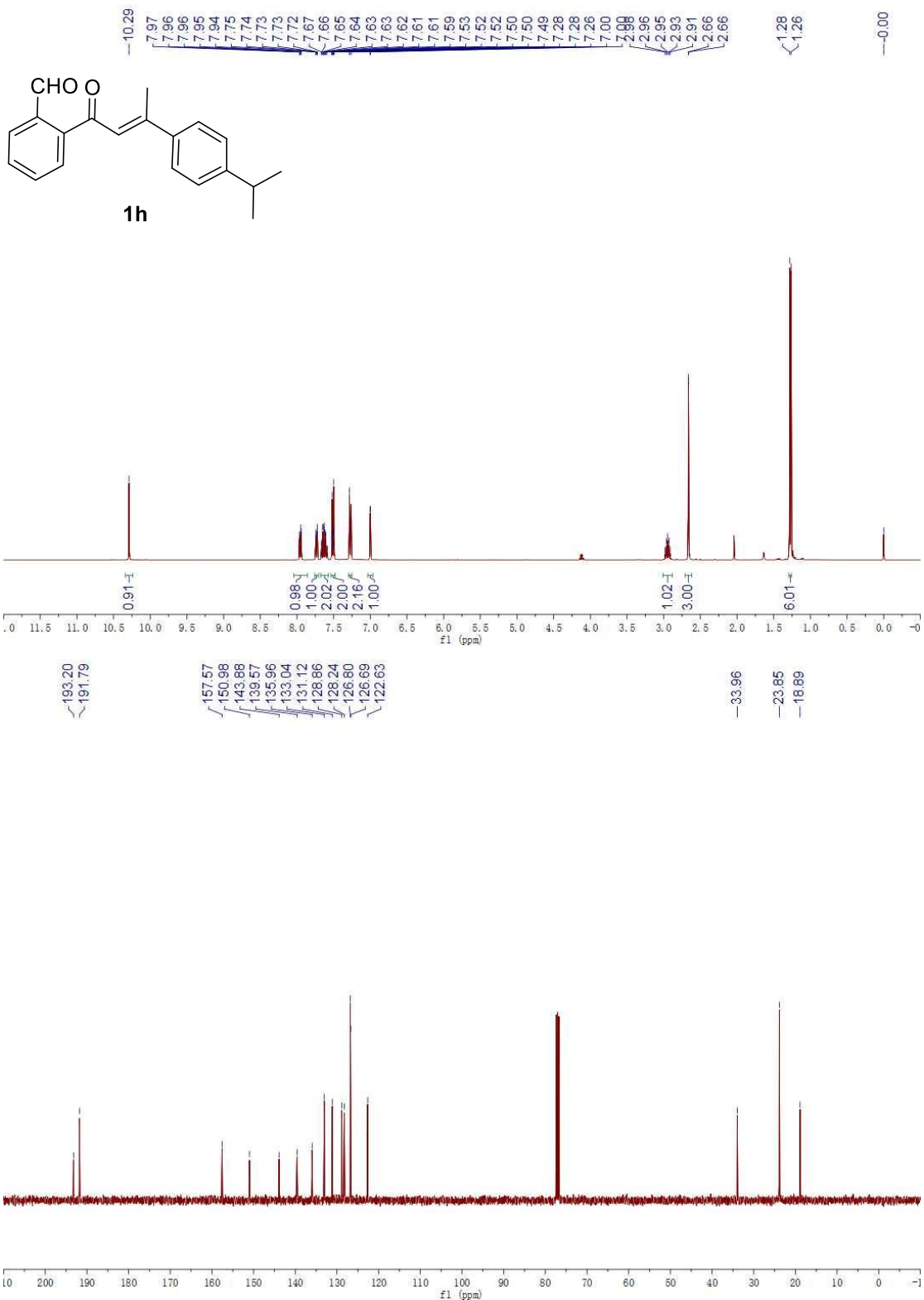


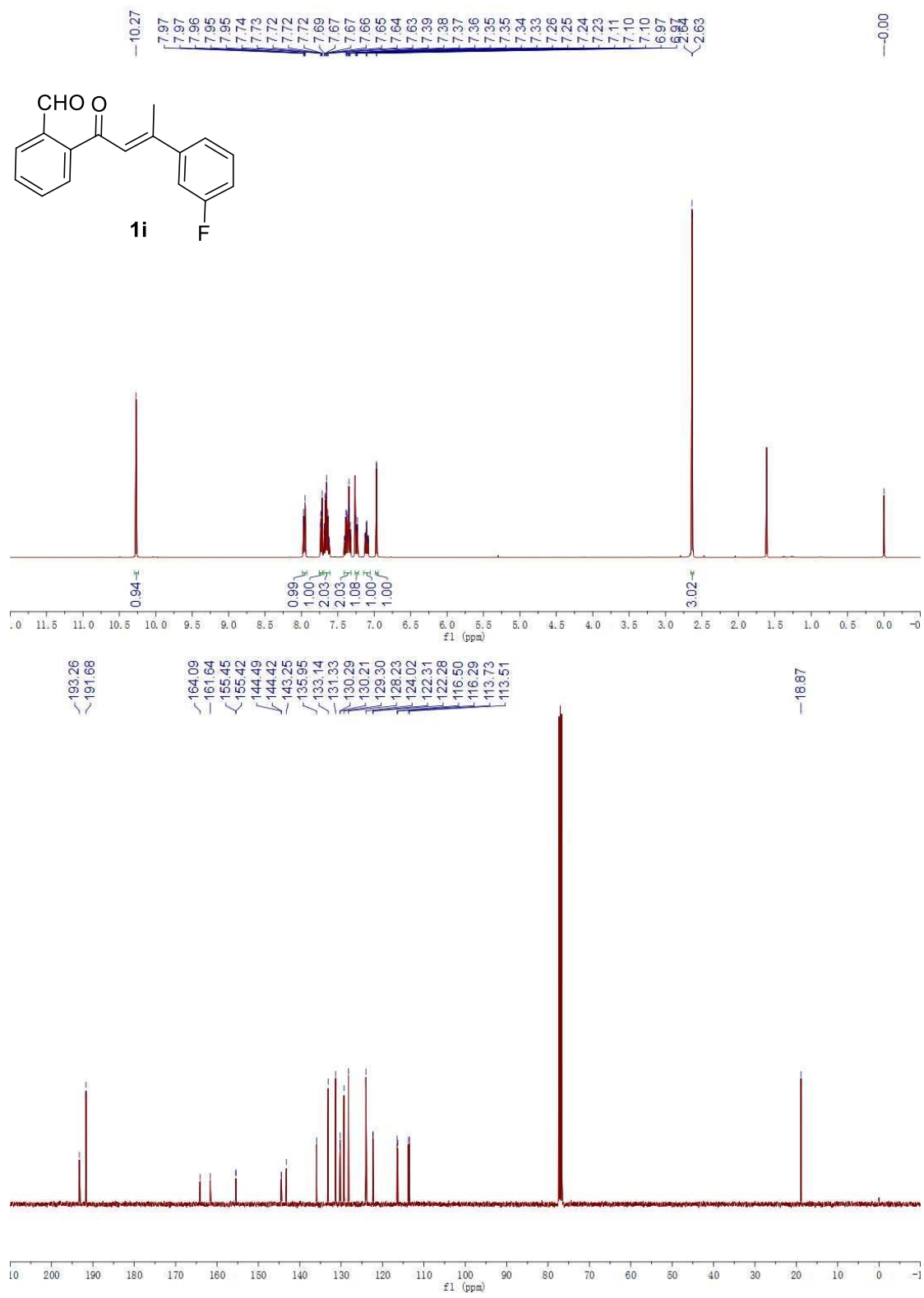


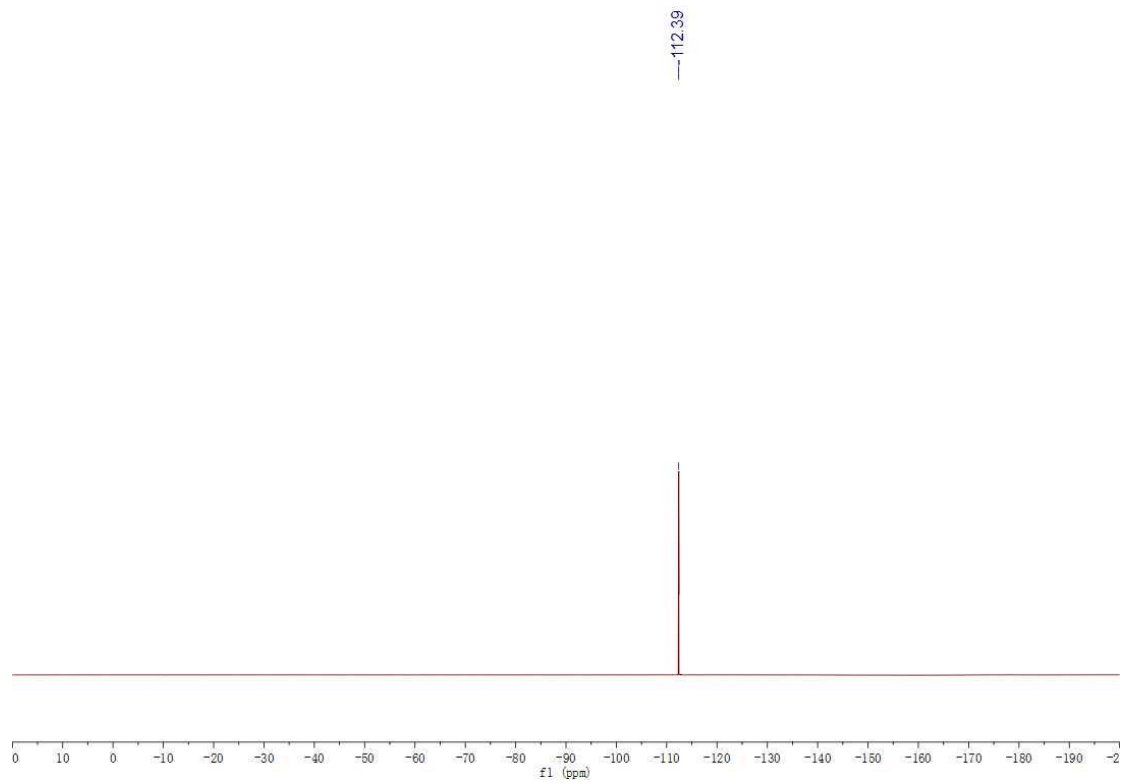


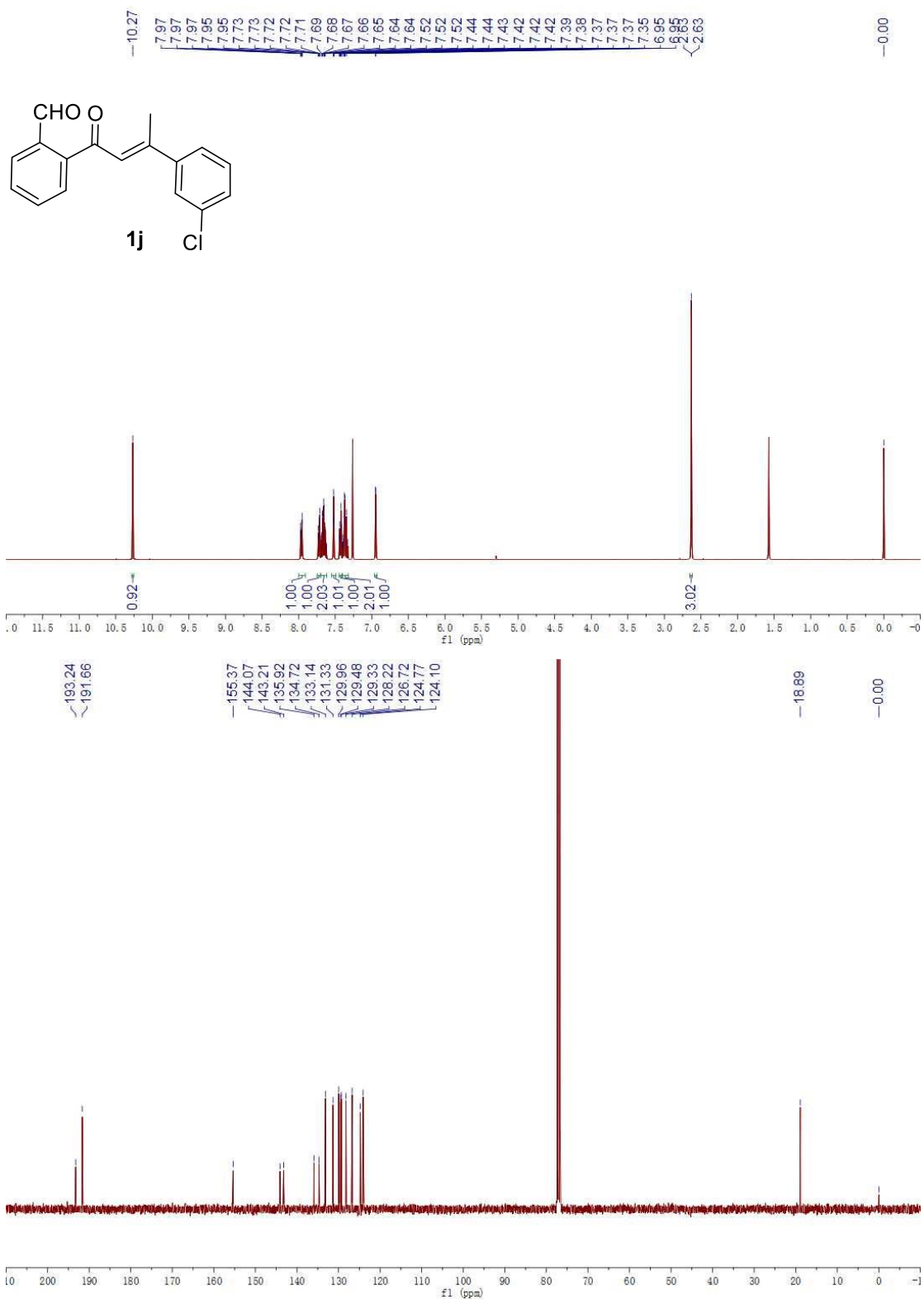


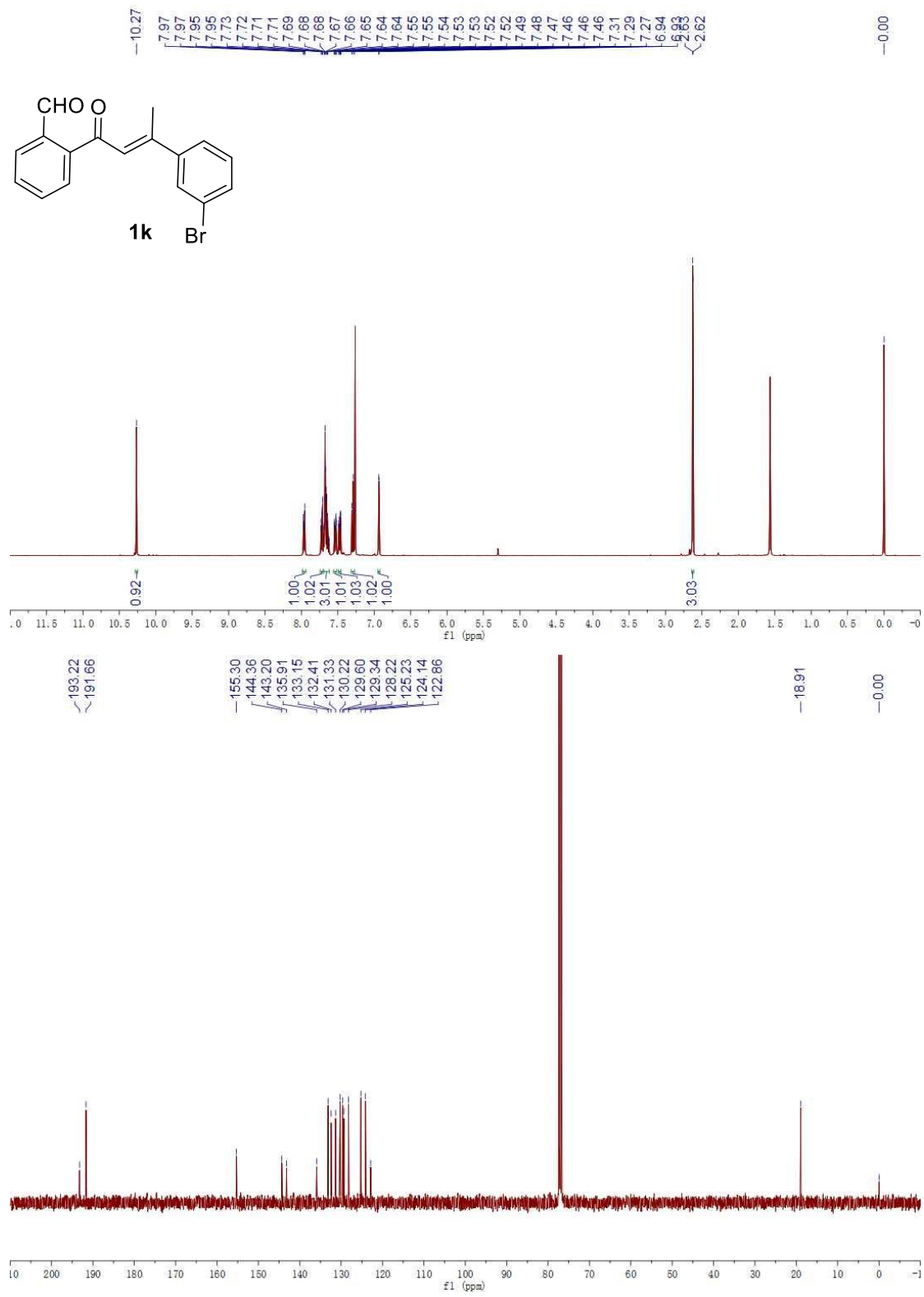


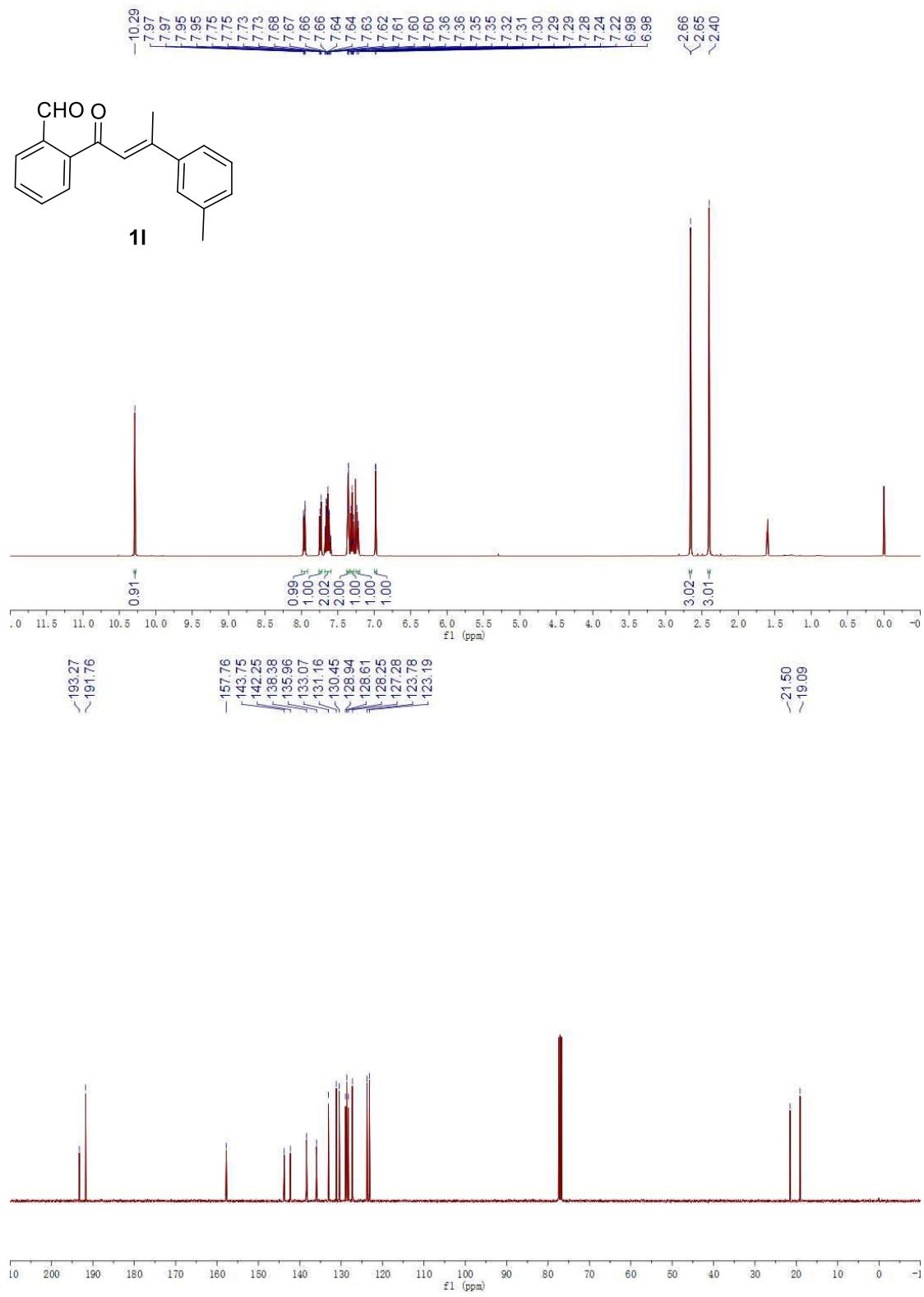


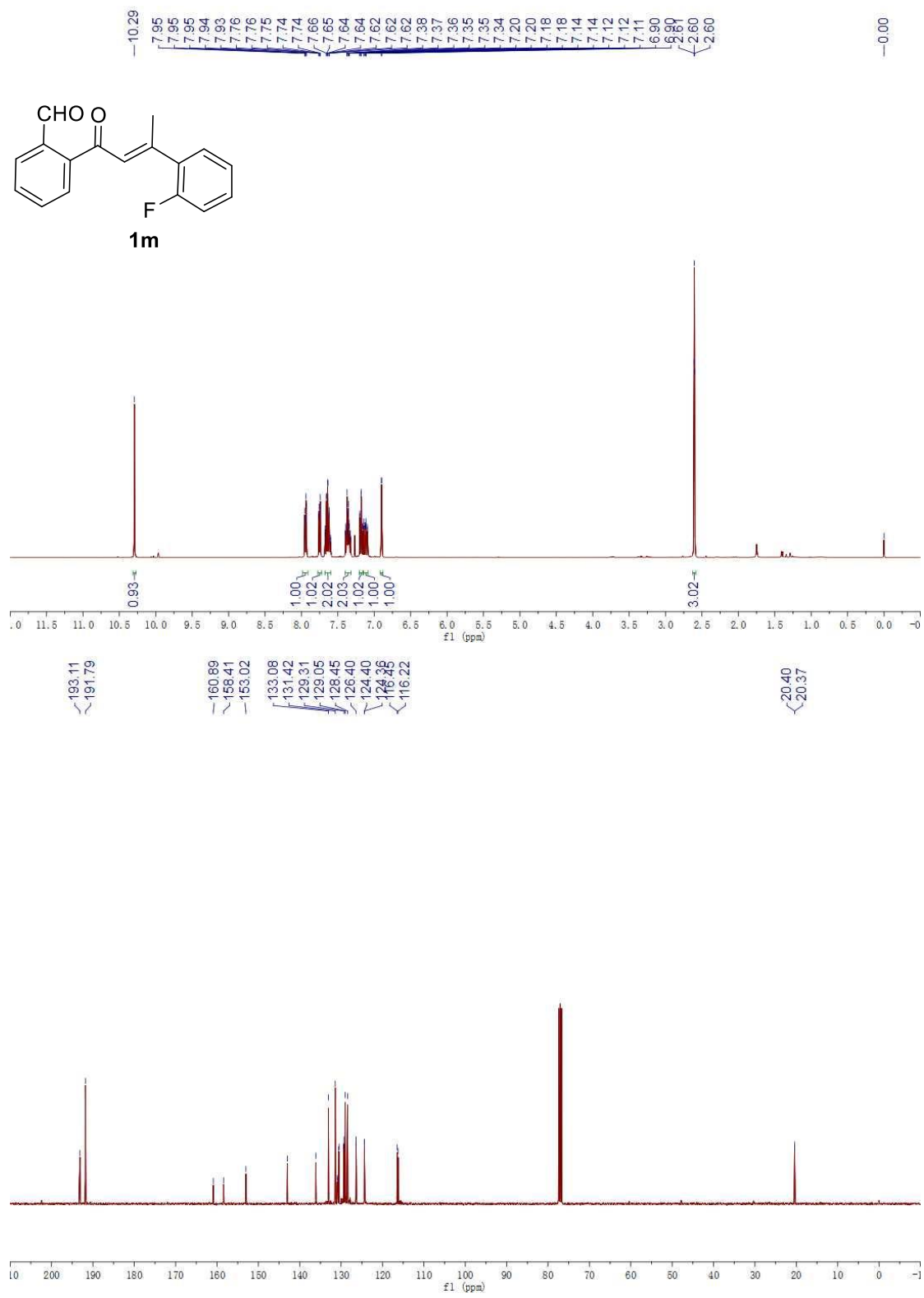


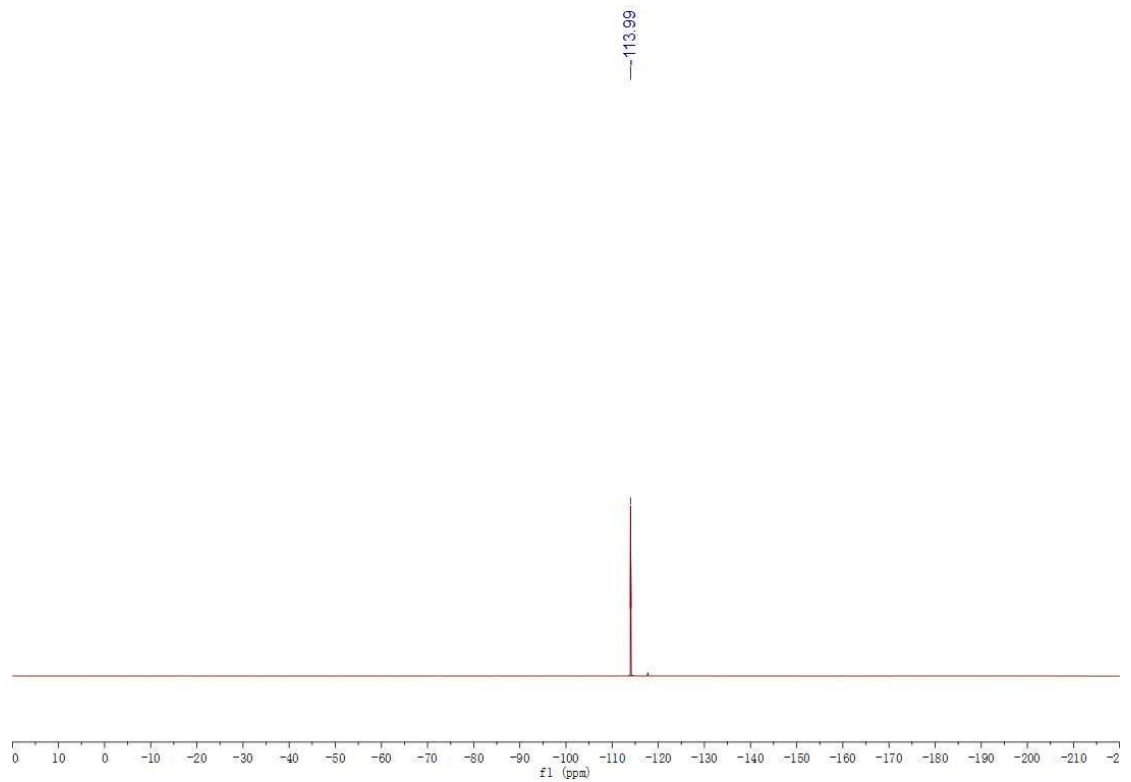


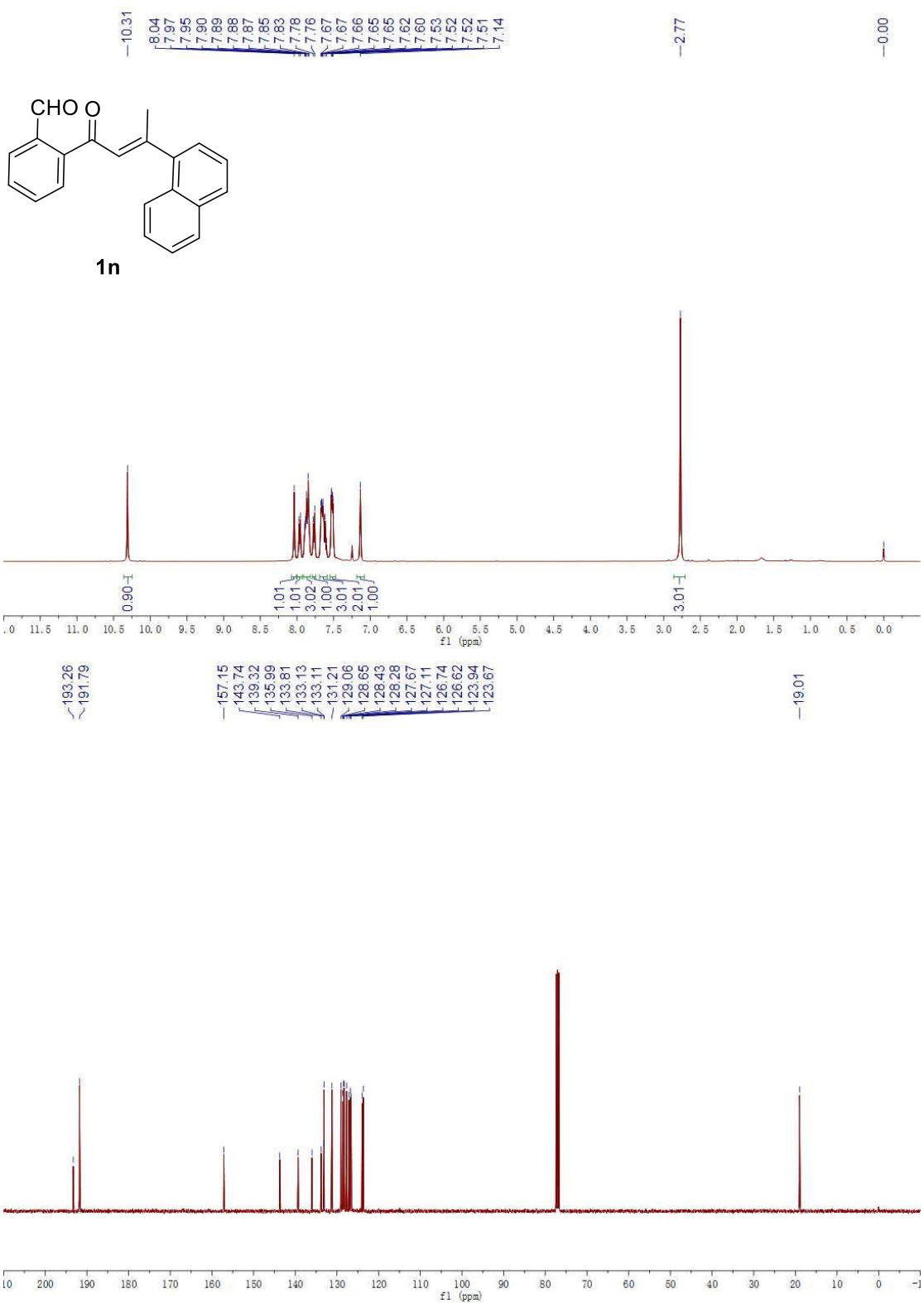


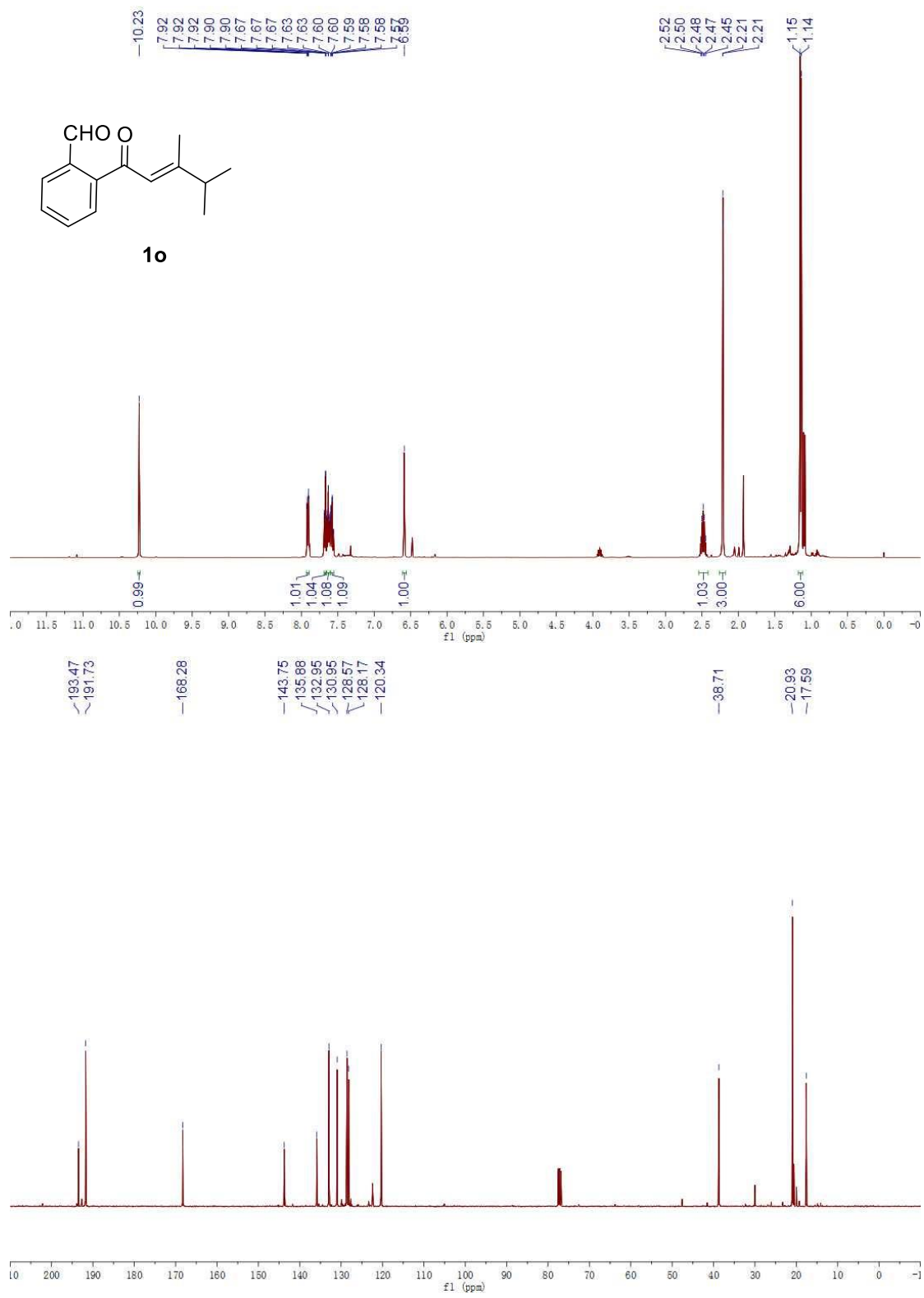


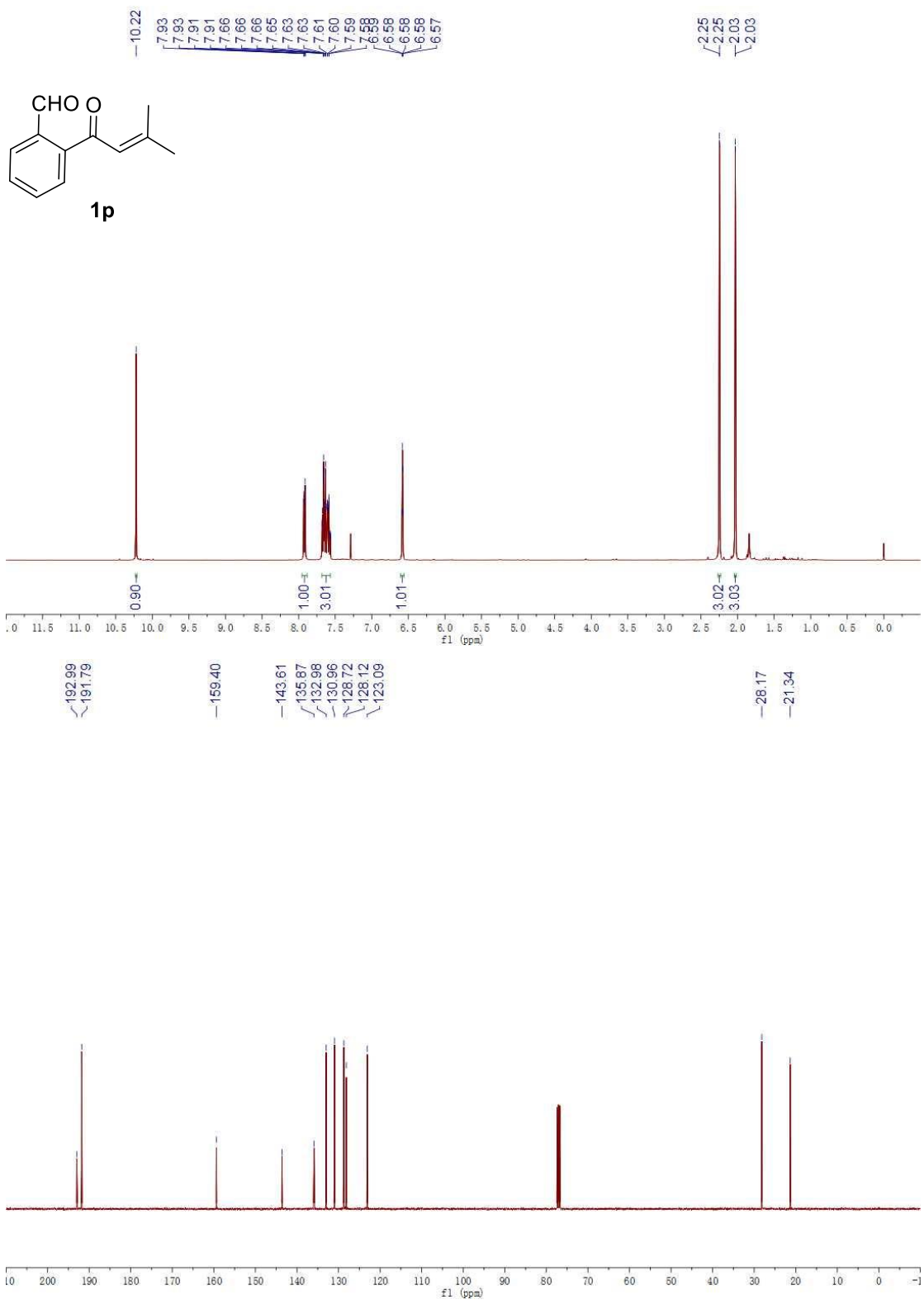


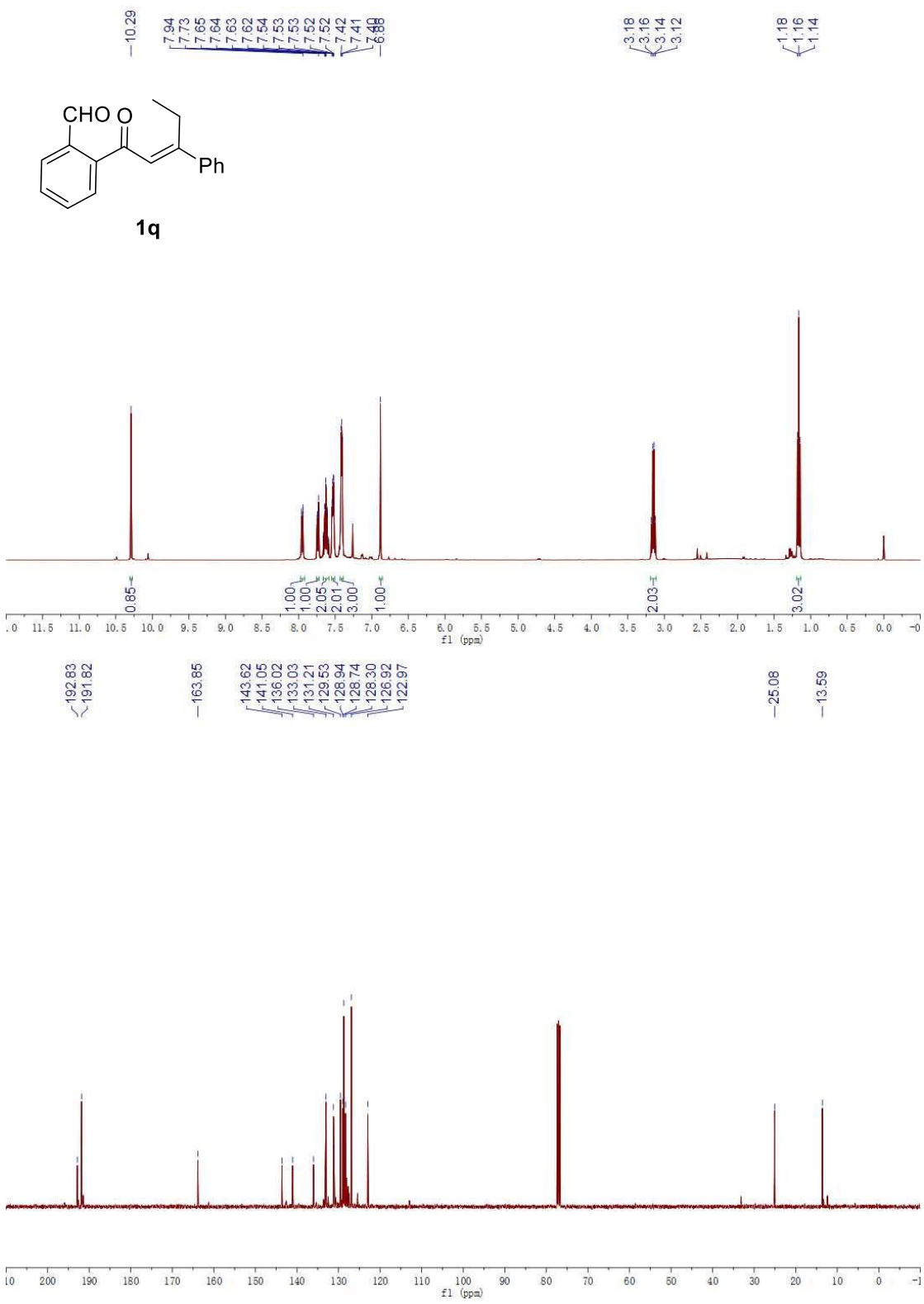


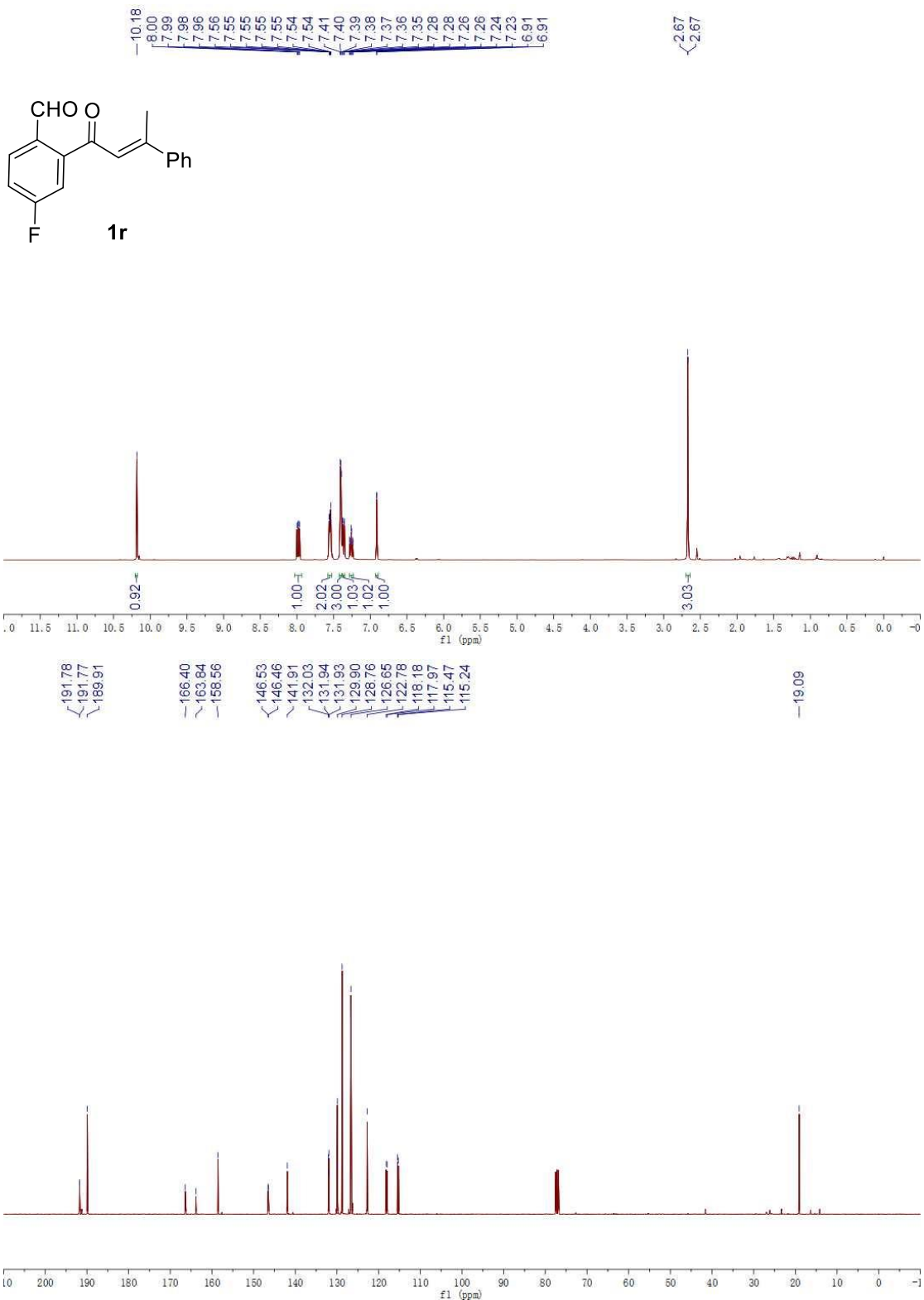


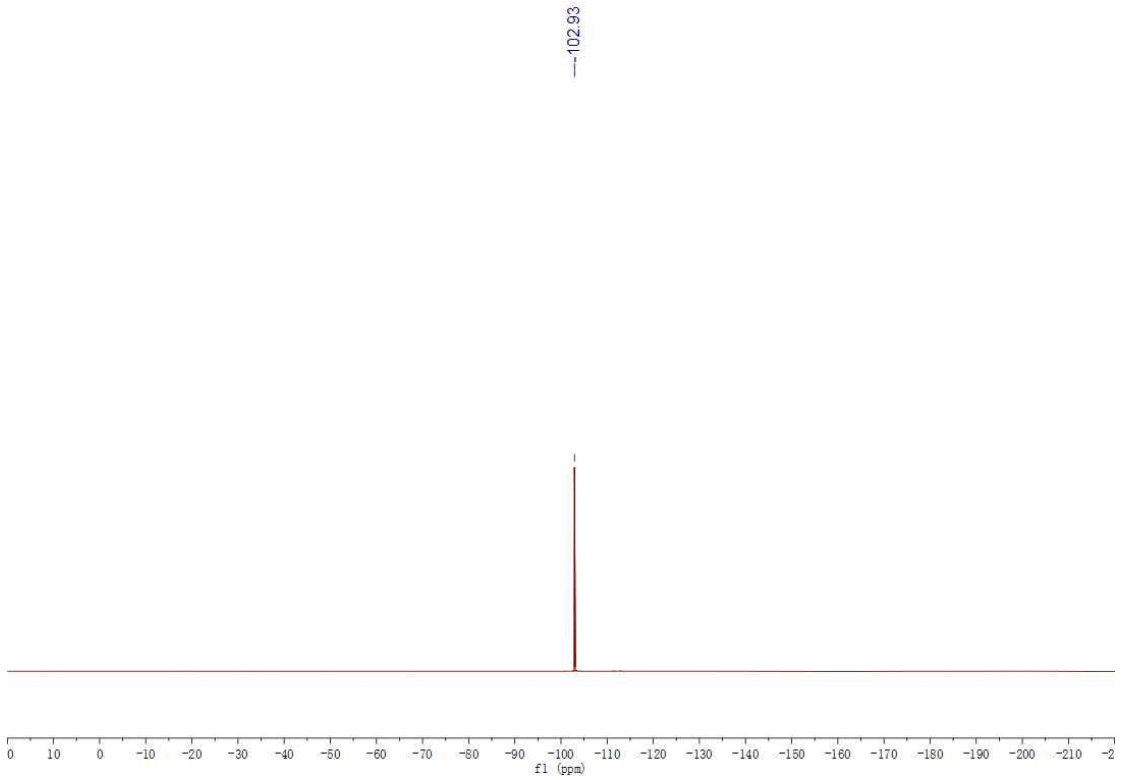


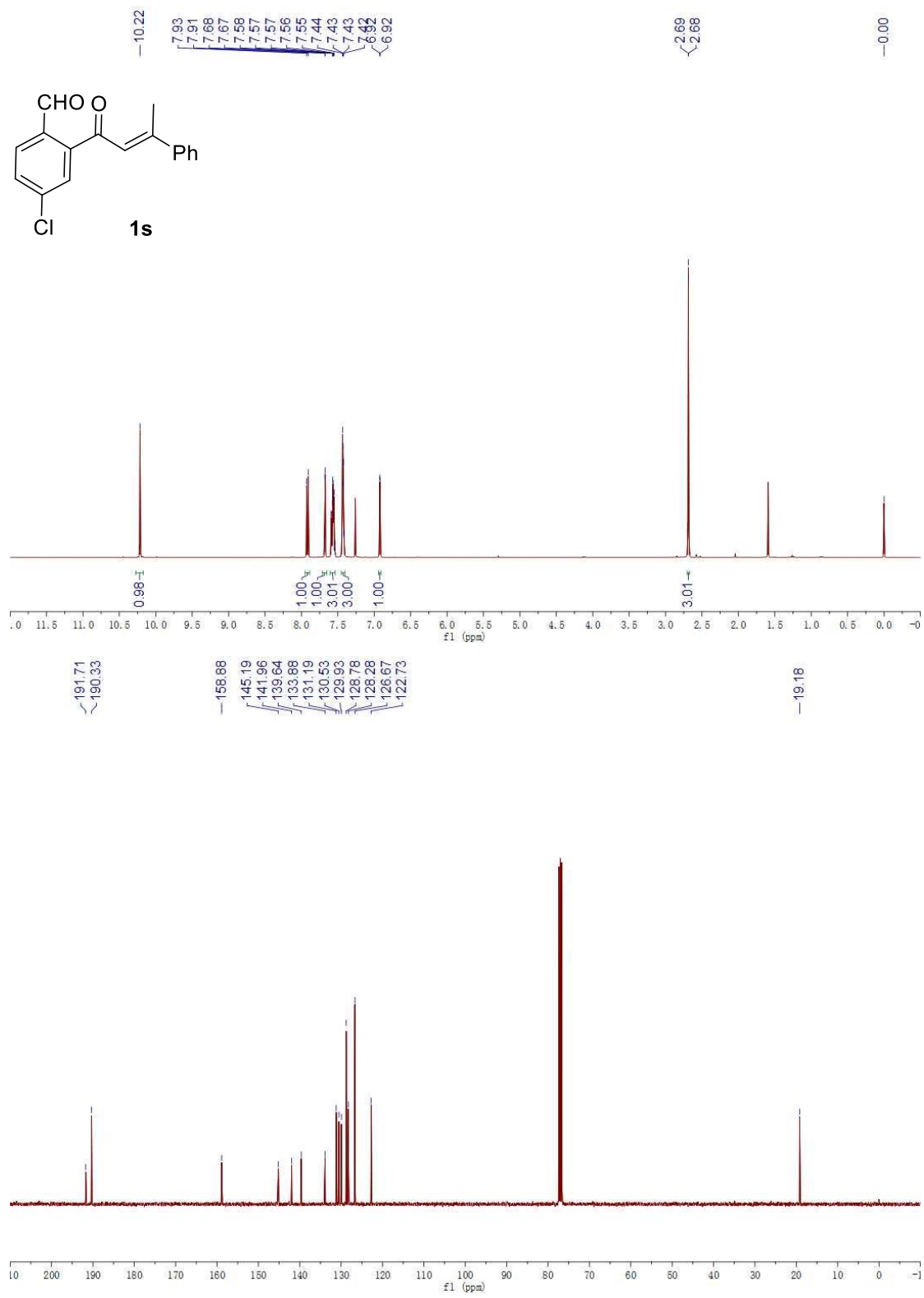


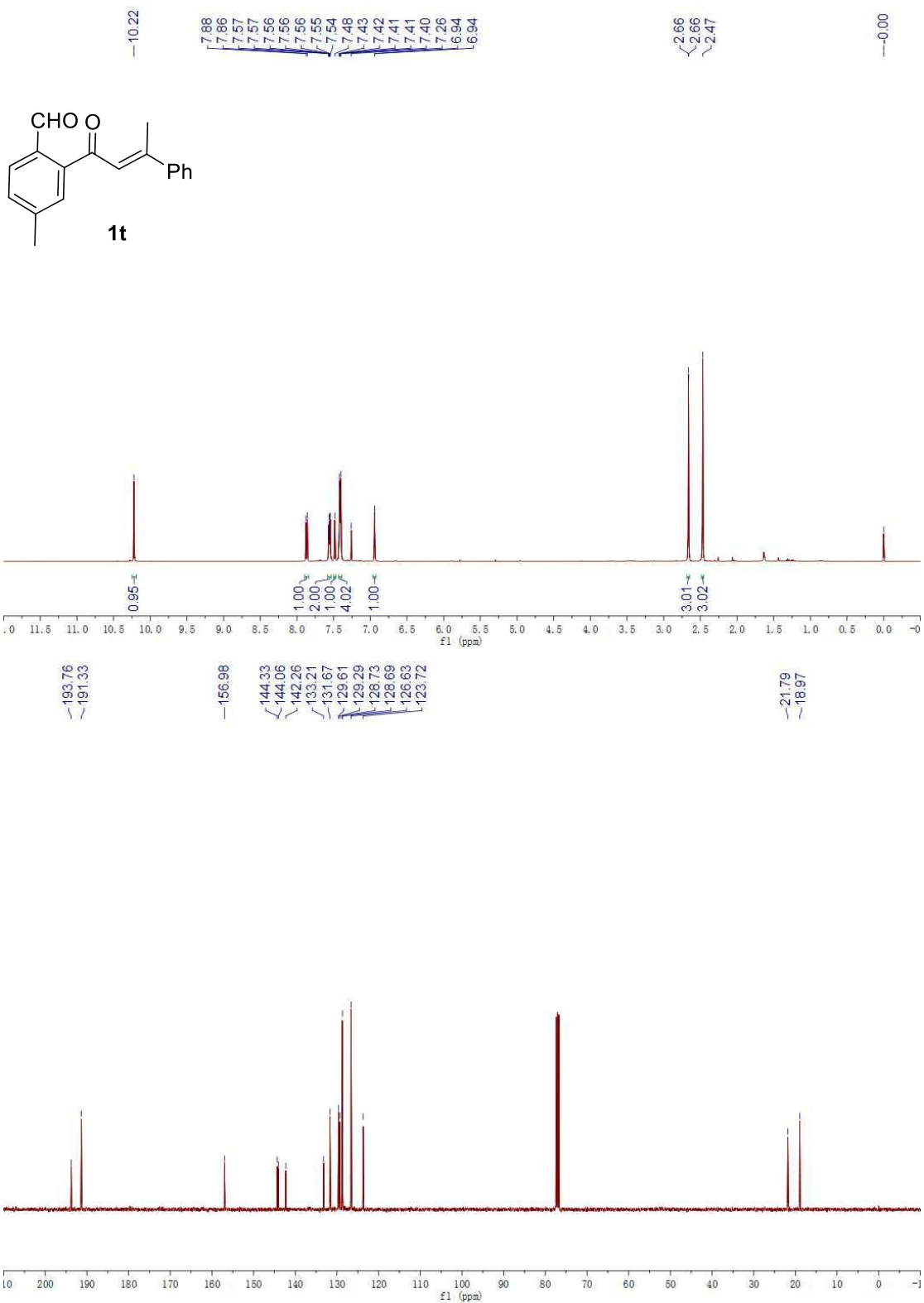


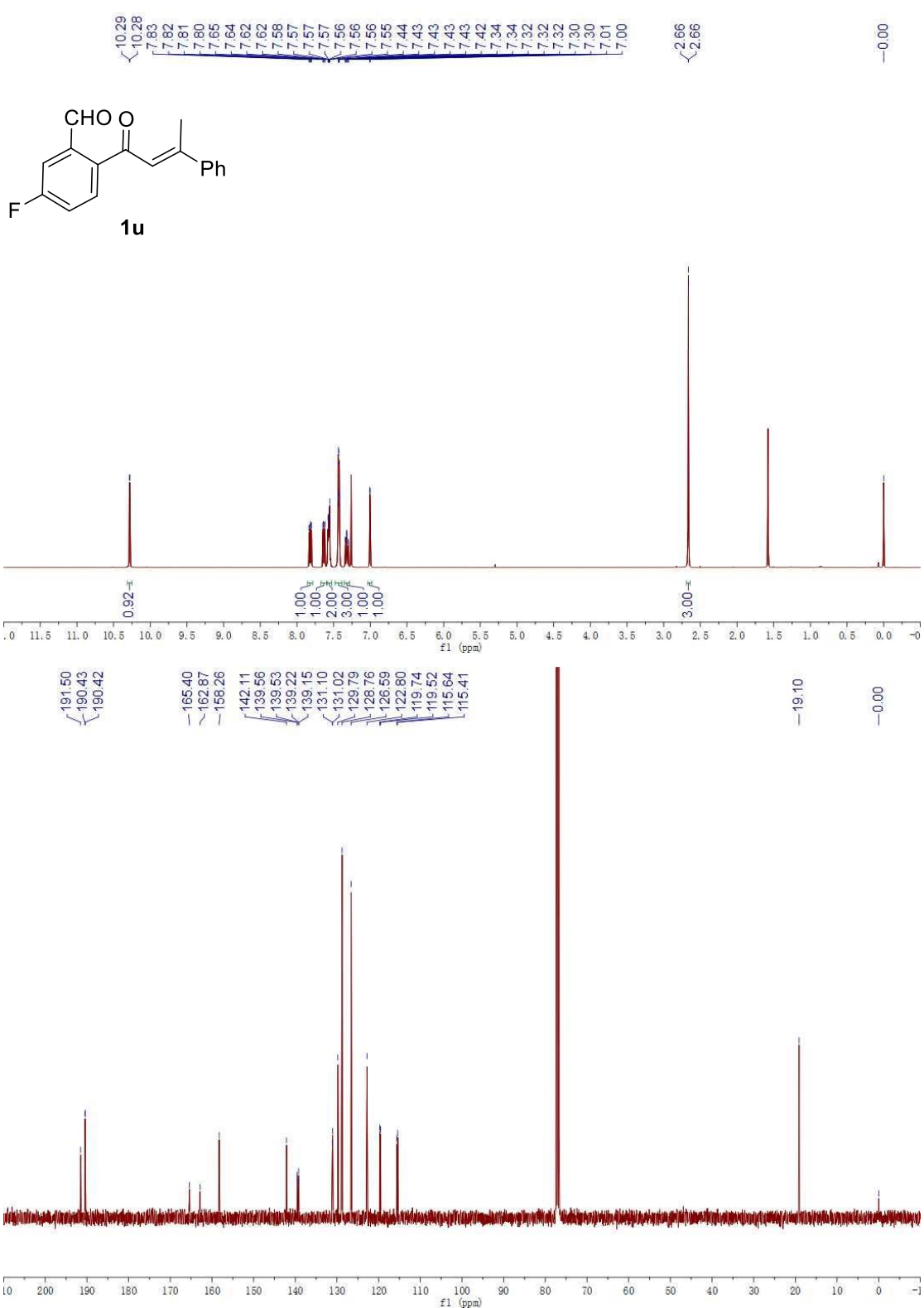


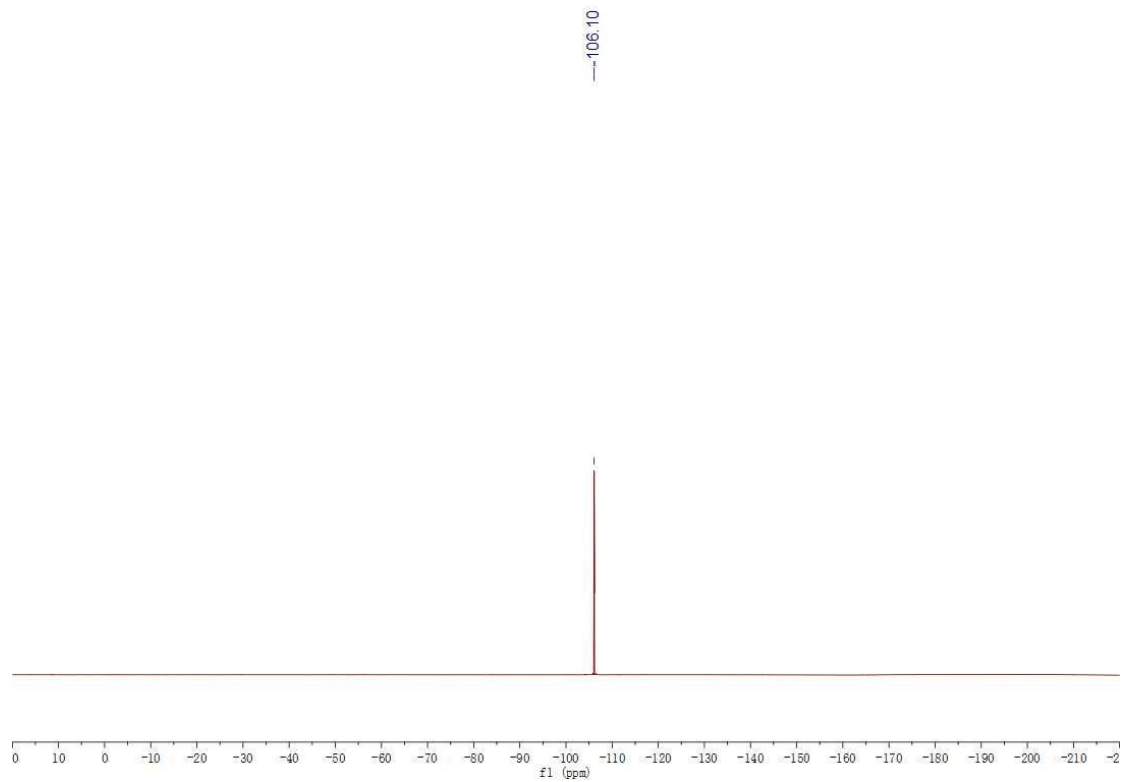


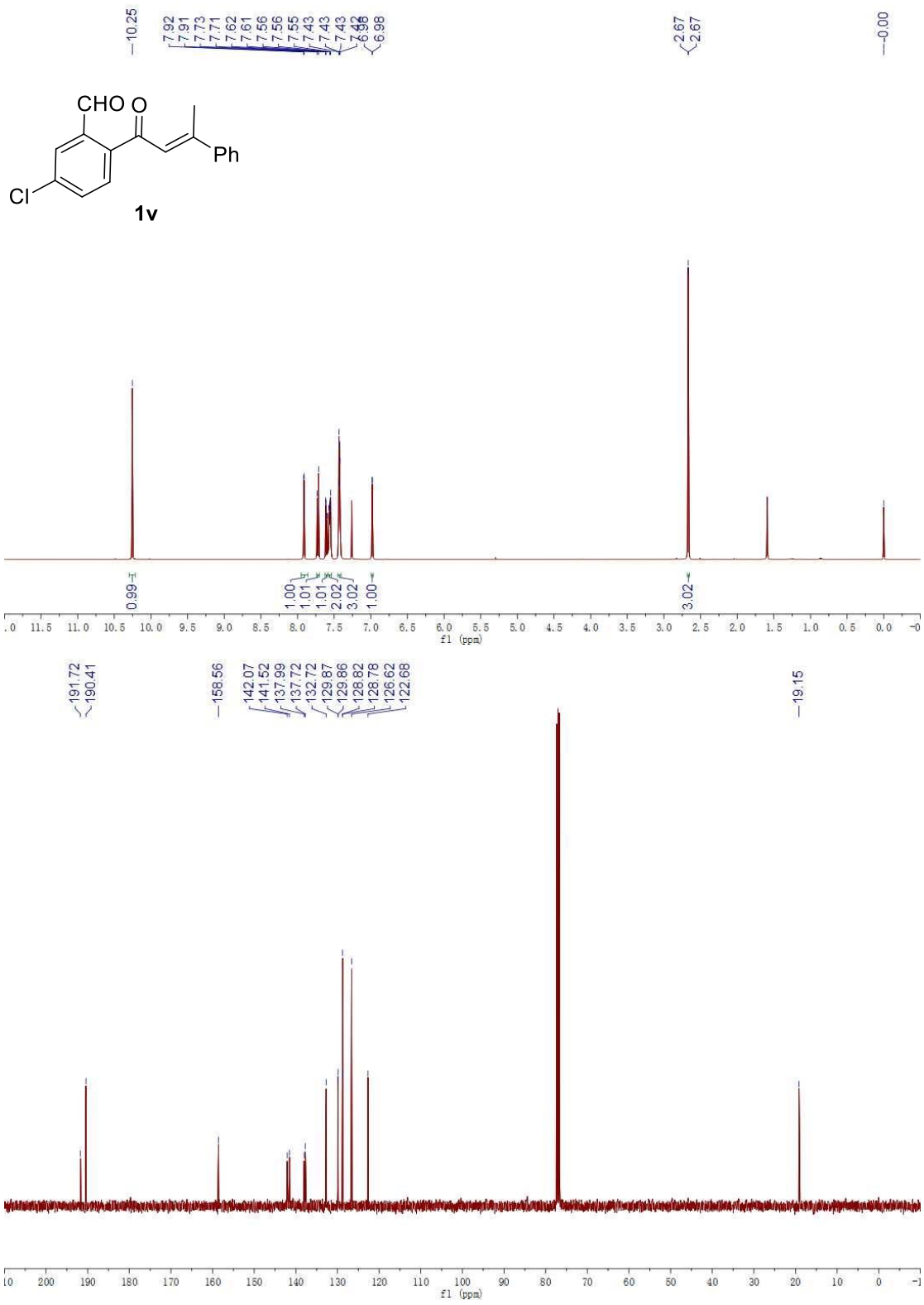


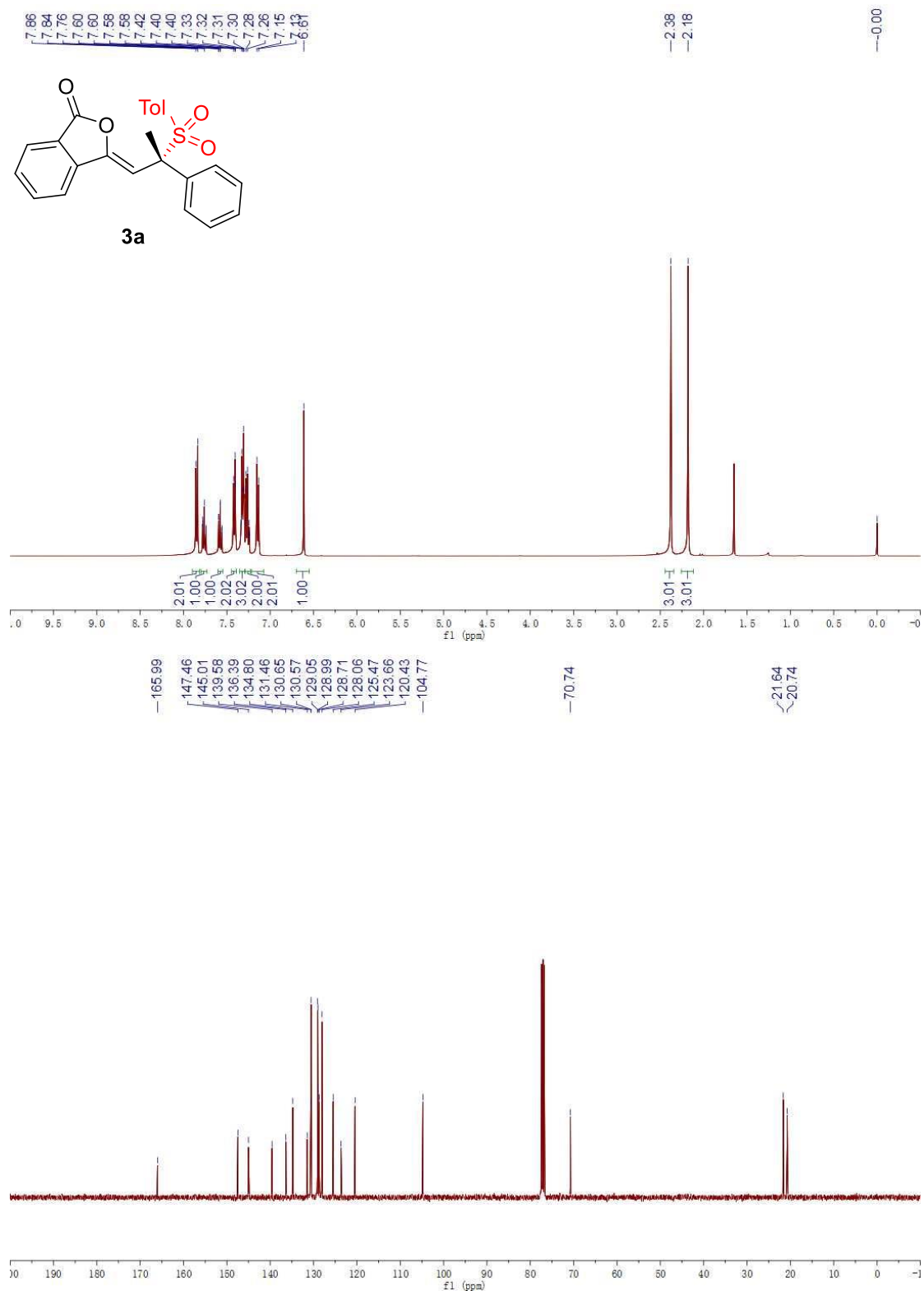


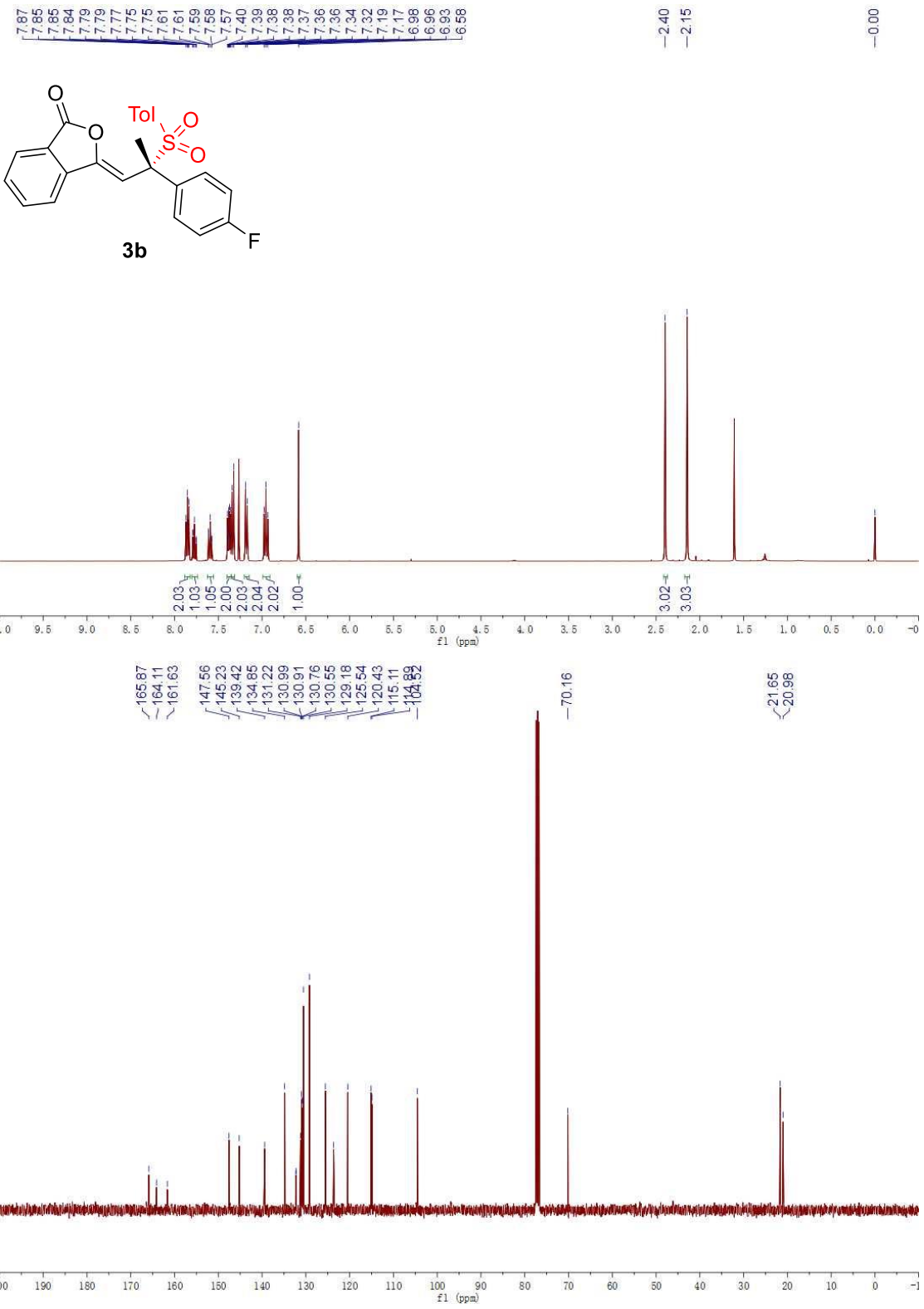


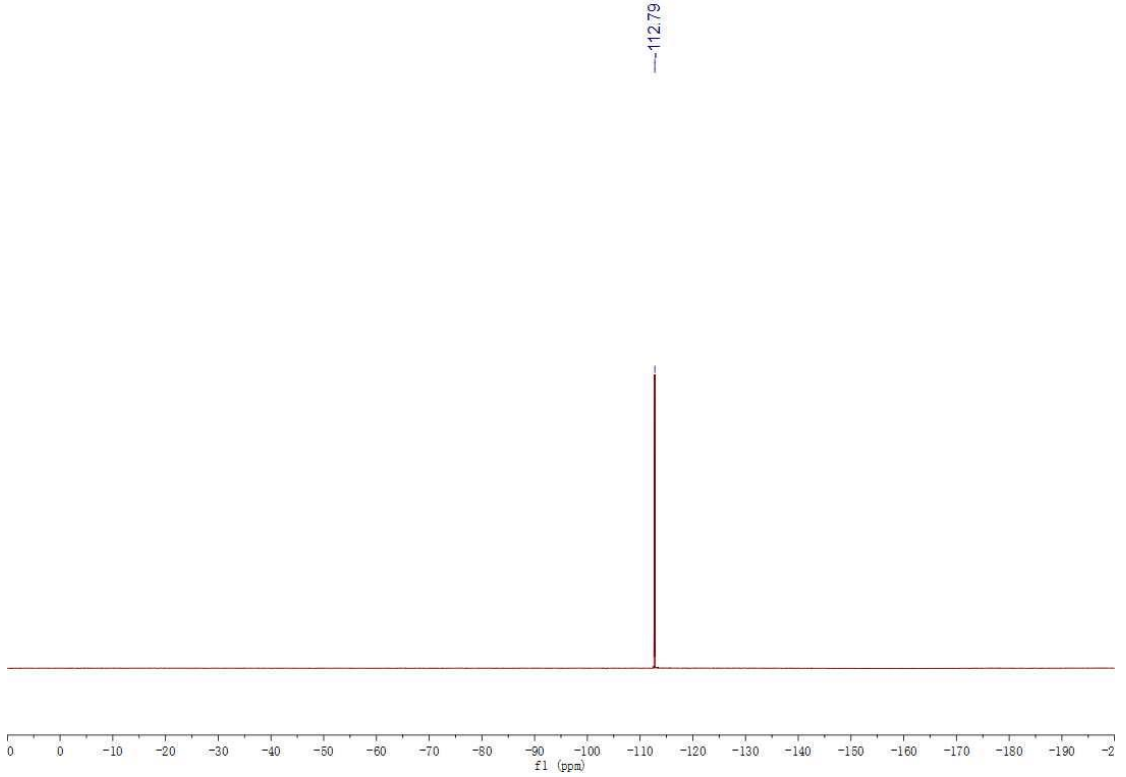


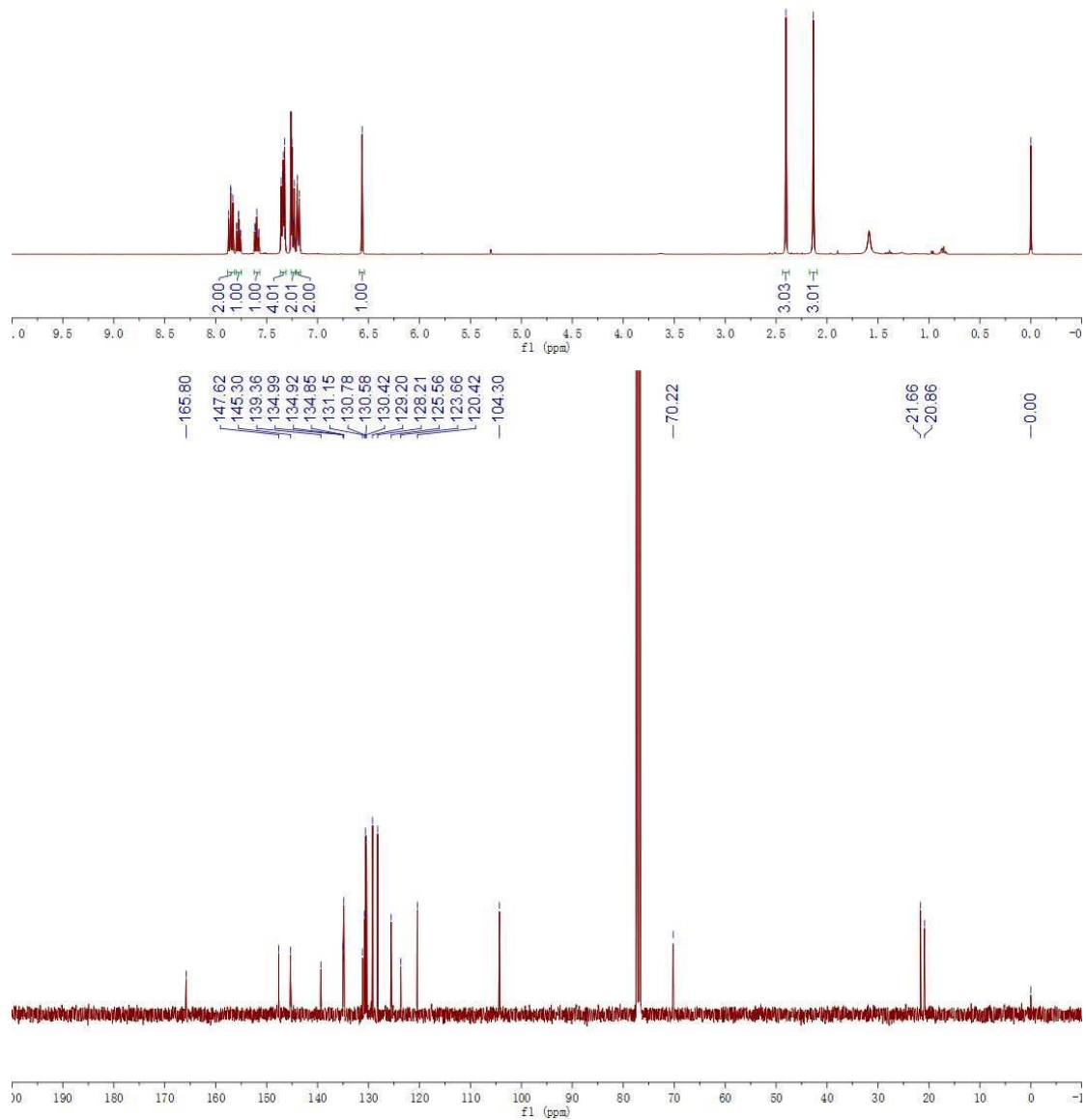
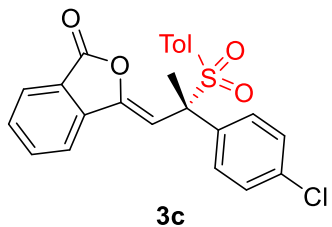


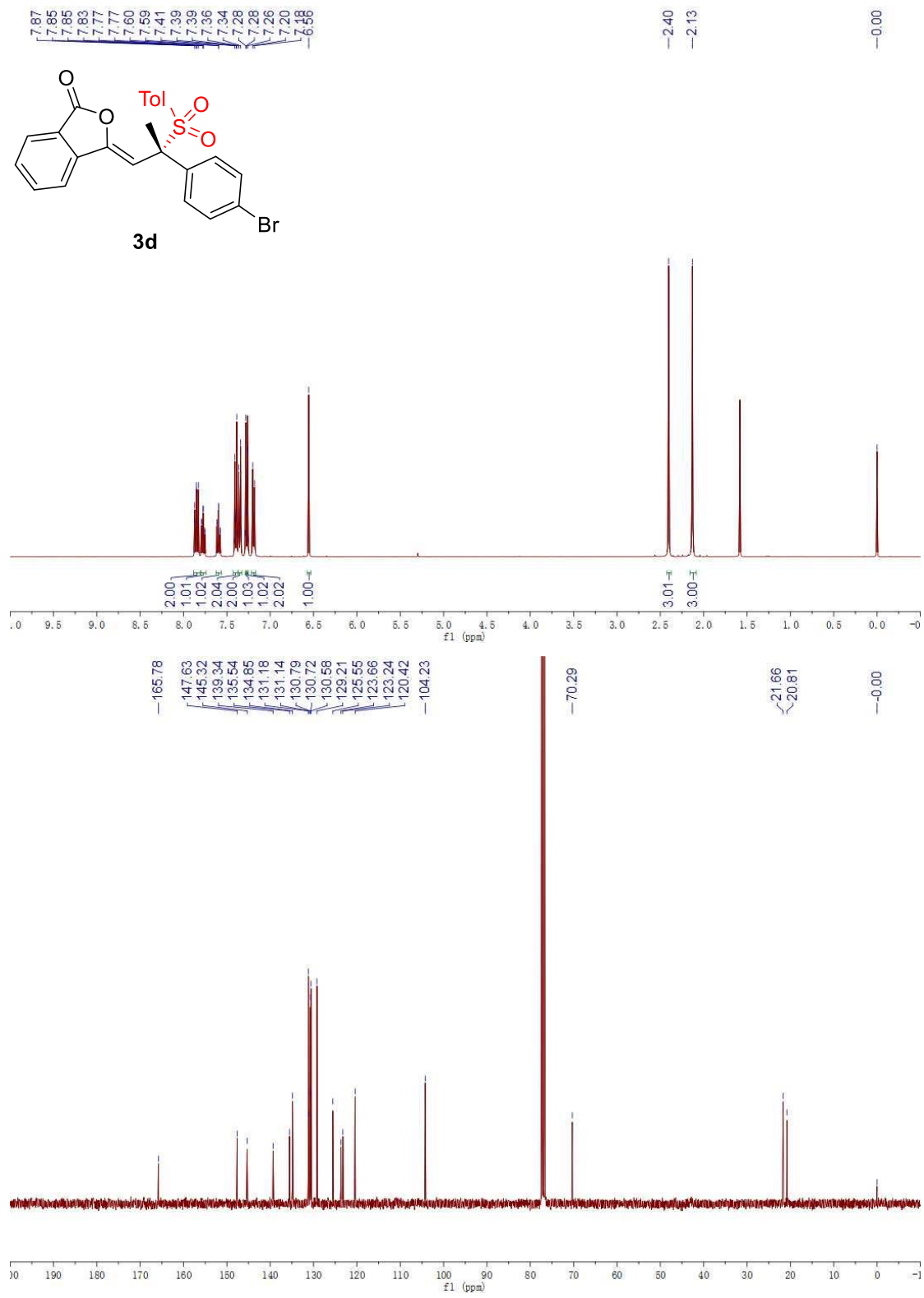


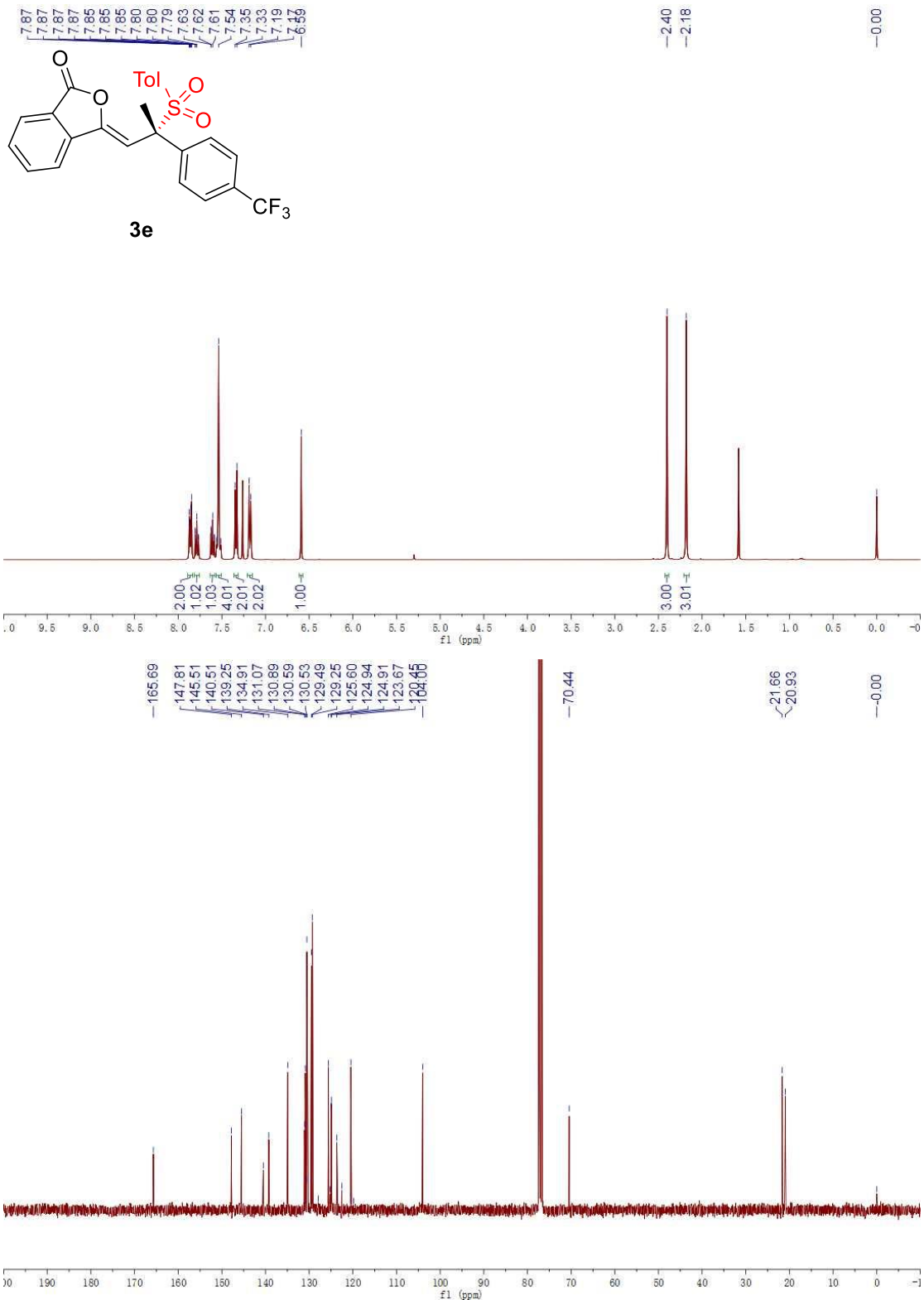


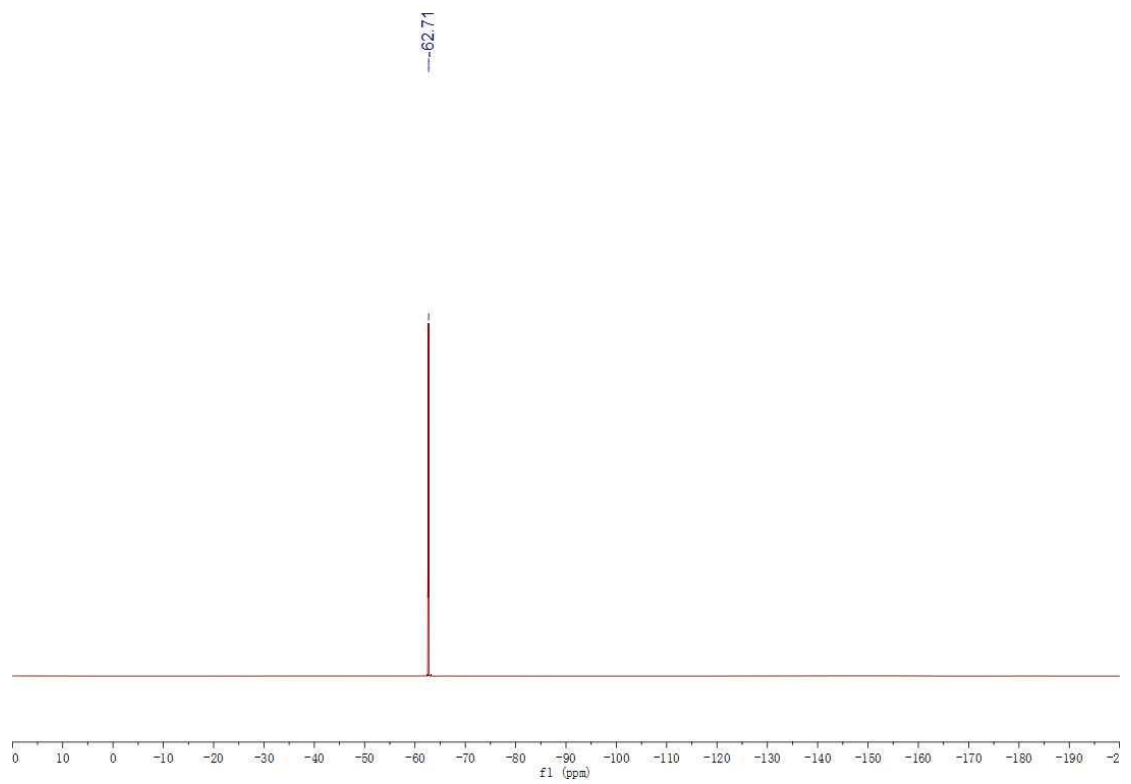


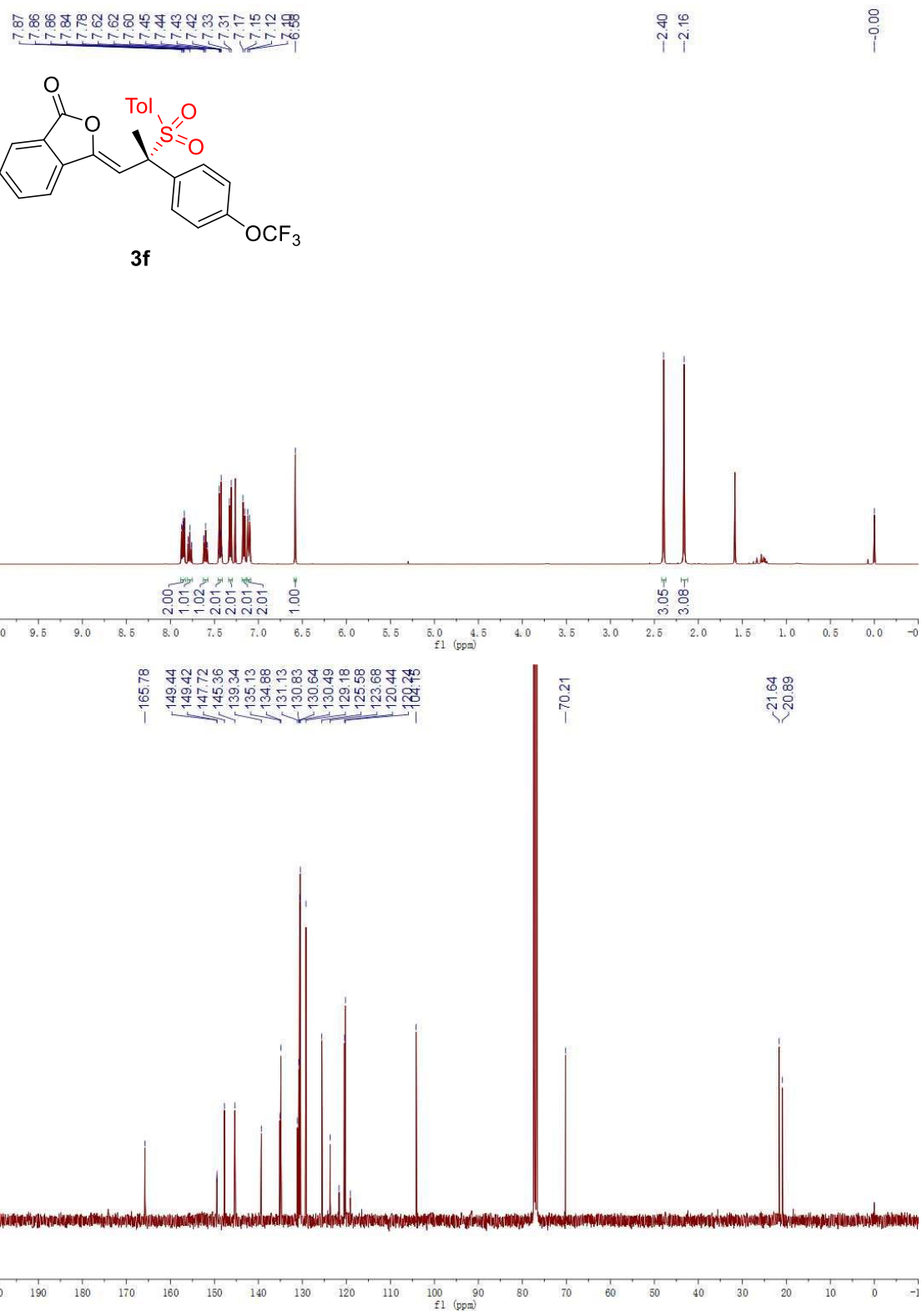


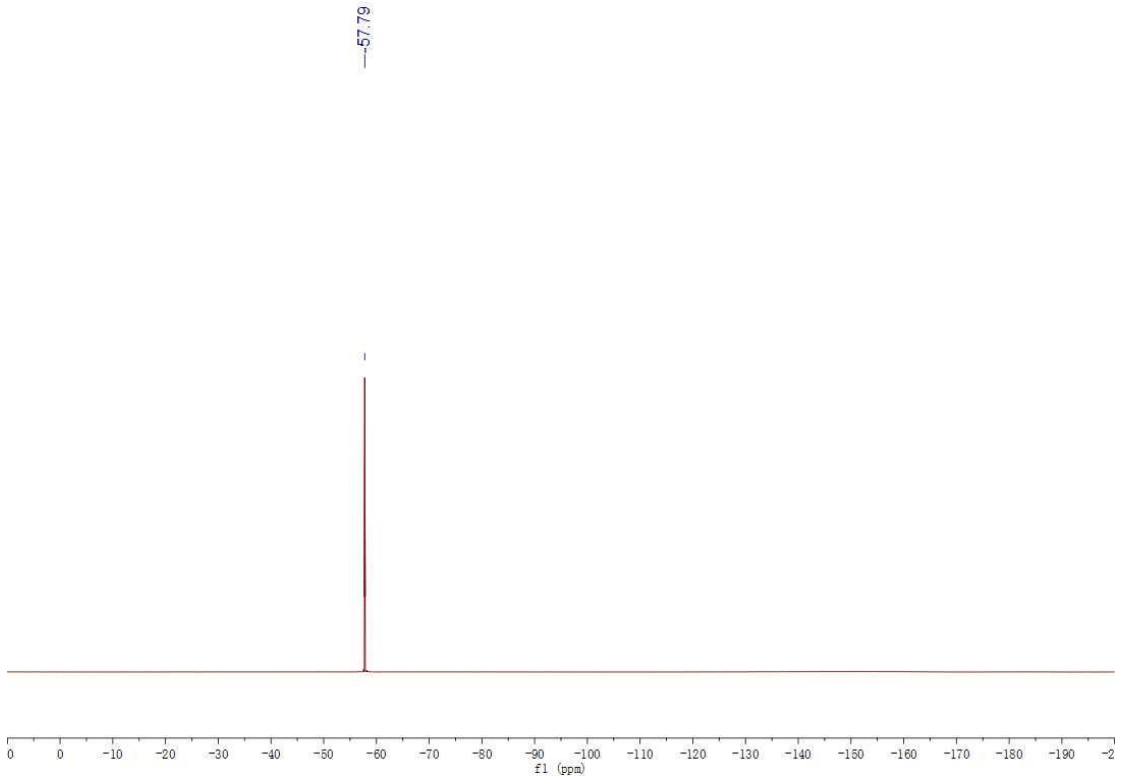


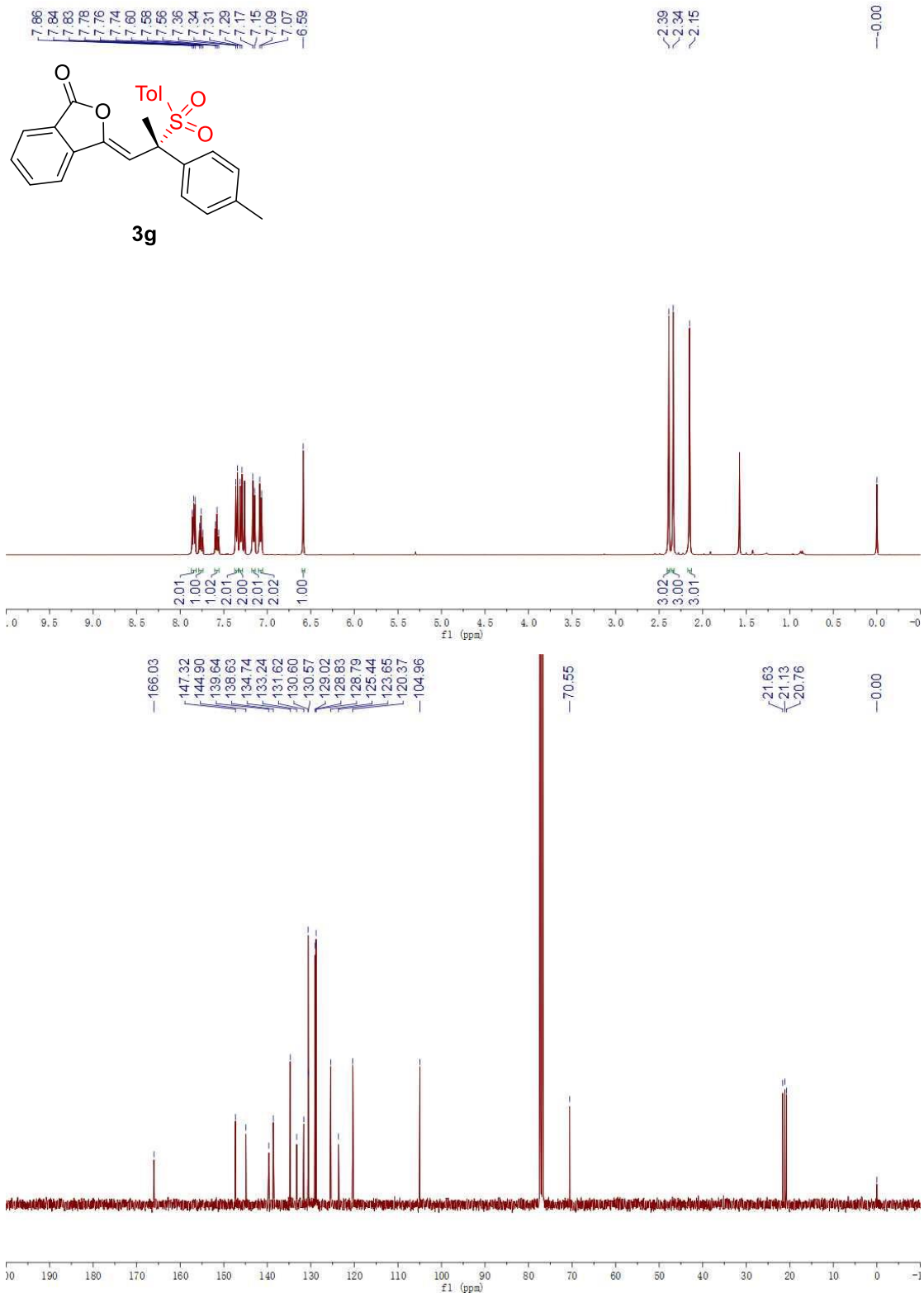


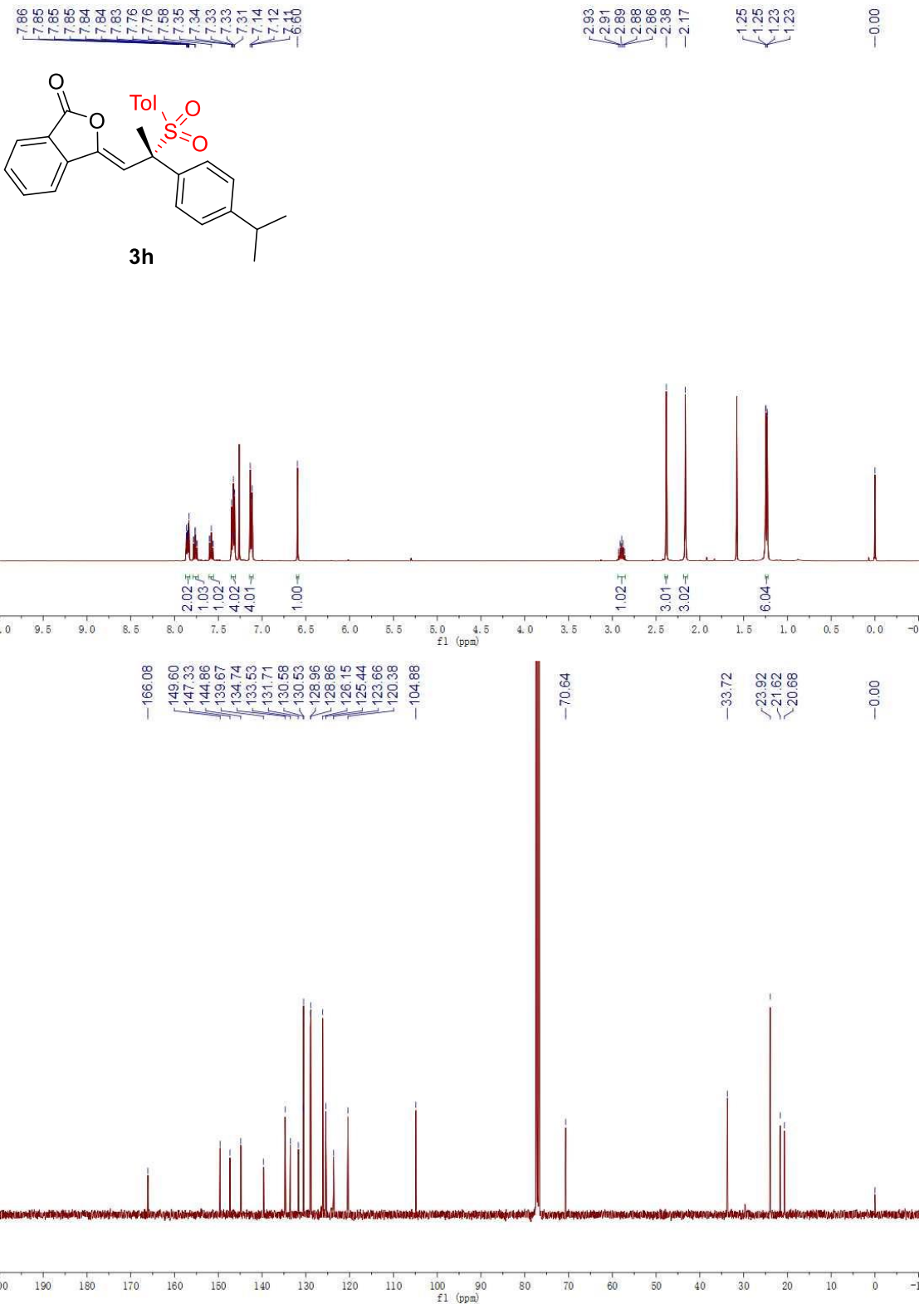


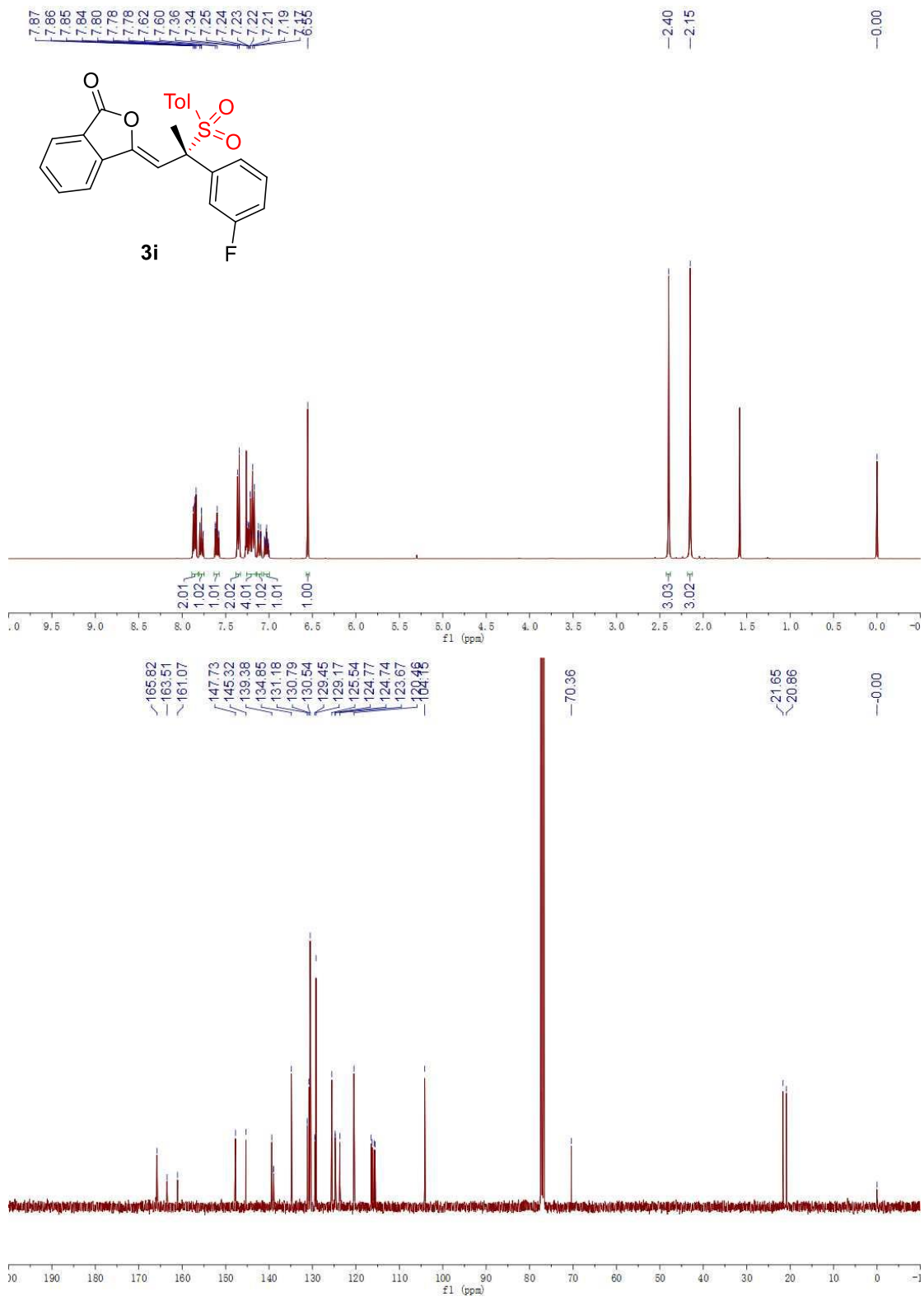


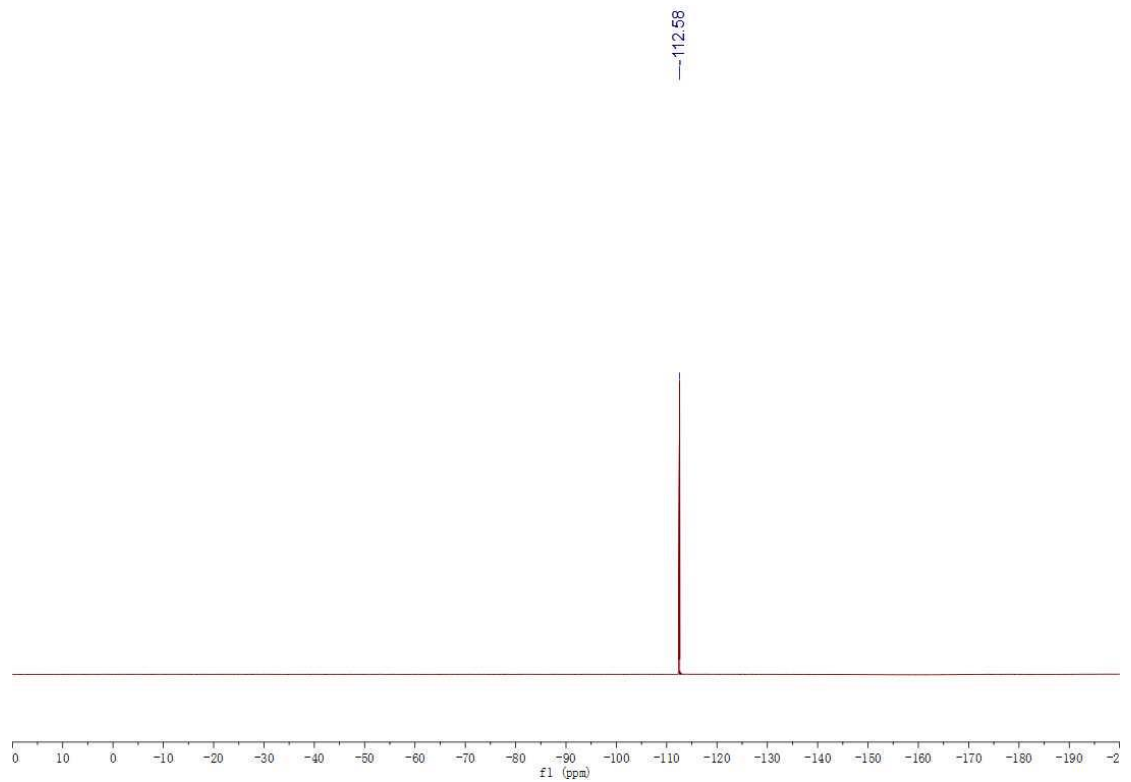




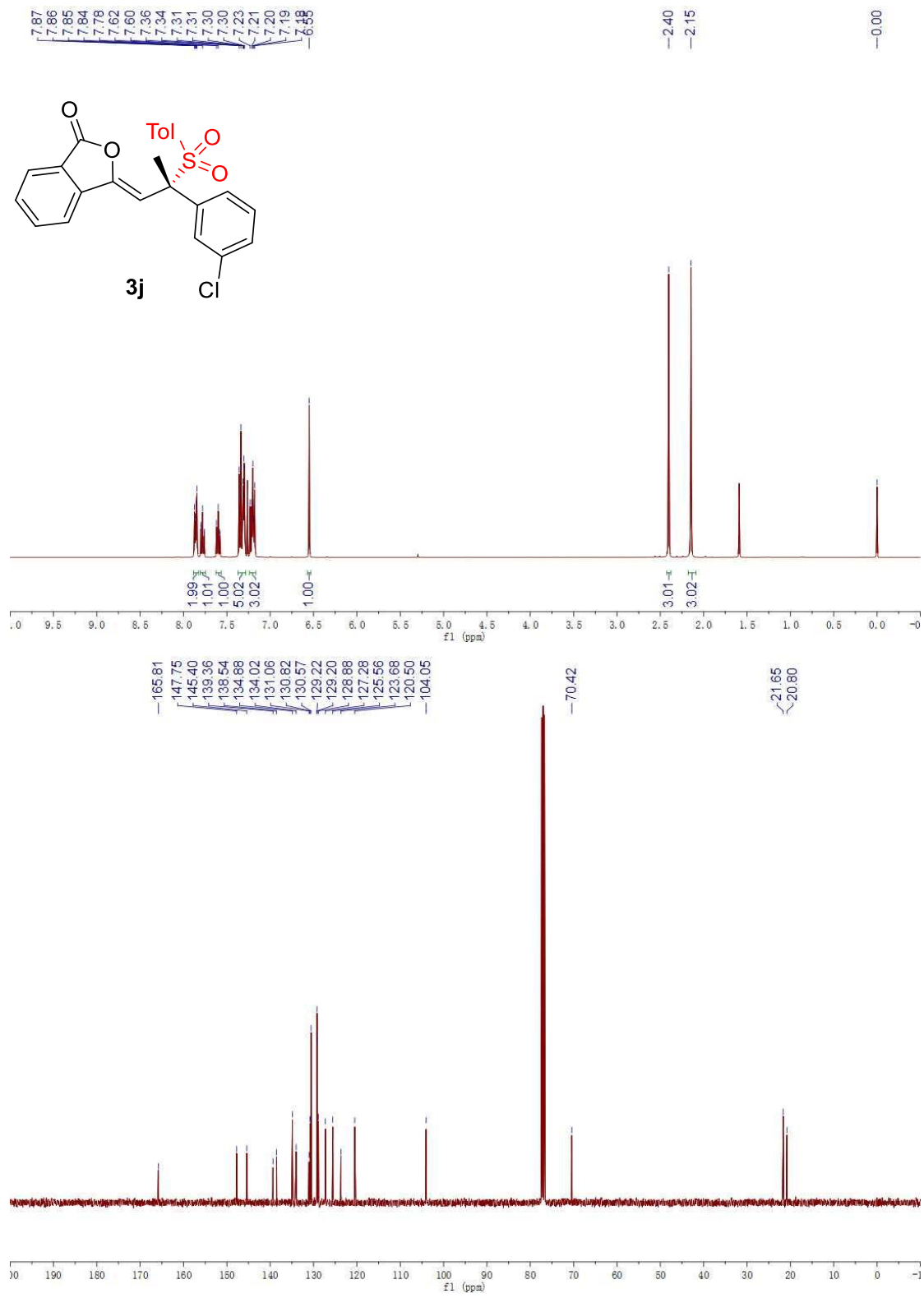


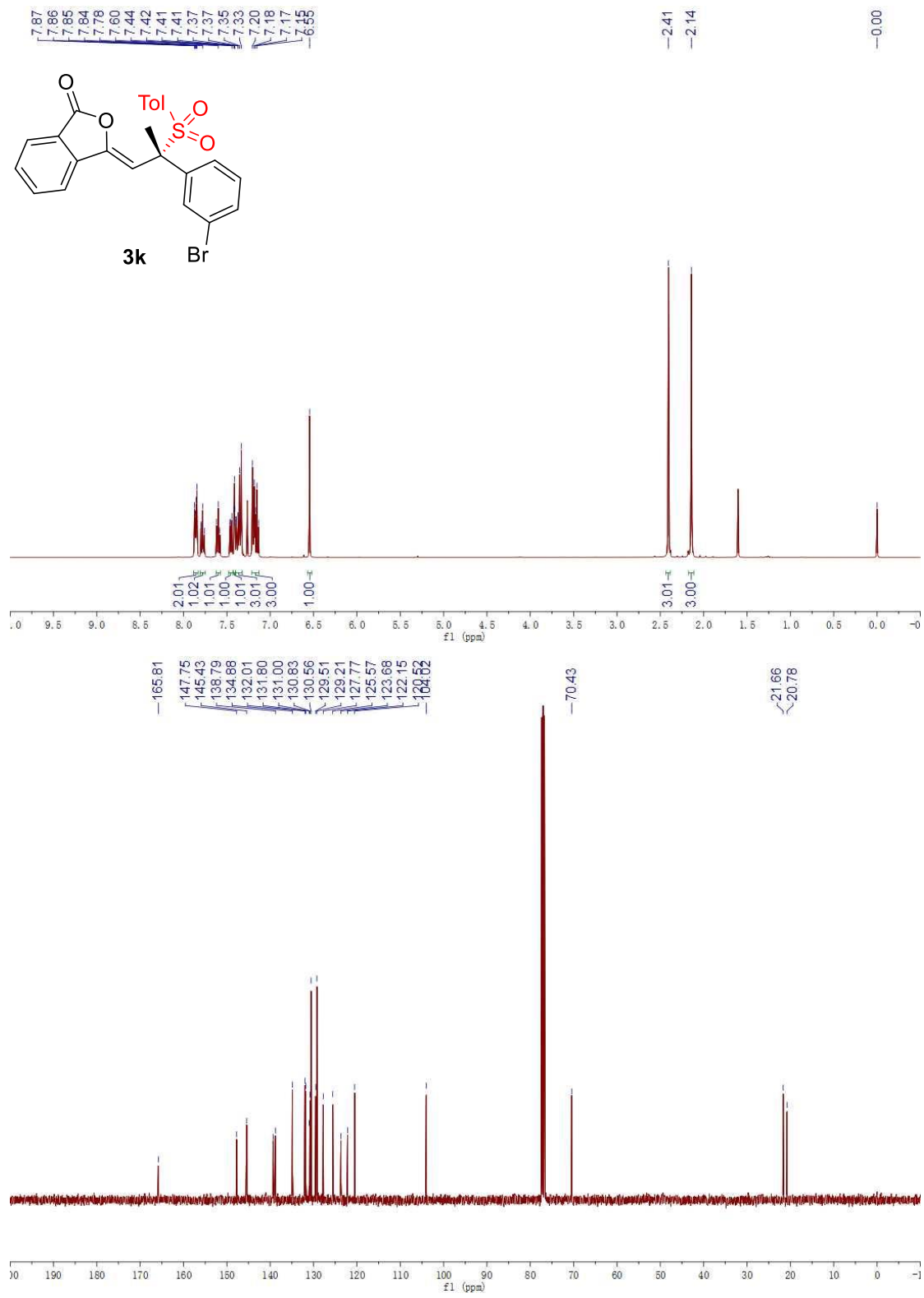


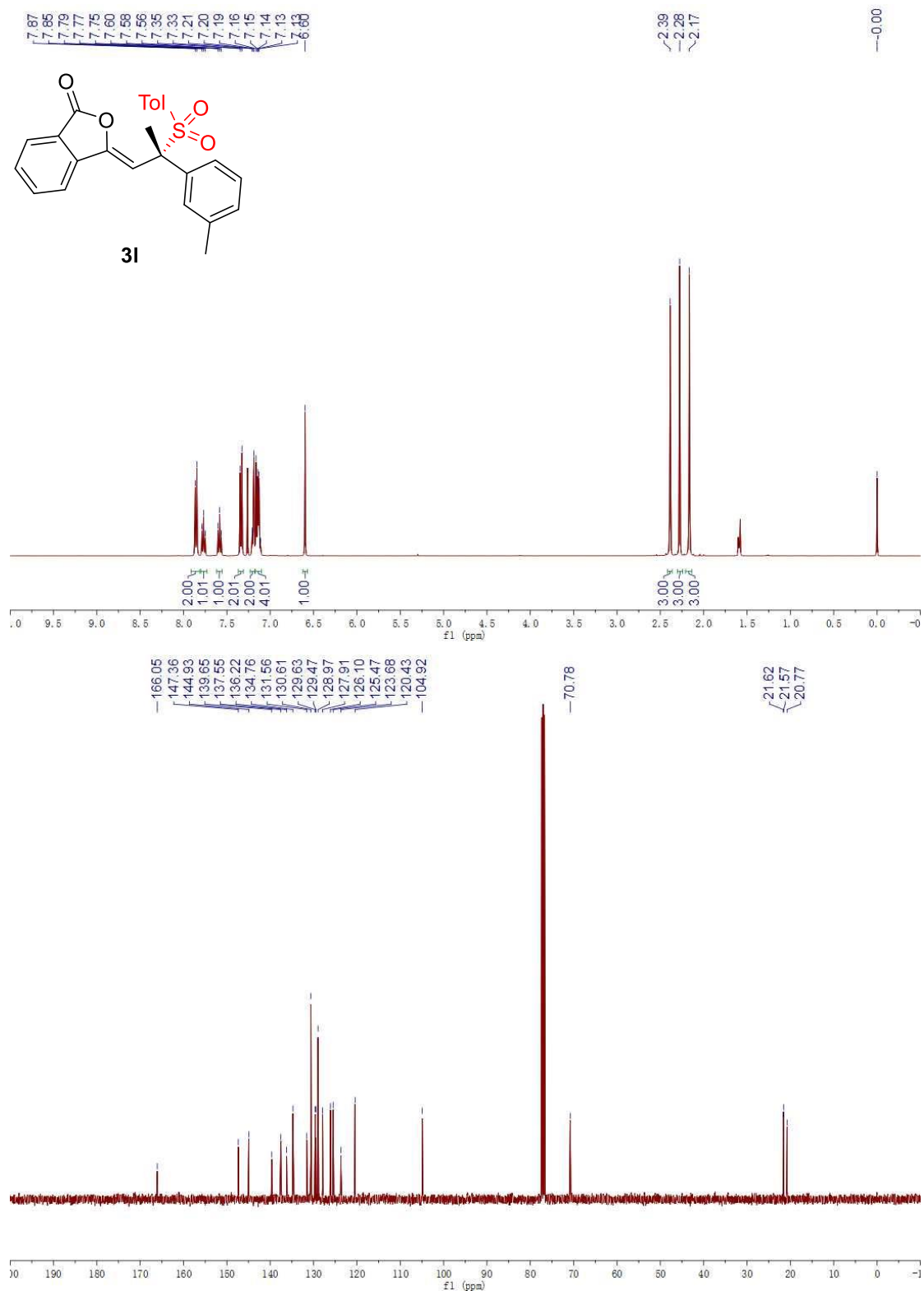


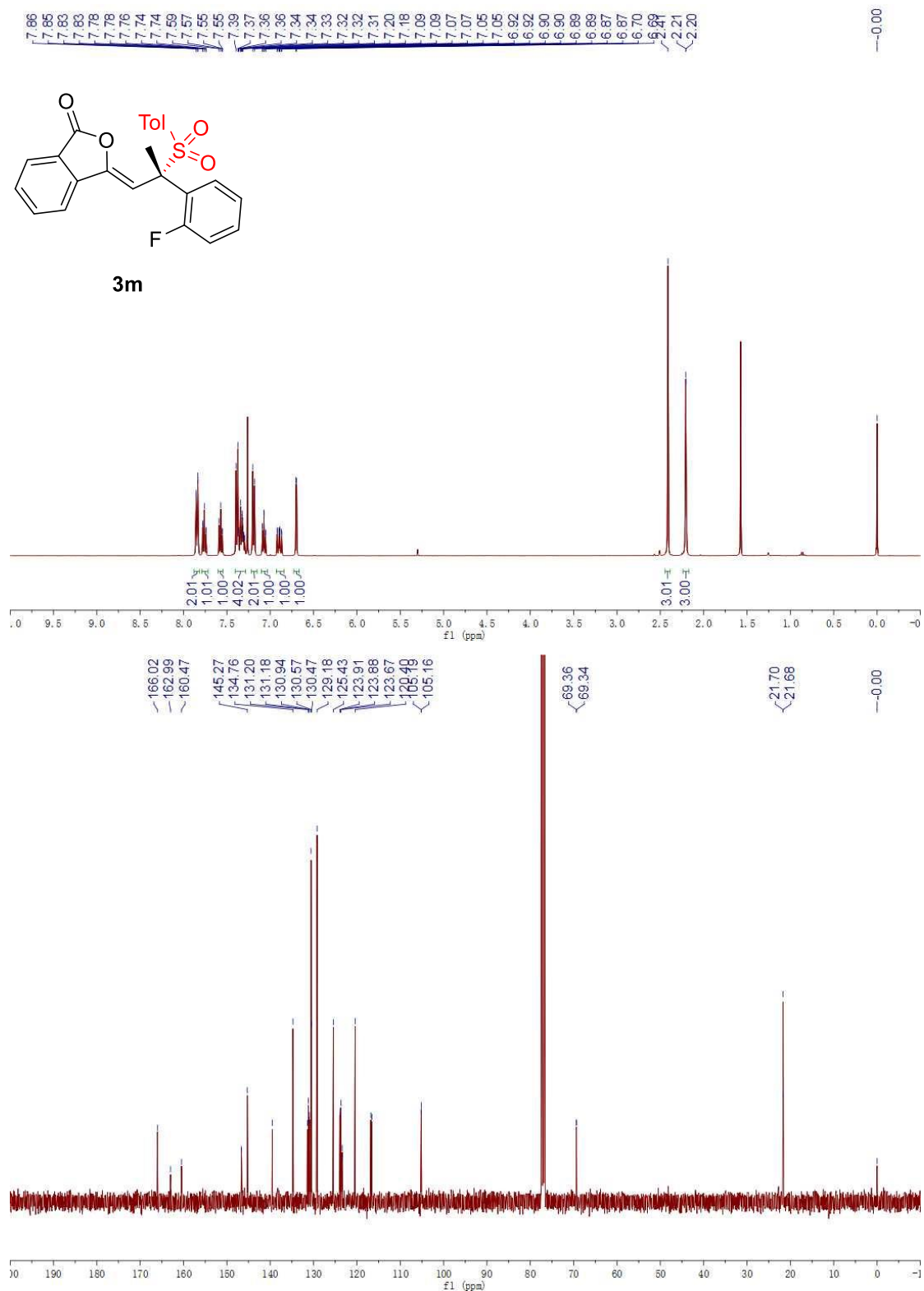


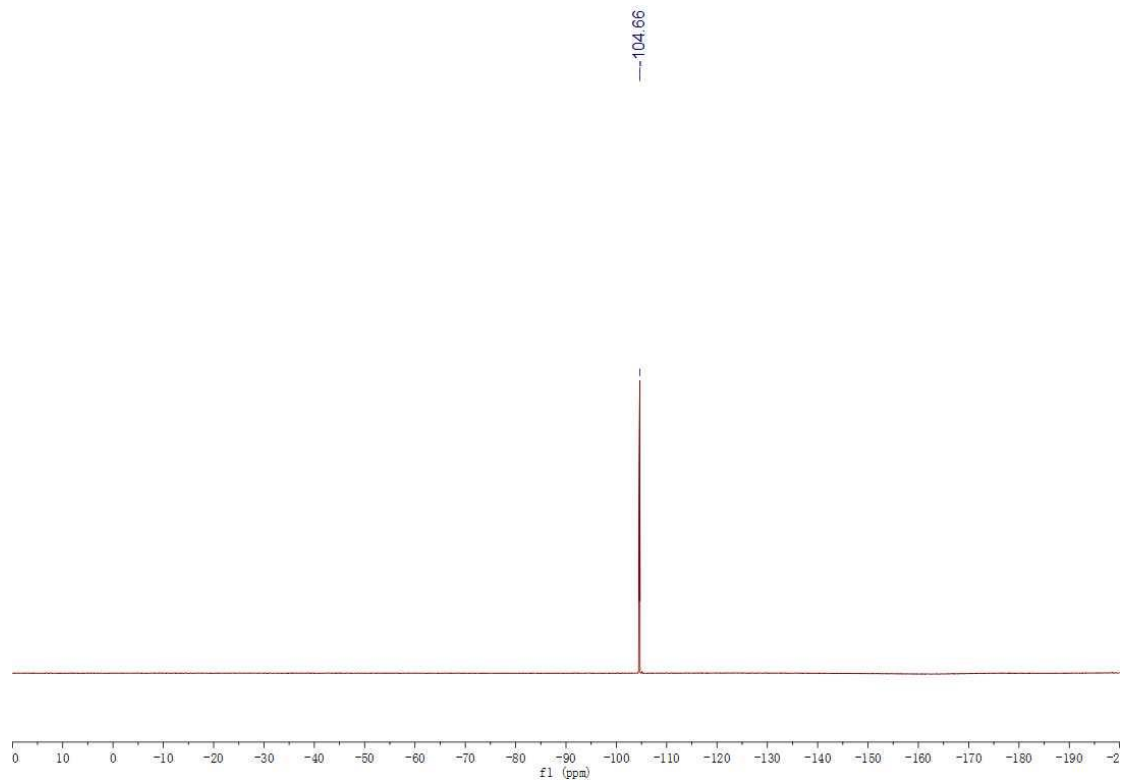
S109

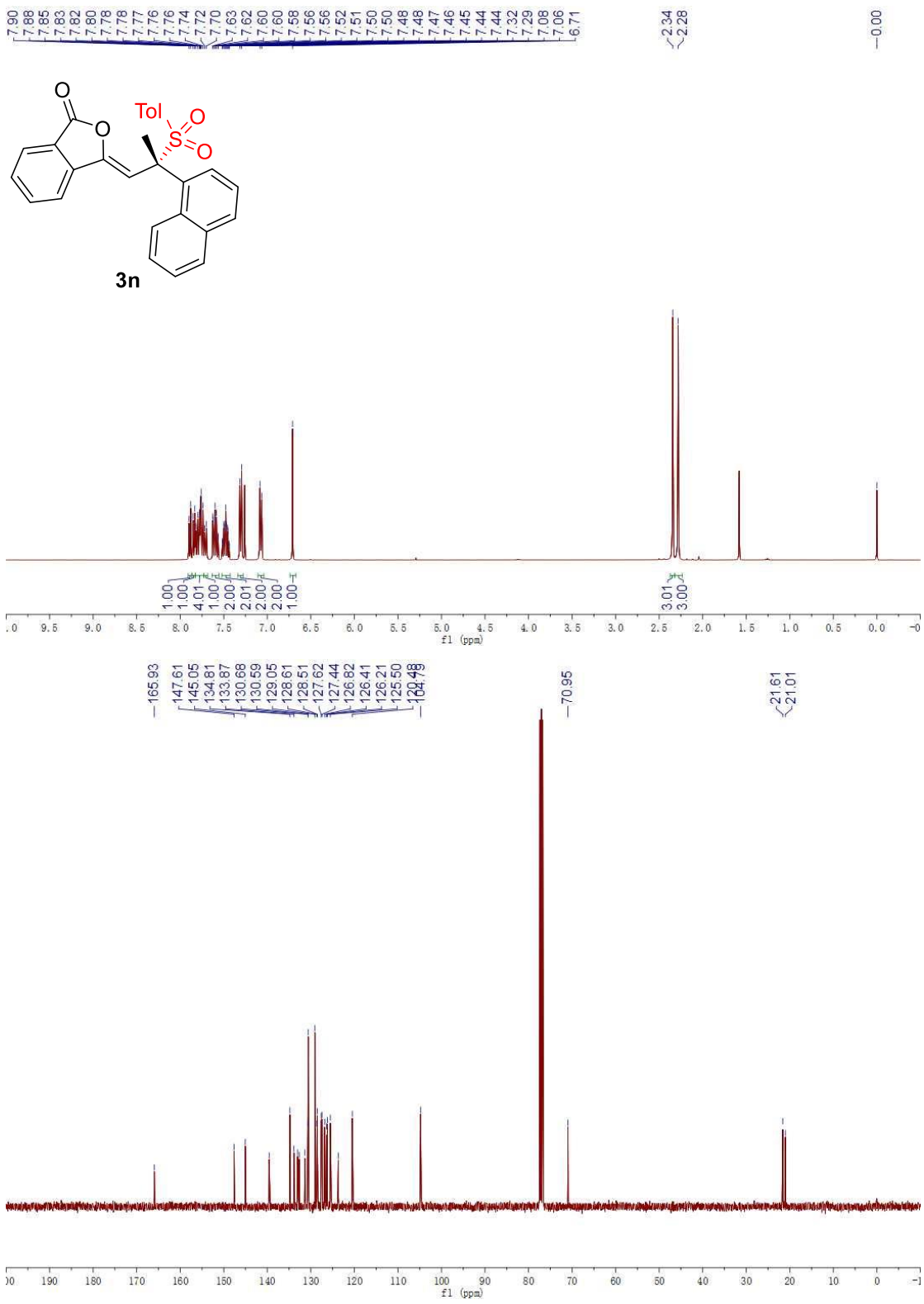


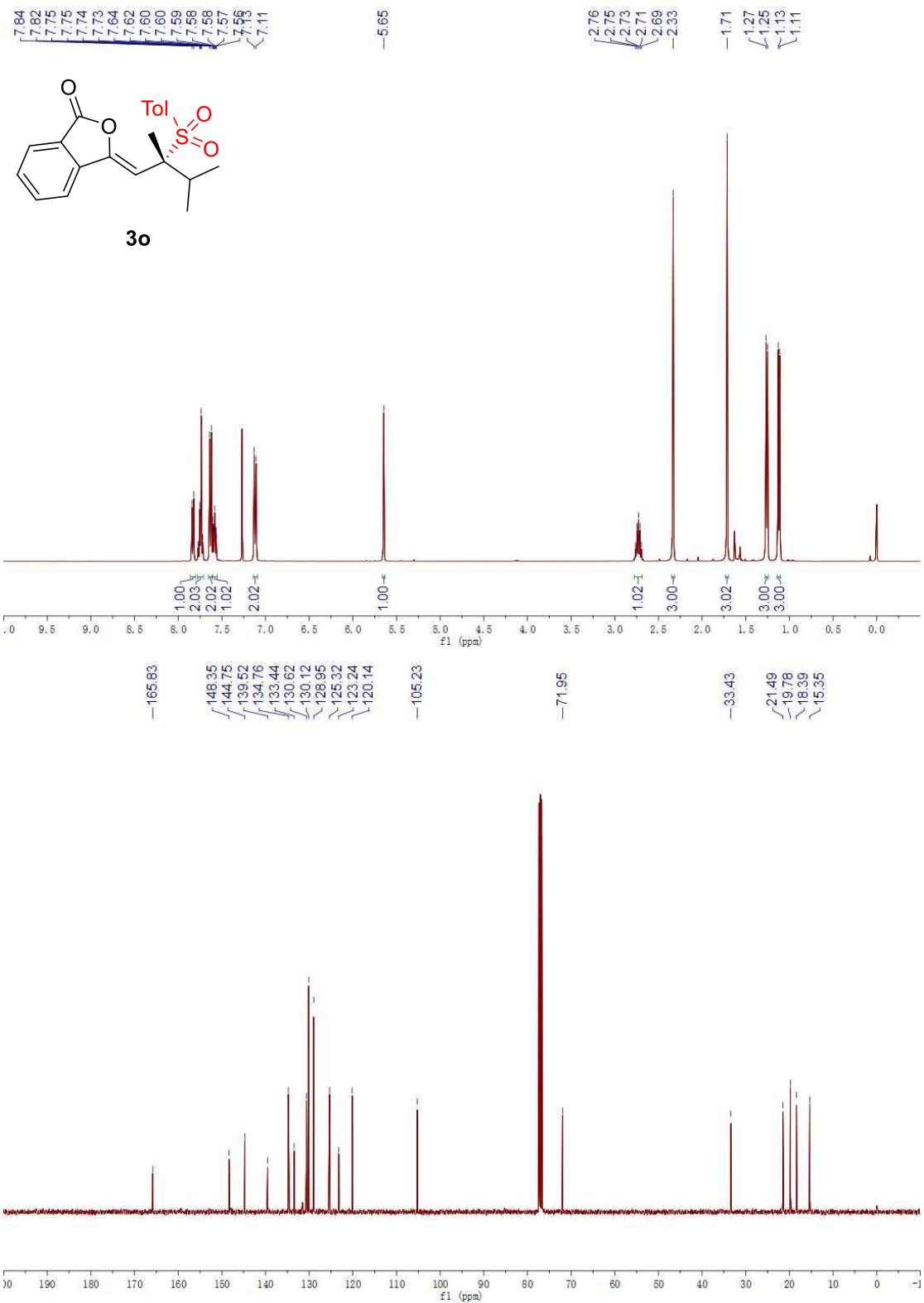


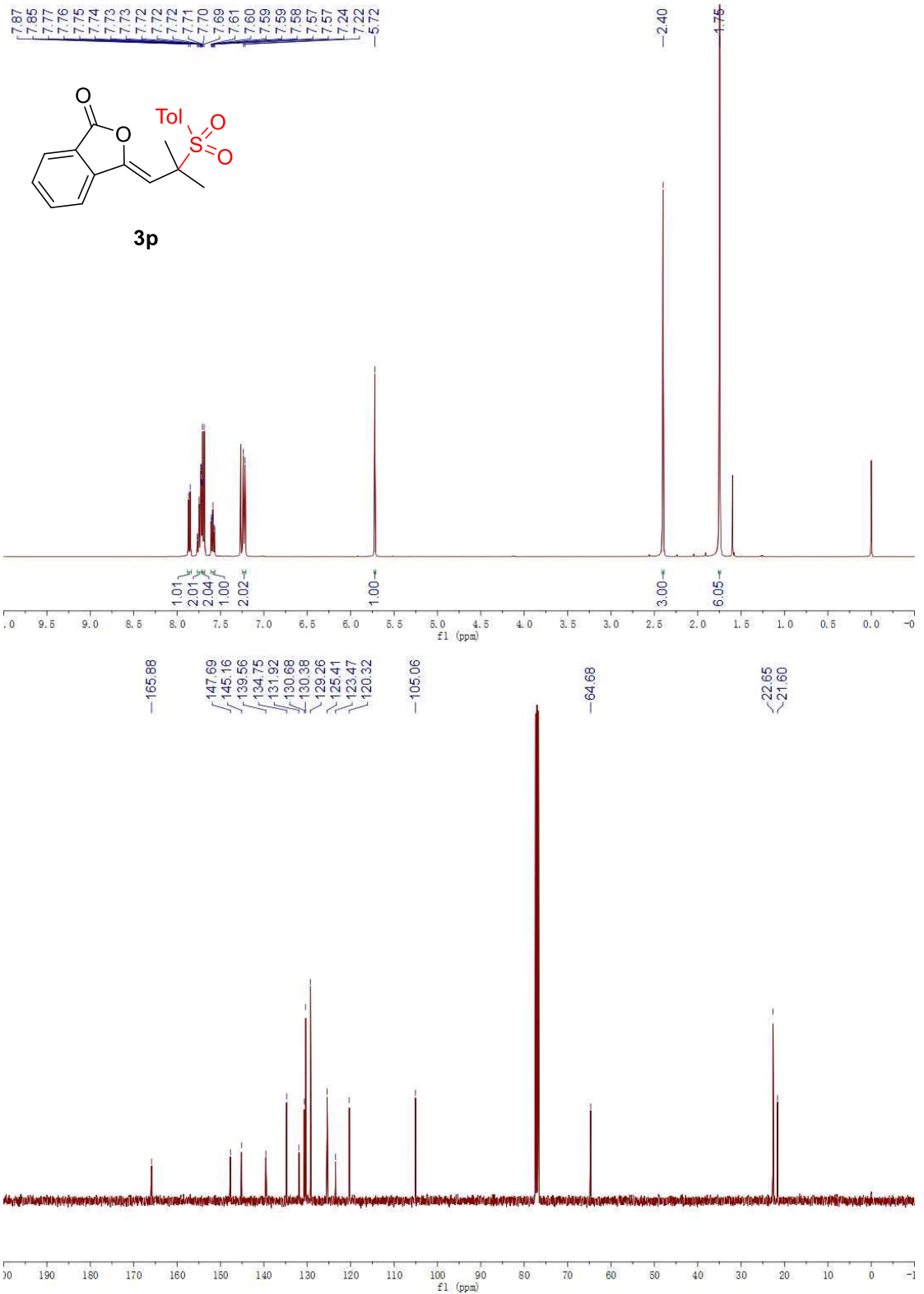


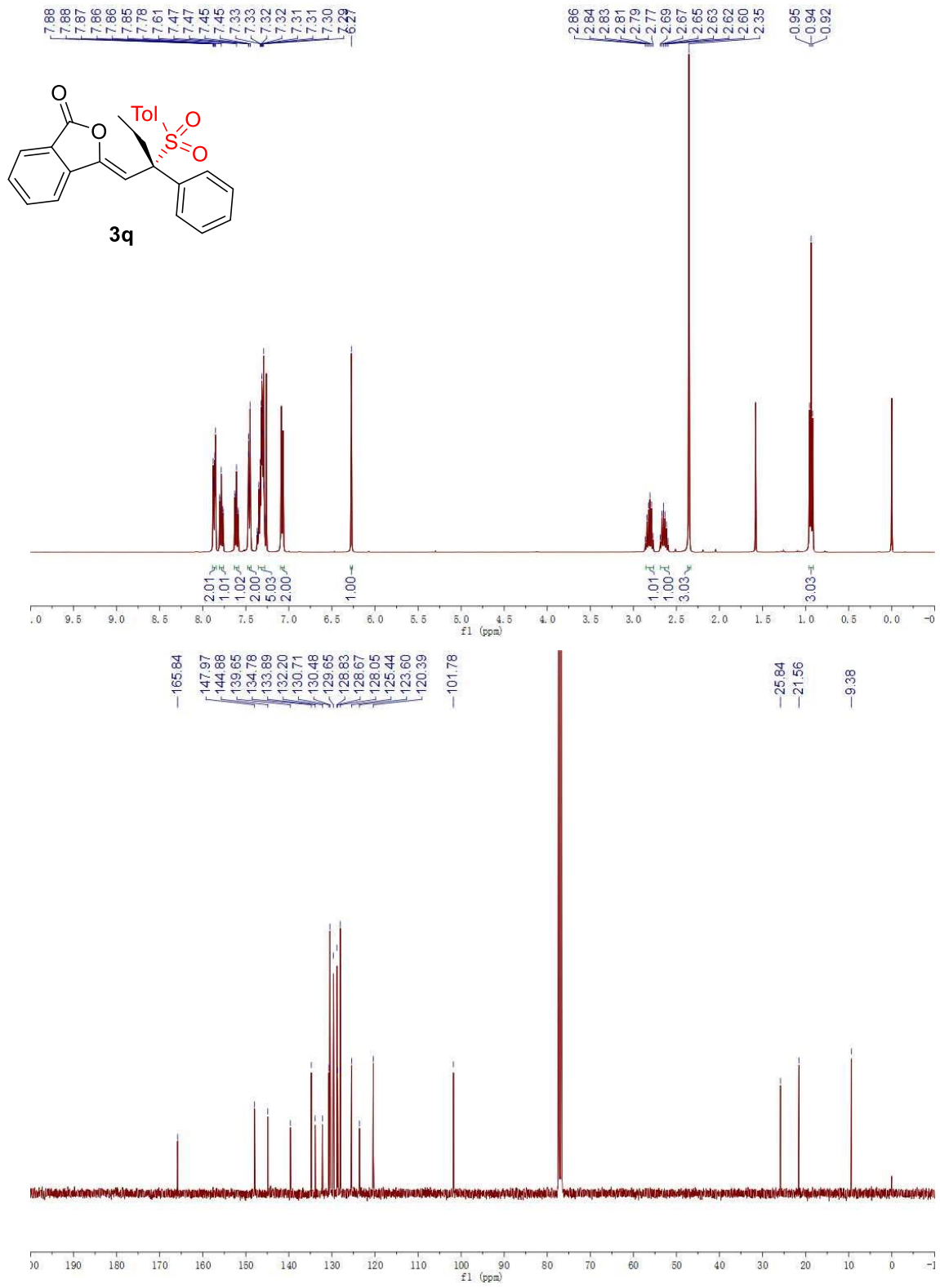


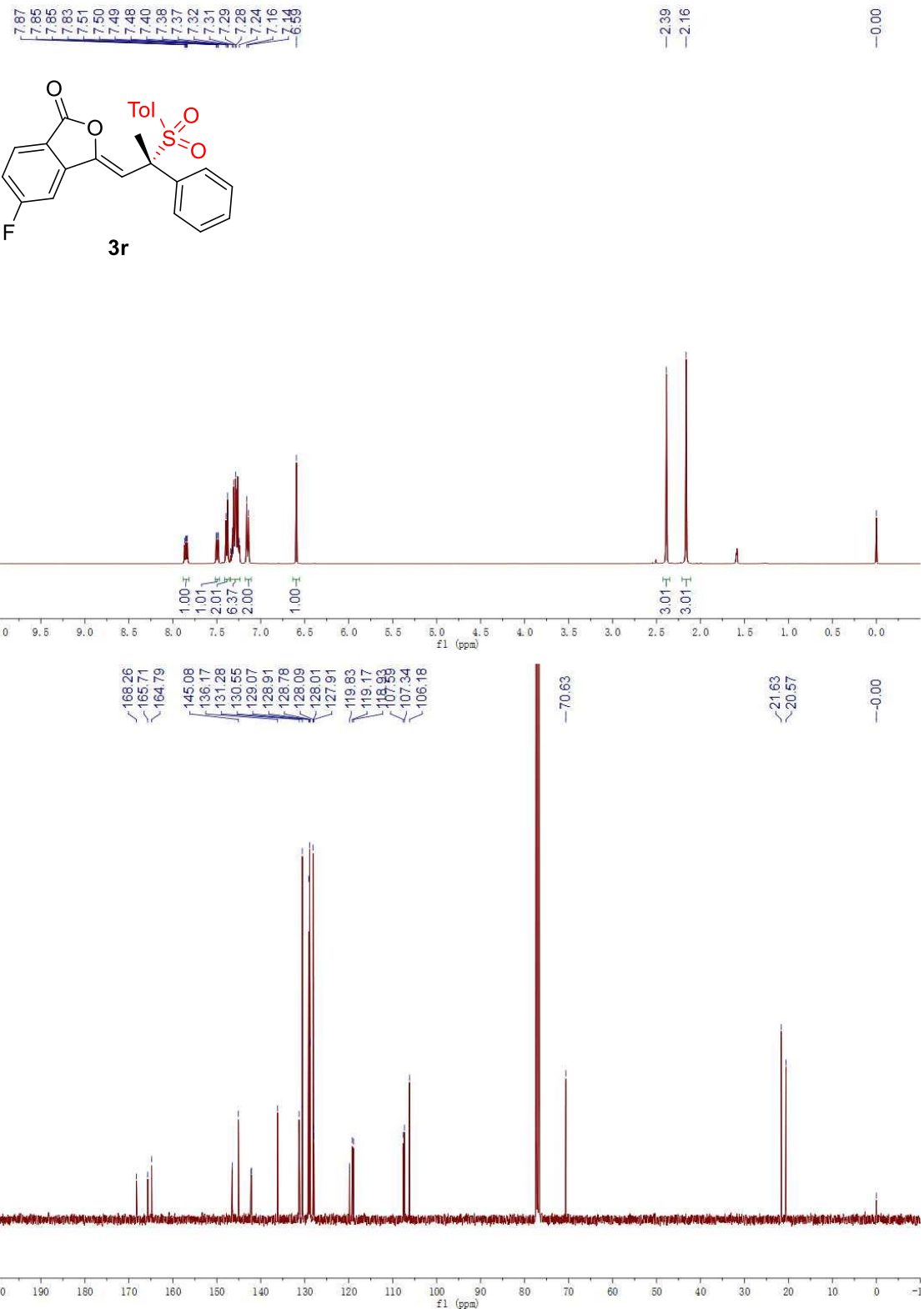


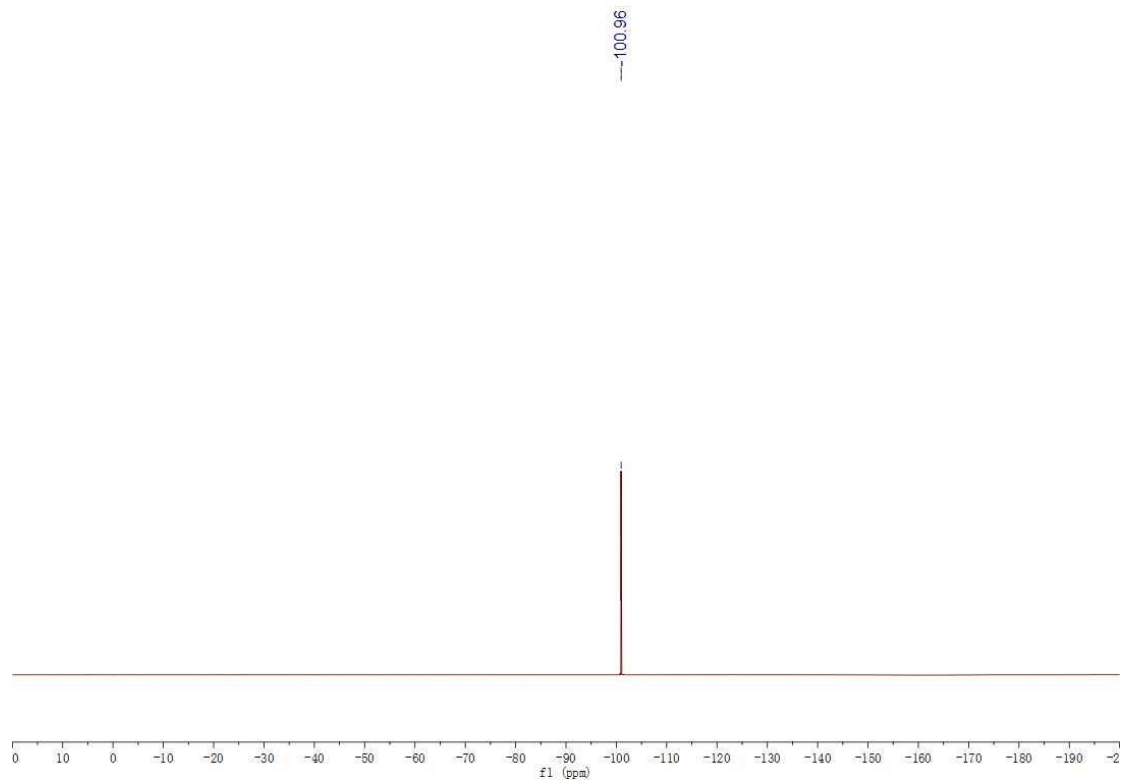




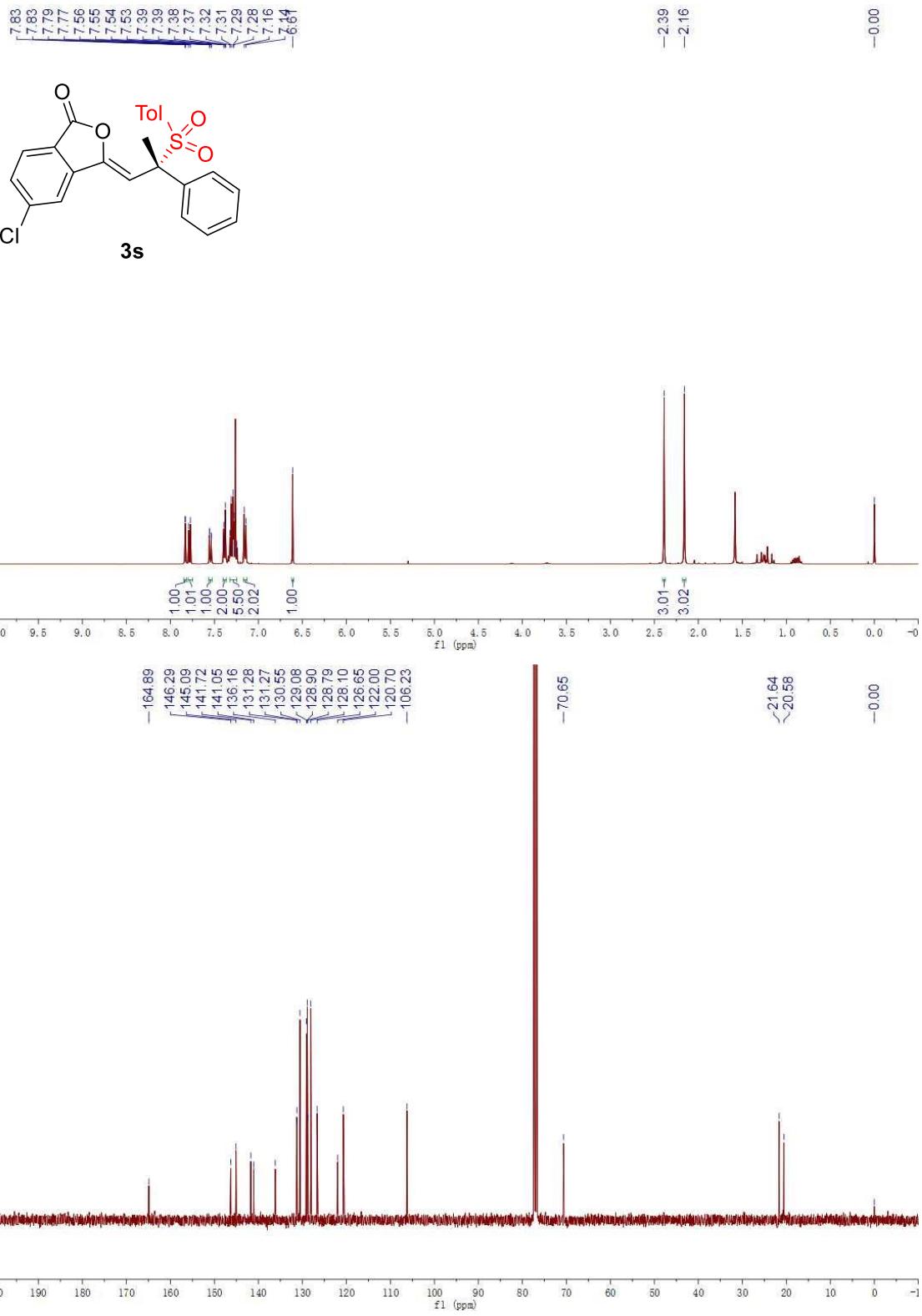


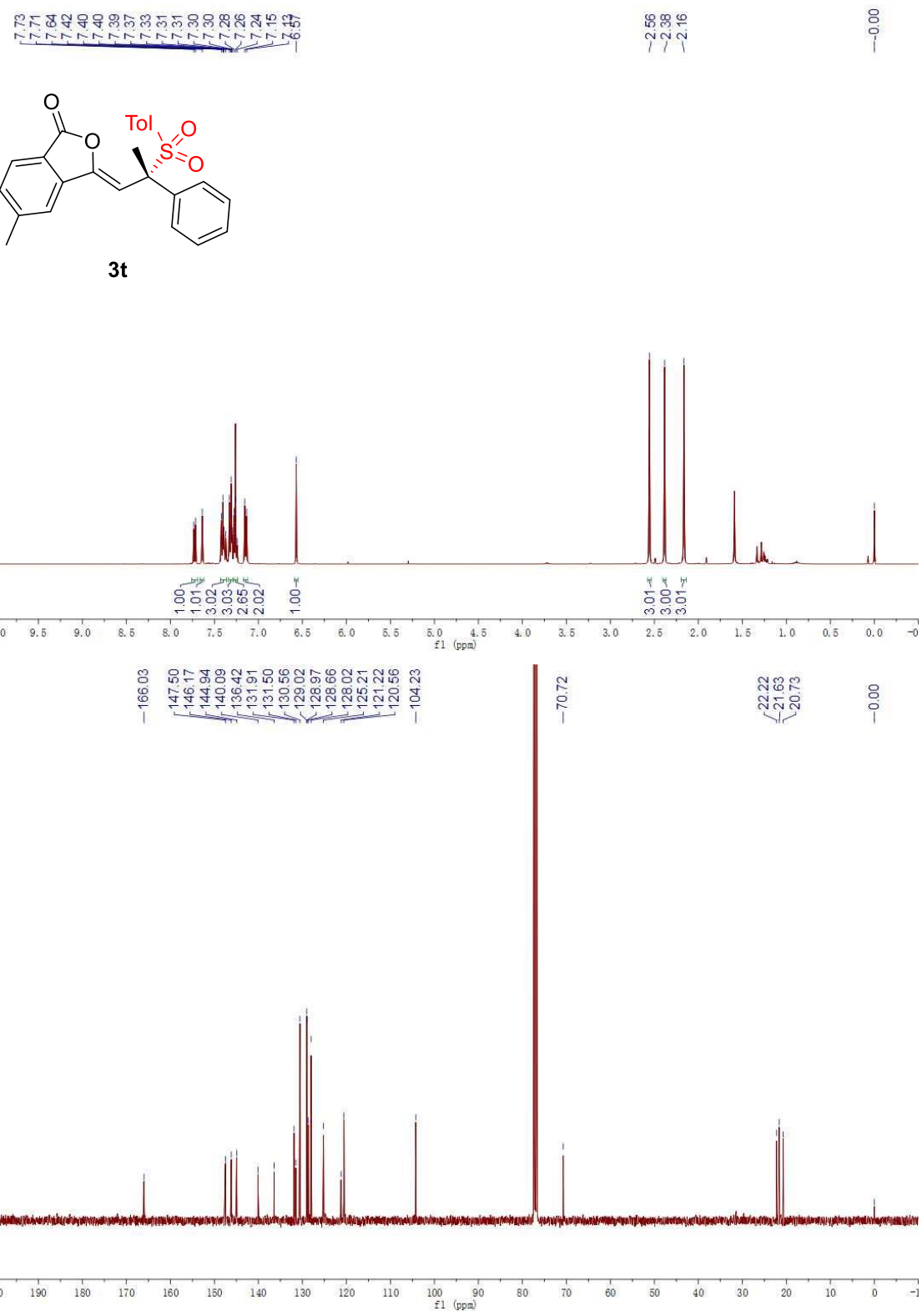


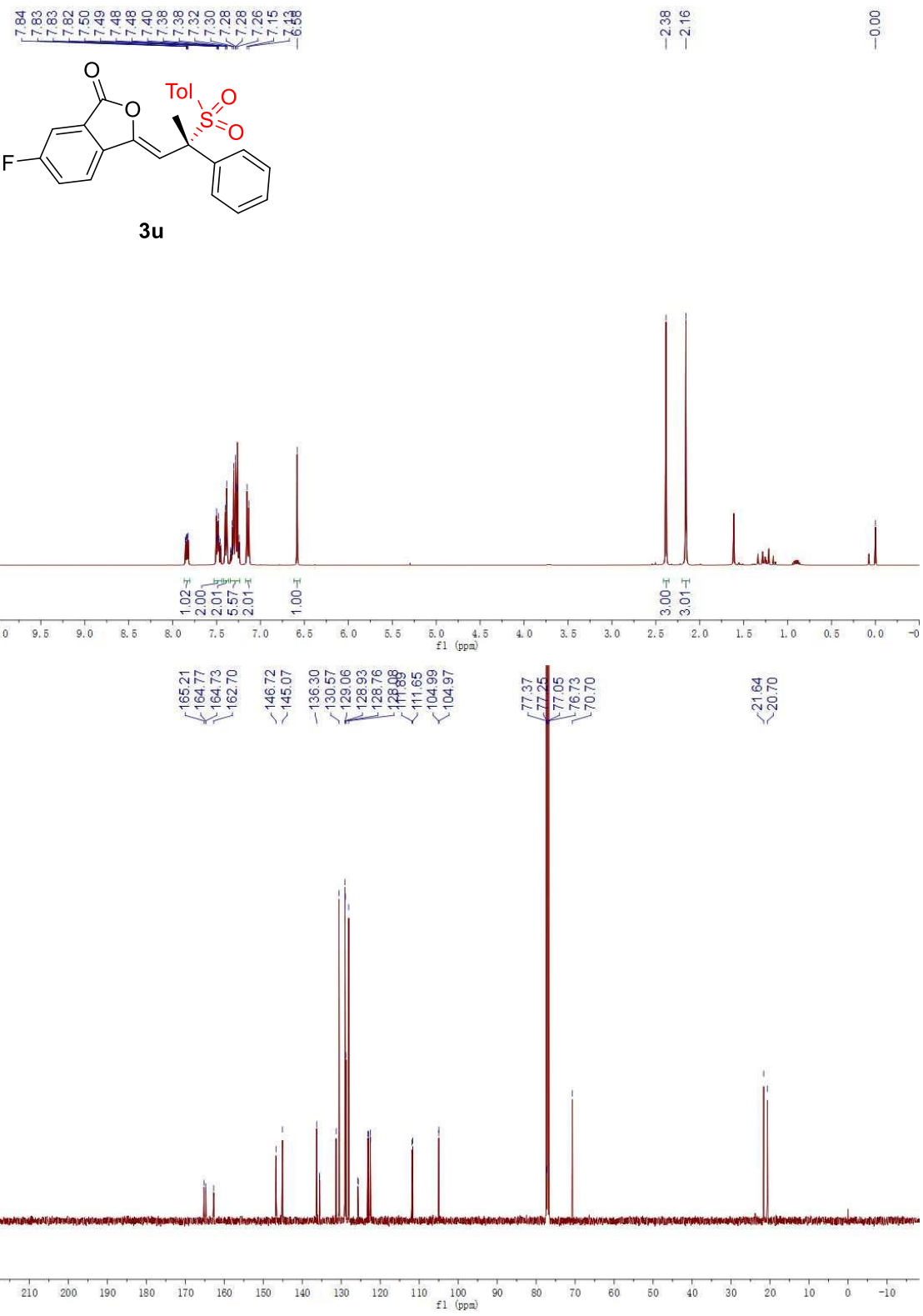


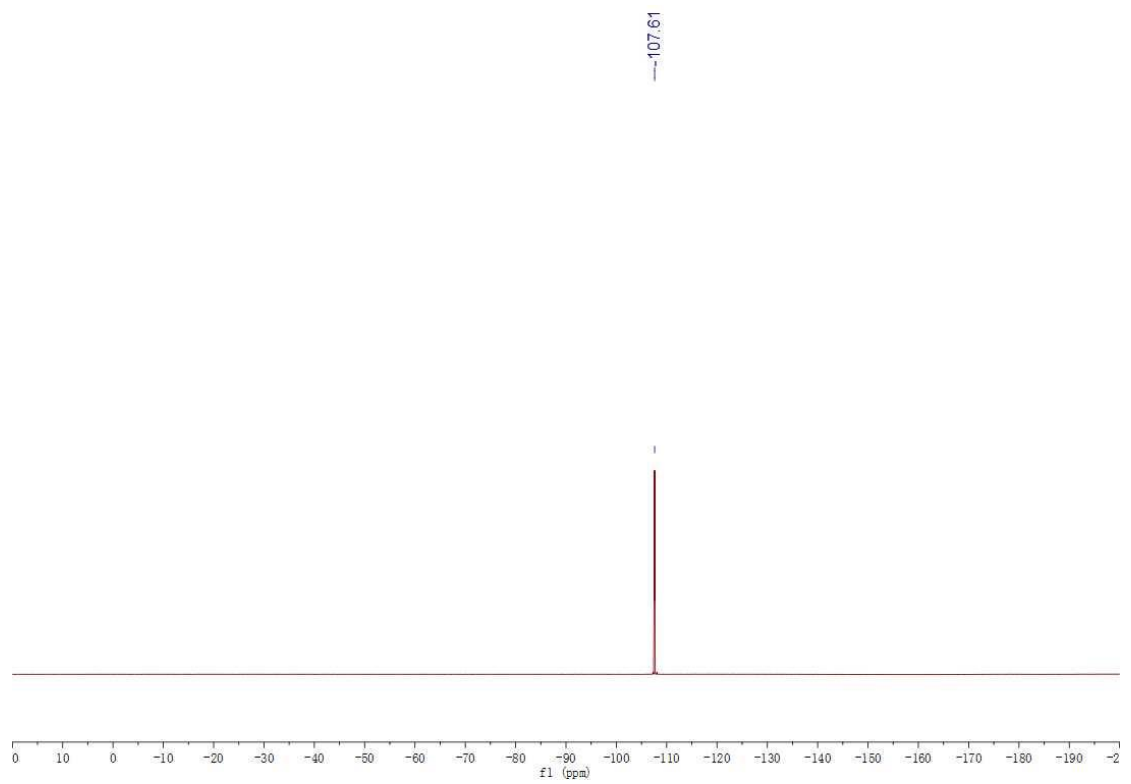


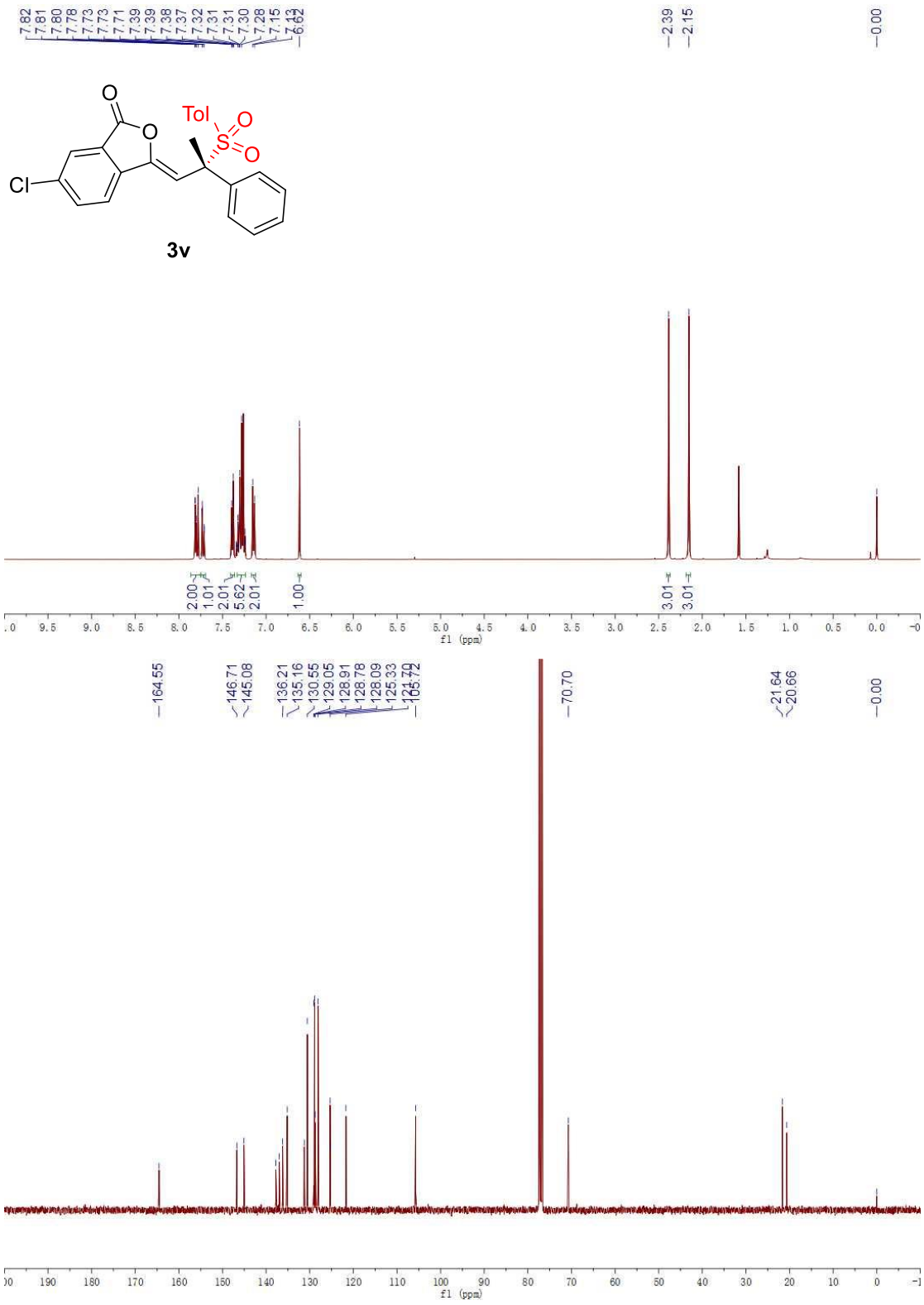
S120

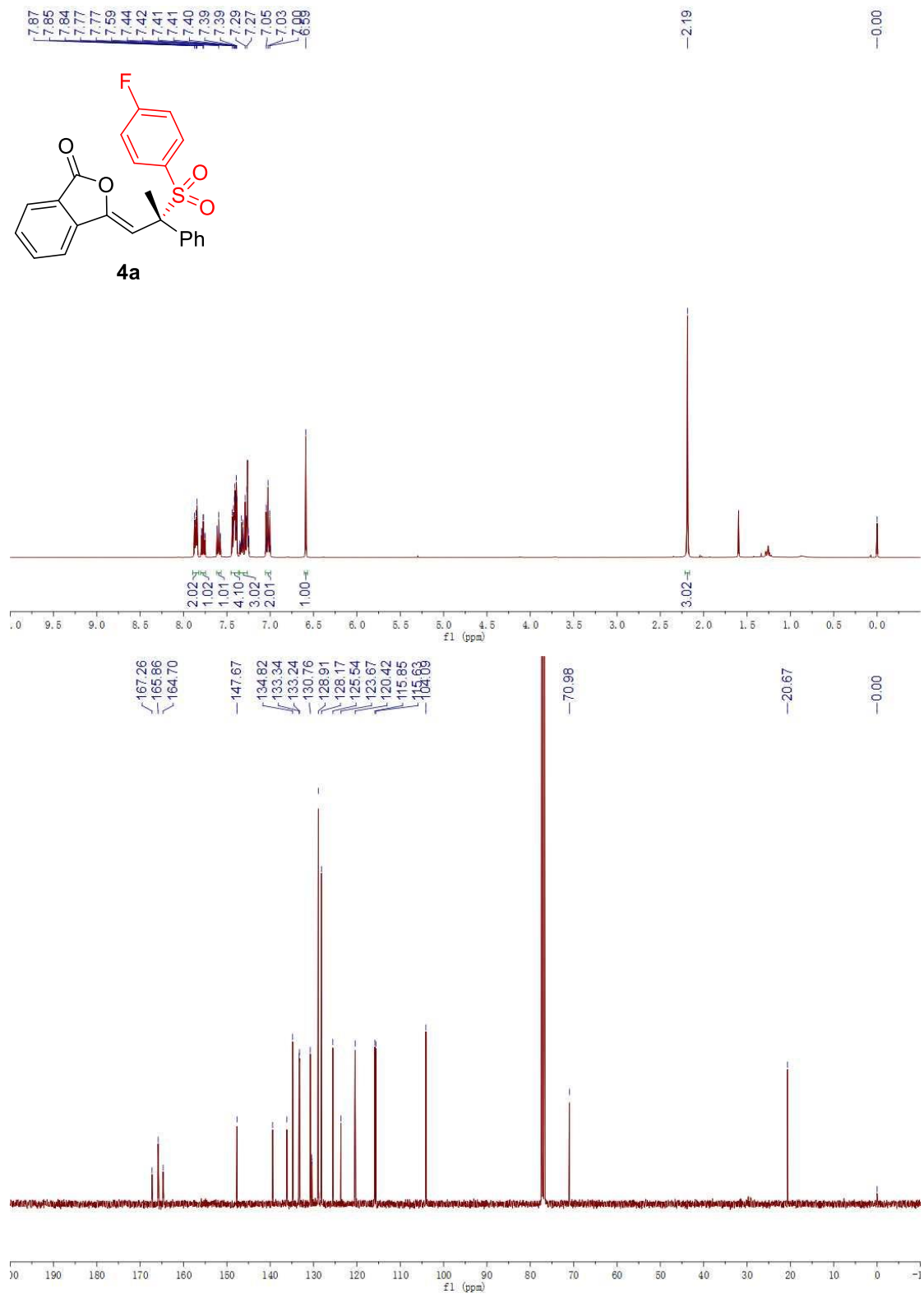


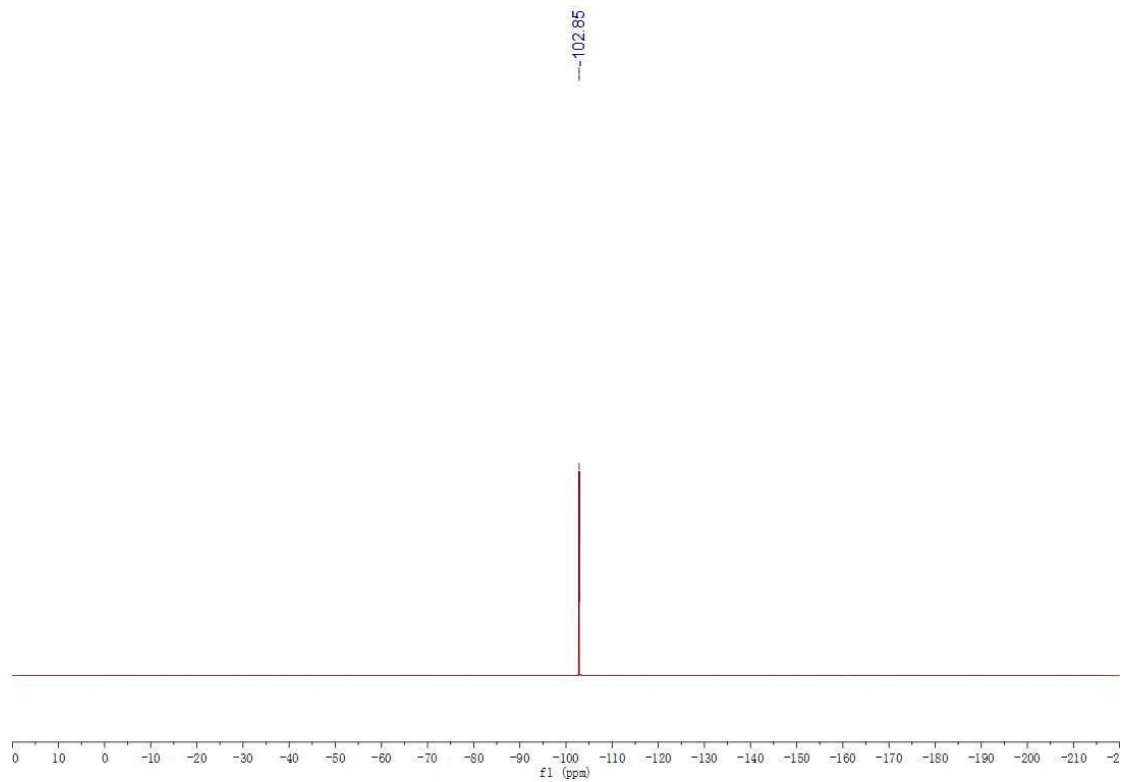


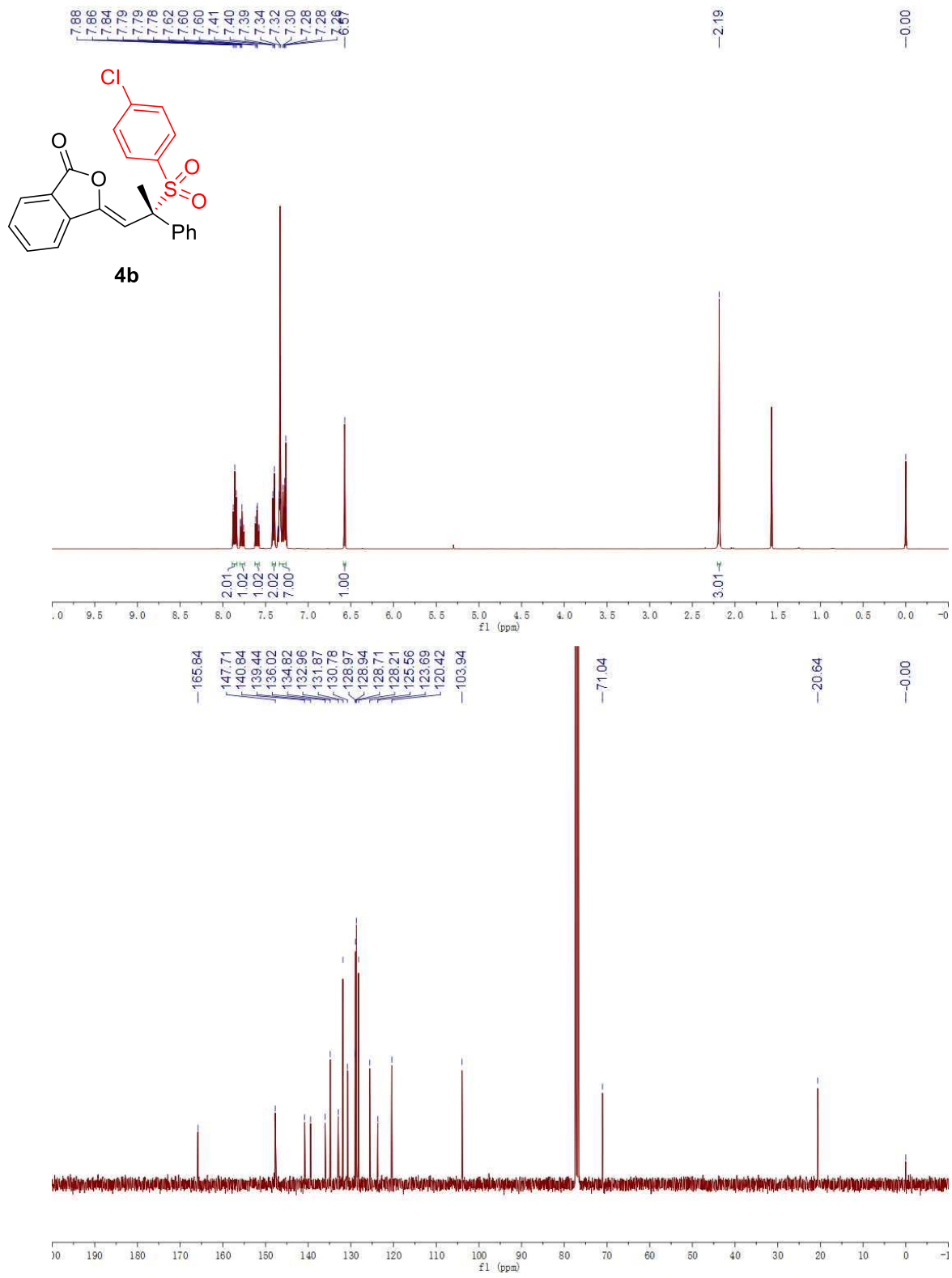


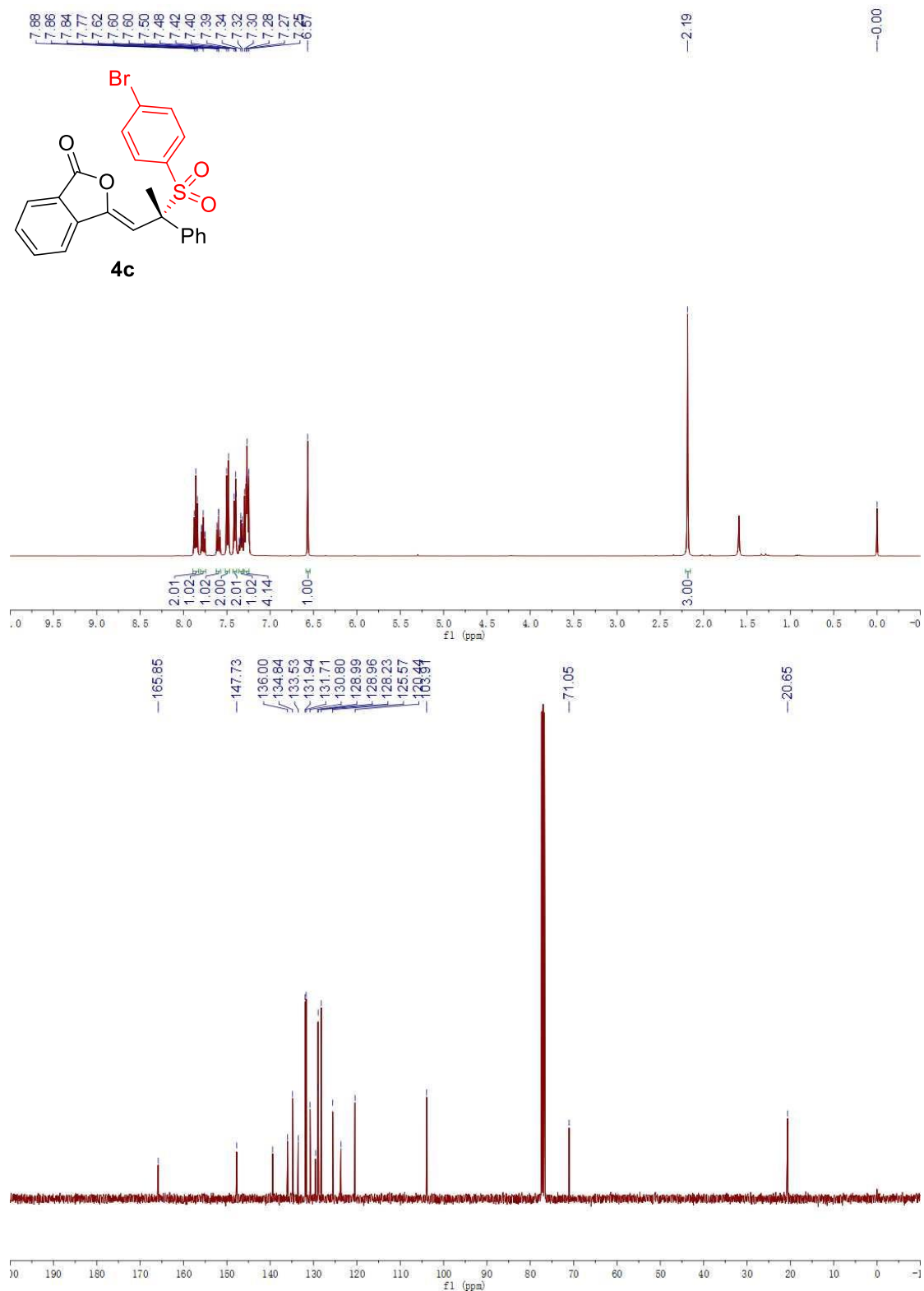


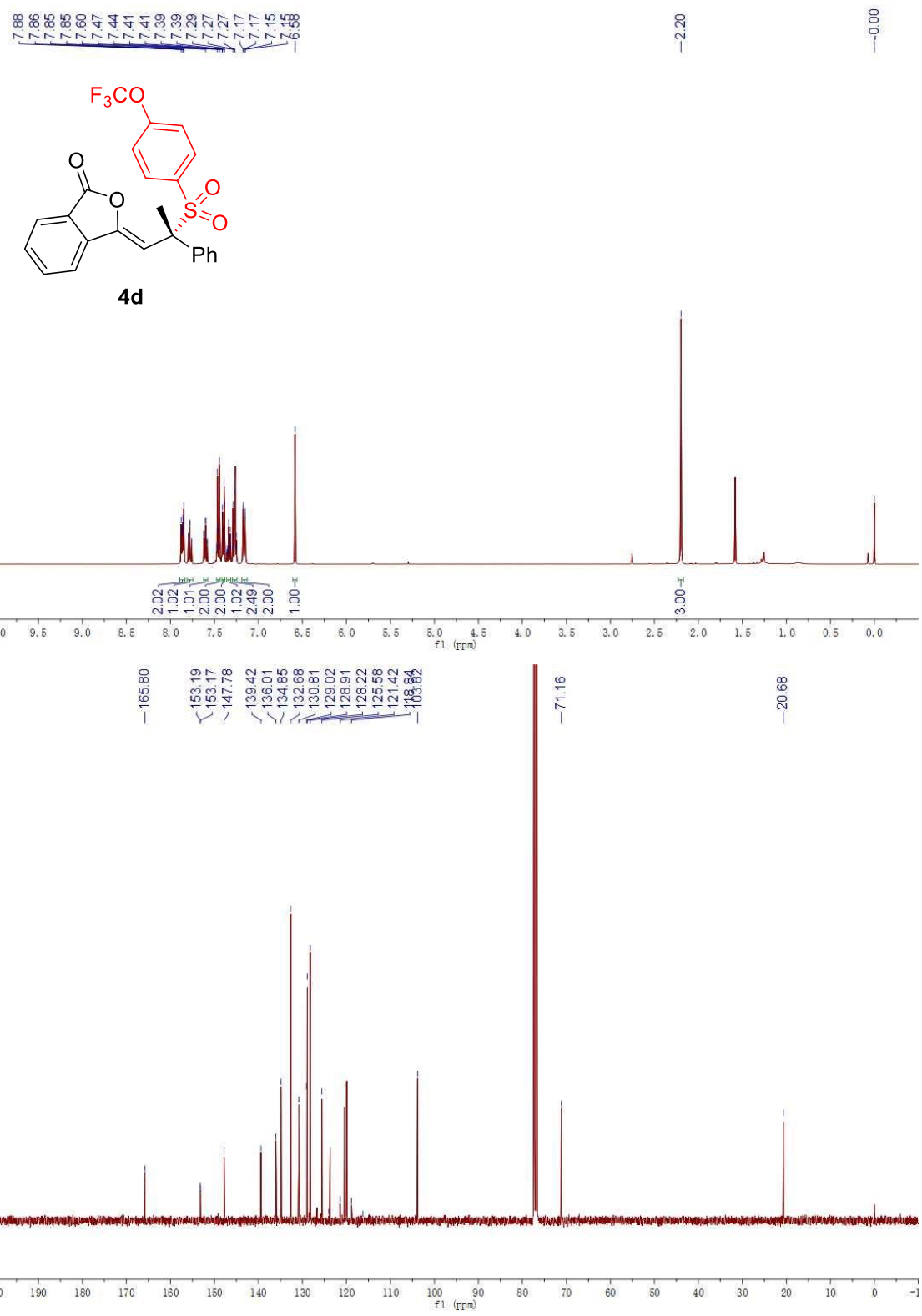


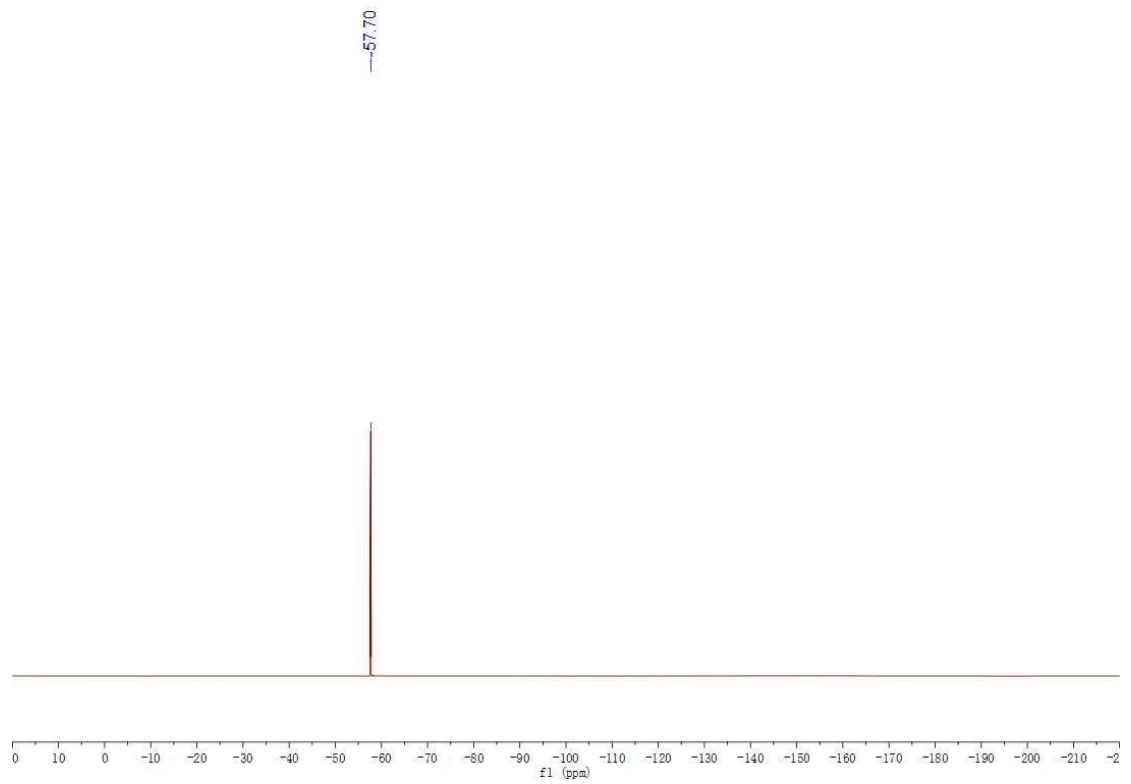


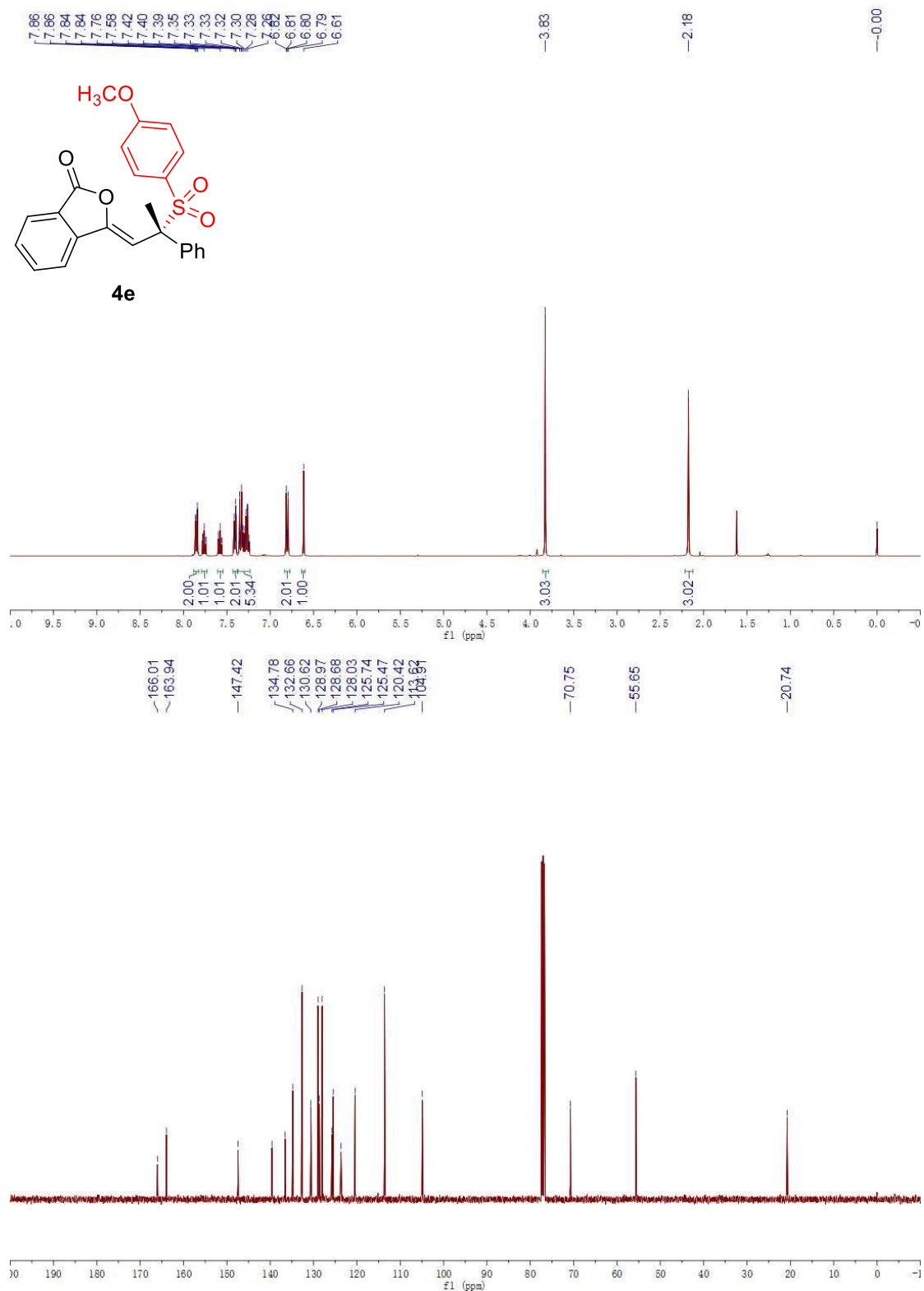


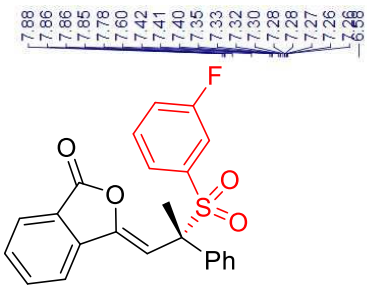




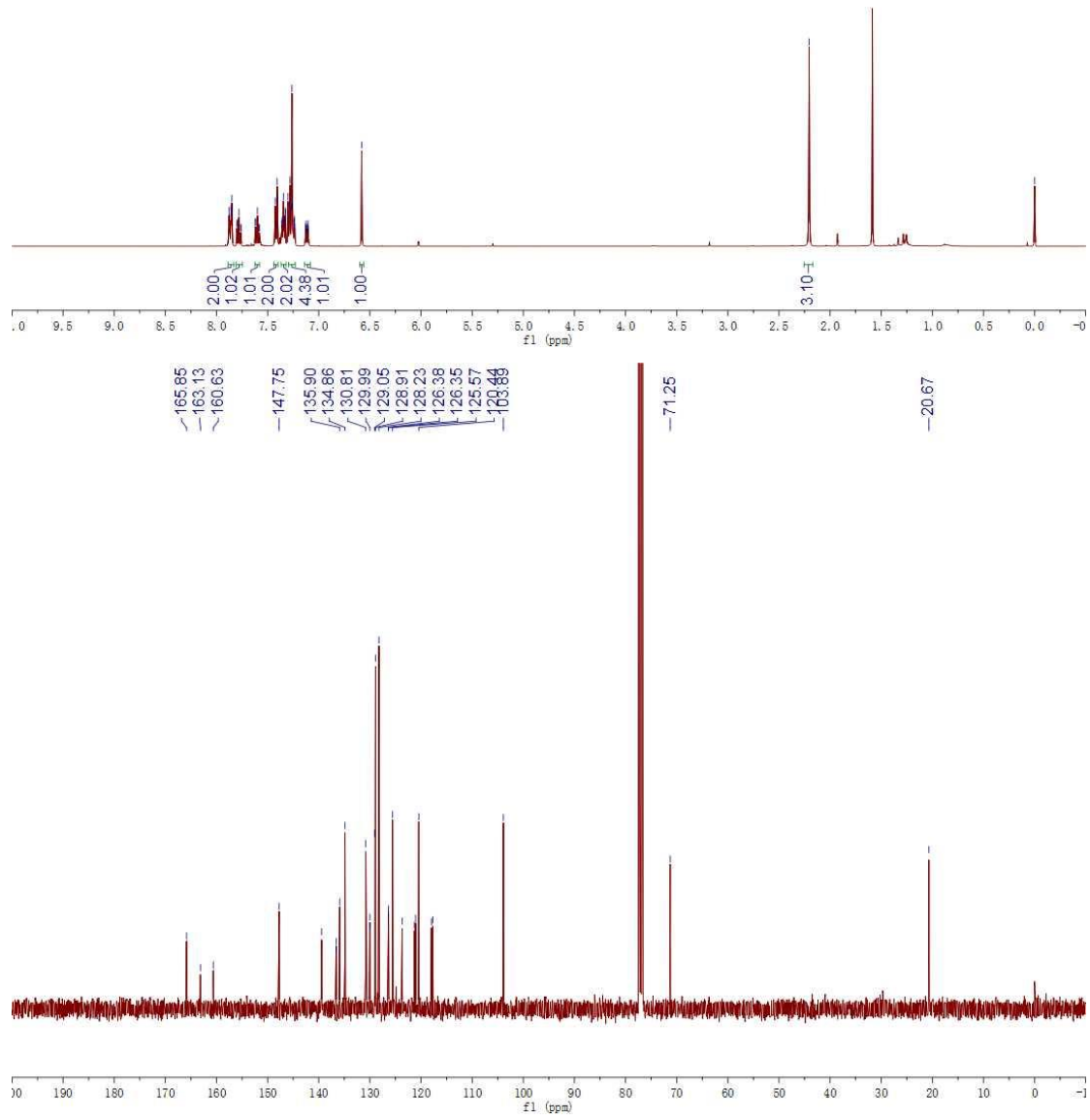


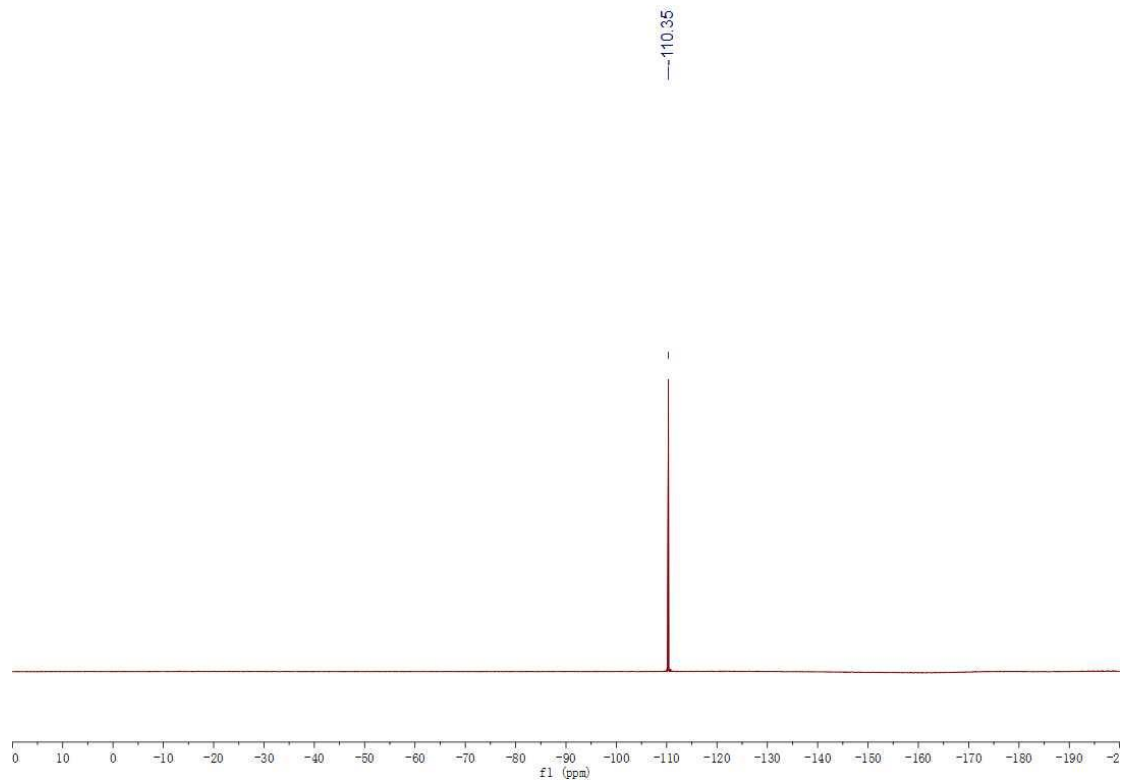


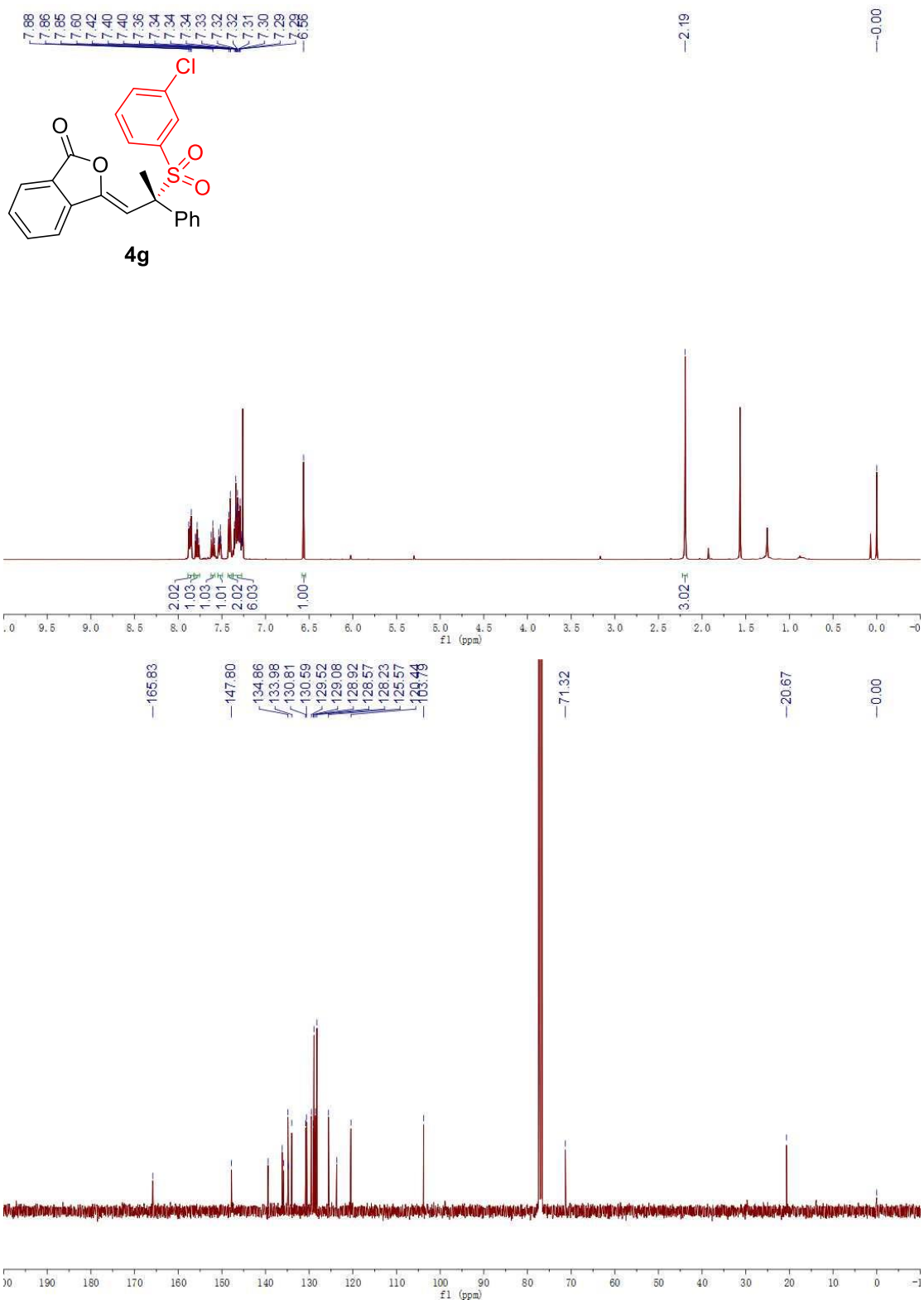


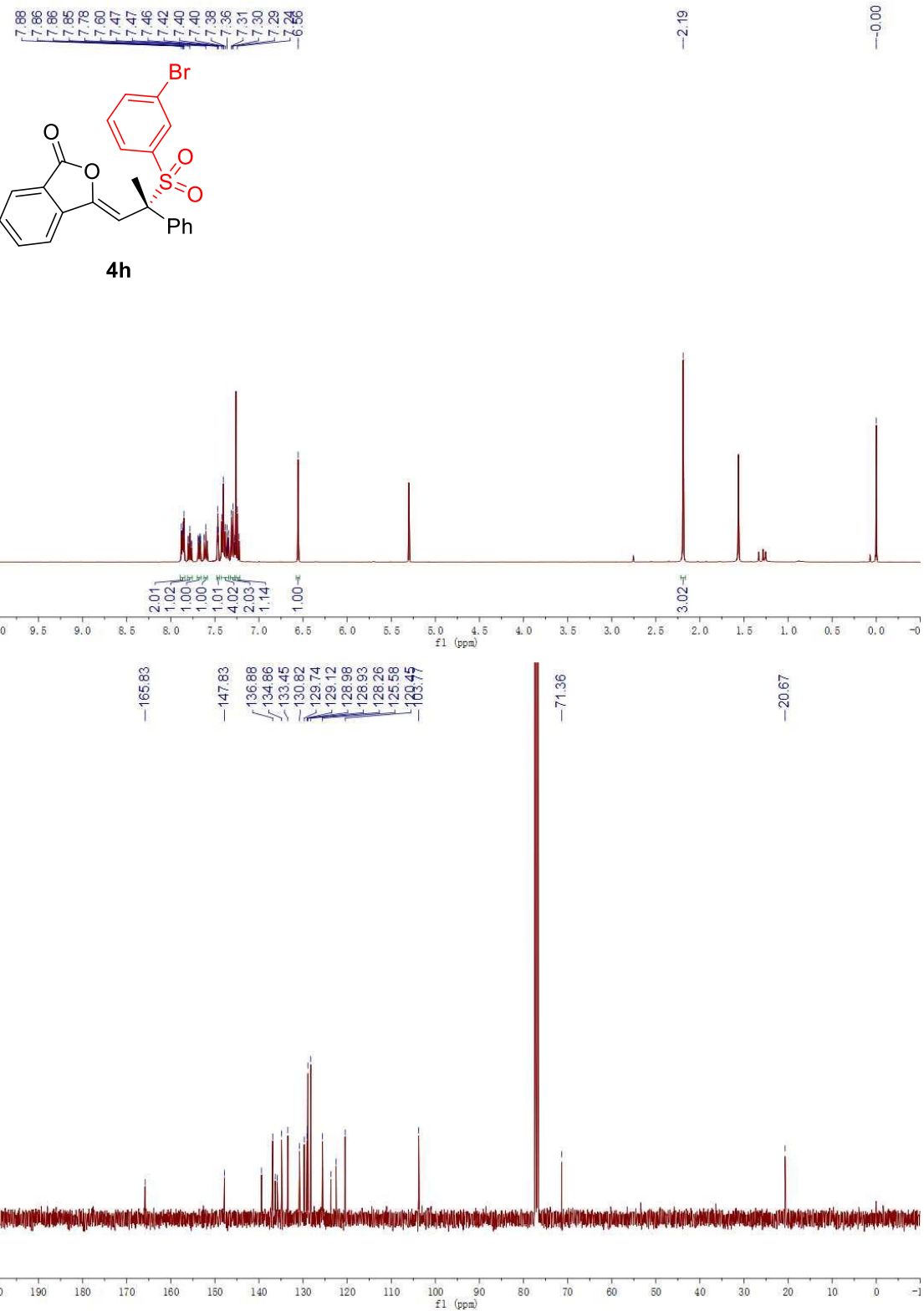


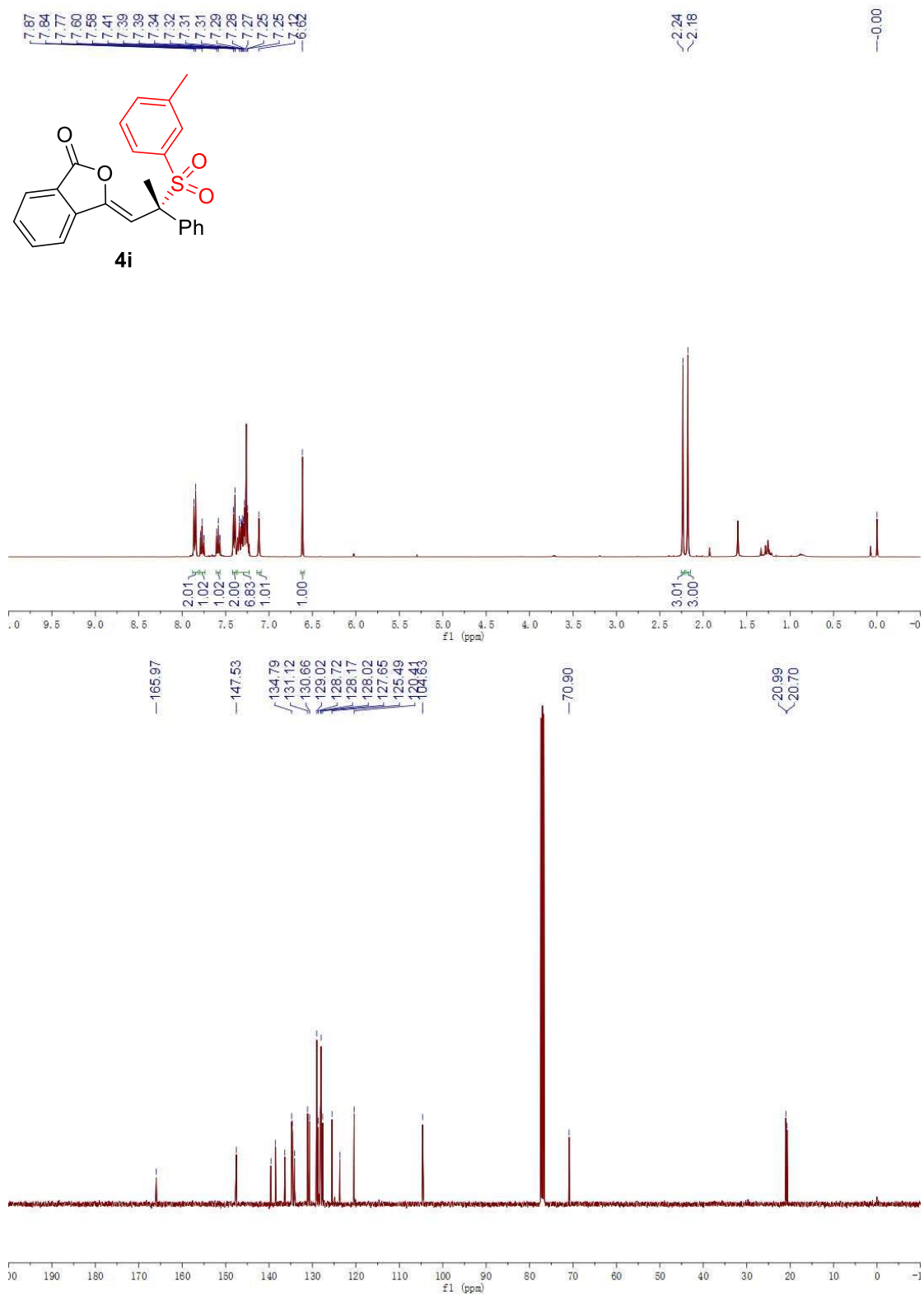
4f

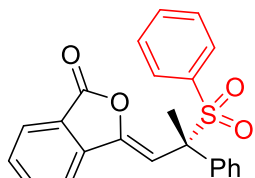




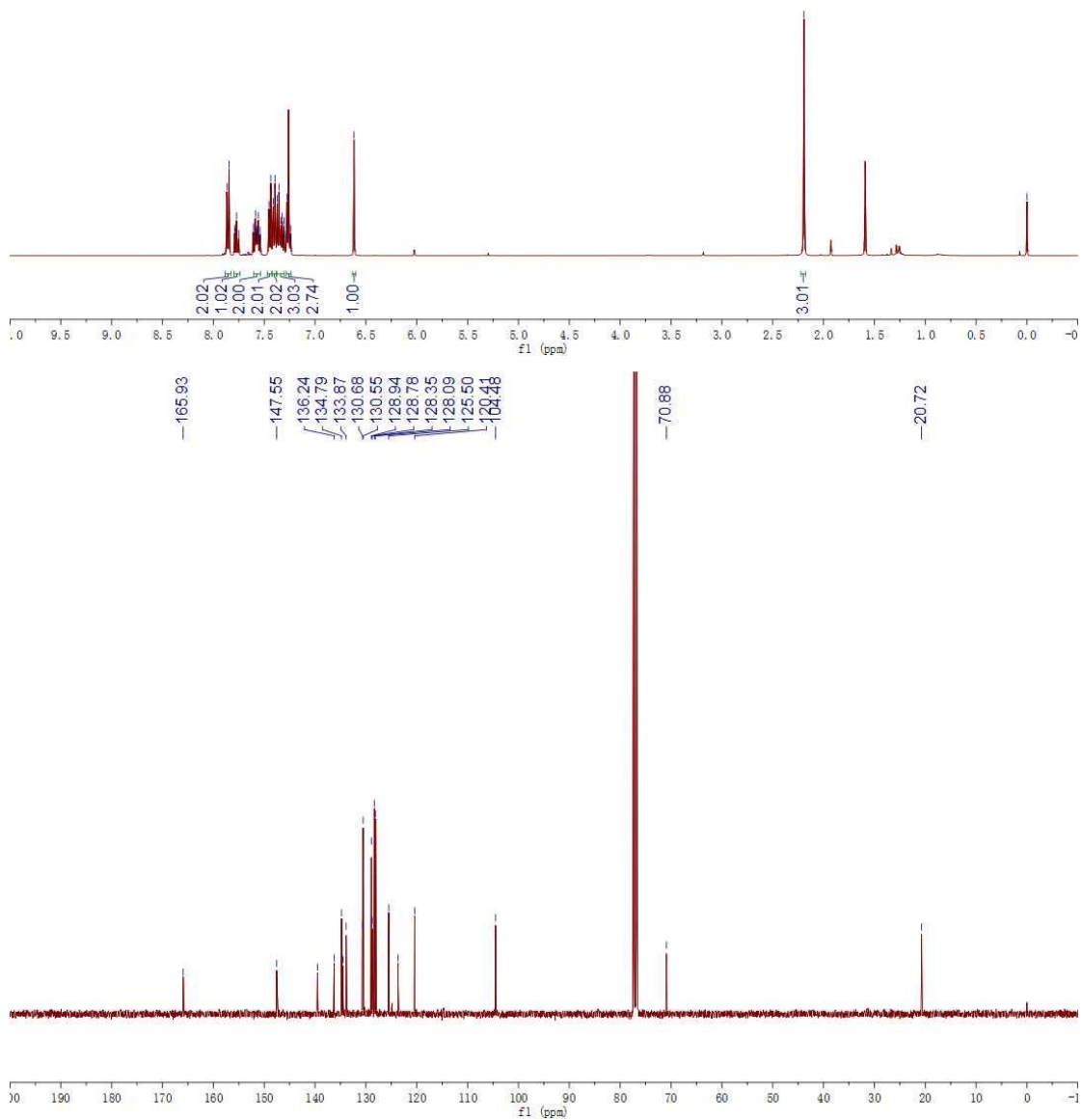


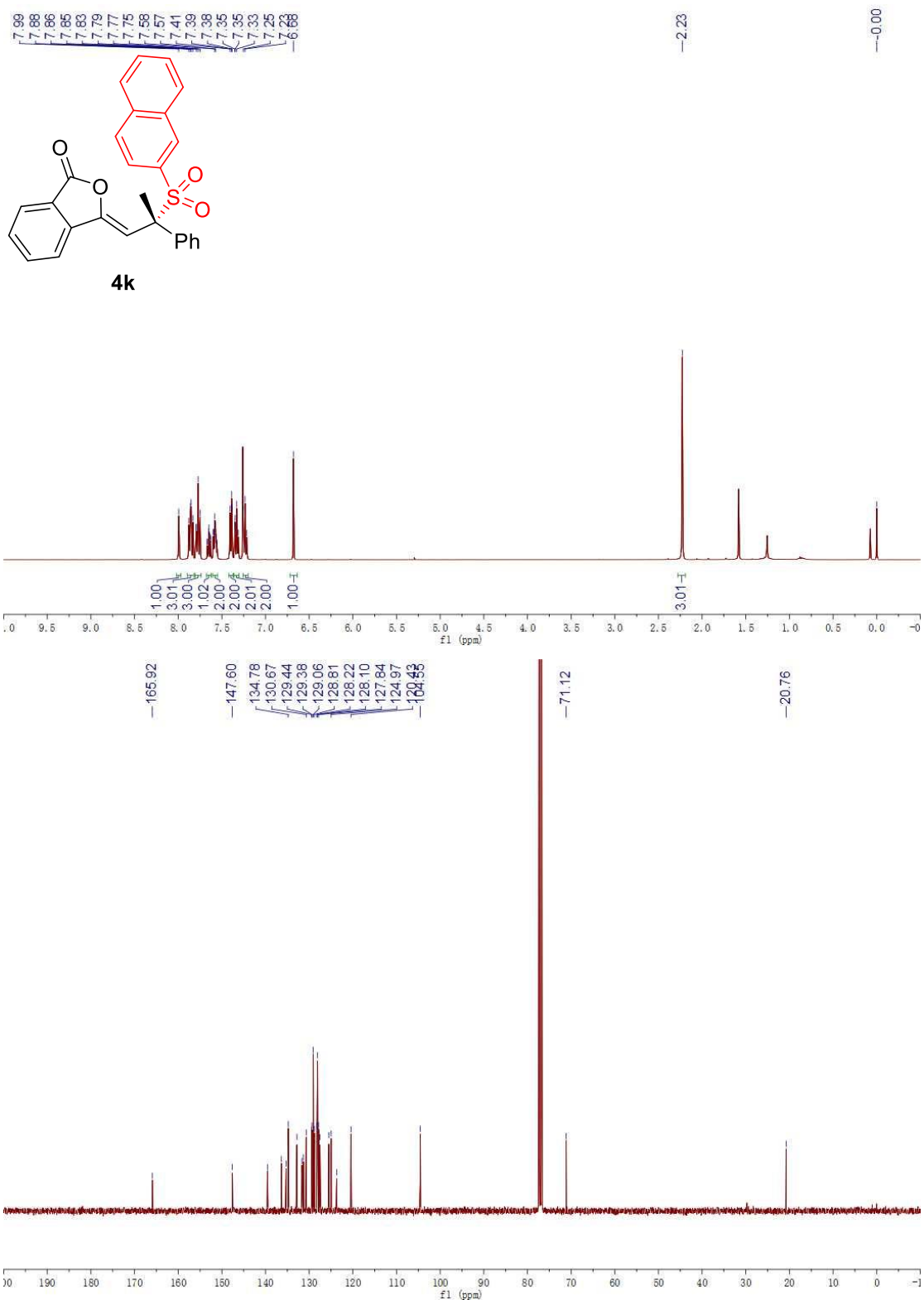


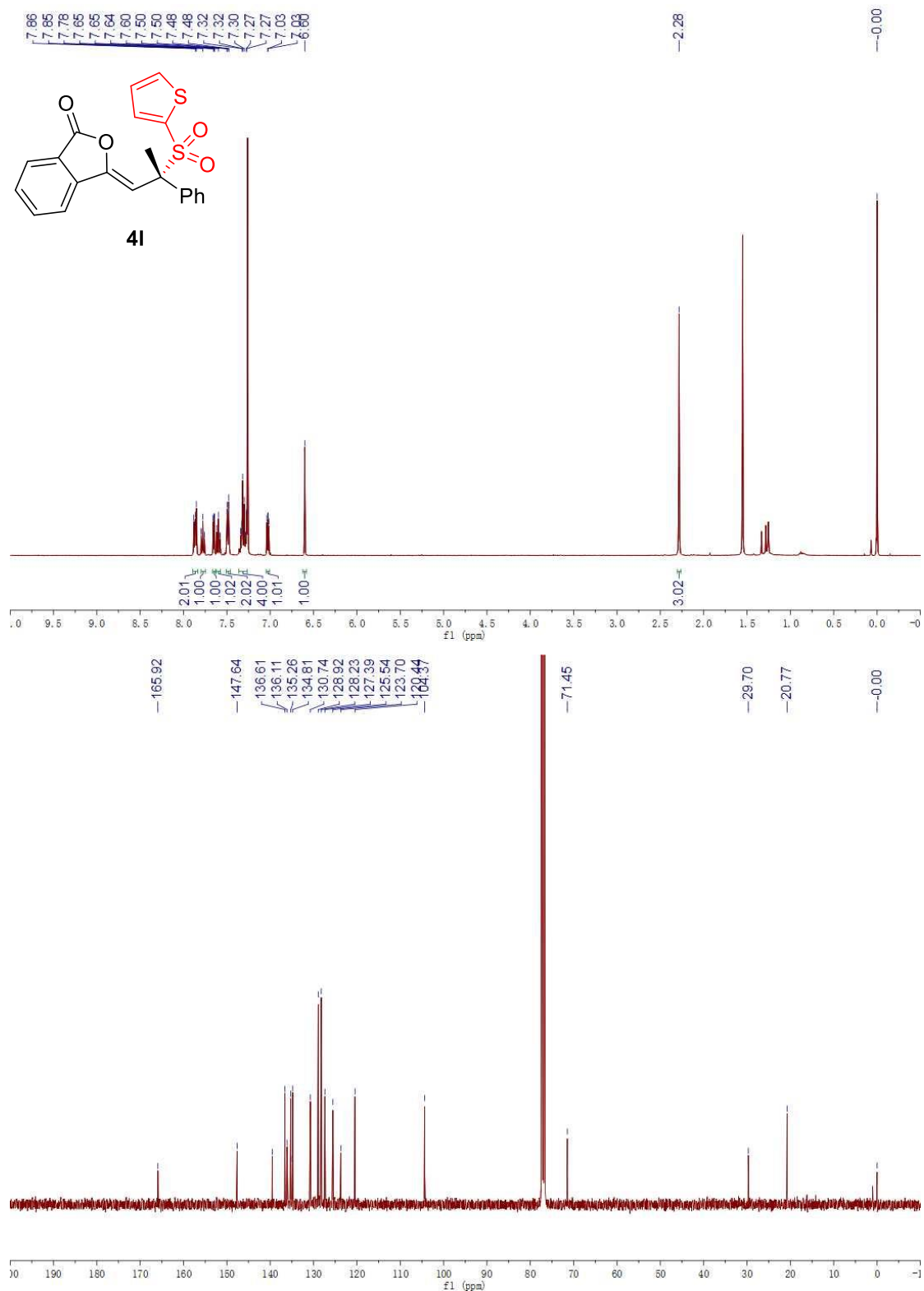


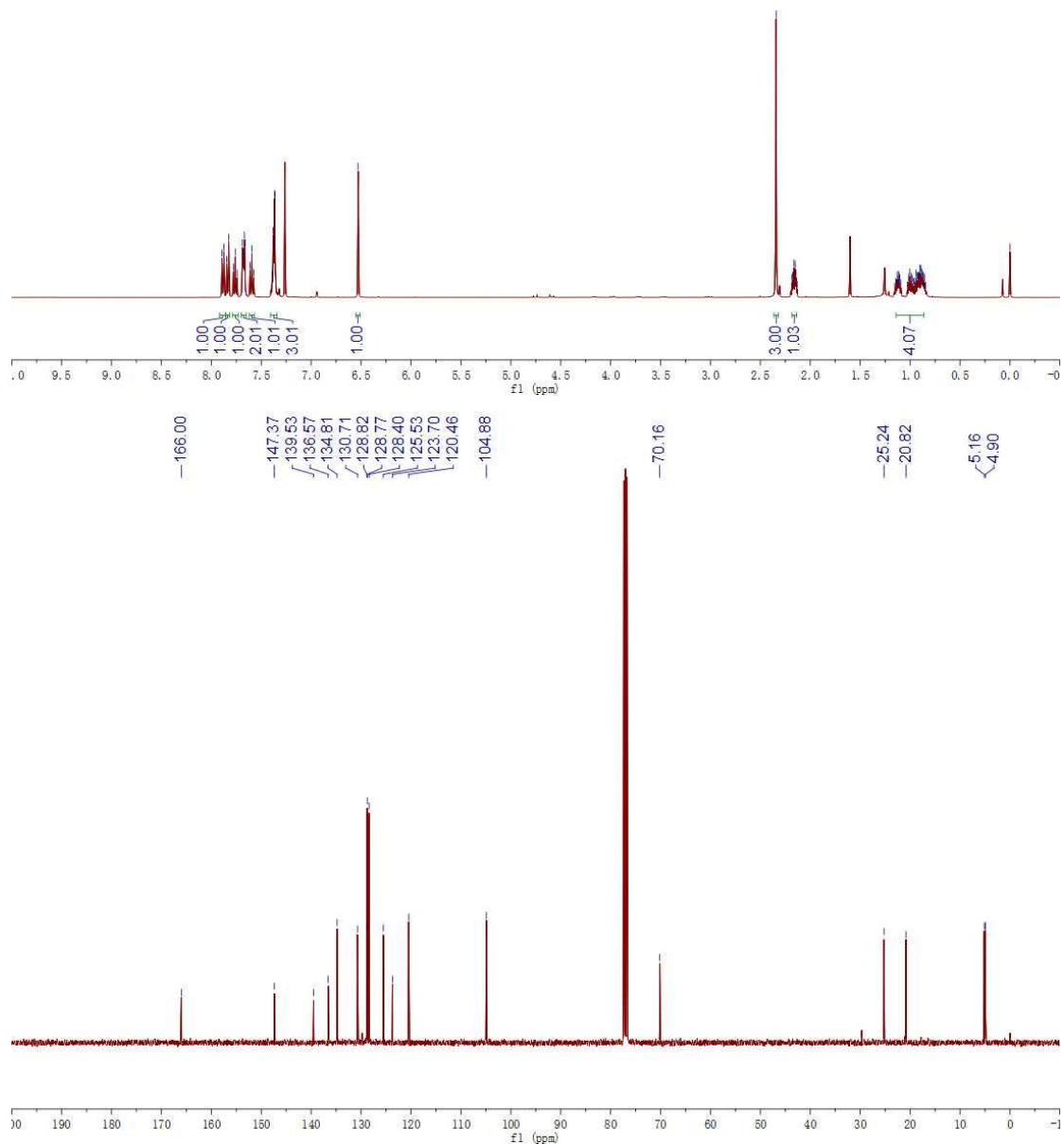
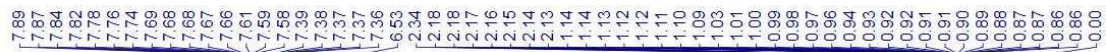


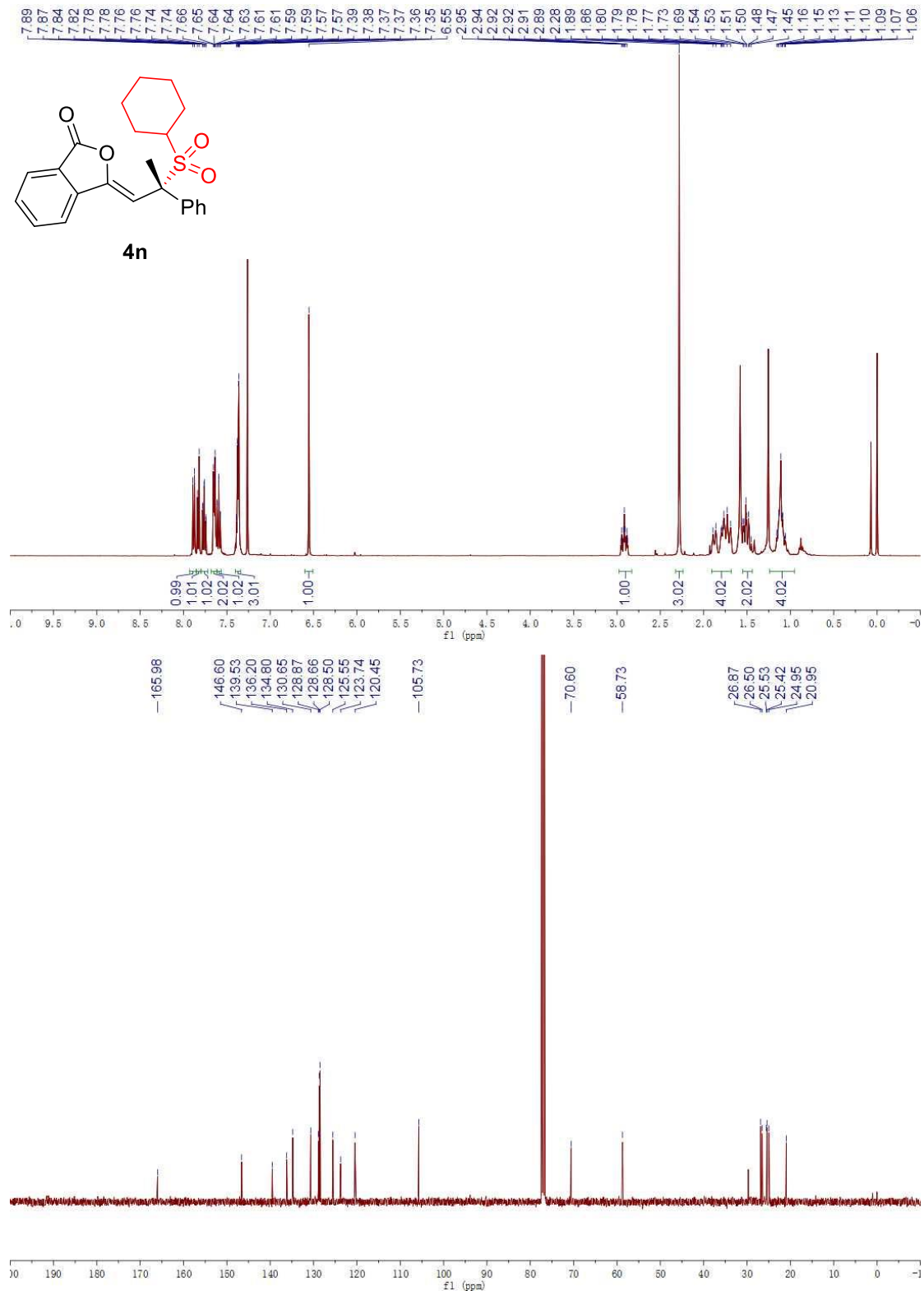
4j

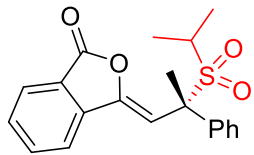
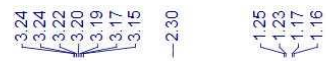
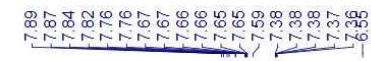




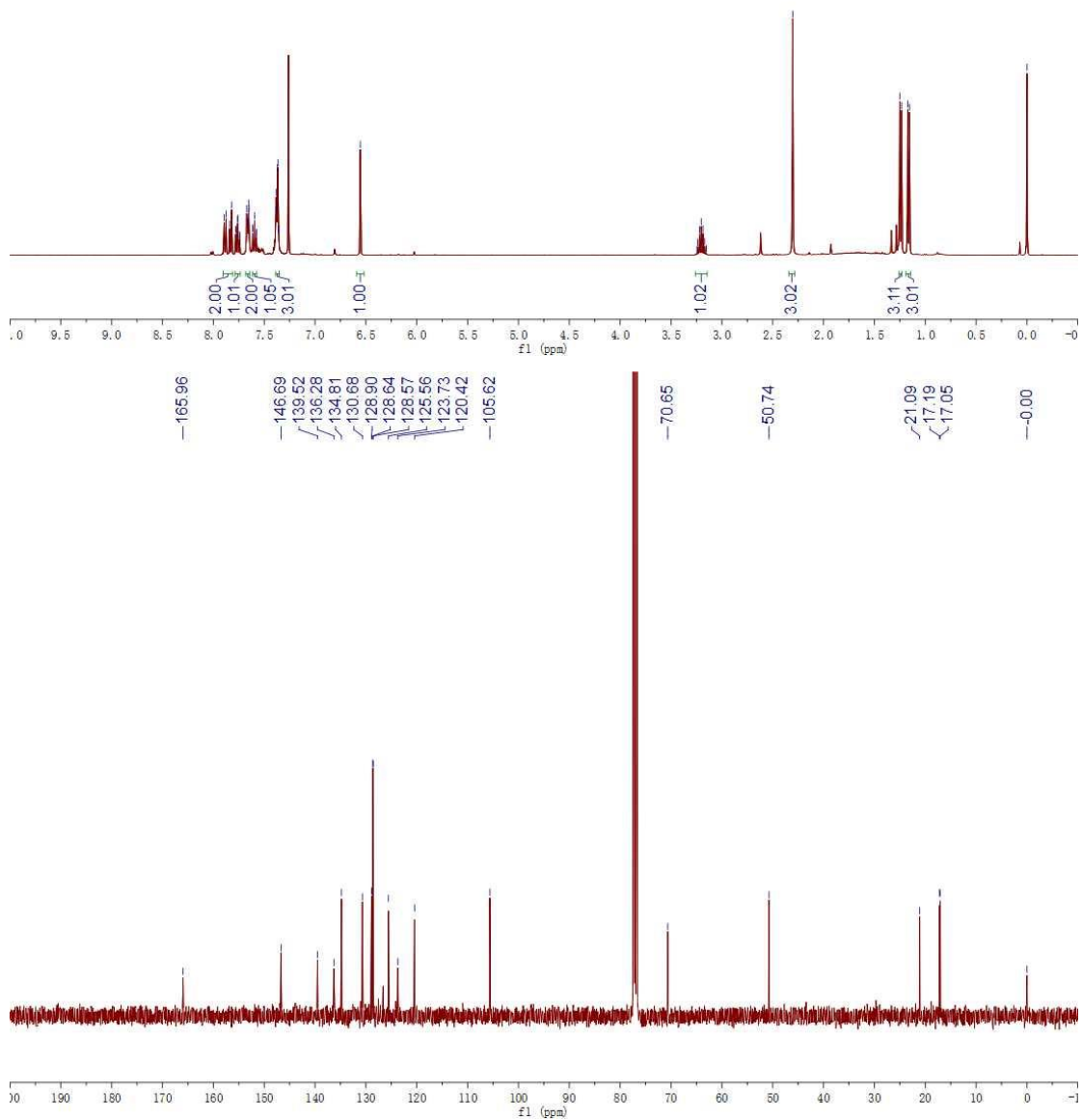


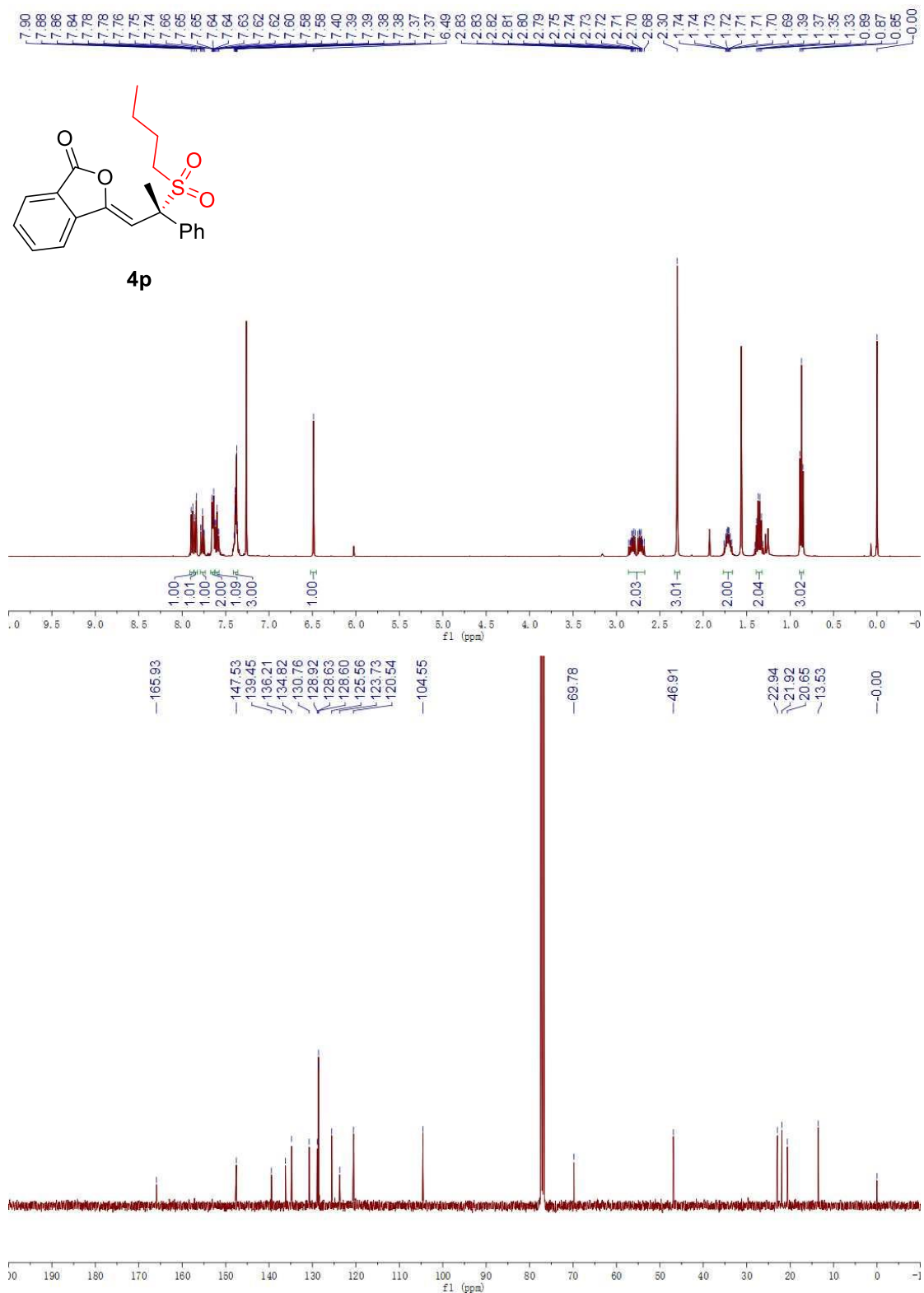


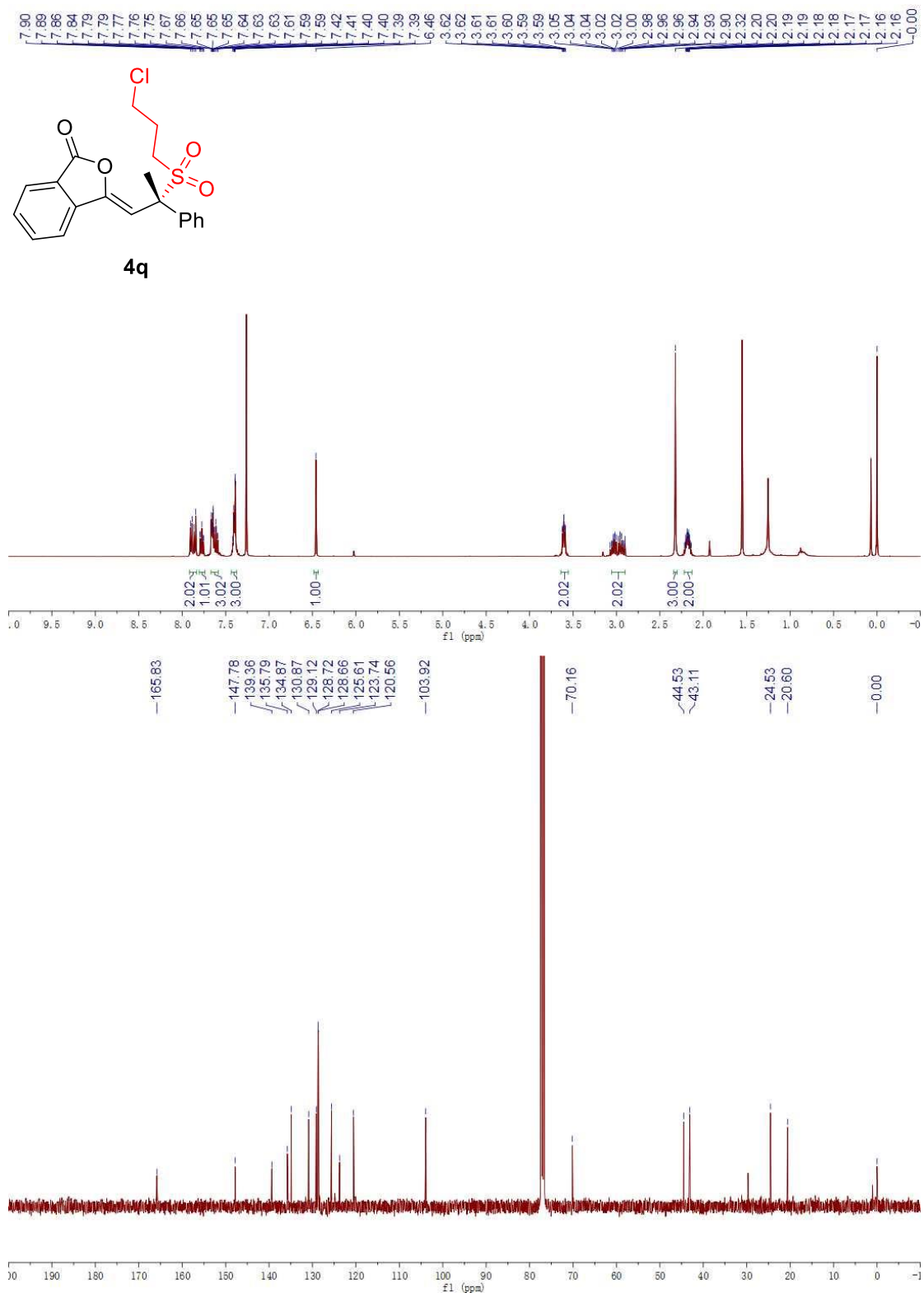


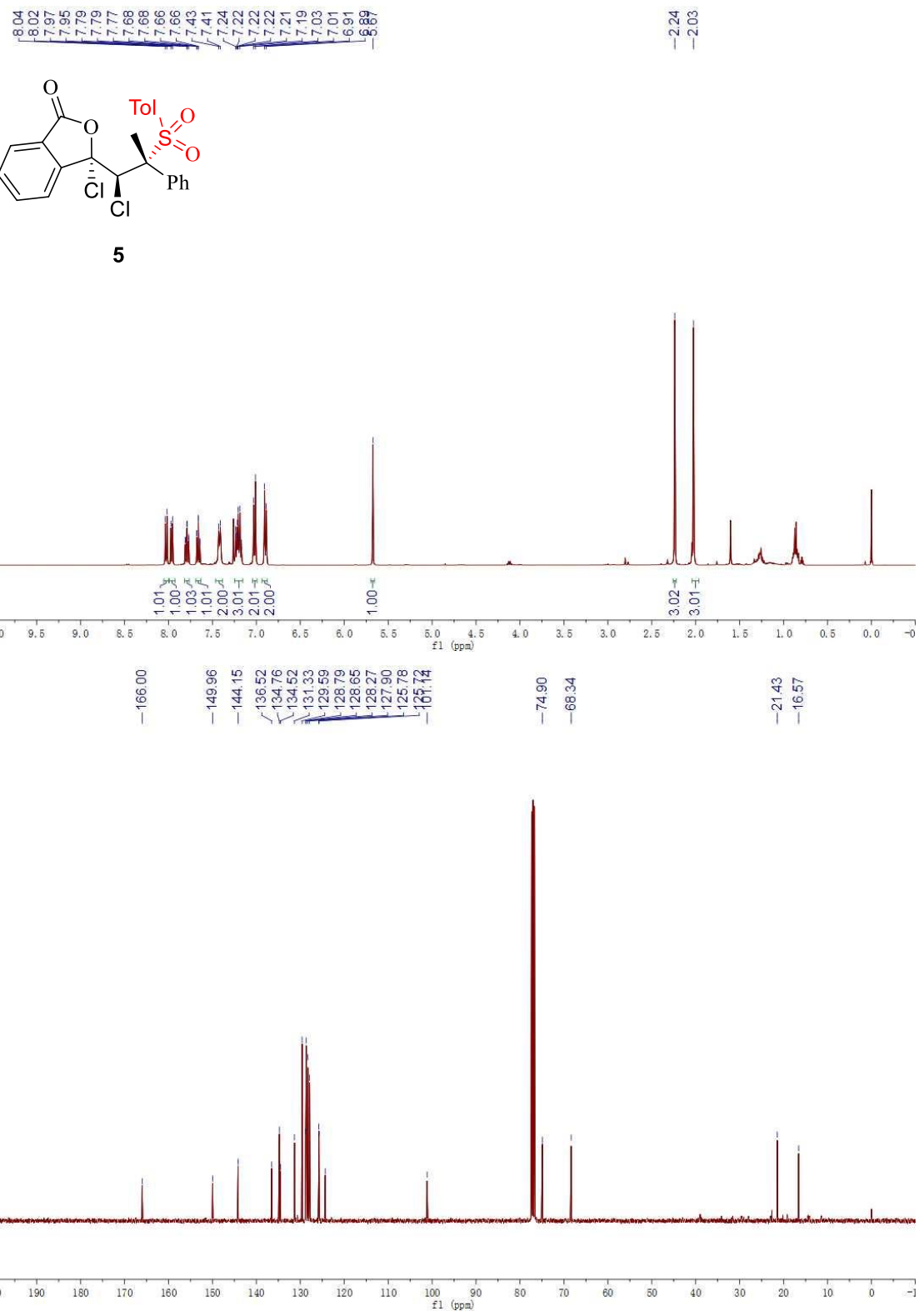


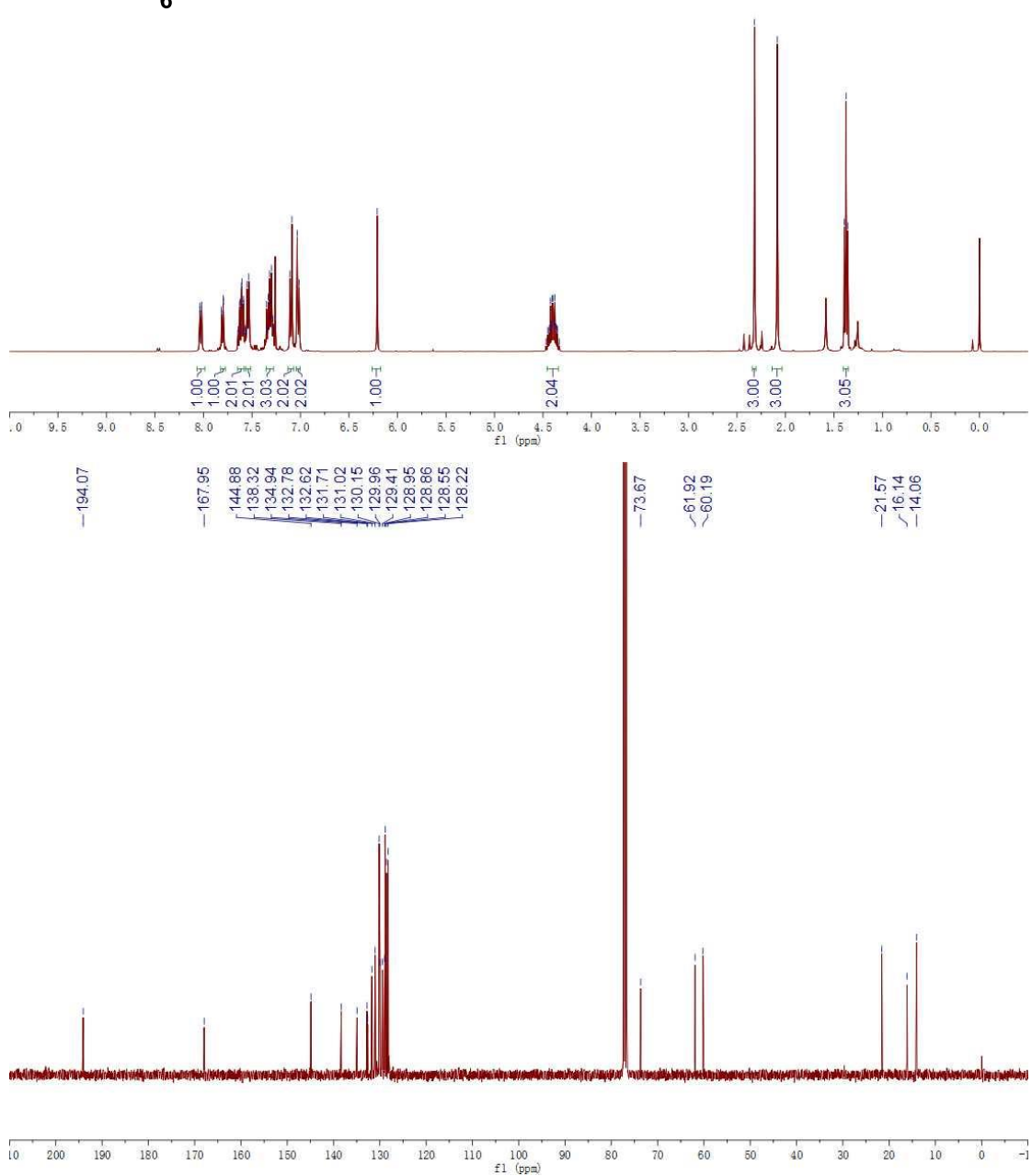
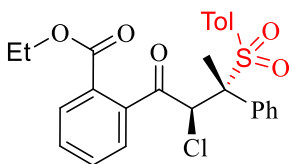
40

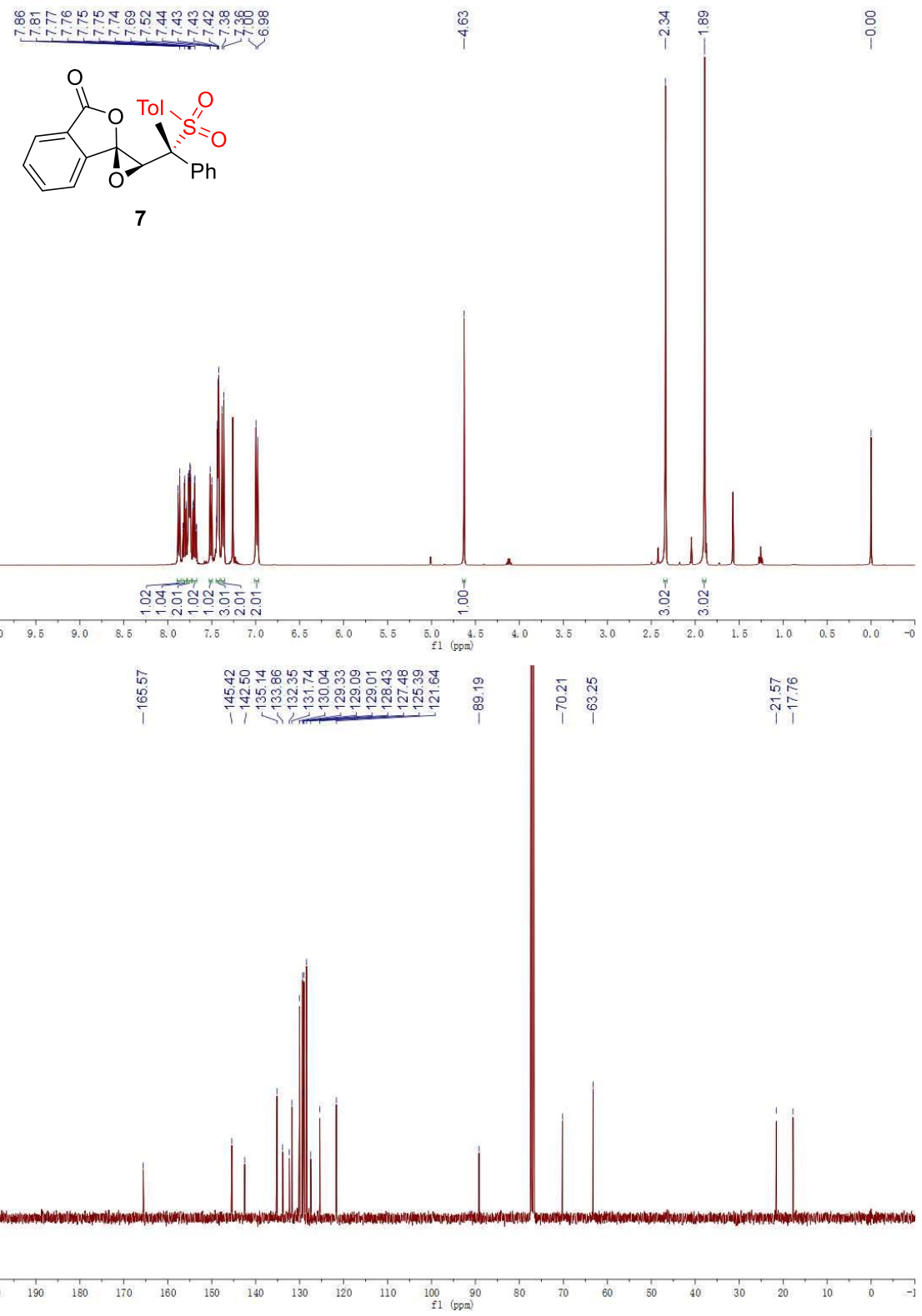


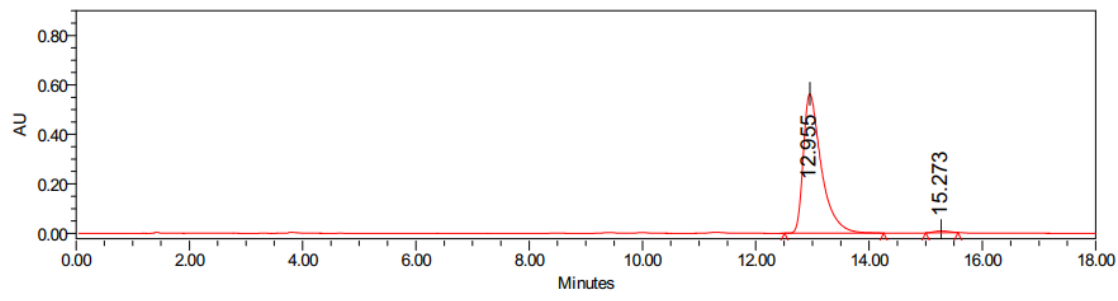
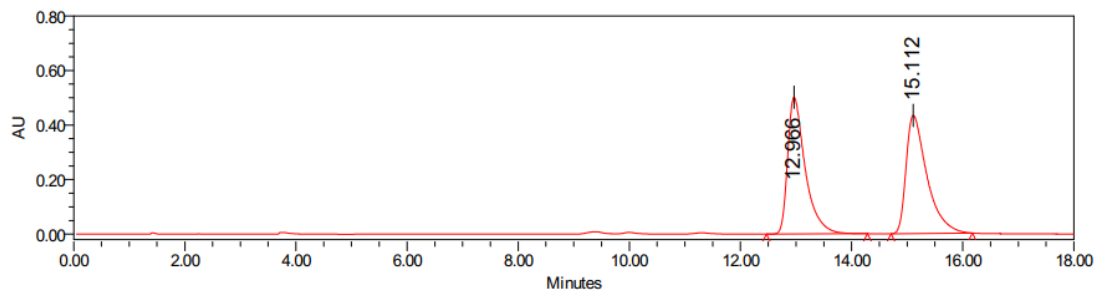
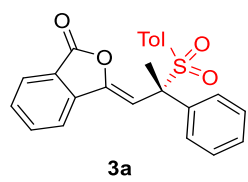


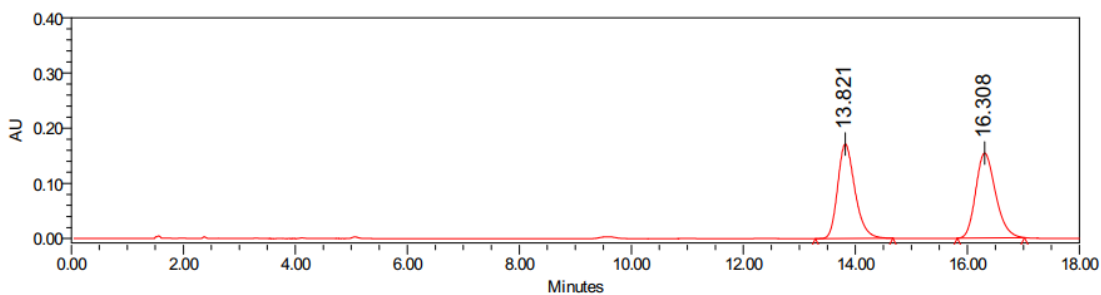
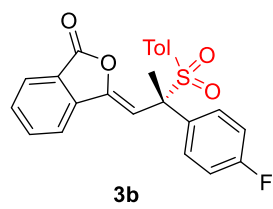






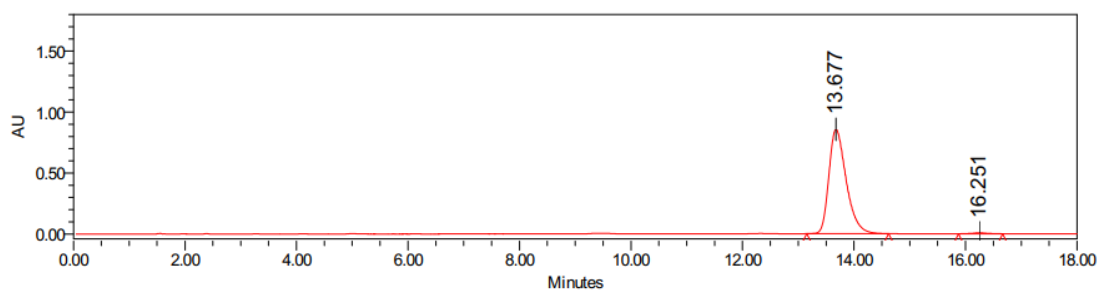






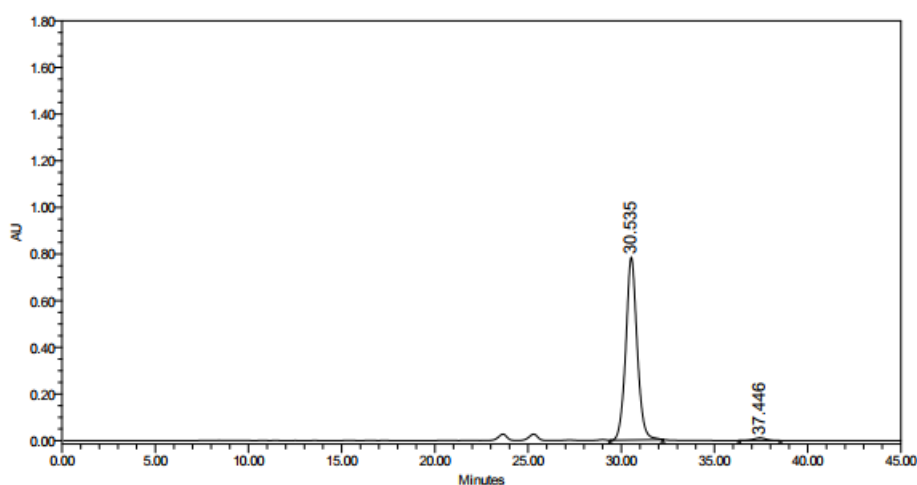
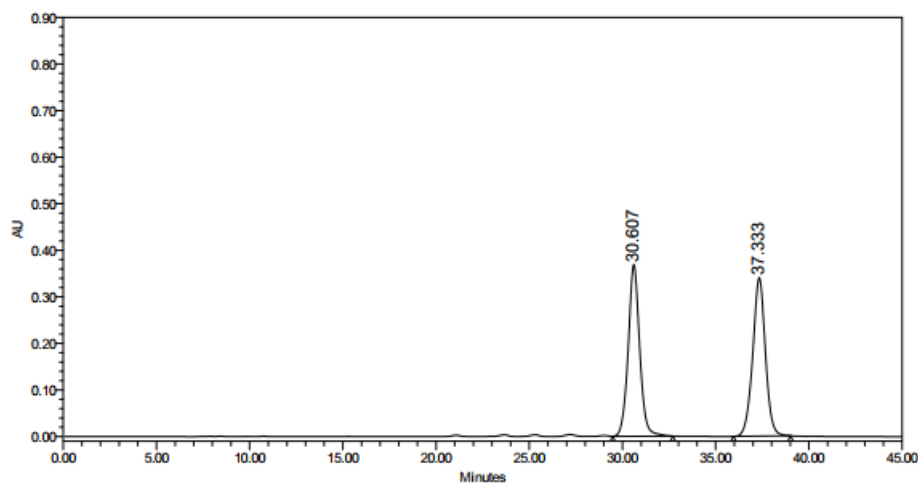
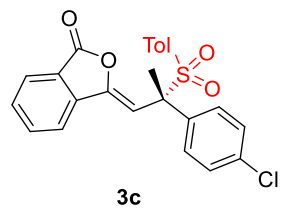
Peak Results

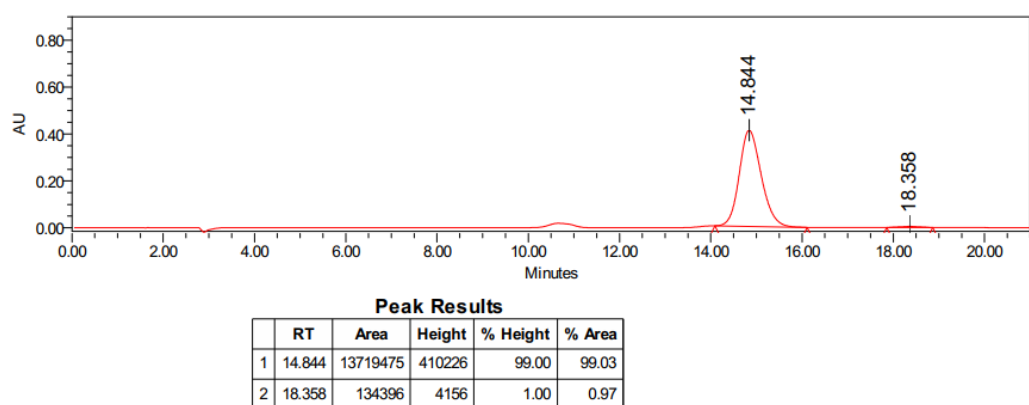
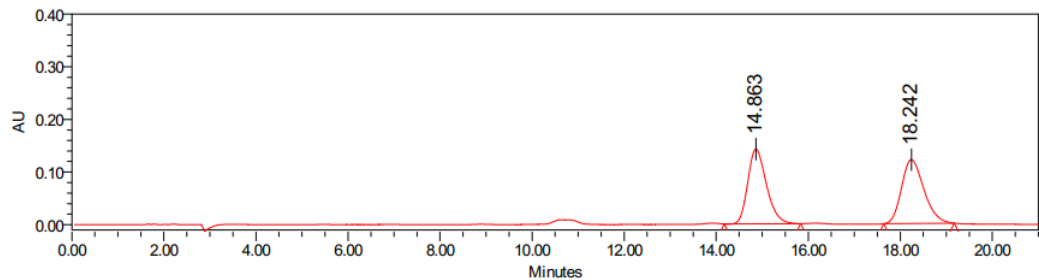
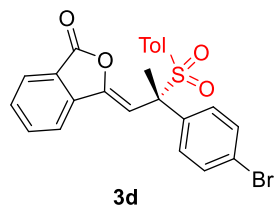
	RT	Area	Height	% Height	% Area
1	13.821	3666406	171204	52.66	49.22
2	16.308	3782744	153928	47.34	50.78

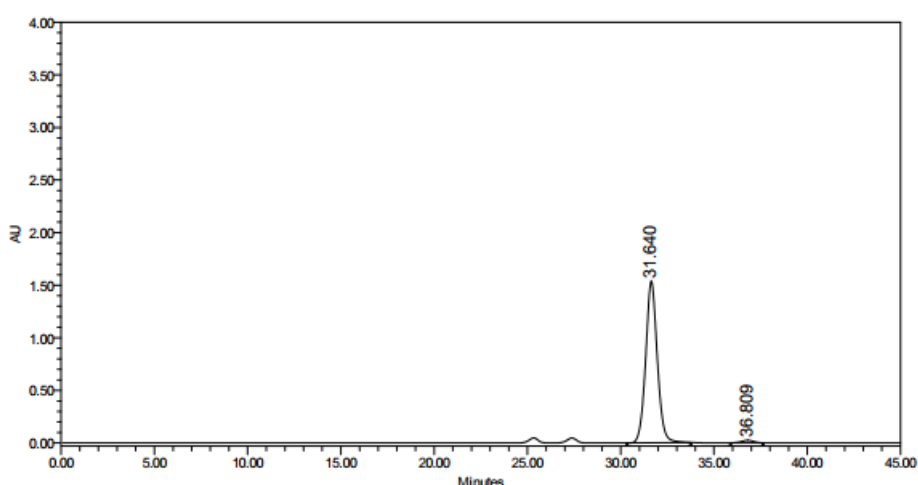
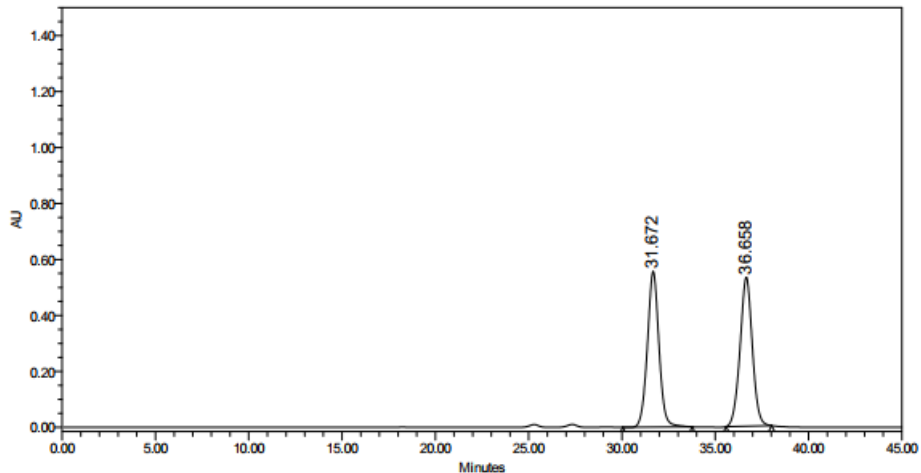
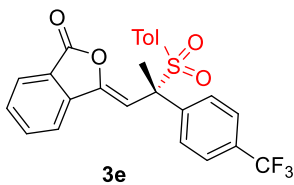


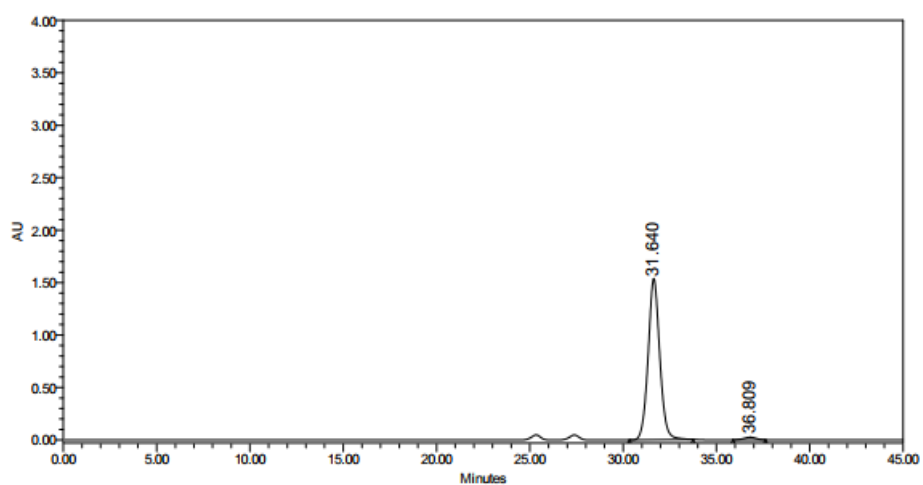
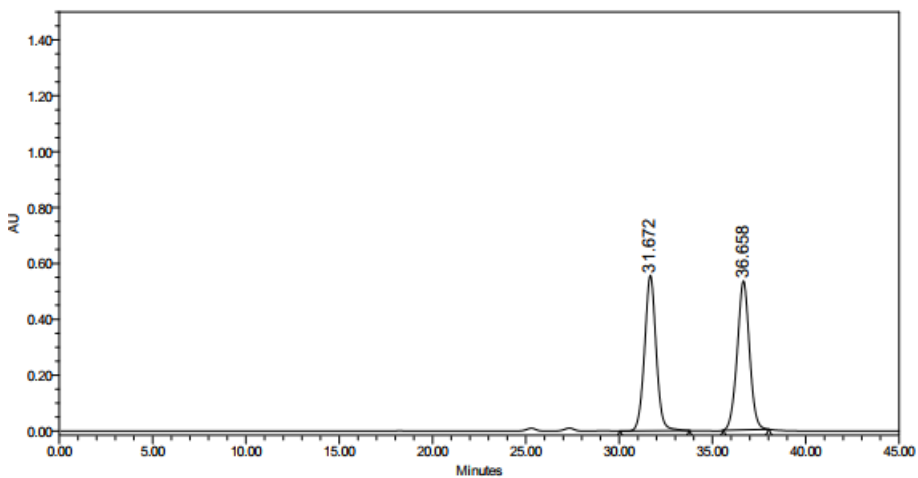
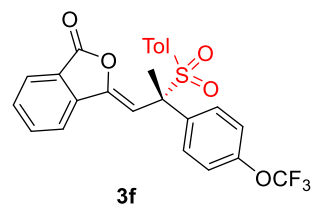
Peak Results

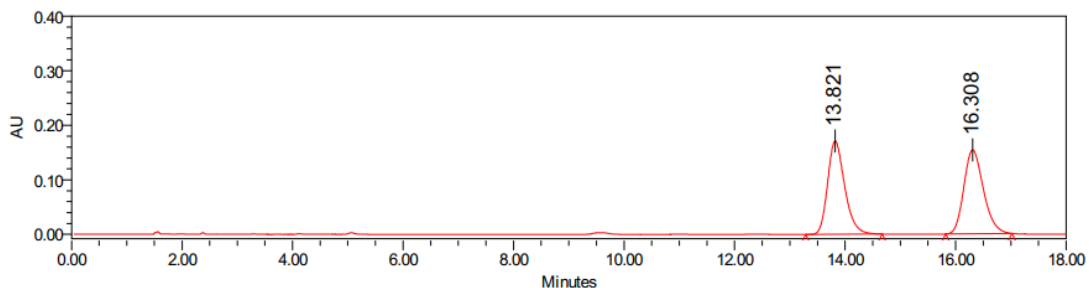
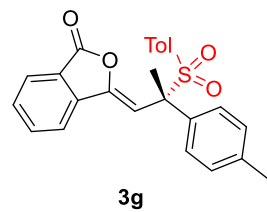
	RT	Area	Height	% Height	% Area
1	13.677	18448233	856635	99.19	99.17
2	16.251	154225	6990	0.81	0.83





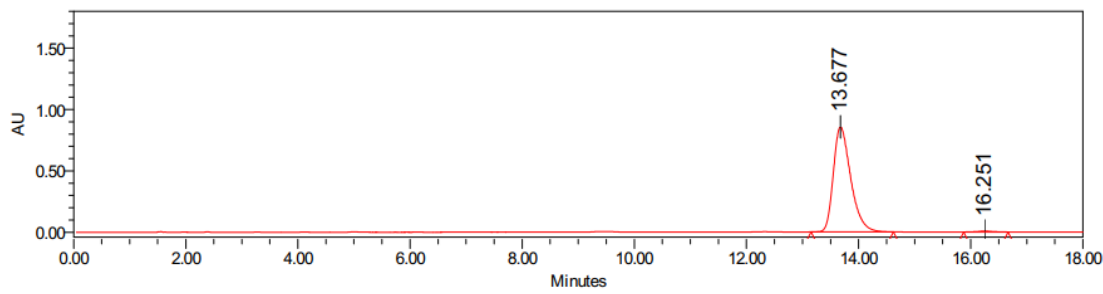






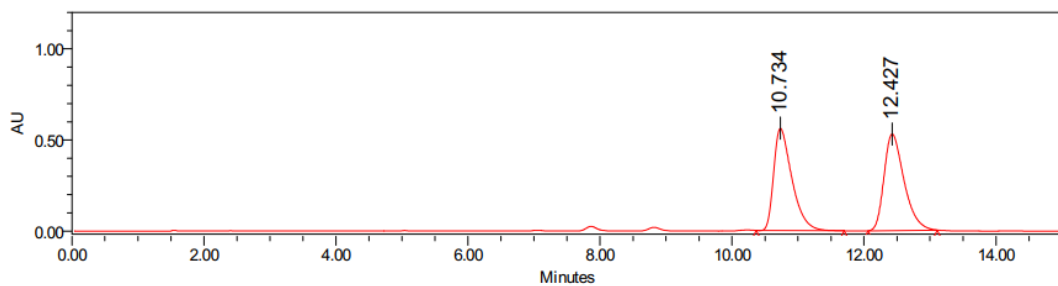
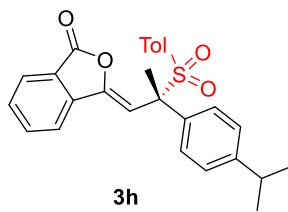
Peak Results

	RT	Area	Height	% Height	% Area
1	13.821	3666406	171204	52.66	49.22
2	16.308	3782744	153928	47.34	50.78



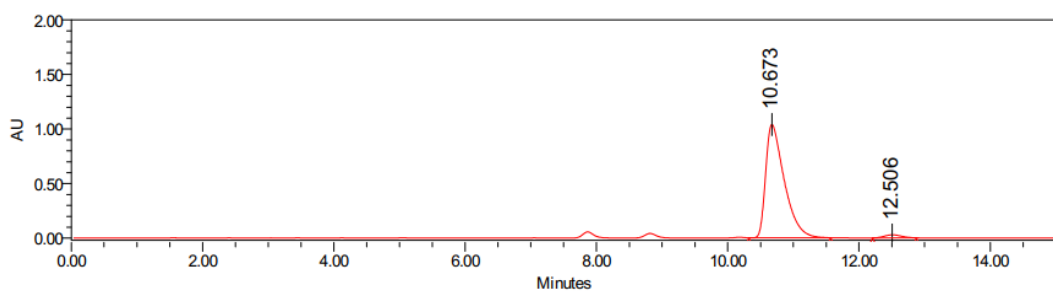
Peak Results

	RT	Area	Height	% Height	% Area
1	13.677	18448233	856635	99.19	99.17
2	16.251	154225	6990	0.81	0.83



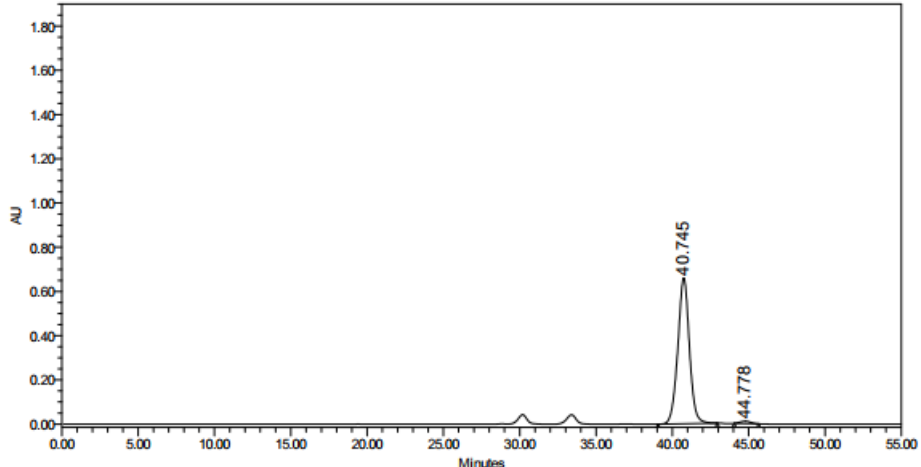
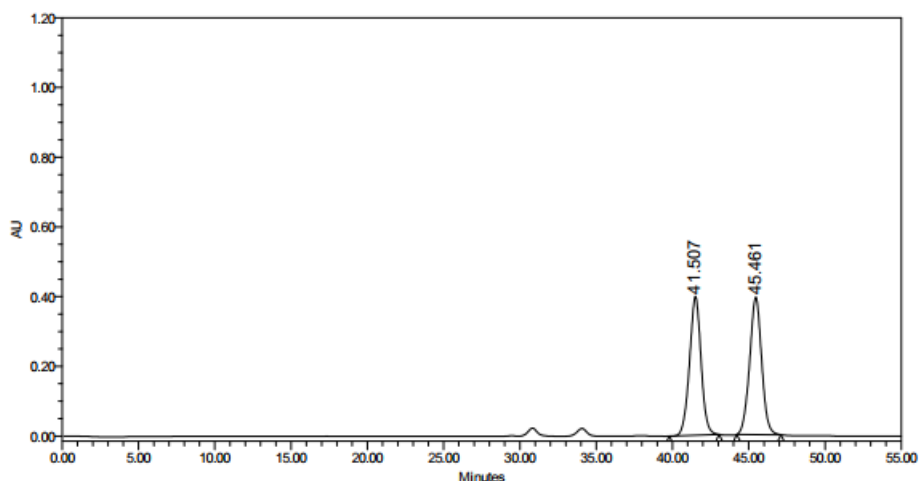
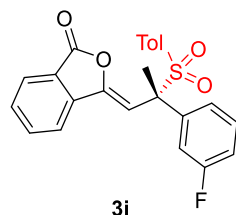
Peak Results

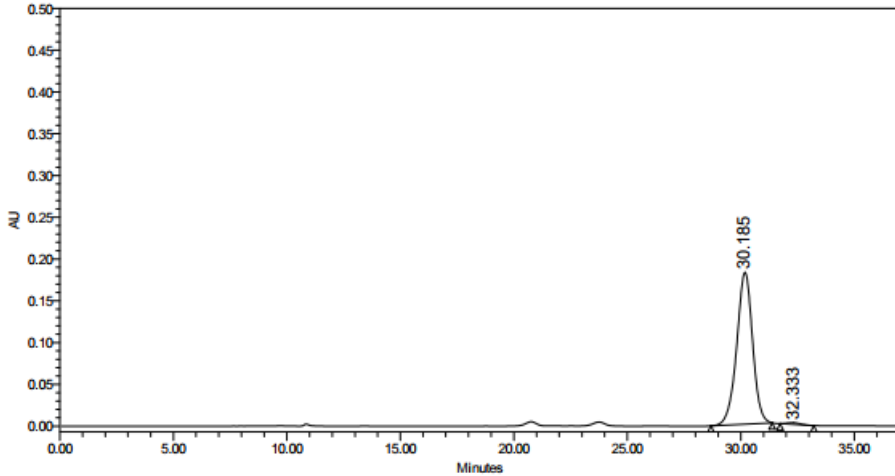
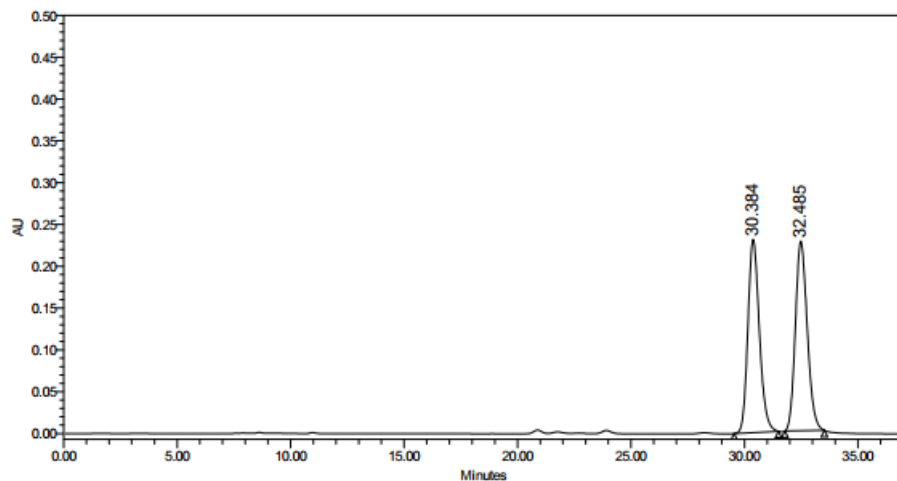
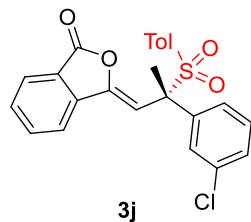
	RT	Area	Height	% Height	% Area
1	10.734	10764657	561443	51.44	49.12
2	12.427	11149506	530100	48.56	50.88

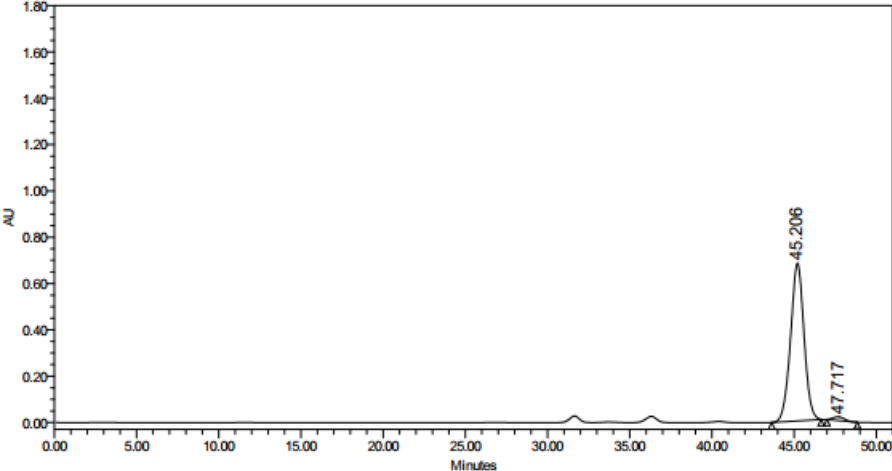
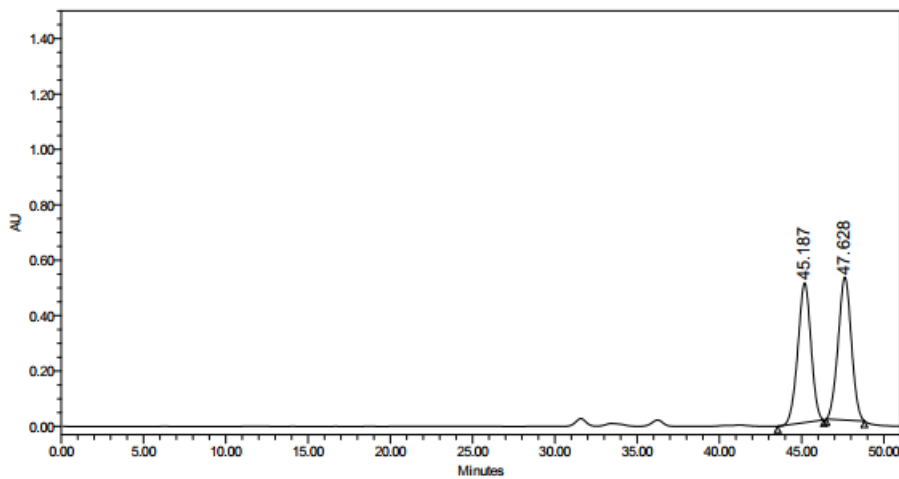
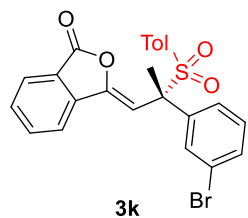


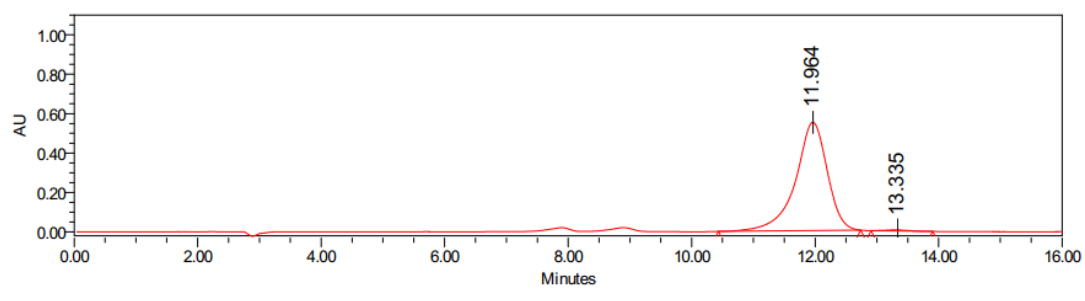
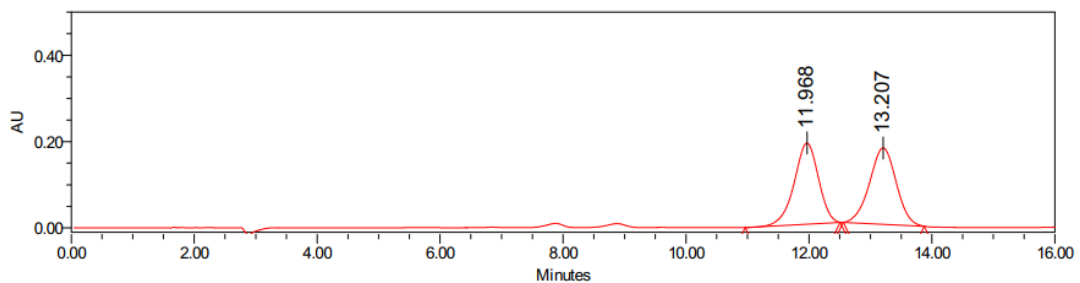
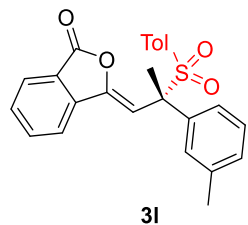
Peak Results

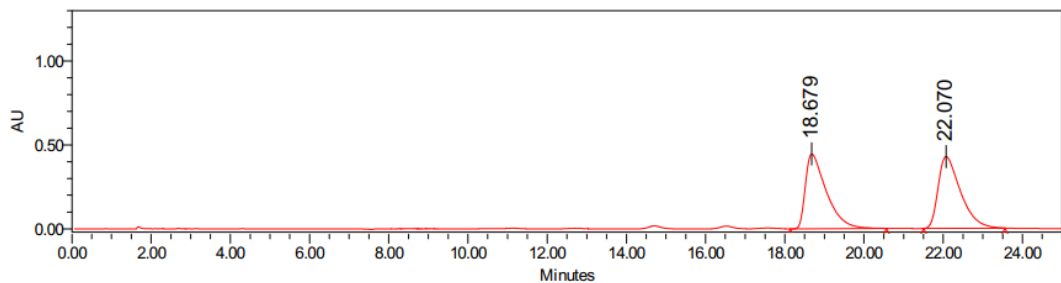
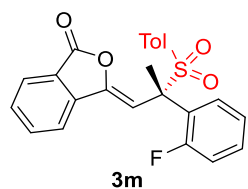
	RT	Area	Height	% Height	% Area
1	10.673	20371538	1038632	97.33	97.55
2	12.506	511329	28486	2.67	2.45





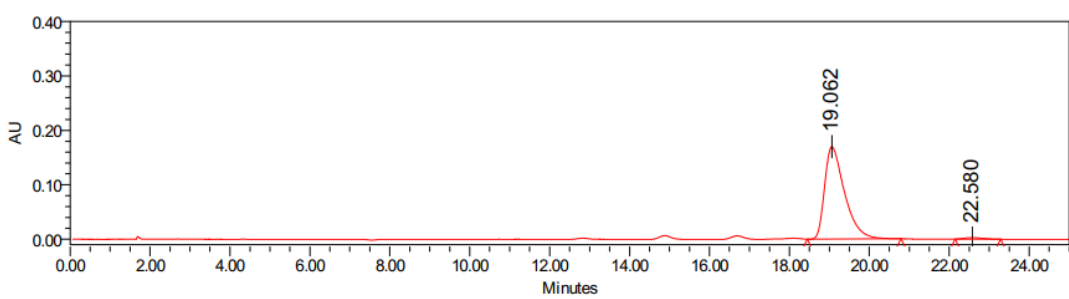






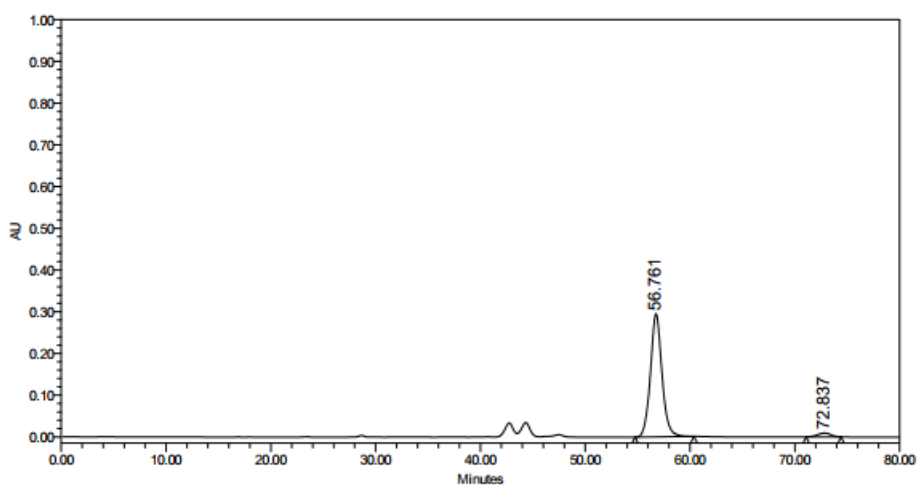
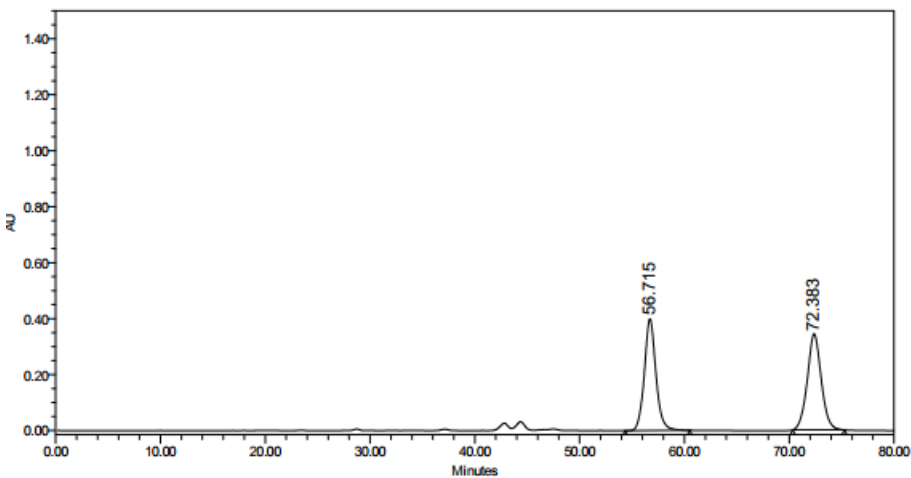
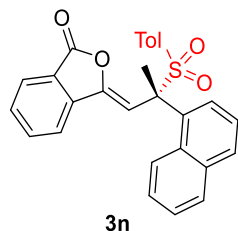
Peak Results

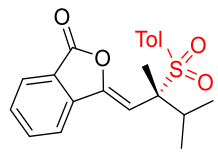
	RT	Area	Height	% Height	% Area
1	18.679	16324641	446216	51.03	49.31
2	22.070	16783019	428173	48.97	50.69



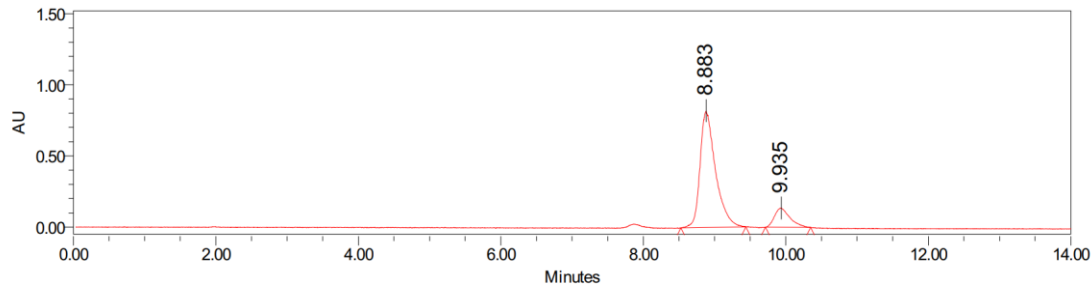
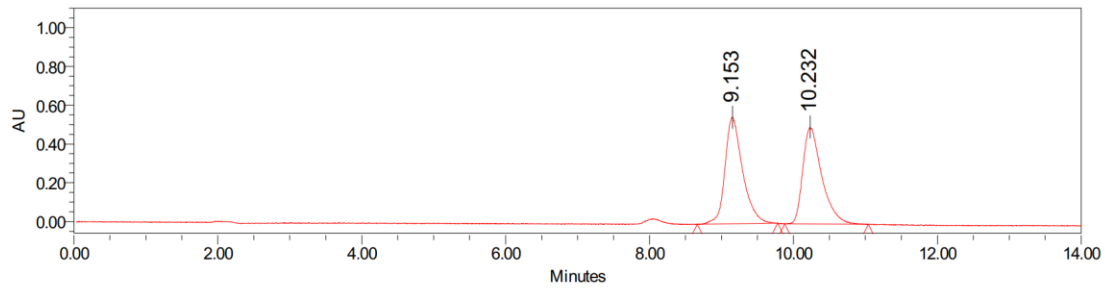
Peak Results

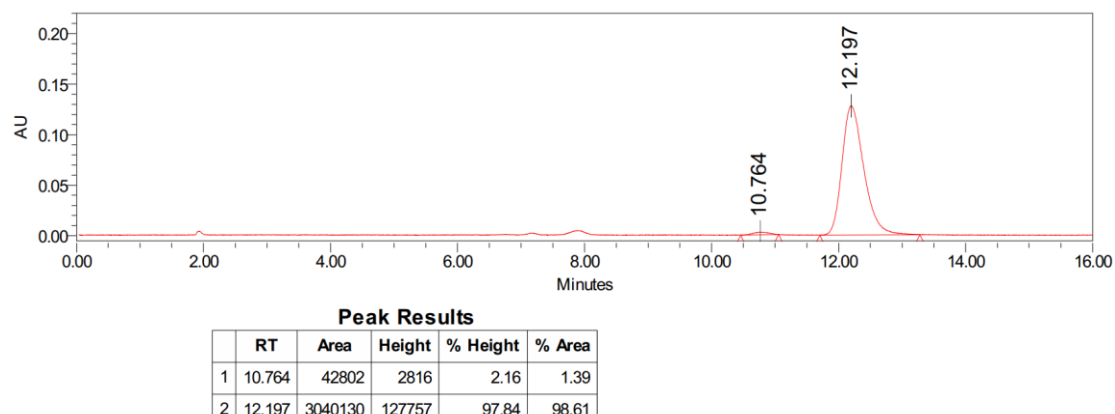
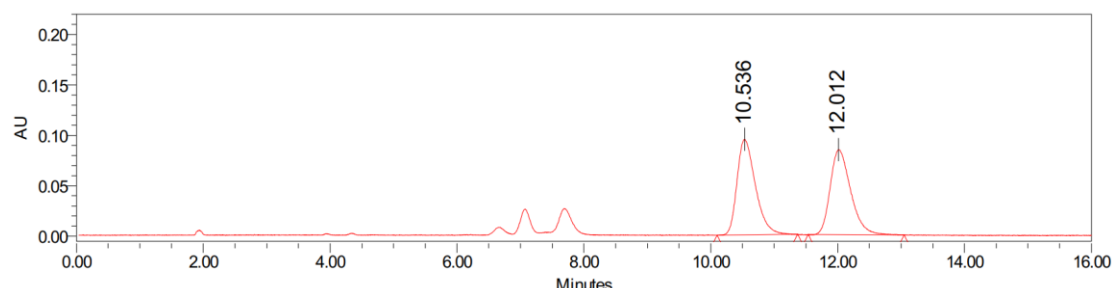
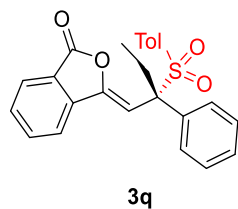
	RT	Area	Height	% Height	% Area
1	19.062	5873039	169718	98.46	98.58
2	22.580	84816	2655	1.54	1.42

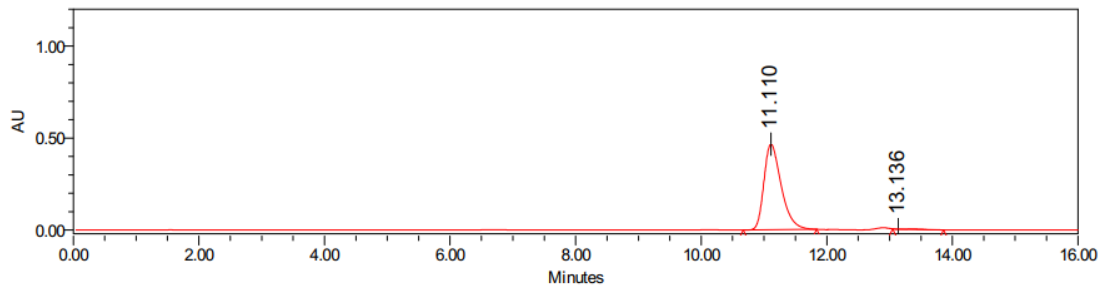
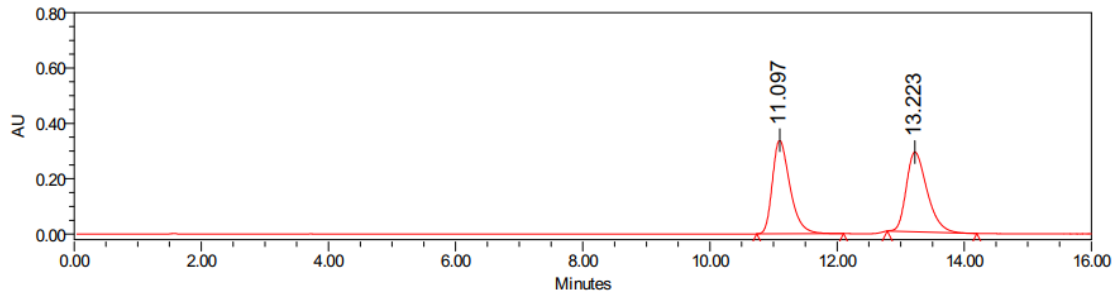
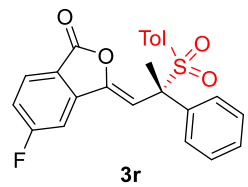


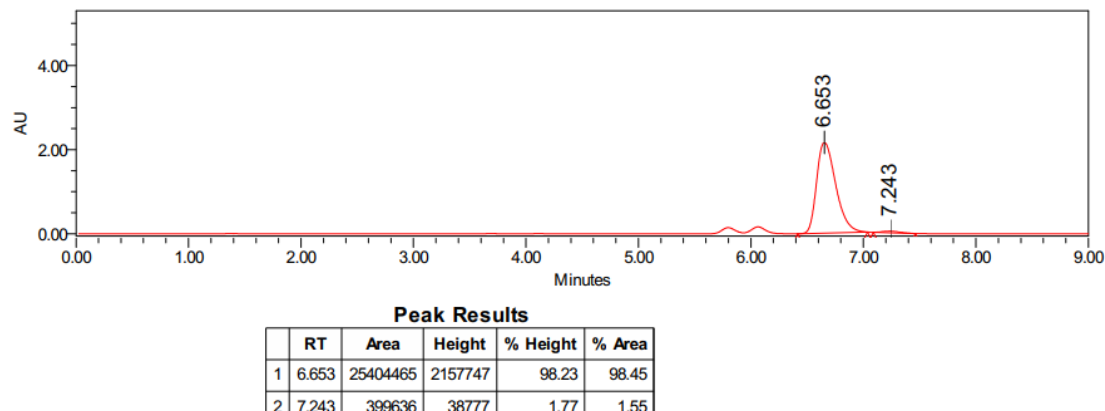
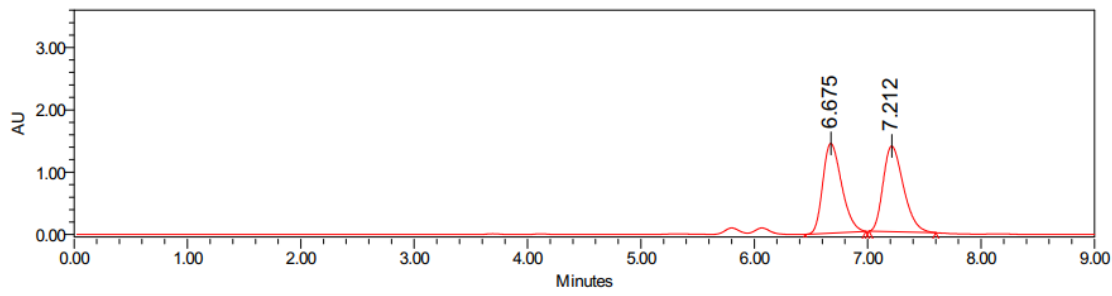
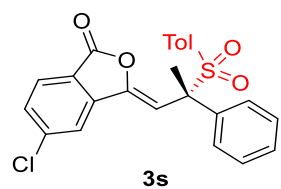


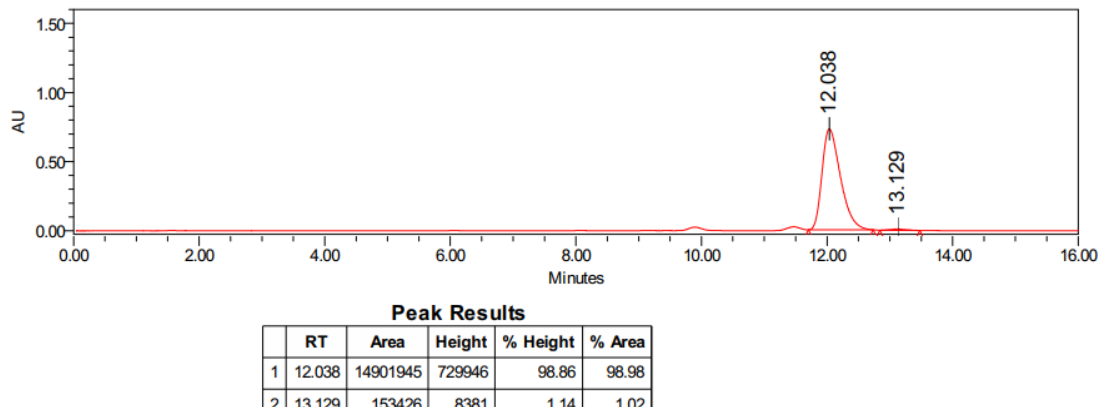
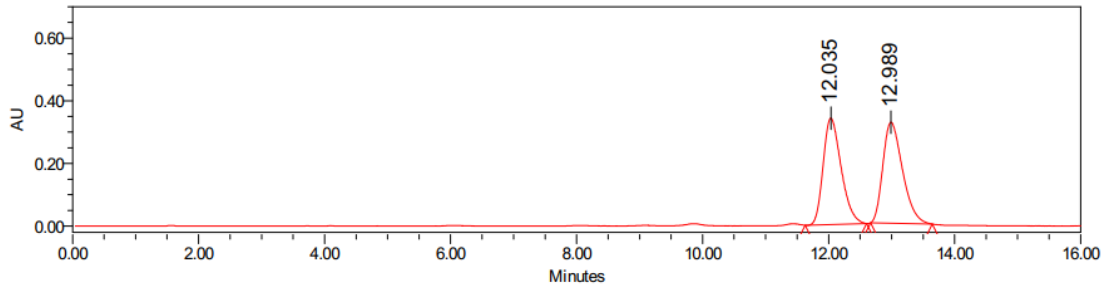
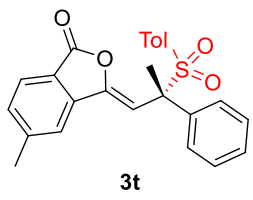
3o

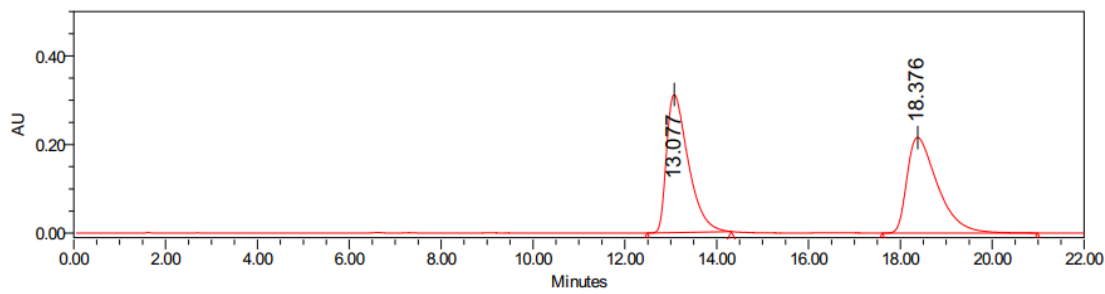
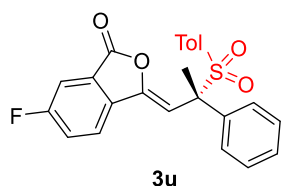






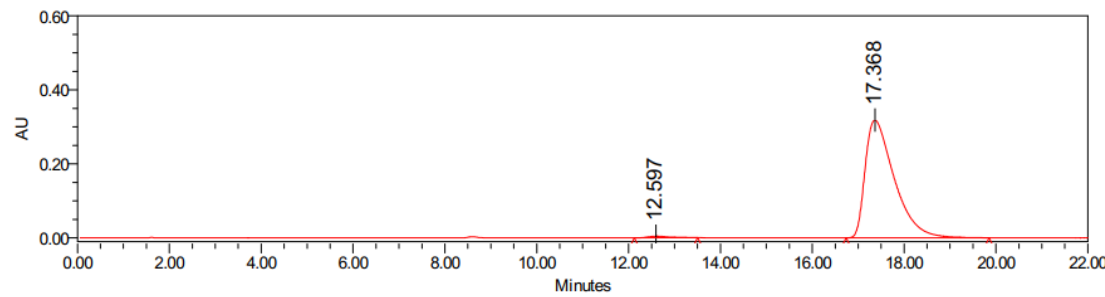






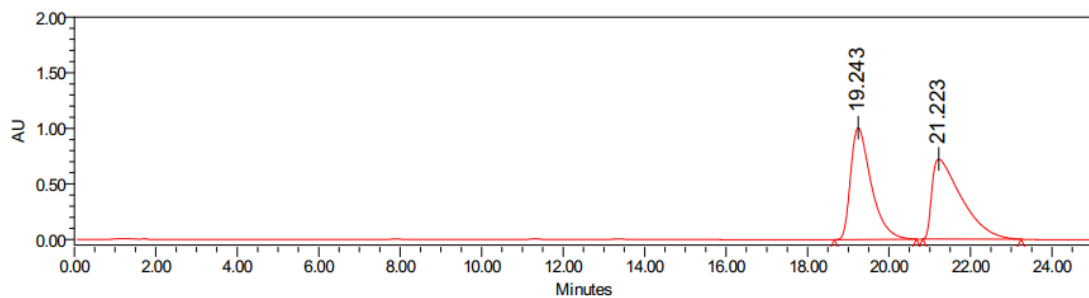
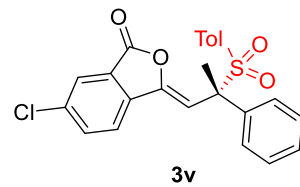
Peak Results

	RT	Area	Height	% Height	% Area
1	13.077	10208995	311494	59.07	50.64
2	18.376	9951463	215826	40.93	49.36



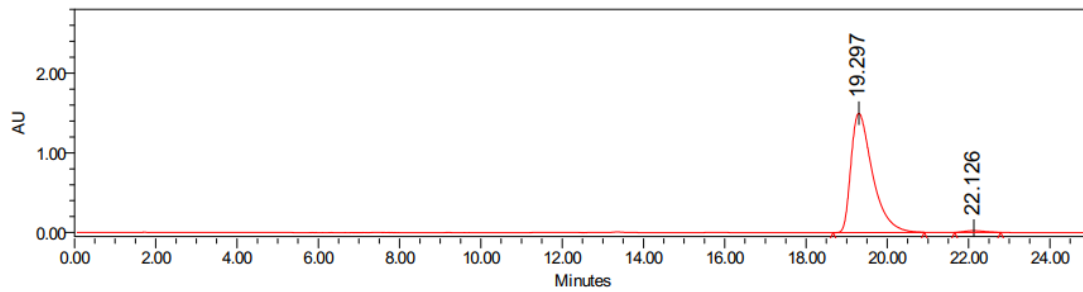
Peak Results

	RT	Area	Height	% Height	% Area
1	12.597	146220	4396	1.36	1.03
2	17.368	14022677	318295	98.64	98.97



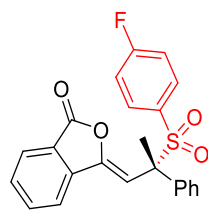
Peak Results

	RT	Area	Height	% Height	% Area
1	19.243	35240748	1006646	58.31	49.31
2	21.223	36227788	719717	41.69	50.69

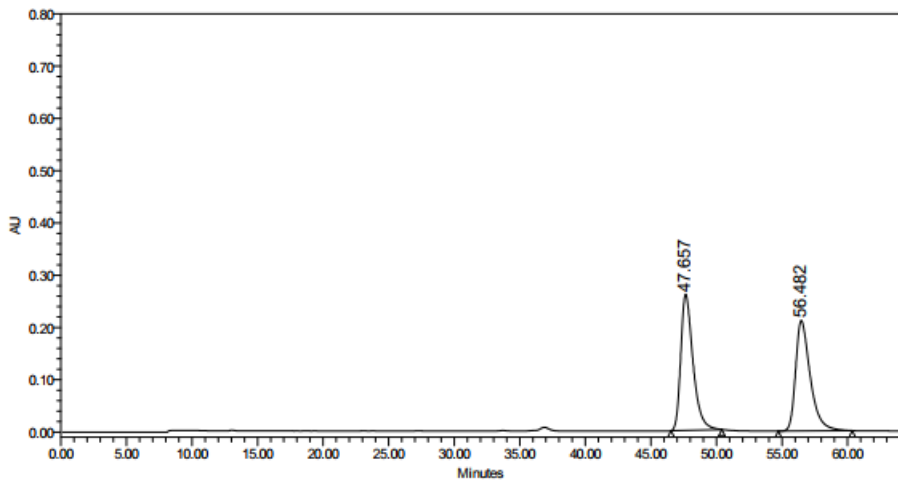


Peak Results

	RT	Area	Height	% Height	% Area
1	19.297	54918648	1498360	98.55	98.68
2	22.126	736785	22007	1.45	1.32

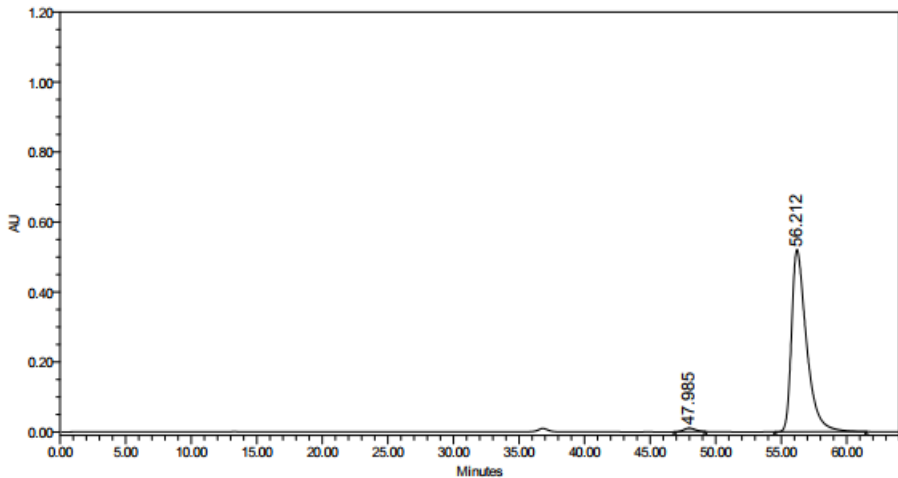


4a



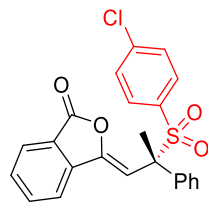
Peak Result

	RT	Area	Height	% Height	% Area
1	47.657	16896758	259876	55.22	50.73
2	56.482	16410386	210760	44.78	49.27

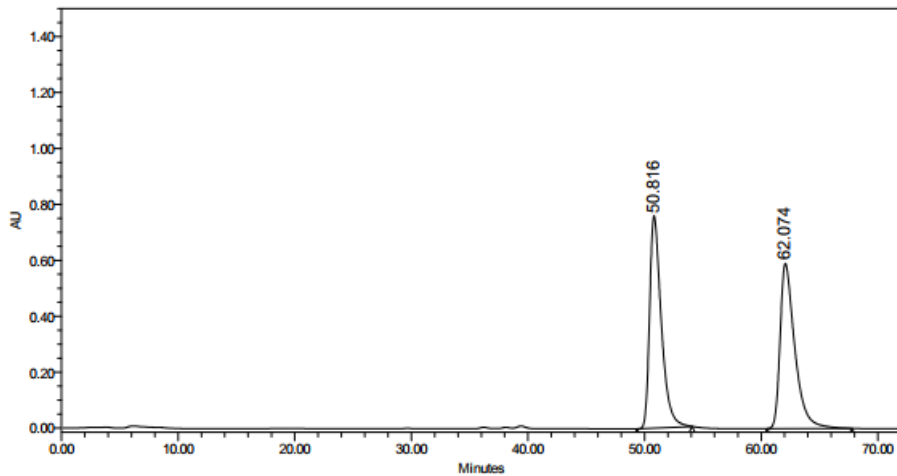


Peak Result

	RT	Area	Height	% Height	% Area
1	47.985	628212	10379	1.96	1.49
2	56.212	41460901	520392	98.04	98.51

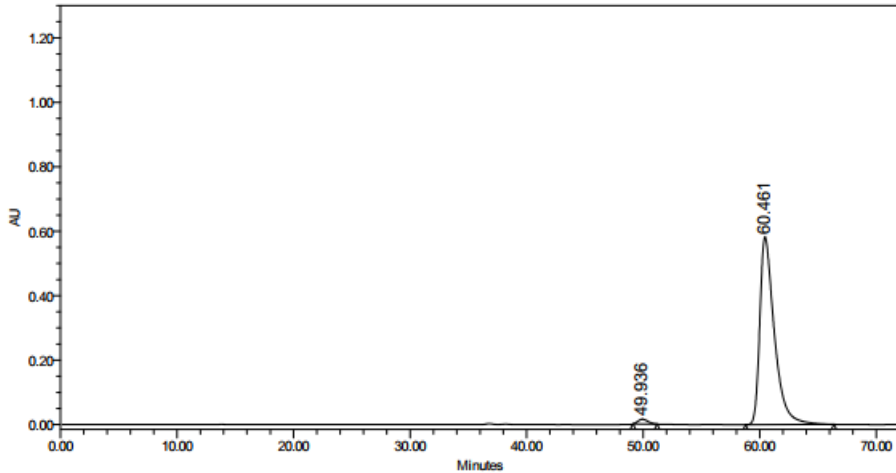


4b



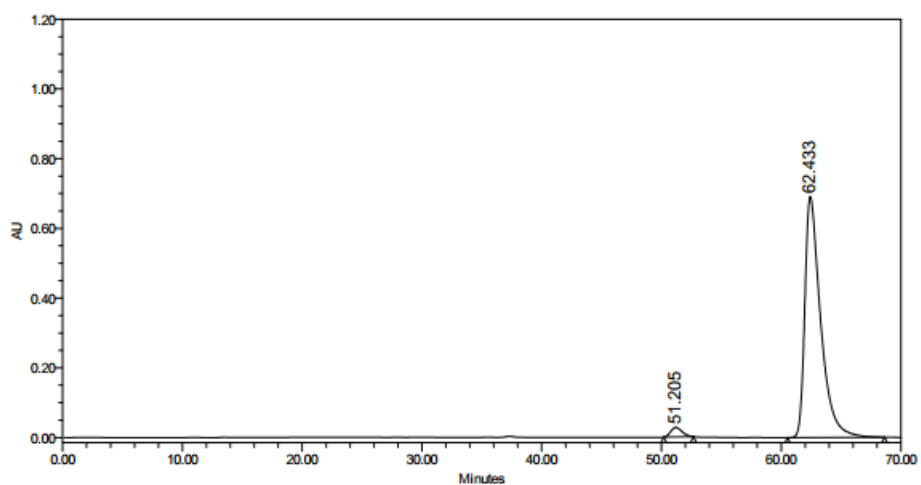
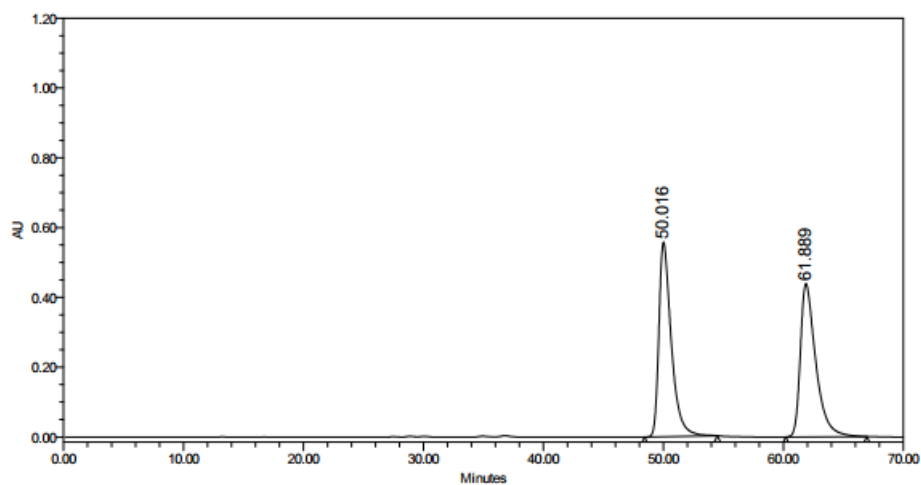
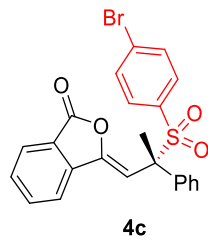
Peak Result

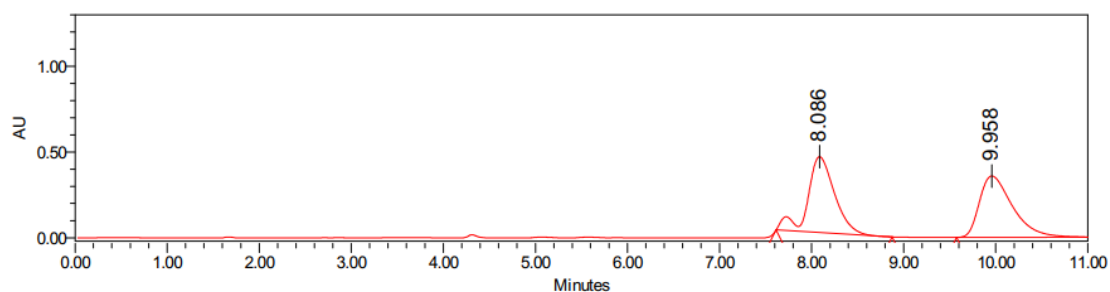
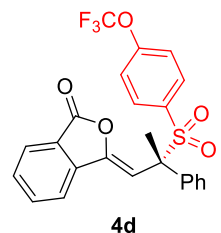
	RT	Area	Height	% Height	% Area
1	50.816	52729472	758562	56.24	50.43
2	62.074	51830459	590192	43.76	49.57



Peak Result

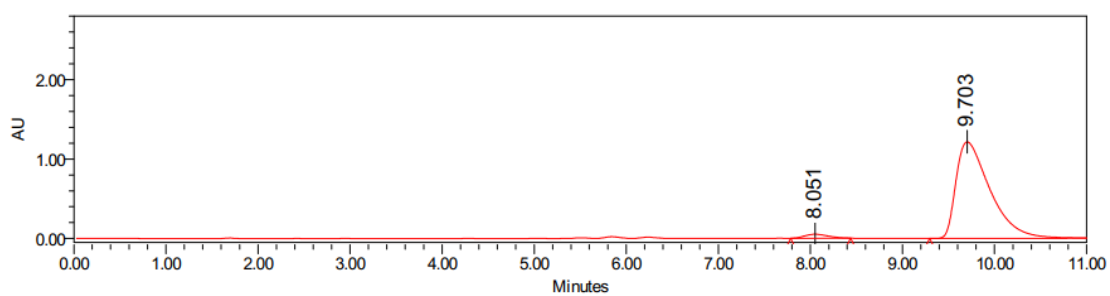
	RT	Area	Height	% Height	% Area
1	49.936	887041	14916	2.50	1.72
2	60.461	50670713	581857	97.50	98.28





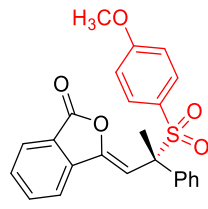
Peak Results

	RT	Area	Height	% Height	% Area
1	8.086	8998218	442387	55.26	50.16
2	9.958	8940272	358153	44.74	49.84

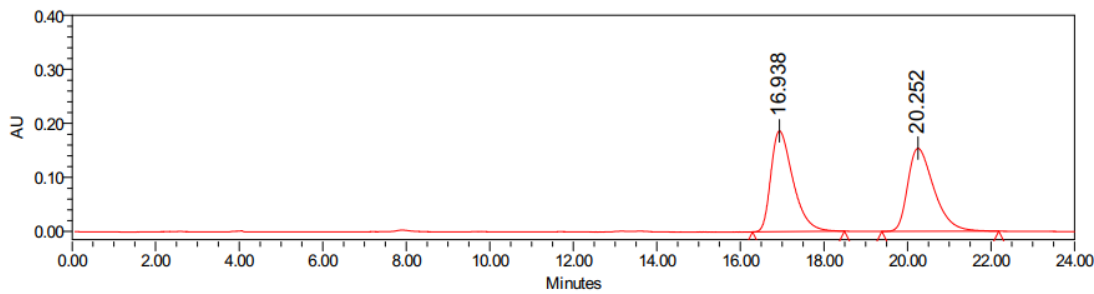


Peak Results

	RT	Area	Height	% Height	% Area
1	8.051	866479	49583	3.92	2.70
2	9.703	31268489	1215682	96.08	97.30

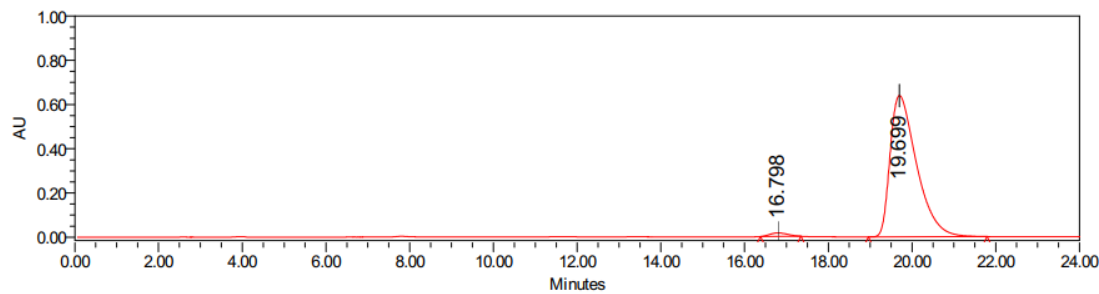


4e



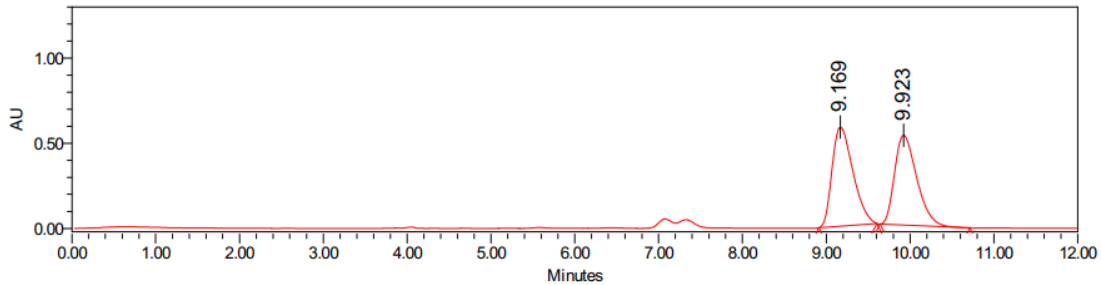
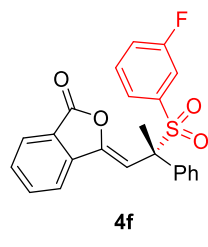
Peak Results

	RT	Area	Height	% Height	% Area
1	16.938	6852818	186528	54.83	50.68
2	20.252	6668963	153673	45.17	49.32



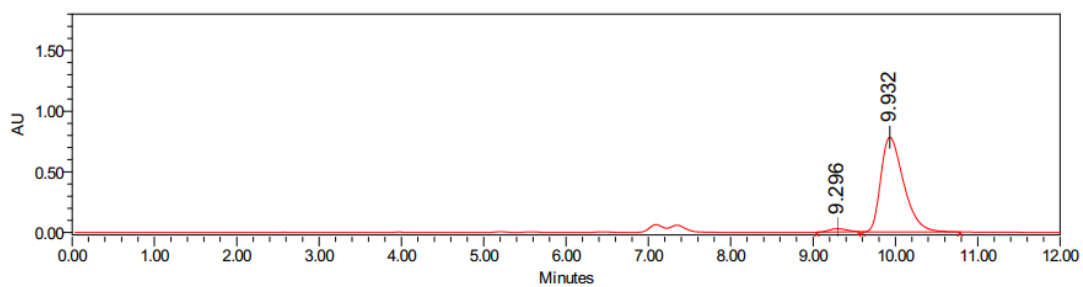
Peak Results

	RT	Area	Height	% Height	% Area
1	16.798	471541	15833	2.42	1.65
2	19.699	28062126	639123	97.58	98.35



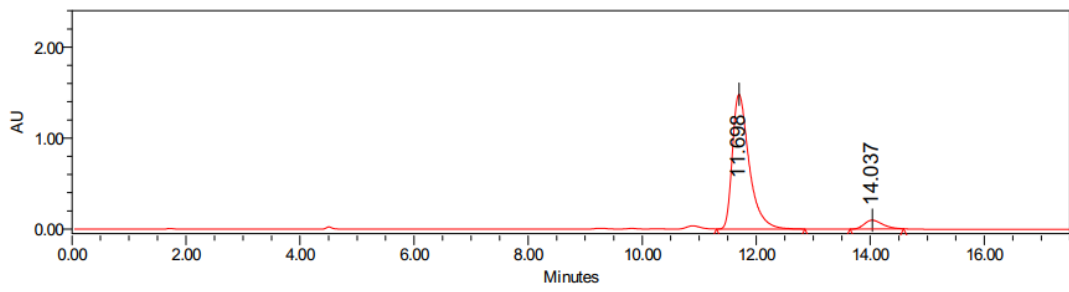
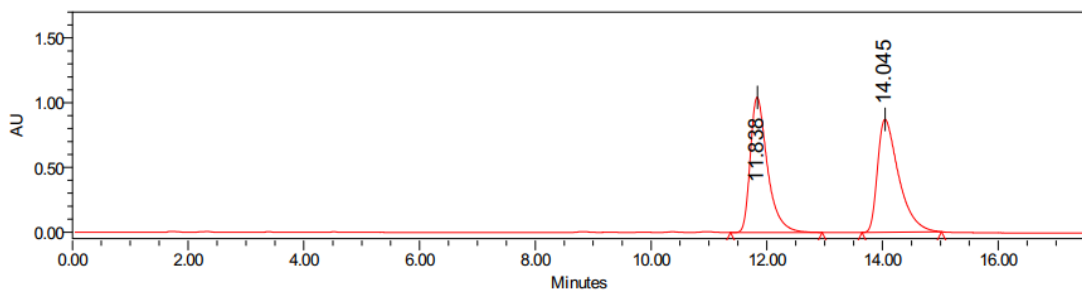
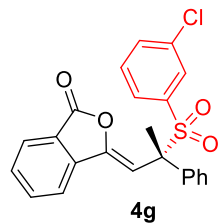
Peak Results

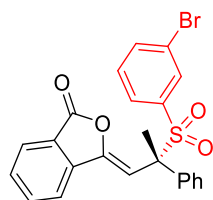
	RT	Area	Height	% Height	% Area
1	9.169	10040700	581454	52.43	50.82
2	9.923	9717339	527654	47.57	49.18



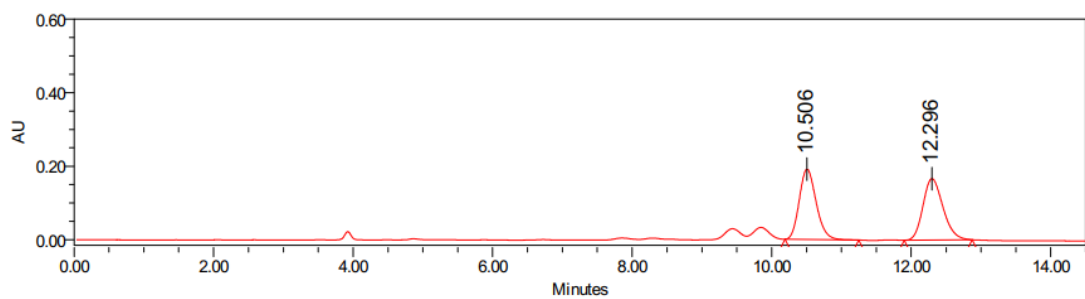
Peak Results

	RT	Area	Height	% Height	% Area
1	9.296	415073	27089	3.35	2.69
2	9.932	15039532	781180	96.65	97.31



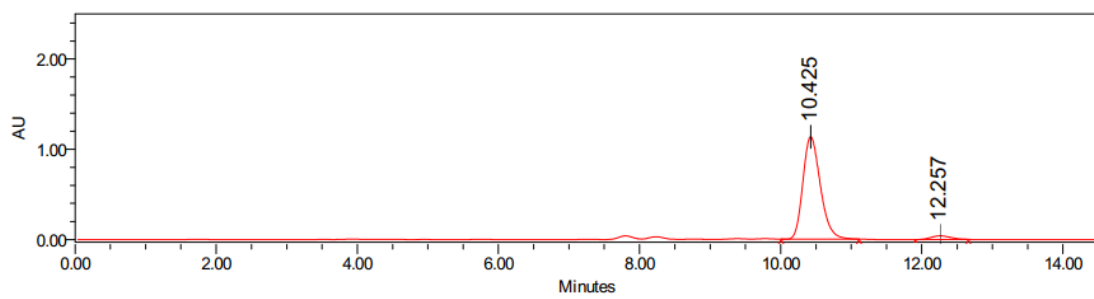


4h



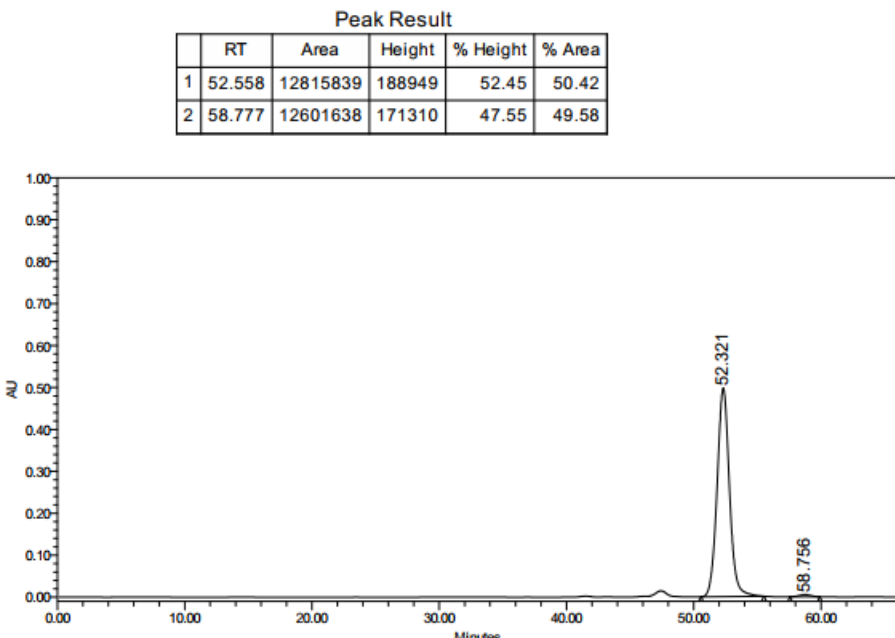
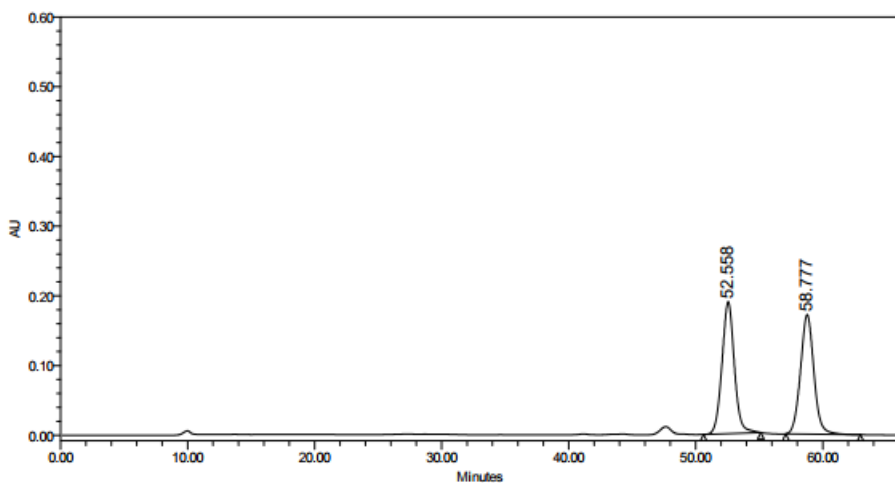
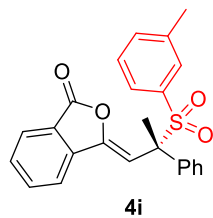
Peak Results

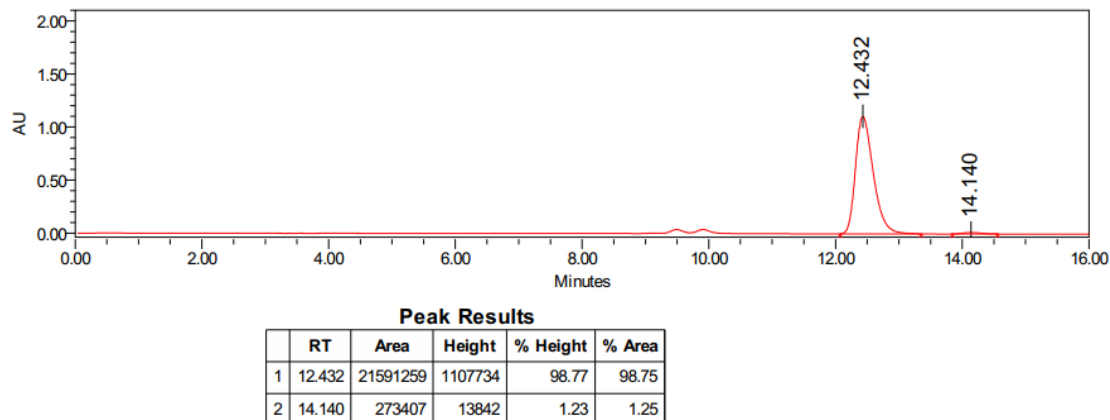
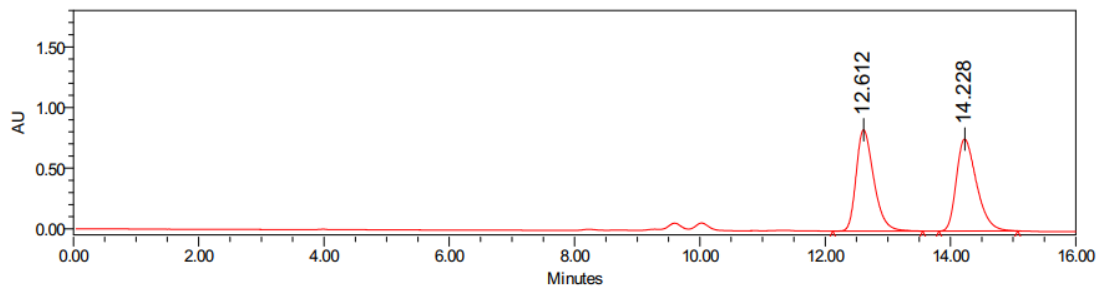
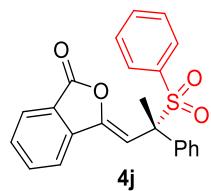
	RT	Area	Height	% Height	% Area
1	10.506	3211080	191310	53.37	49.16
2	12.296	3321415	167151	46.63	50.84

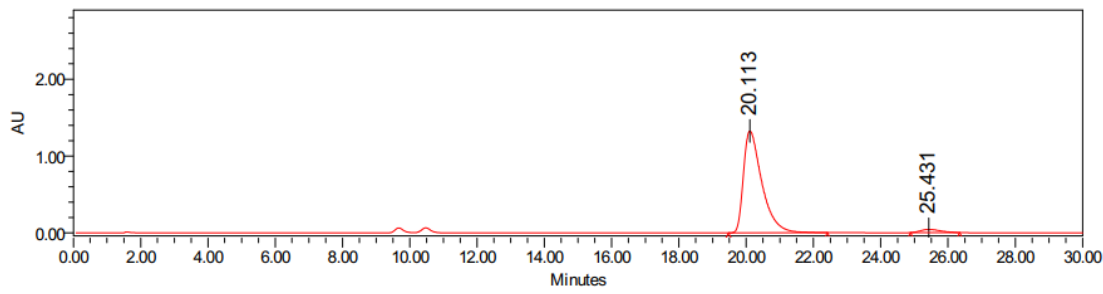
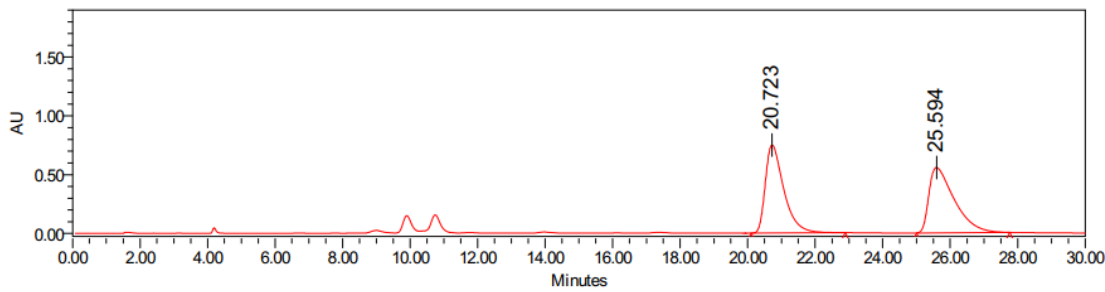
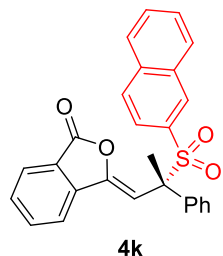


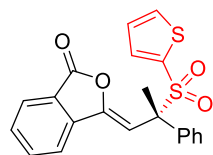
Peak Results

	RT	Area	Height	% Height	% Area
1	10.425	19461191	1135607	96.57	96.12
2	12.257	785640	40339	3.43	3.88

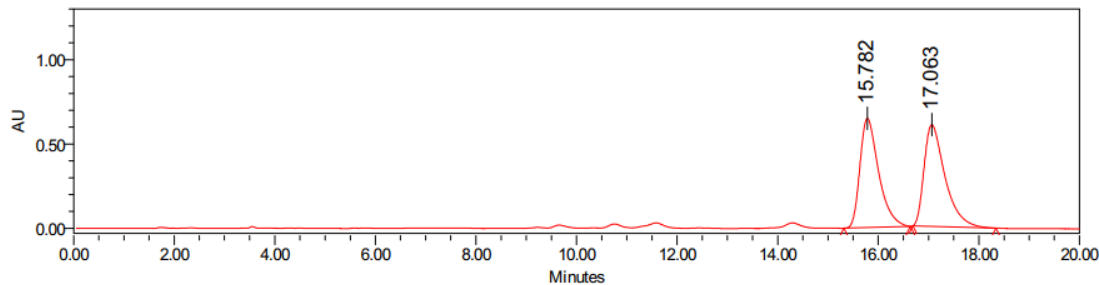






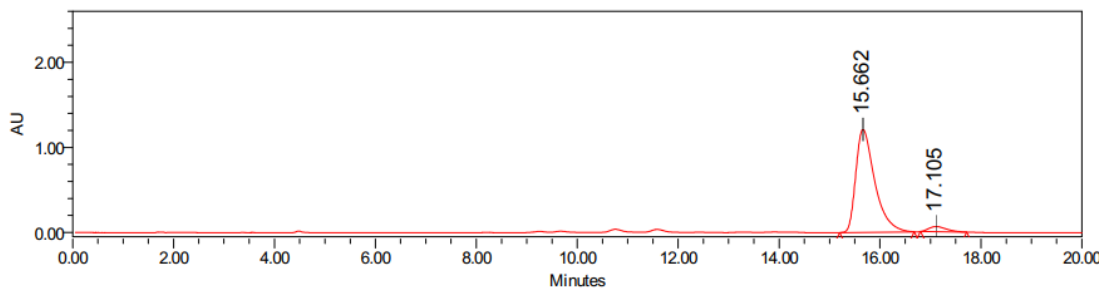


4l



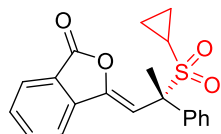
Peak Results

	RT	Area	Height	% Height	% Area
1	15.782	16792159	647938	51.80	49.12
2	17.063	17393799	602853	48.20	50.88

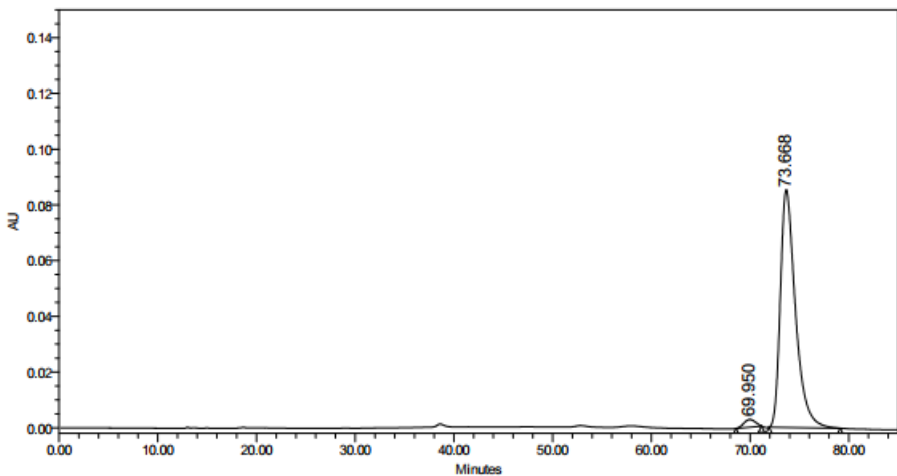
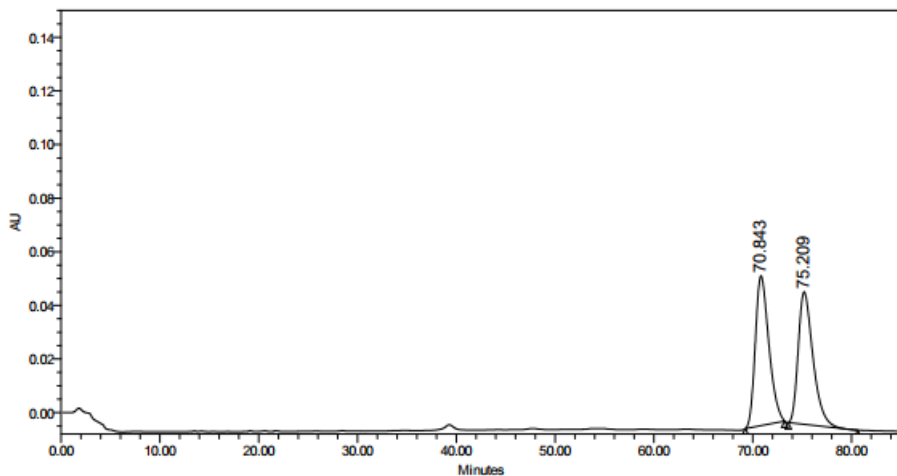


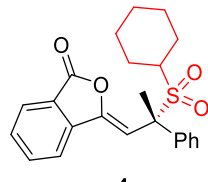
Peak Results

	RT	Area	Height	% Height	% Area
1	15.662	31582130	1210263	95.13	95.43
2	17.105	1513963	61908	4.87	4.57

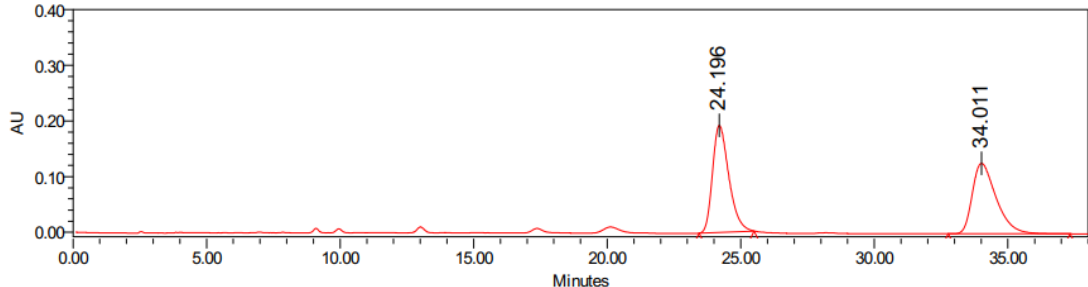


4m



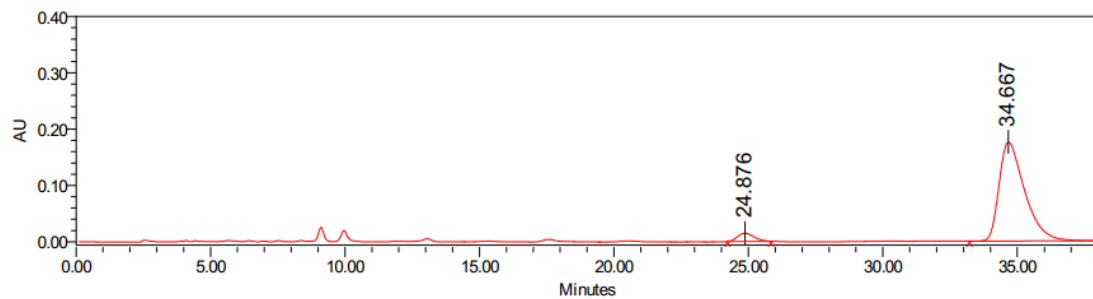


4n



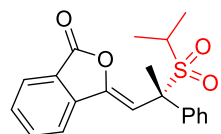
Peak Results

	RT	Area	Height	% Height	% Area
1	24.196	8131444	192233	60.28	50.88
2	34.011	7848720	126670	39.72	49.12

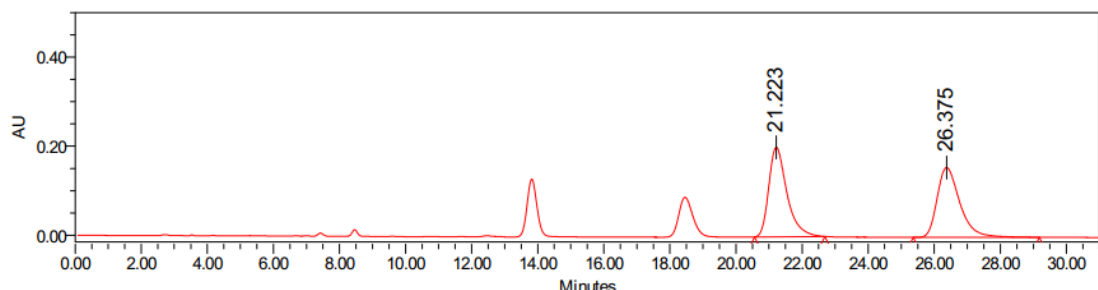


Peak Results

	RT	Area	Height	% Height	% Area
1	24.876	617863	14578	7.67	5.07
2	34.667	11573720	175500	92.33	94.93

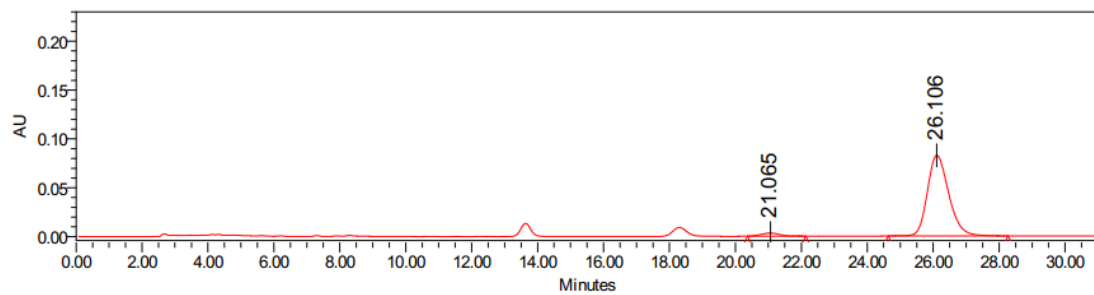


4o



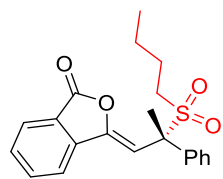
Peak Results

	RT	Area	Height	% Height	% Area
1	21.223	7656811	201180	56.20	50.67
2	26.375	7456197	156801	43.80	49.33

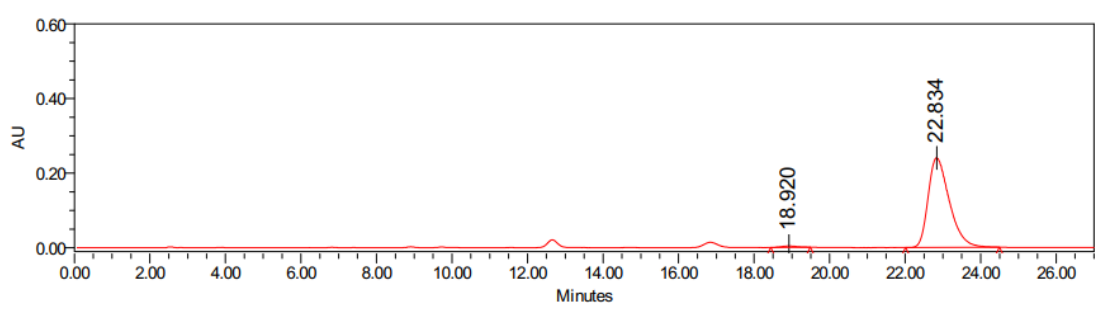
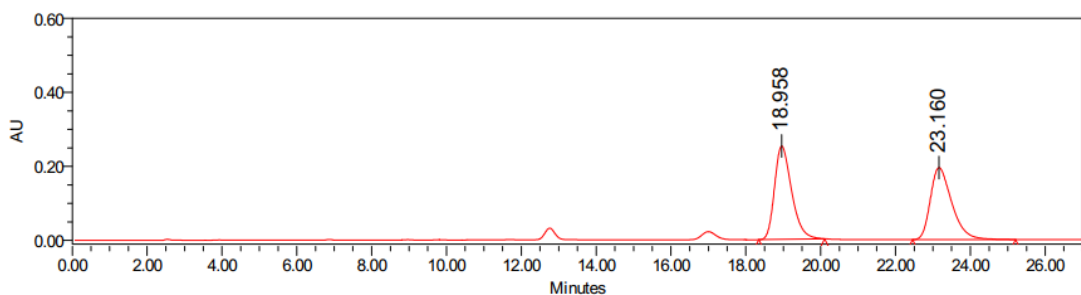


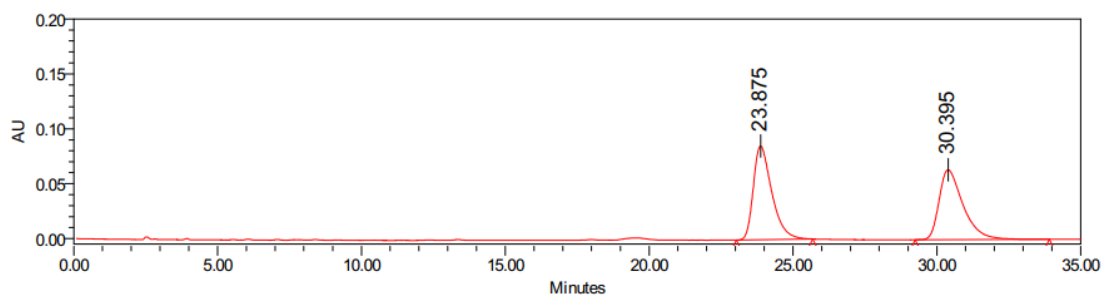
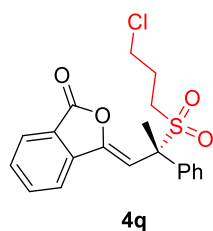
Peak Results

	RT	Area	Height	% Height	% Area
1	21.065	121122	3155	3.68	3.16
2	26.106	3706045	82625	96.32	96.84



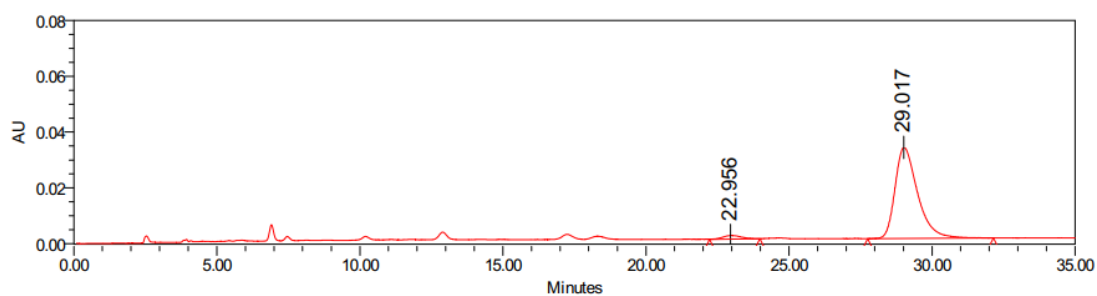
4p





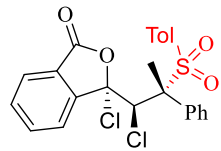
Peak Results

	RT	Area	Height	% Height	% Area
1	23.875	3806604	85395	57.29	50.72
2	30.395	3698014	63650	42.71	49.28

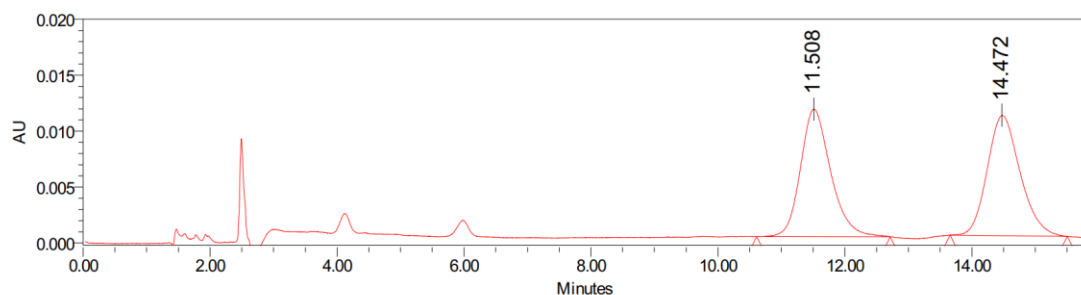


Peak Results

	RT	Area	Height	% Height	% Area
1	22.956	54044	1278	3.76	2.94
2	29.017	1781378	32656	96.24	97.06

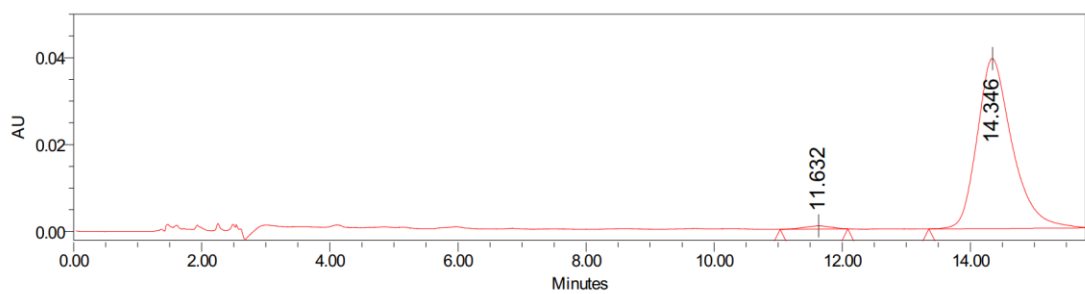


5



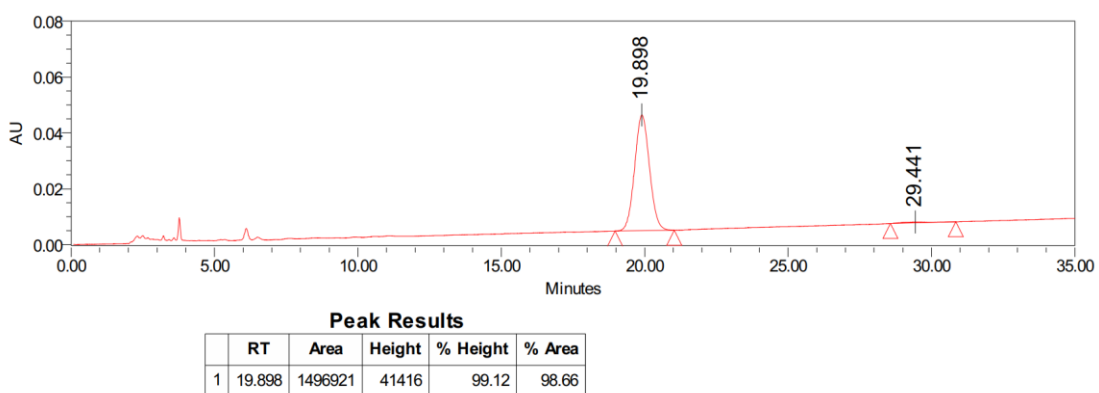
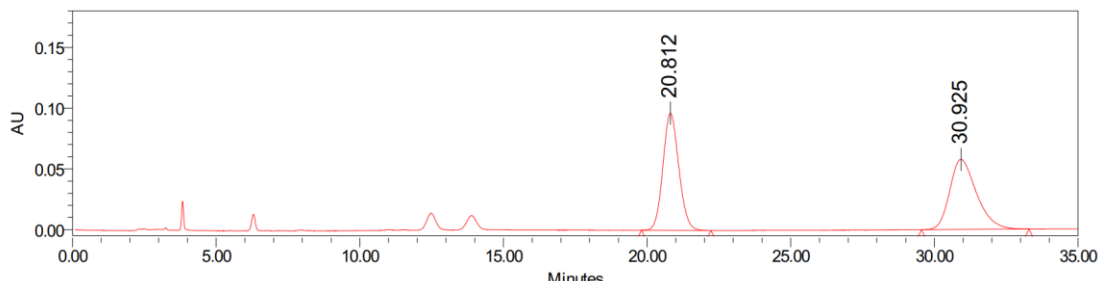
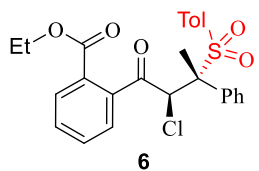
Peak Results

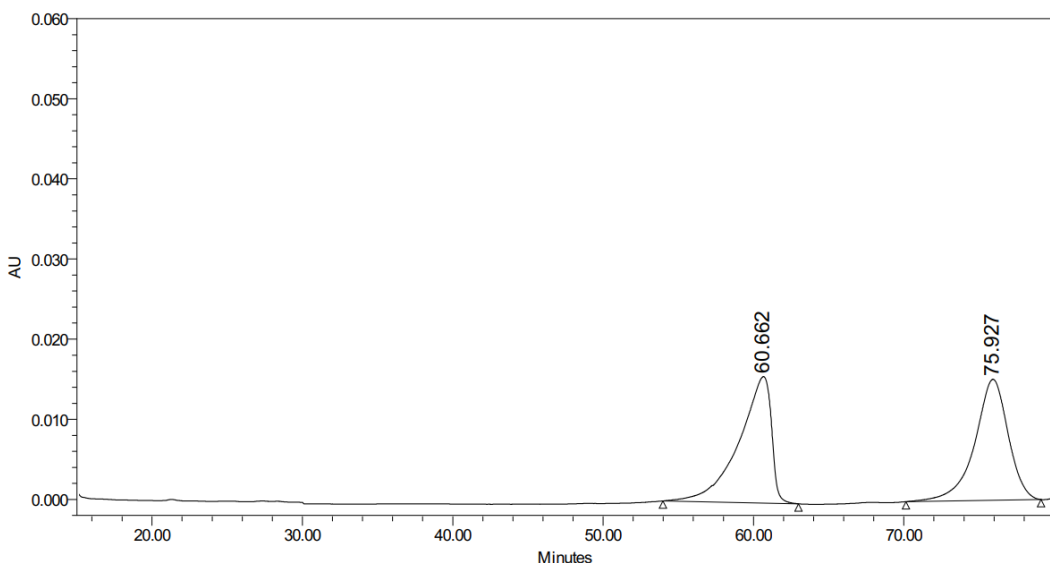
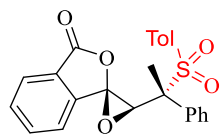
	RT	Area	Height	% Height	% Area
1	11.508	377563	11415	51.48	49.37
2	14.472	387245	10761	48.52	50.63



Peak Results

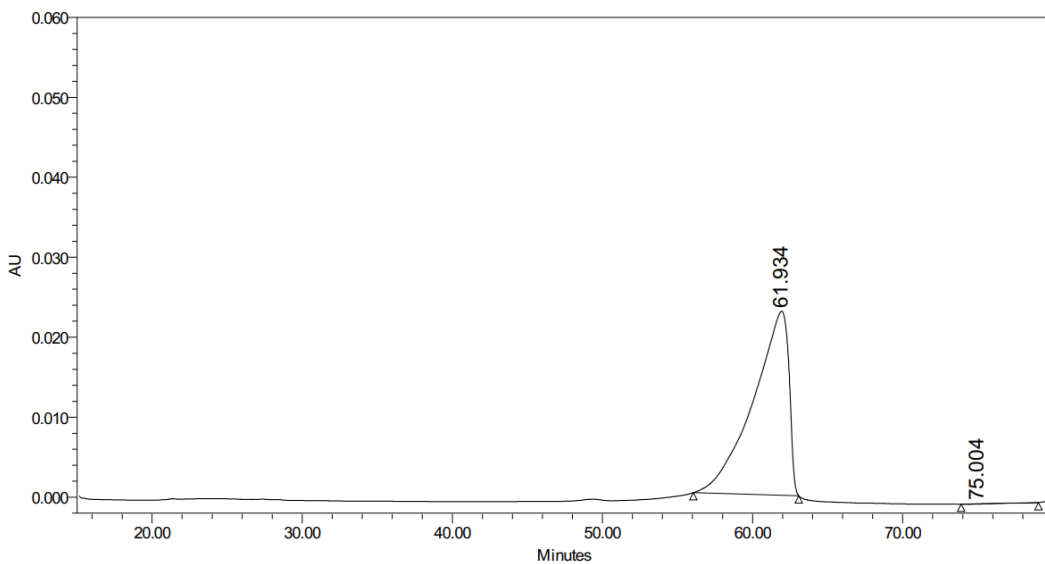
	RT	Area	Height	% Height	% Area
1	11.632	20751	724	1.82	1.38
2	14.346	1483958	39122	98.18	98.62





Peak Result

	RT	Area	Height	% Height	% Area
1	60.662	2363992	15784	51.11	50.34
2	75.927	2331836	15101	48.89	49.66



Peak Result

	RT	Area	Height	% Height	% Area
1	61.934	3792501	23009	99.83	99.84
2	75.004	6205	-38	0.17	0.16